PERFORMANCE EVALUATION OF TREATED RICE HUSK ACTIVATED CARBON IN WATER TREATMENT AND REMOVAL OF PHENOL

By

YAHAYA SAYYADI MOHAMMAD

DEPARTMENT OF WATER RESOURCES AND ENVIRONMENTAL ENGINEERING
FACULTY OF ENGINEERING
AHMADU BELLO UNIVERSITY
ZARIA, NIGERIA.

APRIL, 2015

PERFORMANCE EVALUATION OF TREATED RICE HUSK ACTIVATED CARBON IN WATER TREATMENT AND REMOVAL OF PHENOL

By

Yahaya Sayyadi MOHAMMAD
B.Eng-Chemical (FUTMin) 2004
M.Eng-Environmental (UniPort) 2009
(PhD/ENG/12353/2011-12)

A DISSERTATION SUBMITTED TO THE SCHOOL OF POSTGRADUATE STUDIES, AHMADU BELLO UNIVERSITY, ZARIA

IN PARTIAL FULFILMENT OF THE REQUIREMENTS FOR THE AWARD OF THE DEGREE OF
DOCTOR OF PHILOSOPHY IN ENVIRONMENTAL ENGINEERING

DEPARTMENT OF WATER RESOURCES AND ENVIRONMENTAL ENGINEERING
FACULTY OF ENGINEERING
AHMADU BELLO UNIVERSITY, ZARIA
NIGERIA

APRIL, 2015

DECLARATION

I declare that the work in this dissertation entitled **"Performance Evaluation of Treated Rice Husk Activated Carbon in Water Treatment and Removal of Phenol,"** has been carried out by me in the Department of Water Resources and Environmental Engineering under the supervision of Dr. E.M. Shaibu-Imodagbe, Dr. S.B. Igboro and Dr. A. Giwa. The information derived from the literature has been duly acknowledged in the text and a list of references provided. No part of this dissertation was previously presented for another degree or diploma at this or any other institution.

MOHAMMAD, Yahaya Sayyadi

(Name of Student) _____ Sign _____ Date

CERTIFICATION

This dissertation entitled "**Performance Evaluation of Treated Rice Husk Activated Carbon in Water Treatment and Removal of Phenol**" by YAHAYA SAYYADI MOHAMMAD meets the regulations governing the award of the degree of Doctor of Philosophy of Ahmadu Bello University, Zaria, and is approved for its contribution to knowledge and literary presentation.

Dr. E.M. Shaibu-Imodagbe Chairman, Supervisory Committee	Sign	Date
Dr. S.B. Igboro Member, Supervisory Committee	Sign	Date
Dr. A. Giwa Member, Supervisory Committee	Sign	Date
Dr. A. Ismail Head of Department	Sign	Date
Prof. A.Z. Hassan Dean, School of Postgraduate Studies	Sign	Date

DEDICATION

This is dedicated to the memory of my *late* mother. May Allah forgive her all her sins, have mercy on her and make her among the dwellers of Al-Jannatu Firdaus.

ACKNOWLEDGEMENT

Glory is to Allah for seeing me through to this stage of life. I also remained profusely thankful to my parent for their care, concern and support especially during childhood which invariably set the basis for my continued educational pursuit in both western and Islamic knowledge. I really cannot thank them enough. I am also sincerely grateful to my supervisory team: Dr. E.M. Shaibu-Imodagbe, Dr. S.B. Igboro and Dr. A. Giwa for their motivational guidance and support. Let me say that this study is a direct consequence of their collective contributions. With high sense of gratitude to my major supervisor sir, let me also proudly say that his academic advice to me on the first day of introduction as his research student have remained memorable and became the strongest driving force and pillar of inspiration and encouragement throughout my study.

I wish to also express my profound appreciation to the entire staff of my department particularly Prof. C.A. Okuofu, Dr. D.B. Adie and Dr. A. Ismail for their fatherly role and contributions that have added much value to this work, and Engr. B.S. Salauwa for his warmest welcome to the department. Let me also acknowledge the support and contributions of Ibrahim Badamasi Babangida University, Lapai, Petroleum Technology Development Fund, Abuja, as well as the members of staff of the following: Multi-User Laboratory, Ahmadu Bello University (ABU), Zaria, Chemical Engineering Laboratory, ABU, Zaria, Biochemistry Laboratory, Federal University of Technology (FUT), Minna, Central Teaching Laboratory, FUT, Minna, Center for Genetic Engineering and Biotechnology, FUT, Minna, Scientific Equipment Development Institute, Minna and National Research Institute for Chemical Technology, Zaria.

I wish to also express my appreciation and gratitude to my wife (Amina) and children (Rahma and Hasana) for their much-needed understanding and patience which became a source of moral support throughout the study. I will like to also appreciate my family members and friends for their concern throughout the period of my study. Finally, I wish to also thank the management of Ahmadu Bello University, Zaria for providing the enabling environment for this programme of study.

ABSTRACT

Rice husk, a potential source of activated carbon, is locally available in Nigeria but underutilized thereby constituting solid waste menace in the environment. Incidentally, large volume of wastewater containing high concentrations of toxic contaminants such as phenol and other contaminants are continuously being generated as a result of increased industrial activities. Agricultural waste materials including rice husk, when suitably modified could serve as activated carbon for efficient removal of wastewater contaminants. In this study, rice husk activated carbon was produced by carbonization followed by activation with phosphoric acid. Batch adsorption experiment was conducted on effect of process variables (carbonization temperature, initial phenol concentration, adsorbent dosage, contact time, solution pH and temperature) on the adsorption of phenol onto rice husk activated carbon. Equilibrium isotherm, kinetics and thermodynamics of the adsorption process were studied. Response surface methodology was then employed for modeling and optimization of the process variables. Under the optimum condition for the production of rice husk activated carbon developed, characterization of the rice husk activated carbon was carried out and column adsorption experiment was conducted in two modes: Rapid Small Scale Column Test (RSSCT) and Large Scale Column Test (LSCT) using process wastewater collected from Kaduna refinery and Samaru stream water. RSSCT was utilized to study the effect of process variables: flow rate and bed depth and the experimental data obtained were fitted into column models (BDST, Thomas and Yoon-Nelson), while the LSCT was employed to obtain the peak adsorption performance. For the batch adsorption, process variables were observed to have significant effect on the performance of the adsorption process. Adsorption capacity and removal efficiency of 2.4 mg/g and 96 % were attained and equilibrium was found to occur between 10-20

minutes. Adsorption capacity and removal efficiency were also observed to be maximum at pH=4 and better favoured at lower temperatures. The adsorption process was found to be inconsistent with the assumption of Langmuir monolayer but conformed to Freudlinch assumption of multilayer and physical adsorption. The data followed pseudo-second order kinetic model and intra-particle diffusion was not the only rate-limiting step. The adsorption process was also found to be exothermic. The model equations developed have correlation coefficient (R^2) values of 0.9979 and 0.9981 for removal efficiency and adsorption capacity respectively. Optimization revealed that the optimum temperature for the production of rice husk activated carbon is 441.46 ^{o}C. The models were experimentally validated under optimum condition. Phosphoric acid modification of rice husk was also observed to enhance the surface area from 12.47 to 102.4 m^2/g and micropores from 2.4 to 1.82 nm. This was confirmed from the SEM micrographs while FTIR analysis revealed the existence of oxy- and phosphorous-oxy-containing functional groups. RSSCT shows that performance of the column adsorption was significantly affected by bed depth and flow rate. The column experimental data fitted well to Thomas and Yoon-Nelson models. LSCT shows that the column experiment attained relatively high adsorption capacity of 55.106 mg/g at exhaustion point of 0.9; this implies the peak adsorption capacity of the rice husk activated carbon.

TABLE OF CONTENTS

Contents **Page**

Title Page……..i

Declaration ……..ii

Certification……iii

Dedication ……iv

Acknowledgement……...v

Abstract……vi

Table of Contents……vii

List of Figures……..xiv

List of Tables……...xvii

List of Appendices……..xiv

CHAPTER ONE - INTRODUCTION

1.1 Preamble……1

1.2 Rice and Rice Husk……..2

1.3 Phenol……4

1.4 Statement of the Problem ……...5

1.5 Justification of the Study……7

1.6 Aim and Objectives…….....7

1.7 Limitation of the Study……..8

CHAPTER TWO - LITERATURE REVIEW

2.1 Adsorption Technology……...9

2.1.1 Factors affecting adsorption……...9

2.1.2 Adsorbents……....10

2.2 Activated Carbons…….....11

2.2.1 History of activated carbons……...12

2.2.2 Classification of activated carbon…….……13

2.2.3 Agricultural waste: Emerging source of activated carbon……13

2.3 Production of Activated Carbons……..14

2.3.1 Thermal (physical) pretreatment…….……..14

2.3.2 Chemical pretreatment……..15

2.3.3 Combined pretreatment (Two-Step process)……17

2.4 Characterization of Activated Carbon…….19

2.4.1 Pore size …….……..19

2.4.2 Surface area…….....20

2.4.3 Morphology…….….20

2.4.4 Surface functional group…….……..21

2.5 Application of Activated Carbons……...…..21

2.6 Application of Activated Carbon in Removal of Inorganic Contaminant..22

2.7 Mode of Operation of Adsorption Process……....23

2.7.1 Batch mode……..……..23

2.7.2 Column mode…….....24

2.8 Batch Experimental Data Analysis ……..….24

2.8.1 Adsorption capacity and removal efficiency…….……....24

2.8.2 Adsorption equilibrium isotherms…….….....26

2.8.3 Adsorption kinetic models…….……....29

2.8.4 Adsorption thermodynamics ……..……..…32

2.9 Column Experimental Data Analysis…….....33

2.9.1 Breakthrough curve…….…….....33

2.9.2 Column models…….....33

2.10 Response Surface Methodology……..…..…35

2.11 Review of Batch Adsorption Processes……...…..37

2.12 Review of Column Adsorption Processes…….……...37

2.13 Review of Activated Carbon Production……..37

CHAPTER THREE - MATERIALS AND METHOD

3.1 Materials and Sample Collection……..….**.....**48

3.1.1 Materials/reagents**.....**48

3.1.2 Sample collection/processing…….**.....**48

3.2 Production of Activated Carbon….**.....**50

3.2.1 Thermal pretreatment……..….50

3.2.2 Chemical pretreatment….**.....**50

3.3 Batch Adsorption……**....**50

3.3.1 Preparation of simulated wastewater…….50

3.3.2 Batch experiment……...51

3.3.3 Determination of unadsorbed phenol…….52

3.3.4 Determination of adsorption capacities and removal efficiency……...52

3.3.5 Adsorption equilibrium isotherm study…….53

3.3.6 Adsorption kinetic study……54

3.3.7 Adsorption thermodynamic study…….**.....**55

3.4 Modeling and Optimization……....56

3.4.1 Experimental design……**...**56

3.4.2 Regression model…….…..…58

3.4.3 Statistical and graphical analysis……**....**58

3.4.4 Optimization……**...**59

3.4.5 Model validation…….**.....**59

3.4.6 Software application……59

3.5 Characterization of Activated carbon……..60

3.5.1 Thermogravimetric analysis (TGA)……....60

3.5.2 Scanning electron microscopy (SEM) analysis……60

3.5.3 Fourier transform infrared (FTIR) spectroscopy analysis……..…..60

3.5.4 Surface area and pore size analysis……...61

3.6 Column Adsorption……61

3.6.1 Adsorption of phenol from refinery wastewater……61

3.6.2 Breakthrough curve …… ……..64

3.6.3 Column adsorption models ……65

3.6.4 Treatment of raw water from Samaru stream……67

3.6.5 Determination of raw water parameters……68

CHAPTER FOUR - RESULTS AND DISCUSSION

4.1 Batch Adsorption Capacity and Removal Efficiency ……..69

4.2 Effect of Process Variables on Phenol Adsorption……...79

4.2.1 Effect of initial concentration……79

4.2.2 Effect of adsorbent dosage……87

4.2.3 Effect of contact time…….93

4.2.4 Effect of pre-treatment (carbonization) temperature…….……..……..98

4.2.5 Effect of solution pH…….....101

4.2.6 Effect of solution temperature……..103

4.3 Adsorption Isotherm, Kinetics and Thermodynamic Models……....105

4.3.1 Adsorption isotherm……105

4.3.2 Adsorption kinetics……...113

4.3.3 Adsorption thermodynamic…….....120

4.4 Comparative Study……..120

4.5 Modeling and Optimization…**.....**122

4.5.1 Design of experiment……122

4.5.2 Development of model equations……..123

4.5.3 Comparison of actual (experimental) and predicted values…….**.....**129

4.5.4 Combined effect of factors on response……**....**132

4.5.5 Optimization……..136

4.5.6 Model validation…….…...136

4.6 Characterization of Activated Carbon……..138

4.6.1 Themo-gravimetric analysis (TGA) profiles……138

4.6.2 Fourier transformed infrared spectroscopy (FTIR) spectrum……140

4.6.3 Scanning electron microscopy (SEM) micrograph……142

4.6.4 Surface area and pore size……144

4.7 Column Adsorption……146

4.7.1 Adsorption of phenol from refinery wastewater *(RSSCT mode)*……..146

4.7.2 Effect of bed depth and flow rate……**..**…148

4.7.3 Bed Depth Service Time model……**.**151

4.7.4 Thomas model ……**...**151

4.7.5 Yoon Nelson model……**...**154

4.7.6 Adsorption of phenol from refinery wastewater *(LSCT mode)*..……**..**156

4.7.7 Treatment of raw water from Samaru stream……**....**160

4.8 Important Outcome of this Study……**...**163

CHAPTER FIVE - CONCLUSION AND RECOMMENDATIONS

5.1 Conclusion……**....**166

5.2 Recommendations…….……**...**167

REFERENCES……...168

APPENDIX A…….....……....197

APPENDIX B.....207

LIST OF FIGURES

Fig. 3.1: Availability of Rice Husk.....49

Fig. 3.2: Dry Rice Husk.....49

Fig. 3.3: Sketch of the Column Experimental Set-up.....62

Fig. 4.1: Effect of Initial concentration on Adsorption Capacity (*RH300)*…….81

Fig. 4.2: Effect of initial concentration on Adsorption Capacity (*RH400)* ……81

Fig. 4.3: Effect of Initial concentration on Adsorption Capacity (*RH500)* ……82

Fig. 4.4: Effect of Initial concentration on Removal Efficiency *(RH300*……85

Fig. 4.5: Effect of Initial concentration on Removal Efficiency (*RH400)* ……..85

Fig. 4.6: Effect of Initial concentration on Removal Efficiency (*RH500)* …….86

Fig. 4.7: Effect of Adsorbent dosage on Adsorption Capacity *(RH300)* ……88

Fig. 4.8: Effect of Adsorbent Dosage on Adsorption Capacity (*RH400)*…….....88

Fig. 4.9: Effect of Adsorbent Dosage on Adsorption Capacity (*RH500)* ……...89

Fig. 4.10: Effect of Adsorbent dosage on Removal Efficiency *(RH300)* ……91

Fig. 4.11: Effect of Adsorbent Dosage on Removal Efficiency *(RH400)* ……..91

Fig. 4.12: Effect of Adsorbent Dosage on Removal Efficiency *(RH500)* ……..92

Fig. 4.13: Effect of Contact time on Adsorption Capacity *(RH300)* ……..95

Fig. 4.14: Effect of Contact time on Removal Efficiency *(RH300)* ……...95

Fig. 4.15: Effect of Contact time on Adsorption Capacity *(RH400)* ……..96

Fig. 4.16: Effect of Contact time on Removal Efficiency *(RH400)* ……...96

Fig. 4.17: Effect of Contact time on Adsorption Capacity *(RH500)* ……..97

Fig. 4.18: Effect of Contact time on Removal Efficiency *(RH500)* ……97

Fig. 4.19: Effect of Pretreatment Temperature on Removal Efficiency, m=2g……99

Fig. 4.20: Effect of Pretreatment Temperature on Removal Efficiency, m=4g……99

Fig. 4.21: Effect of Pretreatment Temperature on Adsorption Capacity, m=2g ….100

Fig. 4.22: Effect of Pretreatment Temperature on Adsorption Capacity, m=4g….100

Fig. 4.23: Effect of Solution pH on Adsorption Capacity ……..102

Fig. 4.24: Effect of Solution pH on Removal Efficiency……102

Fig. 4.25: Effect of Solution Temperature on Adsorption Capacity……104

Fig. 4.26: Effect of Solution Temperature on Removal Efficiency ……104

Fig. 4.27: Intra-particle Diffusion Plot *(RH300)* ……118

Fig. 4.28: Intra-particle Diffusion Plot *(RH400)* ……..118

Fig. 4.29: Intra-particle Diffusion Plot *(RH500)* ……119

Fig. 4.30: Predicted-Actual Plot for Response Y_1……130

Fig. 4.31: Predicted-Actual Plot for Response Y_2……130

Fig. 4.32: Combined Effect of Factors A-B on Response Y_1 ……134

Fig. 4.33: Combined Effect of Factors A-B on Response Y_2……..134

Fig. 4.34: Combined Effect of Factors A-C on Response Y_1……..134

Fig. 4.35: Combined Effect of Factors A-C on Response Y_2……..134

Fig. 4.36: Combined Effect of Factors A-C on Response Y_1 …… …135

Fig. 4.37: Combined Effect of Factors A-C on Response Y_2…….135

Fig. 4.38: TGA profile for %weight loss against temperature……139

Fig. 4.39: TGA profile for %weight loss against time……139

Fig. 4.40: FTIR spectrum before phosphoric acid modification…….141

Fig. 4.41: FTIR spectrum after phosphoric acid modification……141

Fig. 4.42: SEM Micrographs before phosphoric acid modification……143

Fig. 4.43: SEM Micrographs after phosphoric acid modification……..143

Fig. 4.44: Breakthrough Curve for bed Depth, 6cm and Flow rate, 4.5ml/min.....146

Fig. 4.45: Breakthrough Curve for different Bed Depths ……..149

Fig. 4.46: Breakthrough Curve for different Flow Rates……150

Fig. 4.47: Bed Depth Service Time Model Plot for different Breakthrough Points....152

Fig. 4.48: Thomas Model Plot……..…..153

Fig. 4.49: Yoon Nelson Model Plot…….155

Fig. 4.50: Breakthrough Curve for bed depth 60cm (359.84g) ……..156

LIST OF TABLES

Table 2.1: Summary of Modification Processes and Variables with their Expected Characteristic…….....…..…..18

Table 2.2: Review of Batch Adsorption Processes…….....38

Table 2.3: Review of Column Adsorption Processes…….....42

Table 2.4: Review of Activated Carbon Production Processes……....44

Table 4.1: Adsorption capacity and Removal efficiency as a function of adsorbent dosage and initial concentration of phenol *(RH300)*….....71

Table 4.2: Adsorption capacity and Removal efficiency as a function of Contact time at a Fixed Initial Phenol concentration (C_o*=50mg/l, RH300)*.....…...72

Table 4.3: Adsorption capacity and Removal efficiency as a function of adsorbent dosage and initial concentration *(RH400)*…….....74

Table 4.4: Adsorption capacity and Removal efficiency as a function of Contact time at a Fixed Initial Phenol concentration (C_o*=50mg/l, RH400))*…….....75

Table 4.5: Adsorption capacity and Removal efficiency as a function of adsorbent dosage and initial concentration *(RH500)*…….....77

Table 4.6: Adsorption capacity and Removal efficiency a function of Contact time at a Fixed Initial Phenol concentration (C_o*=50mg/l, RH500)*…….....78

Table 4.7: Langmuir Adsorption isotherm data *(RH300)*…….106

Table 4.8: Langmuir Adsorption isotherm data *(RH400)*….....107

Table 4.9: Langmuir Adsorption isotherm data *(RH500)*…….108

Table 4.10: Freunlich Adsorption isotherm data *(RH300)*……...110

Table 4.11: Freunlich Adsorption isotherm data *(RH400)*……...111

Table 4.12: Freunlich Adsorption isotherm data *(RH500)*……..….112

Table 4.13: Pseudo Second Order kinetics data *(*C_o*=50mg/l, RH300)*…….114

Table 4.14: Pseudo Second Order kinetics data *(*C_o*=50mg/l, RH400)*…….115

Table 4.15: Pseudo Second Order kinetics data *(*C_o*=50mg/l, RH500)*…….116

Table 4.16: Adsorption Thermodynamics Data……....121

Table 4.17: Comparison of Thermal and Combined Pre-Treatment…….....121

Table 4.18: Design Matrix for Factors and Respective Response from Experiment..122

Table 4.19: Model Summary Statistics for Response Y_1 (Removal Efficiency)…….125

Table 4.20: Model Summary Statistics for Response Y_2 (Adsorption Capacity)……125

Table 4.21: Model ANOVA for Response Y_1 (Removal Efficiency)…….…...127

Table 4.22: Model ANOVA for Response Y_2 (Adsorption Capacity)…….....128

Table 4.23: Actual-Predicted Values and Residual…….….....131

Table 4.24: Desirability for Optimum Operating Conditions……..137

Table 4.25: Model Validation…….....137

Table 4.26: Surface Area and Pore Size before and after Acid Modification.....145

Table 4.27: Breakthrough Curve data for *z=6cm, f=4.5ml/min,* C_o*=51.32mg/l*…….147

Table 4.28: Breakthrough Characteristics…….....149

Table 4.29: Bed Depth Service Time (BDST) model parameters…….....152

Table 4.30: Thomas model parameters……...153

Table 4.31: Yoon Nelson model parameters …….……..…..155

Table 4.32: Breakthrough Curve data for *z = 60 cm (359.84 g), f = 56.58 ml/min,* C_o*=78.32mg/l*……..157

Table 4.33: Raw and Treated Values of Water Parameters collected at different Points *z=6cm, f=3ml/min, t=300min*…….....162

Table 4.34: Outcome of Batch Adsorption…….....163

Table 4.35: Outcome of Activated Carbon Modification……164

Table 4.36: Outcome of Column Adsorption…….....165

LIST OF APPENDICES

Appendix A1: Results on Effect of Solution pH……197

Appendix A2: Results on Effect of Solution Temperature……197

Appendix A3: Breakthrough Curve, Yoon Nelson and Thomas model plot data for *z=4.5cm, f=3ml/min, C_o=51.32mg/l*…….....198

Appendix A4: Breakthrough Curve, Yoon Nelson and Thomas model plot data for *z=6cm, f=3ml/min, C_o=51.32mg/l*…….....199

Appendix A5: Breakthrough Curve, Yoon Nelson and Thomas model plot data for *z=7.5cm, f=3ml/min, C_o=51.32mg/l*…….....200

Appendix A6: Breakthrough Curve, Yoon Nelson and Thomas model plot data for *z=6cm, f=4.5ml/min, C_o=51.32mg/l*…….....201

Appendix A7: Langmuir Isotherm Plot *(RH300)* ……...202

Appendix A8: Langmuir Isotherm Plot *(RH400)* ……..202

Appendix A9: Langmuir Isotherm Plot *(RH500)* ……...203

Appendix A10: Freundlich Isotherm Plot *(RH300)* …….203

Appendix A11: Freundlich Isotherm Plot *(RH400)* ……..…204

Appendix A12: Freundlich Isotherm Plot *(RH500)* …….204

Appendix A13: Pseudo-Second Order Kinetics Plot *(RH300)* ……205

Appendix A14: Pseudo-Second Order Kinetics Plot *(RH400)* …….205

Appendix A15: Pseudo-Second Order Kinetics Plot *(RH500)* …….206

Appendix A16: Thermodynamic model plot…….....……..206

CHAPTER ONE

INTRODUCTION

1.1 Preamble

Biomass waste especially agricultural wastes have, in recent times, been receiving increased attention for many reasons; among which are depletion of global fossil fuel reserves, economic and environmental benefit, availability and renewability (Deng *et al*., 2010; Igboro, 2010; Mohamed *et al*., 2010; Liu and Zhang, 2011; Wang *et al*., 2011a; Lim *et al*., 2012; Chen *et al*., 2013). These agricultural wastes constitute a great source of emerging bio-products (bio-fuel, bio-chemicals and bio-materials) and their efficient utilization will provide a viable platform for effective solid waste management (Kalderis *et al*., 2008a; Singh *et al*., 2008; Purnomo *et al*., 2011; Boumaza *et al*., 2012; Sahin and Saka, 2013). Adsorbents that are used in removal of contaminants from water and wastewater include activated alumina, zeolites and activated carbon (Ahmaruzzaman, 2008; Lin and Juang, 2009; Soto *et al*., 2011; Ali *et al*., 2012; Han *et al*., 2013). Nowadays, activated carbons (bio-materials) prepared from agricultural wastes are receiving increasing attention due to their relatively low cost, availability and ease in processing (Krishnani *et al*., 2008; Sahu *et al*., 2009b; Chand *et al*., 2009; Njoku and Hameed, 2011).

Water is an essential necessity for the well being of all living things. It is unique in its physiological roles to all living resources and hence indispensable to all life forms. Therefore, among the various forms of pollution, water pollution is of greatest concern (Bhatnagar and Minocha, 2006). It is a known fact that increasing global industrialization has led to the continuous generation of large amounts of wastewater containing toxic pollutants. The presence of these toxic contaminants is associated with adverse effect and has therefore led to increased strict regulation of water pollution

hence; making the treatment of wastewater generated from industrial activities a necessity before being discharged into the environment (Sahu *et al*., 2009b; Calero *et al*., 2013; Moussavi *et al*., 2013).

Consequently, pollution control and management have evolved many technologies for the treatment of wastewater (Qadeer and Akhtar, 2005; Bhatnagar and Minocha, 2006). These technologies and methodologies which differ in their performance and effectiveness include coagulation, filtration, ion exchange, sedimentation, solvent extraction, adsorption, electrodialysis, chemical oxidation, disinfection, chemical precipitation and membrane separation (El-Naas *et al*., 2010; Liu *et al*., 2010). Among the various available technologies for water pollution control, adsorption process is considered relatively more promising because of its convenience, ease in operation and simplicity of design (Han *et al*., 2008; Kadhim and Al-Seroury, 2012; Song *et al*., 2013). Various kind of contaminants can be removed from polluted water by adsorption process due to the availability of diverse form of adsorbents especially activated carbon which makes it have a broader applicability in water pollution control (Kalderis *et al*., 2008b; Fierro *et al*., 2008; Liu *et al*., 2010; Aidan, 2012).

1.2 Rice and Rice Husk

Rice is the third most important cereal crop grown around the world with an annual output of more than 650 million tons (Song *et al.,* 2013). Nigeria has an annual local production of 3-4 million tons of paddy rice (Cadoni and Angelucci, 2013) and about 20-25 % of this is rice husk. Rice husk which is a layer protecting rice grain (Nhapi *et al*., 2011) is the major by-product obtained from rice processing (Zhang *et al*., 2011a). It consists of cellulose (32.24 %), hemicelluloses (21.34 %), lignin (21.44 %), water (8.11 %), extractives (1.82 %) and mineral ash (15.05 %) as well as high percentage of

silica in its mineral ash, which is 94.5-96.34 % (Ngah and Hanafiah, 2008; Demibras, 2009; Masoud *et al*., 2012). Rice husk also has an average particle diameter of 4-5mm and bulk density of 96-160 kg/m^3 (Bansal *et al*., 2009). In recent times, there have been deliberate attempts to utilize large quantities of rice husks from rice mills for useful purposes. These include the use as animal feed, bedding materials, soil conditioner, fertilizer, solid fuel for steam generation, bio-fuel, a source of organic and inorganic chemicals, porous carbon, catalyst, abrasives components, refractory and insulating materials, paper and board manufacturing, among others (Patel, 2005; Srivastava *et al*., 2008; Lin *et al*., 2013). Rice husk is insoluble in water, has good chemical stability, high mechanical strength and possesses a granular structure, making it a potential adsorbent material (Ngah and Hanafiah, 2008; Chakraborty *et al*., 2011). It constitutes approximately 20-25 % of the total grain weight depending on the variety and it is abundantly and locally available at almost no-cost but underutilized thereby constituting solid waste in the environment (Masoud *et al*., 2012). It is very difficult to decompose and traditionally, it is being disposed on land resulting in aesthetic pollution, eutrophication and perturbation in aquatic life (Foo and Hameed, 2009; Li *et al*., 2011a; Zhu *et al*., 2012). Application of heat treatment on rice husk can lead to different type of residue depending on oxygen supply (Foo and Hameed, 2009). When rice husk is burnt in air, a residue, white rice husk ash consisting of pure silica (95 %) is obtained. But heating rice husk in limited supply or absence of oxygen (pyrolysis) produces a black rice husk ash containing varying amount of carbon and silica. This residue when appropriately modified can be of useful purposes such as in water and wastewater treatment. The suitability of rice husk for removal of wastewater contaminants largely depends on its modification processes (Ye *et al*., 2010).

1.3 Phenol

Over 2000 wastewater chemical contaminants have been identified among which over 600 are of organic origin (Agarry and Aremu, 2012a). Phenolic compounds are among the most common organic pollutants and are present in effluents from coal processing, plastic, disinfectant, pesticides, pharmaceutical, petroleum and steel industries (Kennedy *et al*., 2007; Beker *et al*., 2010). Phenol, an aromatic compound with the following properties, molecular formula: C_6H_5OH, molecular weight: 94.11g/mol, molecular size: 0.42-0.72 nm, cross sectional area: 0.414 nm^2, melting point: 40.9 ^oC, boiling point: 181.75 ^oC, water solubility: 93 g/l, has always been chosen as a model pollutant in the field of environmental research (Busca *et al*., 2008; Liu *et al*., 2010; Liu *et al*., 2011; Song *et al*., 2013). Phenol is an important toxic compound listed as a priority pollutant by environmental protection agencies because of its high toxicity and possible accumulation in the environment (Suresh *et al*., 2011; Moreno-Virgen *et al*., 2012). Phenol is the 11^{th} of the 126 chemical priority pollutants by United State Environmental Protection Agency (USEPA) with odour threshold of 0.04 ppm (Omar, 2012). The concentration of phenol in wastewater varies from 0.1-6,800 mg/l and the permissible limit of phenol concentration in wastewater by Federal Environmental Protection Agency (FEPA) is 0.5 mg/l (Otekunefor and Obiukwu, 2005) while concentration in portable water by World Health Organization (WHO) is 0.001 mg/l (Bada, 2007; Kamble *et al*., 2008). Long exposure to low level of phenol in water can cause severe health hazard which include liver damage, diarrhea, dark urine and mouth ulcer. Phenol is a strong eye and respiratory irritant (Belgin *et al.*, 2008). Bad taste and odor is an indication of the presence of phenol in water (Kermani *et al.*, 2006). As a result of toxic and inhibitory characteristics, phenols are very difficult or impossible to remove by biological treatment processes, hence studies are being conducted with the

aim of decreasing their concentrations to allowable limits or converting them to less toxic and hazardous forms that may be released easily into the environment (Ahmaruzzaman 2008; Blanco-Martinez *et al*., 2009; Soto *et al*., 2011; Girish and Ramachandra, 2012). In view of these characteristics, it was chosen for focus in this study.

1.4 Statement of the Problem

High concentration of chemical contaminants in industrial wastewater can cause hazard when discharged into the environment (Abdelkareem, 2013). These hazards include aesthetics, health disorder, damage to aquatic life and environment (Girods *et al*., 2009; Nabais *et al*., 2009; Lazo-Cannata *et al*., 2011). Phenols are among the most common water pollutants that can cause hazards including health hazard which may lead to death. Amongst hydrocarbons present in refinery wastewater, phenol is one of the main dissolved components and it is also one of the most difficult hydrocarbons to degrade biologically (Benyahia, 2004; Kamble *et al*., 2008). Industries such as Kaduna Refinery continuously generate large volume of wastewater that contains high concentration of phenol (Alhamed, 2009; Nadavala *et al*., 2009) thereby making wastewater treatment an integral part of their activities. Ultimately, this results in increased cost of production and has led to the continuous search for simple, cleaner and cost-effective treatment approach.

Most of the treatment methods for wastewaters are not without their drawbacks such as high capital and operational cost, regeneration cost and residual disposal (Bansal *et al*., 2009; Lakshmi *et al*., 2009; Chowdury *et al*., 2011). Treatment cost for these methods ranges from 10-450 US Dollars per cubic meter of treated water except for adsorption which is in the range of 5-200 US Dollars (Ali *et al*., 2012). Consequently, adsorption

has been identified as one of the most efficient techniques for the removal of wastewater contaminants because of the potentials of low-cost adsorbents especially activated carbon from agricultural wastes (Singh *et al*., 2008; Krishnani *et al*., 2008; Naiya *et al*., 2009). More so that the increasing demands for food production will lead to additional generation of agricultural wastes such as rice husk which increase additional challenges in solid waste disposal. For example, in an attempt to become self-sufficient in rice production, Nigeria has been on the path of boosting its rice production (Cadoni and Angelucci, 2013) which will invariably lead to increased generation of rice husk (as solid waste) in the environment.

As a result of the above, there is ongoing research into modification of these agricultural wastes with the aim of improving their efficiencies and effectiveness in adsorption process. Rice husk is an agricultural waste material that is cheaply available as a by-product of rice processing but requires pretreatment (modification) for better performance as an adsorbent. These modification processes may be very complex, sometimes comprising of several stages of production, elevated temperatures for pyrolysis and gas activation as well as being time-consuming (Kalderis *et al*., 2008a; Liu *et al*., 2011). Influence of thermal and chemical pretreatment of rice husk for phenol adsorption from wastewater has been studied but little is known of the combined techniques in batch and column studies especially direct pyrolysis preceding phosphoric acid activation. Therefore, this research is on the production of rice husk activated carbon by direct pyrolysis preceding phosphoric acid modification for adsorption of phenol and other wastewater contaminants.

1.5 Justification of the Study

The outcome of this research will be of immense economic benefit to the rice processing centers that generate rice husk by adding value to their by-product. It will also be of benefit to industries that generate phenol-containing wastewater like petroleum refinery through the availability of simple and cost-effective treatment approach. It will also be of benefit by adding value to the by-product (bio-char) of pyrolysis of rice husk for the production of bio-fuel and/or chemicals. It will also be of environmental benefit to the government and public.

1.6 Aim and Objectives

The aim of this research is to produce combined thermal and chemical pretreated rice husk activated carbon and apply it in the adsorption of phenol and water treatment.

The obtectives of this research are:

i. To investigate the influence of combined thermal and chemical pretreatment of rice husk on phenol adsorption.
ii. To investigate the effect of adsorbent dosage, initial phenol concentration, contact time, pretreatment temperature, pH and temperature on batch adsorption of phenol using the thermal and chemically treated rice husk activated carbon.
iii. To study the equilibrium isotherm, kinetics and thermodynamics of the adsorption process.
iv. To develop model equations for the process variables and determine the optimum operating conditions (using Response Surface Methodology).
v. To characterize the rice husk activated carbon under optimum condition.

vi. To investigate the effect of flow rate and bed depth on column adsorption of phenol using the thermal and chemically treated rice husk activated carbon as well as to analyze the column experimental data using column models.

1.7 Limitation of the Study

This study is specifically limited to the use of thermal and chemically treated rice husk activated carbon in the adsorption of phenol from simulated and refinery wastewater and treatment of general contaminants from communal raw water. While the use may have prospects in application to no-phenolic wastes in industrial effluent, these were not specifically covered in this study due to obvious constraint of finance, equipment and time. Another limitation encountered in this study was that the heating rate of the furnaces available could not be preset thereby making it difficult to study the effect of heating rate. However, heating rate was estimated by taking note of the temperature attained in 1 hour and dividing it by 60 minutes.

CHAPTER TWO

LITERATURE REVIEW

2.1 Adsorption Technology

Adsorption is a surface phenomenon by which a component or multi-component of a fluid (gas or liquid) is attracted to a surface of a solid and form attachment via physical or chemical bond (Hameed and Foo, 2010; Ibrahim *et al*., 2011). Adsorption may be physical or chemical. Physical adsorption is known as Vander Waals adsorption (Sincero and Sincero, 2006) and it occurs when intermolecular Vander Waals forces bind the adsorbing molecule to the solid (Patel, 2005) and the process is reversible. Patel (2005); Sincero and Sincero (2006) also described chemical adsorption as chemisorption which they further described as the covalent or ionic bonding between the adsorbing molecules and the solid with the process being irreversible. The solute is called the adsorbate and the solid that adsorbs is called the adsorbent. Adsorption is effective in most natural, biological, physical and chemical system and it is widely used in industrial applications (Charles and Odoemelam, 2010).

2.1.1 Factors affecting adsorption

Factors affecting adsorption include (Basonde, 2002; Busca *et al.*, 2008; Soto *et al*., 2011):

(i) Physical and chemical characteristics of the adsorbent such as surface area, pore size, surface functional groups.

(ii) Characteristics of the adsorbate such as pKa (acid dissociation/ ionization constant), binary or multicomponent solution.

(iii) Concentration of the adsorbate in the liquid phase.

(iv) Characteristics of the liquid phase (solution) e.g. temperature and pH.

(v) Residence time of the process.

(vi) Adsorbent dosage.

2.1.2 Adsorbents

Low-cost or cheap adsorbents are waste materials or by-products of other processes that are readily available in large quantity and require little processing (Ngah and Hanafiah, 2008). Adsorbents that can be used for removal of contaminants from wastewater include:

Zeolites: Due to their chemical properties and good surface area, zeolites with their natural or synthetic hydrated alumino-silicate minerals are used as adsorbent, molecular sieve, ion-exchangers and catalysts. Unlike activated carbons that are amorphous in nature, molecular sieves (zeolites) posses a crystalline structure with the characteristics of uniform pore diameter consequent upon which they can be used for separation processes on the basis of molecular size and shape. These molecular sieves are principally used for the removal of moisture from exhaust streams and hydrocarbons separation in refining operations (Bada, 2007; Oscar and Stuart, 2008).

Activated alumina as an amorphous product mainly consisting of aluminum oxide is a porous, high surface area adsorbent commonly used as catalyst and desiccants that is also used as an adsorbent for wastewater treatment (Bada, 2007). It was first used in adsorption process for the removal of water vapour from gases (Bhatnagar and Minocha, 2006).

Activated carbons: Traditionally, activated carbons used in wastewater treatment are obtained from coal, wood or animal bones but nowadays, there is a growing interest in the use of alternative and low-cost agricultural materials for their production. Among

the main reasons for the extensive applications of activated carbons are low-cost with respect to other adsorbents, wide availability, high performance in adsorption processes, surface reactivity and the versatility to modify its physical and chemical properties for synthesizing adsorbents with very specific characteristics (Moreno-Virgen *et al.*, 2012).

2.2 Activated Carbons

These are identified to be carbonaceous materials that are predominantly amorphous and can be distinguished from elemental carbon by the oxidation of the carbon atoms found on the outer and inner surfaces. They are characterized by their extraordinary large specific surface areas, well-developed porosity and tunable surface-containing functional groups that result in high degree of surface reactivity (Lori *et al*., 2008; Al-Qodah and Shawabkah, 2009; Abechi *et al*., 2013). They are noted to contain not only carbon, but also small amounts of chemically bonded oxygen and hydrogen in the form of various functional groups and mineral matter which is usually indicated as ash or residue (Mohammad-Khan and Ansari, 2009; Bhatnagar *et al*., 2013). The ash has catalytic effects during carbonization and modification and the minerals such as silica, aluminum, iron, magnesium and calcium may negatively affect or inhibit the improvement in surface area and development of open pores (Ahmad *et al.*, 2013). Characteristics of activated carbons depend on the composition of the biomass waste (raw materials) as well as processes of production and modification (Zanzi *et al*., 2001; Verla *et al*., 2012). Commercial activated carbons have been identified to be among the most widely used adsorbent in the adsorption process, but regeneration is difficult and expensive (Bada, 2007; Agarry and Aremu, 2012b). Recently, however extensive research has focused on new, efficient, renewable, low-cost and readily available

materials to be used as adsorbent (Sud *et al.*, 2008; Yadanaparthi *et al*., 2009; Hameed and Foo, 2010).

2.2.1 History of activated carbons

Historical developments of activated carbons were compiled by Gottipati (2012) as follows:

In ancient times (1500 B.C), activated carbons have been used for medicinal purposes. In 1773, the adsorptive powers of the carbons (charcoal) were identified by measuring the volumes of various gases adsorbed by carbons obtained from different source materials. The effectiveness of charcoal in decolorizing various aqueous solutions was investigated in 1785 and this appears to be the first systematic account for application of charcoal in liquid phase. In 1793, carbon prepared from animal tissues was successfully used for color removal from solutions. An English sugar company used wood charcoal for the decolorization of sugar syrups in 1974 but kept the method of preparing the carbon a secret.

In 1805, the decolorizing power of charcoal for sugar-beet liquor was established. It was discovered in 1822 that activated carbon produced by heating blood with potash has 20-50 times the decolorizing power of bone char. This was the first known step in producing an activated carbon by a combination of thermal and chemical processes. In 1856, decolorizing chars were produced by heating a mixture of flour, tar, and magnesium carbonate. Carbons were produced and applied to purify potable water in 1862. Activated carbon prepared from coconut shells was identified for gas adsorption properties in 1865 and in 1868 activated carbon was produced by heating paper mill waste with phosphates.

2.2.2 Classification of activated carbon

According to appearance, activated carbons are generally classified as granular activated carbons (GAC) or powdered activated carbons (PAC). While powered activated carbons have particles predominantly smaller than 80 mesh in size with a typical particle size less than 0.1mm and common particle size ranging between 0.015 to 0.025 mm, granular activated carbons have at least 90 % of the particles greater than 80 mesh in size and their particle size range between 0.6 to 4 mm. Granular activated carbons have the advantage of adaptability to continuous contacting and with no need of separation of adsorbent from the bulk fluid, while powdered activated carbons require the separation of adsorbent from the bulk fluid, however lower capital cost and less contact time make them relatively attractive (Bhatnagar *et al*., 2006; Gottipati, 2012). However, Dwivedi *et al*. (2008) reported that granular activated carbon have larger surface area and smaller internal pores while powdered activated carbon have smaller surface area and larger internal pores consequent upon which powdered activated carbons have relative faster adsorption rate.

2.2.3 Agricultural waste: Emerging source of activated carbon

Foo and Hameed (2009) reported that increasing demand for commercial activated carbons has resulted in their skyrocketing prices in the global market. This has also led to the search for alternative low-cost activated carbons which require little or no processing and are naturally available in abundance or are by-products or waste materials from other processes (Demibras, 2009). Activated carbon can be produced from biomass plant or waste but production from biomass waste is favored because the former competes for land and water with food crops which may lead to rise in food prices (Godliving, 2009). Biomass wastes such as agricultural wastes are available in

large quantities and constitute one of the most abundant renewable resources in the world. The abundance and availability of agricultural wastes make them good and cheap raw materials sources for activated carbon (Sud *et al*., 2008; Rangabhashiyam *et al*., 2013). Hence, attention is increasingly focused on the production of activated carbons from these agricultural wastes (Bhatnagar and Minocha, 2006) as they are renewable, very cheap, readily available and utilization of these wastes for the production of activated carbons will constitute a viable option for material recovery and efficient solid waste management. Agricultural wastes to be used as absorbent need further modification for suitability and improved performance (Srinivasakannan, 2003; Mohammad *et al*., 2012). Composition of these agricultural waste have a significant influence on the properties of the activated carbon produced as high content of cellulose yield predominantly microporous materials whereas high content of lignin favors the development of macroporous structure (Agarry and Aremu, 2012a).

2.3 Production of Activated Carbons

Process type and conditions for the production of activated carbon determine its characteristics (Rivera-Utrilla *et al*., 2011). These processes as presented in Table 2.1 can be classified as: thermal (physical), chemical and combined pretreatment.

2.3.1 Thermal (physical) pretreatment

Thermal pretreatment involves direct pyrolysis to remove moisture and volatile matter or physical activation of the biomass waste (Ibrahem *et al.,* 2012). The volatile matter consists of liquids and gasses that can be conveniently collected and utilized for the production of bio-fuel and/or chemicals (Schroder *et al*., 2011; Mohammad *et al*., 2012). The remaining solid charred residue exhibit different properties from the parent

biomass waste. The major differences are mainly in porosity, surface area and pore structures. These changes in the properties usually lead to high reactivity, and hence, an alternative usage of char becomes possible (Ioannidou and Zabaniotou, 2007).

During thermal decomposition (pyrolysis) of biomass which was reported to occur between 200-800 ^{o}C, significant decomposition occur at temperatures between 200-400 ^{o}C after which the rate of decomposition is much lower. This is more likely due to the impact of decomposition of cellulose which decomposes quickly at 200-400 ^{o}C. The decomposition of lignin which is slower but spans over the entire temperature range is thought to be responsible for additional weight loss between 400-800 ^{o}C (Zahangir-Alam *et al*., 2007; Mohammad *et al*., 2012; Verla *et al*., 2012). Among the variables of biomass pyrolysis, temperature was identified to have the most significant effect on the characteristics of activated carbons, followed by heating rate and residence time though residence time does not result in significant change in the performance of activated carbon (Ioannidou and Zabaniotou, 2007; Chandra *et al*., 2009; Alicia Peláez-Cid and Margarita, 2012). Physical (gas) activation have been described as thermal decomposition but at elevated temperatures (700-1100 ^{o}C) in the presence of suitable oxidizing gases such as carbon dioxide, steam and/or air (Zanzi *et al*., 2001; Hapazari *et al.*, 2011*;* Fathy *et al*., 2012; Ceyhan *et al*., 2013).

2.3.2 Chemical pretreatment

Chemical pretreatment is usually carried out by impregnation (the addition of a suitable activating agent) of a carbonaceous material (Wong *et al*., 2003; Jimenez *et al*., 2009; Mahmoud *et al*., 2012), followed by heating in the absence of oxygen usually at temperature less than 200^{o}C, and after cooling, the residual impregnating agent is removed by leaching or washing with water (Mohammad-Khan and Ansari, 2009,

Khare, 2011; Gundogdu *et al*., 2013). The impregnation ratio has influence on the characteristics of activated carbons. Therefore, complete saturation is necessary with minimum activating agent consumption (Alicia Peláez-Cid and Margarita, 2012). Thus a balance is maintained between a proper consumption of activating agent and a better elimination of the excess during the leaching or washing process.

The widely used activating agents include sodium hydroxide, calcium hydroxide, hydrochloric acid, sulphuric acid, phosphoric acid, nitric acid, citric acid, formaldehyde, ethylenediamine, sodium carbonate, zinc chloride and potassium hydroxide (Lori *et al*., 2008; Nabais *et al*., 2008; Ngah and Hanafiah, 2008; Fathy *et al*., 2012; Islam *et al*., 2012; Sugumaran *et al*., 2012). Zinc chloride is one of the most effective and common activating agent employed in chemical activation (Yang and Qui, 2011; Gundogdu *et al*., 2013), however Girgis *et al*. (2009); Ucar *et al*. (2009); Somasundaram *et al*. (2013) reported that the introduction of zinc on the surface of activated carbon is restricting or limiting the application of zinc chloride because of its resultant effects such as corrosion and poor recovery. Therefore, preference is on phosphoric acid because of its relative ease in recovery (washing with water) and development of heterogeneous surface (Ucar *et al*., 2009; Zuo *et al*., 2009; Wang *et al*., 2011b). Hence, in spite of its smaller surface area effect, phosphoric acid is the preferred choice in large scale production of activated carbon (Juarez-Galan *et al*., 2009). Phosphoric acid activation at 150-350 ^{o}C has been reported (Zuo *et al*., 2009) to yield predominant microporosity while 350-450 ^{o}C result in predominant mesoporosity. Somasundaram *et al*. (2013) reported that there is little study on the use of phosphoric acid for the production of activated carbon from rice husk.

2.3.3 Combined pretreatment (Two-Step process)

Two-step process involves the application of both thermal and chemical pretreatment in the production of activated carbon which can be carried out in different approaches. One approach involves simultaneous use of thermal and chemical pretreatment on the biomass waste. The process involves the biomass waste being mixed with a suitable impregnating agent and thereafter, subjected to thermal pretreatment (direct pyrolysis or gas activation) to efficiently produce activated carbon (Malik *et al*., 2006; Stavropoulos *et al*., 2008; Cuhadaroglu and Uygun, 2008; Yakout and Sharaf-El-Deen, 2011; Baseri *et al*., 2012; Kwaghger and Ibrahim, 2013). However other approaches include that first, the biomass waste is carbonized via thermal pretreatment process and thereafter, the charred residue obtained is subjected to chemical pretreatment to produce activated carbons (Mohd Din *et al*., 2009; Nhapi *et al*., 2011; Al-Swaidan and Ahmad, 2011; Amuda *et al*., 2012; Dim and Okafor, 2012; Abechi *et al*., 2013). Also, the combination of direct pyrolysis and physical gas activation, by the application of physical gas activation on the biomass waste subsequent to direct pyrolysis successfully produced activated carbon (Zhang *et al*., 2007; Islam *et al*., 2012; Herawan *et al*., 2013; Mukosha *et al*., 2013; Saetea and Tippayawong, 2013).

Table 2.1: Summary of Modification Processes and Variables with their Expected Characteristic

Techniques	Processes	Process Variables	Characteristics
Thermal (Physical)	Direct Pyrolysis	Temperature Heating rate Residence time	Large Surface Area Development of Pores
	Physical (gas) Activation	Temperature Heating rate Residence time Gas Flow Rate	Large Surface Area Development of Pores Introd. of Surface Oxide
Chemical	Impregnation	Impregnation Ratio Nature of Impregnating Agent	Introd. of Functional Groups
Combined (Two-Step)	Impregnation followed by Direct Pyrolysis	Impregnation Ratio Nature of Impregnating Agent Temperature Heating rate Residence time	Introd. of Functional Groups Large Surface Area Development of Pores
	Impregnation followed by Physical (Gas) Activation	Impregnation Ratio Nature of Impregnating Agent Temperature Heating rate Residence time Gas Flow Rate	Introd. of Functional Groups Large Surface Area Development of Pores
	Direct Pyrolysis followed by Impregnation	Temperature Heating rate Residence time Impregnation Ratio Nature of Impregnating Agent	Large Surface Area Development of Pores Introd. of Functional Groups
	Physical (Gas) Activation followed by Impregnation	Temperature Heating rate Residence time Gas Flow Rate Impregnation Ratio Nature of Impregnating Agent	Large Surface Area Development of Pores Introd. of Functional Groups
	Direct Pyrolysis followed by Physical (Gas) Activation	Temperature Heating rate Residence time Gas Flow Rate	Large Surface Area Development of Pores Introd. of Surface Oxide

2.4 Characterization of Activated Carbon

Characteristics of activated carbon determine its efficiency and suitability for subsequent application in adsorption, principal characterization are pore size, surface area, morphology and surface functional groups (Valix *et al*., 2008; Rivera-Utrilla *et al*., 2011).

2.4.1 Pore size

According to Oscar and Stuart (2008); Sadon *et al*. (2012), pore size is one of the characteristics of activated carbon that significantly influences its performance and application in adsorption. They also reported that thermal pretreatment enable the development of pores through removal of moisture and volatile matter from the biomass waste and these pores become sites for entrapment, attachment or useful application in the adsorption process. Ioannidou and Zabaniotou (2007) reported that small pore size will not trap large molecules and large pores may not be able to retain small molecule, whether they are charged, polar molecules or uncharged, non-polar compounds. The pore size of activated carbons may be microporous which is less than 2nm in diameter, mesoporous which is between 2-50 nm in diameter or macroporous which is greater than 50nm in diameter (Aworn *et al*., 2008; Njoku and Hameed, 2011; Herawan *et al*., 2013). According to Inagaki (2009) pores can also be classified on the basis of origin as inter-particle or intra-particle pores and on state as open or closed pores while micropores can be sub-classified on the basis of size into supermicropores (0.7-2 nm) and ultramicropores (<0.7 nm). Agarry and Aremu (2012a) reported that biomass composition has influence on the pore structure of activated carbon. While those with greater content of lignin yield activated carbon with macroporous structure, biomass with higher content of cellulose yield activated carbon with predominantly

microporous structure. Though, attachment or entrapment of solute molecule in adsorption process sometimes occurs in mesopores, it mostly occurs in the micropores, while macropores and mesopores are usually the transport medium to micropores. Hence, micropores have the greatest significance on the performance of activated carbon.

2.4.2 Surface area

Surface area is also one of the characteristics of activated carbon that has great influence on its performance. Increase in surface area of activated carbon relative to the parent biomass waste is another significant outcome of thermal pretreatment but according to Gundogdu *et al*. (2013) chemical pretreatment also leads to improvement in surface area. According to Tay *et al*. (2009); Nhapi *et al*. (2011), commercial activated carbons possesses surface areas in the range of 300-2000 m^2/g. Gayatri and Ahmaruzzaman (2010) reported that the larger the surface area, the better the performance of activated carbon and that while the pores of activated carbon dictate the size of molecule of a substance that can be adsorbed, the surface area limits the amount of the substance that can be adsorbed.

2.4.3 Morphology

Morphology of activated carbon is characterized by its pore structure and enables the classification of activated carbon as having homogeneous or heterogeneous surfaces (Gayatri and Ahmaruzzaman, 2010).

2.4.4 Surface functional group

Surface functional groups are characteristics of activated carbon that mainly result from chemical pretreatment as the type of impregnating agent employed determines the nature of the functional group retained on the surface of the activated carbon. Though introduction of functional groups can also be achieved through physical gas activation, this is specific to surface oxides only. The specific functional group on the surface of activated carbon can change or significantly improve the performance of activated carbon (Bhatnagar and Minocha, 2006). Surface functional groups induce special surface reactivity that makes activated carbon to develop special affinity towards particular substances or for application (Ahmad *et al*., 2013). Functional groups such as carboxyl group, phenolic groups, lactonic groups, carbonyl groups and amino groups contain heteroatom (oxygen, nitrogen, hydrogen, phosphorus, sulphur, halogen) bonded to the edges of the carbon layer and governs the surface chemistry of the activated carbon. Among these, the oxygen-containing functional groups (surface oxides) are the most commonly formed and have the most significant influence (Li, 2012; Bhatnagar *et al*., 2013).

2.5 Application of Activated Carbons

Activated carbons are materials widely used in water and wastewater treatment, in the removal of toxic substances such as insecticides, herbicides, chlorinated hydrocarbons, organic compounds, heavy metal ions, dyes and phenols (Bhatnagar and Minocha, 2006; Ioannidou and Zabaniotou, 2007). They are also used in solution purification for the removal of taste, color, odors and other objectionable impurities from water and wastewater (Ceyhan *et al*., 2013). As filter materials in air cleaning filters, they remove gases and vapors such as motor vehicles exhaust control and in cigarette filters to

adsorb some of the harmful components of tobacco (Mohammad-Khan and Ansari, 2009; Al-Swaidan and Ahmad, 2011).

In chemical, food and pharmaceutical industries, activated carbons have been used for the purification of products. They have also been used to remove color and other impurities such as those causing foaming or retarding crystallization from sugar (Mohammad-Khan and Ansari, 2009). They are also used for the separation, purification, decolorization and deodorization of vegetable oils and fats (Al-Swaidan and Ahmad, 2011). Due to their higher surface area and larger pore volume, activated carbons are also being used as catalyst and catalyst supports, electronic material and energy storage material (Ioannidou and Zabaniotou, 2007; Shen *et al*., 2008; Dolas *et al*., 2011). In electroplating bath, activated carbon have been identified to be capable of removing impurities and to recover valuable substances from waste streams (Mohammad-Khan and Ansari, 2009).

2.6 Application of Activated Carbons in Removal of Inorganic Contaminants

Heavy Metals: Heavy metals are generally considered a threat to man and the environment because of their potentially high toxicity (Ocholi, 2012). Industrial wastewaters from metal plating, mining activities, smelting, battery manufacture, tanneries, petroleum refining, paint manufacture, pesticides, pigment manufacture, printing and photographic industries contain significant quantities of heavy metals (Demibras *et al*., 2004; Ngah and Hanafiah, 2008; Thamilarasu *et al*., 2012). Chromium, cadmium and lead are considered the most common hazardous heavy metals found in wastewaters of several industries. According to Moreno-Virgen *et al*. (2012), adsorption onto activated carbons has been considered as an efficient method for the removal of these heavy metals from wastewater.

Dyes: Typical dyes used in industrial processes include acid, basic, direct, disperse, reactive, sulphur and metallic dyes (Achmad *et al*., 2012). It has been estimated that about 7 x 10^5 tons of dyes are generated annually worldwide by several industrial activities of which 10-15% is lost in industrial effluents during manufacture and processing operations (Demibras, 2009; Rangabhashiyam *et al*., 2013; Suteu and Malutan, 2013). According to Dharmendirakumar *et al*. (2012), synthetic dyes used by many industries such as dyestuffs, textile, paper, leather, foodstuffs, cosmetic, rubber and plastics along with large amount of water, generate substantial amount of wastewater as effluent. Water pollution by dyes is a major environmental problem because these pollutants are toxic and may be carcinogenic. Dyes can affect the physical and chemical properties of water and the aquatic flora and fauna, making wastewater discharged to be a serious problem due to aesthetics and health disorder as well as light penetration and biodegradation (Albanis *et al*., 2000; Hema and Arivoli, 2007; Santhi *et al*., 2010; Awala and El-Jamal, 2011). In general, dyes are usually resistant to classical biodegradation and the adsorption process is an effective treatment method for their removal (Moreno-Virgen *et al.*, 2012).

2.7 Mode of Operation of Adsorption Process

2.7.1 Batch mode

Batch adsorption experimentation is usually a prelude to the column experiments and it provides basic information on the nature of adsorbent, pattern, mechanism and thermodynamic of the adsorption process. Additionally, batch adsorptions are easy to use in the laboratory but are not economical in actual or large scale application (Kalavathy *et al*., 2010).

2.7.2 Column mode

Adsorption equilibrium data are usually obtained from batch experiments while continuous fixed bed column adsorption gives higher yield and valuable data for scale up (Soto *et al*., 2011). The column mode allows a fixed amount of adsorbent to be continuously contacted with fresh adsorbate solution till bed saturation. This enables the attainment of the actual adsorption performance which is difficult to obtain under batch mode (Dwivedi *et al*., 2008). Column adsorption also provides information on the breakthrough characteristics (Song *et al*., 2011) and it can be operated in different forms including packed bed, fluidized bed and moving bed. Among these, the moving bed is difficult to maintain in industrial settings especially for large flow. The two main bed choices are fixed bed and fluidized bed. Fixed bed has comparative advantage which includes little operator attention, ease in inspection and operation, and fewer instances of adsorbent particles in the effluent. Hence, its informed preference for industrial application (Dwivedi *et al*., 2008; Butland, 2008).

2.8 Batch Experimental Data Analysis

2.8.1 Adsorption capacity and removal efficiency

A. Adsorption Capacity at Equilibrium

Adsorption capacity at equilibrium is the maximum amount of solute that can be adsorbed by a unit mass of an adsorbent. Kumar and Kirthika (2009) mathematically expressed this as in equ (2.1):

$$q_e = \frac{(C_o - C_e)\,V}{m} \tag{2.1}$$

Where

q_e = adsorption capacity at equilibrium (mg/g)

C_o = initial concentration of solute (mg/L)

C_e = equilibrium concentration of solute (mg/L)

V = volume of solution (L)

m = mass of adsorbent used (g)

B. Adsorption Capacity at Time 't'

Adsorption capacity at any time *t* is the amount of solute adsorbed by a unit mass of an adsorbent at that time. According to Hameed *et al.* (2008), this is mathematically represented as in equ (2.2):

$$q_t = \frac{(C_o - C_t)\,V}{m} \tag{2.2}$$

Where

q_t = adsorption capacity at time *t* (mg/g)

C_o = initial concentration of solute (mg/L)

C_t = final concentration of solute at time *t* (mg/L)

V = volume of solution (L)

m = mass of adsorbent used (g)

C. Adsorption Removal Efficiency

According to Al-Anber and Mohammed (2008) this can be mathematically represented as in equ (2.3):

$$RE = \frac{(C_o - C_e)}{C_o} \times 100 \tag{2.3}$$

Where

RE = removal efficiency

C_o = initial concentration of solute (mg/L)

C_e = final concentration of solute (mg/L)

2.8.2 Adsorption equilibrium isotherms

Demibras (2008); Hameed and Foo (2010) reported that adsorption equilibrium is attained when a solute containing phase has been contacted with the adsorbent for sufficient time with the solute concentration in the bulk solution in a dynamic balance with the interface concentration. The state of equilibrium is attained when the sorbed solute tends to desorb into the solution. Equal amounts of solute eventually are being adsorbed and desorbed simultaneously to consequently result in the rates of adsorption and desorption attaining an equilibrium state (Basonde, 2002). In general, adsorption isotherm is a relationship between the amount of solute adsorbed and the remaining in solution at a constant temperature and pH (Gayatri and Ahmaruzzaman, 2010). It is a curve describing the process governing the retention, release or mobility of a solute from solution to a solid surface (Hameed and Foo, 2010). An adsorption isotherm is characterized by certain constant values that express the surface properties and affinity of the adsorbent (Khare, 2011), therefore application of several isotherm models involves not only finding the best fit for experimental data but knowlegde of important information that can be deduced from the estimated parameters such as adsorption patterns and surface property (Gayatri and Ahmaruzzaman, 2010; Mohd-Din *et al*., 2009). Application of isotherm models requires conducting batch adsorption experiments with agitation at constant temperature and volume of solution and either varying the mass of the adsorbent or the concentration of the solute for a predetermined time sufficient enough to reach equilibrium (Gayatri and Ahmaruzzaman, 2010). Isotherm analysis of experimental data is important in order to develop an equation that accurately represents the data and which could be used for design purposes (Mahvi *et al*., 2004)

A. Langmuir Isotherm

Langmuir adsorption isotherm, originally developed by Irving Langmuir in 1916 to describe the dependence of the surface coverage of an adsorbed gas on the pressure of the gas above the surface at a fixed temperature (Patel, 2005), has traditionally been used to quantify and contrast the performance of different bio-sorbents (Hameed and Foo, 2010). It was reported to be the most popular model due to its good agreements with sorption experimental data (Khare, 2011). According to Khare (2011); Basonde (2002), Langmuir isotherm is based on assumptions among which are:

(i) The molecules are adsorbed on definite sites on the surface of the adsorbent.

(ii) At maximum adsorption, only a monolayer is formed: molecules of adsorbate do not deposit on already adsorbed molecules, but only on the free surface of the adsorbent, that is each site can accommodate only one molecule.

(iii) The area of each site is a fixed quantity determined solely by the geometry of the surface, and the adsorption energy is the same at all sites (uniform distribution of energy). In addition, the adsorbed molecules cannot migrate across the surface or interact with neighboring molecules.

(iv) The surface of the adsorbent is uniform (homogenous) that is all the adsorption sites are equivalent.

(v) All adsorption occurs through the same mechanism.

Mahmoud *et al.* (2012) reported that Langmuir isotherm can be mathematically represented as in equ (2.4):

$$q_e = \frac{Q_m b C_e}{1 + b C_e} \quad (2.4)$$

Linearizing equ (2.4) gives equ (2.5):

$$\frac{C_e}{q_e} = \frac{1}{b Q_m} + \frac{C_e}{Q_m} \quad (2.5)$$

Where

q_e = adsorption capacity at equilibrium (mg/g)

C_e = equilibrium concentration of solute (mg/L)

Q_m = maximum monolayer adsorption capacity (mg/g)

b = Langmuir isotherm constant (dm^3/mg)

B. Freundlich Isotherm

Freundlich isotherm was the earliest known relationship describing the non-ideal and reversible adsorption and also not restricted to the formation of monolayer (Soto *et al*., 2011). The empirical model had been reported to apply to multilayer adsorption (Hameed and Foo, 2010) with interaction between adsorbed molecules (Gayatri and Ahmaruzzaman, 2010). It is reported to be most widely used and is applicable to adsorption on heterogeneous surfaces (Khare, 2011) but based on the assumption that the adsorption occurs on heterogeneous sites with non-uniform distribution of energy of adsorption over surfaces (Mohd-Din *et al*., 2009; Gullipali *et al*., 2011). The slope of the plot (1/n) is a measure of adsorption intensity or surface heterogeneity, becoming more heterogeneous as its value gets closer to zero (Hameed and Foo, 2010). If the value of 1/n is equal to unity, the adsorption is linear; if the value is below unity, the adsorption process is chemical; and if the value is above unity, the adsorption is a favourable physical process (Gayatri and Ahmaruzzaman, 2010).

Mathematically expressed, Freundlich isotherm is as in equ (2.6) (Kadhim and Al Seroury, 2012; Albadarin *et al*., 2013):

$$q_e = K_f\, C_e^{1/n} \tag{2.6}$$

On linearization, equ (2.6) becomes equ (2.7):

$$\log q_e = \log K_f + \frac{1}{n} \log C_e \tag{2.7}$$

Where

q_e = adsorption capacity at equilibrium (mg/g)

C_e = equilibrium concentration of solute (mg/L)

K_f = Freundlich isotherm constant (mg/g)

n = adsorption intensity

2.8.3 Adsorption kinetic models

According to Pan *et al.* (2009) adsorption kinetics gives information about the performance and mechanism of a process where its analysis establishes or predicts the solute (adsorbent) uptake rate that determines the residence time required for the completion of the adsorption process. The predicted kinetics is important for the design of an adsorption system and the kinetic parameters are helpful for predicting rate of adsorption while also providing important information for designing and modeling a process (Alzaydien and Waleed, 2009).

A. Pseudo-First-Order Rate Equation

Pseudo-first-order rate equation is also known as Lagergren's first order rate equation which describe the kinetic process of liquid-solid phase adsorption based on its adsorption capacity. Recently, this equation has been widely used to describe the adsorption of pollutants from wastewater in different fields (Pan *et al.*, 2009).

As reported by Ho (2004), Pseudo-first-order kinetic model can be mathematically expressed as in equ (2.8):

$$\frac{dq_t}{dt} = k_1(q_e - q_t) \quad (2.8)$$

Integrating the equation with the boundary conditions of $q_t = 0$ at $t = 0$ and $q_t = q_t$ at $t = t$, and on linearization, equ (2.8) is transformed to equ (2.9):

$$\log(q_e - q_t) = \log q_e - \frac{k_1}{2.303} t \quad (2.9)$$

Where

q_t = adsorption capacity at time t (mg/g)

q_e = adsorption capacity at equilibrium (mg/g)

t = time (min)

k_1 = kinetic rate constant (min^{-1})

B. Pseudo-Second-Order Kinetic Model

Pseudo-second-order rate model is also known as Ho's second-order rate equation which described the kinetic process of the adsorption of divalent metal ions onto peat as chemical bonding between divalent metal ions and polar functional groups on peat as being responsible for the cation-exchange capacity of the peat. Among the assumptions were that the adsorption may be second-order, and that the rate limiting step may be chemical adsorption involving valent forces through sharing or the exchange of electrons between the peat and divalent metal ions (Pan *et al*., 2009).

Similarly, this model is mathematically expressed as in equ (2.10) (Ho *et al*., 2010):

$$\frac{dq_t}{dt} = k_2(q_e - q_t)^2 \quad (2.10)$$

Integrating the above equation with the boundary conditions of $q_t = 0$ at $t = 0$ and $q_t = q_t$ at $t = t$, and on linearization, equ (2.10) transformed to equ (2.11):

$$\frac{t}{q_t} = \frac{1}{k_2 q_e^2} + \frac{1}{q_e} t \quad (2.11)$$

Where

q_t = adsorption capacity at time *t* (mg/g)

q_e = adsorption capacity at equilibrium (mg/g)

t = time (min)

k_2 = kinetic rate constant (g mg^{-1} min^{-1})

C. Intra-particle Diffusion Model

Gullipali *et al*. (2011) reported that adsorption process may be controlled by one or more steps. These include film or external diffusion, surface diffusion, and pore diffusion (Shih, 2012; Suteu and Malutan, 2013). Surface and pore diffusion are also known as intra-particle diffusion (Maximova and Koumanova, 2008). Among the three steps, the last step is considered to have negligible effect on the kinetics as it is assumed to be rapid. The rate of adsorption is controlled by either external or intra-particle diffusion depending on the step that is slow, that is rate limiting or controlling. If the plot satisfies a linear relationship with experimental data and passes through the origin, then intra-particle diffusion is the sole rate-limiting, if not then two or more steps control the rate of adsorption (Shih, 2012).

According to Nadeem *et al*. (2006), Intra-particle diffusion model can be written as in equ (2.12):

$$q_t = k_{id} t^{1/2} + I \quad (2.12)$$

Where

q_t = adsorption capacity at time *t* (mg/g)

t = time (min)

k_{id} = Intra-particle diffusion rate constant (mg/gmin$^{1/2}$)

I = boundary layer constant (mg/g)

2.8.4 Adsorption thermodynamics

Zawani *et al.* (2009) highlighted that thermodynamic parameters such as change in standard free energy (ΔGº), enthalpy (ΔHº) and entropy (ΔSº) are interrelated based on equ (2.13) and equ (2.14):

$$\Delta G° = -RT \ln K_c \tag{2.13}$$

While $\Delta G° = \Delta H° - T\Delta S°$ (2.14)

But equ (2.13) and equ (2.14) can be rationalized to obtain equ (2.15):

$$\ln K_c = \frac{\Delta S°}{R} - \frac{\Delta H°}{RT} \tag{2.15}$$

Where

K_c = thermodynamic equilibrium constant L/g (but $K_c = \frac{q_e}{C_e}$)

q_e = adsorption capacity at equilibrium (mg/g)

C_e = equilibrium concentration of solute (mg/L)

T = absolute temperature (K)

R = gas constant (8.314 J/mol K)

However, Foo and Hameed (2009) reported that ΔG° is the fundamental criterion to determine if a process is feasible or occurs spontaneously as at a given temperature, adsorption is considered to be feasible or spontaneous if the ΔG° has a negative value. Though weak positive values indicate that a process is non-spontaneous but feasible and weaker values at lower temperatures imply that adsorption is favored at lower temperatures. Gueu *et al*. (2007); Soto *et al*. (2011) reported that if ΔH° is positive, the

process is endothermic and if it is negative, the process is exothermic, while positive ΔS° indicates a random organization of the solute at the adsorbent/solution interface.

2.9 Column Experimental Data Analysis

2.9.1 Breakthrough curve

The performance of column adsorption is described through the concept of the breakthrough curve analysis as the time to reach the breakthrough point and shape of the breakthrough curve are necessary characteristics that determine the operation and dynamic response of the column adsorption (Sugashini and Meera, 2013). The breakthrough curve is usually expressed in terms of normalized concentration defined as the ratio of effluent concentration to inlet concentration $\frac{C_e}{C_o}$ which is a function of time or volume of effluent for a given bed height. Successful design of a column adsorption process requires prediction of the concentration–time profile or breakthrough curve for the effluent (Ozturk and Kavak, 2005).

2.9.2 Column models

A. Bed Depth Service Time (BDST) Model

This model which is based on Adam-Bohrat equation is widely employed in column experimental data analysis. The equation is based on surface reaction rate theory and assumes that equilibrium is not instantaneous (Kumar and Bandyopadhyay, 2005; Chowdhury *et al*., 2013). The equation is expressed as in equ (2.16):

$$\ln\left(\frac{C_o}{C_e}-1\right)=\ln\left(e^{k_a N_o {}^{Z}/_{F}}-1\right)-k_a C_o t \qquad (2.16)$$

Where

K_a = adsorption rate constant (L mg^{-1} min^{-1})

F = linear flow velocity to bed (m/min)

C_e = effluent concentration of solute at breakthrough (mg/L)

C_o = influent concentration of solute (mg/L)

N_o = adsorption capacity (mg/L)

Z= bed depth (m)

t = time (min)

But $e^{k_a N_o Z/F}$ is usually greater than one, this simplifies equ (2.16) to equ (2.17):

$$\ln\left(\frac{C_o}{C_e}-1\right)=\ln e^{k_a N_o Z/F}-k_a C_o t \tag{2.17}$$

Linearization of equ (2.17) gives equ (2.18):

$$t=\frac{N_o}{C_o F}Z-\frac{1}{C_o k_a}\ln\left(\frac{C_o}{C_e}-1\right) \tag{2.18}$$

B. Thomas Model

Thomas model is one of the common models used in describing the performance of a column adsorption process which is based on the assumption that the rate driving force obeys pseudo-second order reversible kinetics (Zhang *et al*., 2011b; Nwanbunne and Igbokwe, 2012). The model is mathematically expressed as in equ (2.19):

$$\frac{C_e}{C_o}=\frac{1}{1+exp\left[\frac{K_{Th}q_o M}{Q}-K_{Th}C_o t\right]} \tag{2.19}$$

Where

K_{Th} = Thomas rate constant (L/(min mg)) and

Q = volumetric flow rate (L/min).

$C_e\ and\ C_o$ = effluent and influent solute concentration (mg/L)

q_o = maximum adsorption capacity (mg/g)

M= mass of the adsorbent (g)

t = time (min)

The linearization of equ (2.19) results in equ (2.20):

$$\ln\left(\frac{C_o}{C_e}-1\right)=\frac{K_{Th}q_oM}{Q}-K_{Th}C_ot \qquad (2.20)$$

C. Yoon Nelson Model

According to Ozturk and Kavak (2005), Yoon-Nelson model is a simple model that is relatively less complicated because it does not need detailed data about the adsorbent and adsorbate. The model equation is represented as in equ (2.21):

$$\frac{C_e}{C_o}=\frac{1}{1+exp[k(\tau-t)]} \qquad (2.21)$$

Where

K_{YN} = Yoon Nelson rate constant

C_e = effluent concentration of solute at breakthrough (mg/L)

C_o = influent concentration of solute (mg/L)

τ = breakthrough time at 50% (min)

t = time (min)

On linearization, equ (2.21) transformed to equ (2.22):

$$\ln\left(\frac{C_e}{C_o-C_e}\right)=k_{YN}t-k_{YN}\tau \qquad (2.22)$$

2.10 Response Surface Methodology

In the conventional methods, experiments are carried out varying systematically the studied parameters and keeping constant the others. This is repeated for all the influencing parameters, resulting in an unreliable and large number of experiments which would be very expensive and time consuming, and this approach does not also show the combined effect of factors on the dependent variable (Singh *et al*., 2011a; Sivarajasekar and Baskar, 2013). But nowadays, commonly used experimental design

technique for process analysis and modeling is response surface methodology (RSM) with the main objective of optimizing the response surface that is influenced by various process parameters. It also quantifies the relationship between the controllable input parameters and the obtained response surfaces (Kwak, 2005, Ahmad and Alrozi, 2010).

Response Surface Methodology (RSM) is a collection of mathematical and statistical techniques for modeling and analysis of problems involving multivariate experimental design, statistical modeling and process optimization (Gratuito *et al*., 2008; Singh *et al*., 2010; Xin-hui *et al*., 2012; Roosta *et al*., 2014). As reported, the application of statistical experimental design techniques in the development of the adsorption process can result in reduced process variability combined with the requirement of less resources (time, reagents and experimental work) (Khataee, 2010; Anupam *et al*., 2011; Singh *et al*., 2011b).

Using RSM, it is possible to estimate linear interaction and quadratic effects of the factors and a prediction model for the response. The RSM has several classes of designs, with central composite design, box-behnken design and three-level factorial design being the most widely used and the experimental run required are dependent on the chosen design (Khataee, 2009; Ahmad *et al*., 2009). These are different in the number of runs required and in the combinations of the levels used in the experiments. The central composite design gives almost as much information as a multilevel factorial and has been shown to be sufficient to describe the majority of steady-state process responses (Obeng *et al.*, 2005).

2.11 Review of Batch adsorption

Table 2.2 presents a review of related literature on batch adsorption of phenol onto rice husk activated carbon. Application of other adsorbents in batch adsorption processes as well as removal of other adsorbates such dyes and heavy metals from solution were also reviewed as presented in the table.

2.12 Review of Column Adsorption

Related literature on column adsorption from simulated or real refinery wastewater using rice husk activated carbon were reviwed as presented in Table 2.3. The table also presents application of other adsorbents in column adsorption of phenol and other adsorbates from simulated or real refinery wastewater.

2.13 Review of Activated Carbon Production

Table 2.4 presents a review of related literatue on the processes employed in production of activated carbon from of rice husk and other waste materials.

Table 2.2: Review of Batch Adsorption Processes

Adsorbent Adsorbate	Modification Techniques	Dosage (g)	Initial Conc. (mg/l)	Opti-mum pH	Equil. Contact time (min)	Adsorption Capacity (mg/g)	Isotherm model Kinetic model Thermodynamic model	Reference
Rice Husk Phenol	-Carbonization at 400-600^{o}C	1-10	10-1000	4	240	0.98 - 46.19	Freundlich	Daffalla *et al.* (n.d)
Rice husk Phenol	-H_2SO_4 activation -Carbonization at 850-900^{o}C			5.1	6h	75.15 (q_m)	-	Srihari and Das (2008)
Rice Husk Phenol	-Carbonization at 400^{o}C -H_3PO_4 activation -Heating at 700-900^{o}C			2.5	75	2.35x10^{-4}mol/g	Freundlich Second order Exothermic	Kennedy *et al.* (2007)
Rice Husk Phenol	-Carbonization at 600^{o}C -NaOH activation - Heating at 600-900^{o}C		1000			544.8	Freundlich Second order	Song *et al*. (2013)
Rice Husk Phenol	-$ZnCl_2$ activation -Carbonization at 700^{o}C	0.03-0.18	10 ppm		240	27.58		Kalderis *et al*. (2008b)
Rice Husk Phenol	-Carbonization at 400^{o}C			7	180	0.886 (q_{exp})	Freundlich First order	Mahvi *et al*. (2004)
Rice Husk Phenol	-Carbonization at 300-500^{o}C	1-10	10-300	4	300	0.951 - 1(q_{exp})	Freundlich	Kermani *et al*. (2006)
Rice Husk Phenol	-		10- 70	8		1.23 (q_m)	Langmuir First order	SivaSubramanian *et al*. (2012)

Table 2.2: Review of Batch Adsorption Processes *(Cont'n)*

Adsorbent Adsorbate	Modification Techniques	Dosage (g)	Initial Conc. (mg/l)	Opti-mum pH	Equil. Contact time (min)	Adsorption Capacity (mg/g)	Isotherm model Kinetic model Thermodynamic model	Reference
Rice Husk Cr (VI)	-Formaldehyde activation	4-20 g/l	10-70	2	120	1.77 - 9.5 (q_{exp})	Freundlich	Basal *et al*. (2009)
Rice Husk Cd (II)	-NaOH activation			6.5		126 (q_m)	Langmuir	Ye *et al*. (2010)
Rice husk Cu (II)	-Carbonization at 700^oC -H_2O activation at 750^oC			5		15.78 (q_{exp})	Langmuir Second-order Exothermic	Zhang *et al*. (2011a)
Rice Husk Zn (II)	- H_2SO_4 activation					19.38 (q_m)	Langmuir Second-order	El Shafey (2010)
Rice Husk Ash Cd (II)	-			6	120	0.91 - 2.88 (q_{exp})		Srivastava *et al*. (2008)
Rice Husk Ash Pb (II)	-	1-30	3-100	5	60	91.74 (q_m)	Freundlich Second-order Exothermic	Naiya *et al*. (2009)
Rice Husk Ash α-Picoline	-			6.5	7h	15.46 (q_{exp})	Endothermic	Lataye *et al*. (2009)
Rice husk Crystal Violet	-NaOH activation			8	90	44.87 (q_m)	Second-order Exothermic	Chakrabort y *et al*. (2011)

Table 2.2: Review of Batch Adsorption Processes *(Cont'n)*

Adsorbent Adsorbate	Modification Techniques	Dosage (g)	Initial Conc. (mg/l)	Opti-mum pH	Equil. Contact time (min)	Adsorption Capacity (mg/g)	Isotherm model Kinetic model Thermodynamic model	Reference
Rice Husk Methylene Blue Dye	- Carbonization at 700^{o}C -NaOH activation -Heating at 800^{o}C				30	389.5 (q_{exp})	Langmuir Second-order Endothermic	Li *et al*. (2013)
Rice Husk Methylene Blue Dye	-NaOH activation - H_2SO_4 activation -Heating at 800^{o}C -H_3PO_4 activatn (500^{o}C)				60	578 (q_m)	Langmuir Second-order	Chen *et al*. (2013)
Oil Palm Bunch Phenol	- Carbonization at 600-900^{o}C -CO_2 activation	10g/l	50	6	15	1.02 - 4.81		Alam *et al*. (2009)
Rapeseed / Kenaf Phenol	-Carbonization at 400^{o}C -CO_2 activation at 700^{o}C					50-80 (q_{exp})		Nabais *et al*. (2009)
Date Pit Phenol	-Gas activation (Petroleum Refinery Wastewater)		46-88	8.2	60	56.9 (q_m)	Langmuir Second-order Exothermic	El Naas *et al*. (2010)
Coconut Shell Phenol	-H_2SO_4 activation -Carbonization at 200-800^{o}C					0.53 mmol/g (q_m)	Second-order Endothermic	Singh *et al*. (2008)
Coconut Shell Phenol	- Carbonization at 700^{o}C -KOH activation -CO_2 activatn at 800^{o}C	0.2	100-500		300	205.8 (q_m)	Second-order	Mohd-Din *et al*. (2009)
Rattan Sawdust Phenol	- Carbonization at 700^{o}C -KOH activation -CO_2 activatn at 800^{o}C				240	149.25 (q_m)	Langmuir Second-order	Hameed and Rahman (2008)

Table 2.2: Review of Batch Adsorption Processes *(Cont'n)*

Adsorbent Adsorbate	Modification Techniques	Dosage (g)	Initial Conc. (mg/l)	Opti-mum pH	Equil. Contact time (min)	Adsorption Capacity (mg/g)	Isotherm model Kinetic model Thermodynamic model	Reference
Hazelnut Shell Cu/Pb	-$ZnCl_2$ activation - Carbonization at 700^oC -HCl acid treatment			6.7	60	6 - 13 (q_m)		Imamoglu and Tekir (2008)
Olive Cake Tannery Dye	- H_3PO_4 activation				120h	146.3 (q_m)	Second-order Endothermic	Baccar *et al*. 92013)
Sugar cane Bagasse Ni (II)	- Carbonization at 400^oC -H_2O activation at 600^oC			6.5	240	140.8 (q_m)	First-order	Krishnan *et al*. (2011)
Hazelnut Shell Cu (II)	-H_2SO_4 activation			6	90	58.27 (q_m)	Langmuir Second-order	Demibras *et al*. (2009)
Coconut Husk Basic Dye	- Carbonization at 700^oC -KOH activation -CO_2 activatn at 850^oC					434.78 (q_m)	Langmuir Second-order Exothermic	Tan *et al*. (2008a)
BASS & CON Shell Pb(II)/ Cd(II)	- H_3PO_4 activation - Carbonization at 500^oC	0.5-2.5	2.5-20		150	10.20 - 25.8 (q_m)	Second-order	Osakwe (2011)
Powdered Corn Cob Pb (II)	-	0.3-1.2			18h	0.141(q_m)		Adie *et al*. (2010)
Powdered Corn Cob Cd (II)	-			7.37-11.2	8-10h		Second-order	Ismail *et al*. (2009)

Table 2.3: Review of Column Adsorption Processes

Adsorbent Adsorbate	Type of Wastewater	Internal Diameter (cm)	Column Length (cm)	Carbon Depth (cm)	Initial Conc. (mg/l)	Flow Rate (ml/min)	Breakthrough /Exhaustion Capacity (mg/g)	Reference
Rice Husk Congo Red Dye	Simulated	1.2	50	12-30	18-42	3.6-5.6	2.47-3.08 (q_{Thomas})	Han *et al*. (2008)
Rice Husk Cu (II)	Simulated	3	30	3-9	10-50	5-15	1.4-6.33 ($q_{0.1}$)	Luo *et al*. (2011)
Rice Husk Cd (II)	Simulated	2	55	10-30	10-20	5-15		Kumar and Bandyopadh-yay (2005)
Rice Husk Cr (IV)	Simulated	1.5	40	15-25	100-300	25-50	1731-2535 (q_{Thomas})	Sugashini and Meera (2013)
Rice Husk Methylene Blue	Simulated	1.5	50	8.4-39	35-100	3.4-8.2	3.23-6.63 (q_{Thomas})	Han *et al*. (2006)
Rice Husk Cu (II)	Simulated	1.2	19.5	3-8	5-15	10-30	34.56	Nasehir-Khan *et al*. (2011)
Sugar Cane Bagasse Phenol	Simulated	3	55	16-32	20	33.3	12.02-12.34 ($q_{0.9}$)	Karunarathne and Amarasinghe (2013)
Date Stone Phenol	Simulated	1.1	50	5-25	50-150 ppm	23-141		Alhamed (2009)

Table 2.3: Review of Column Adsorption Processes *(Cont'n)*

Adsorbent Adsorbate	Type of Wastewater	Internal Diameter (cm)	Column Length (cm)	Carbon Depth (cm)	Initial Conc. (mg/l)	Flow Rate (ml/min)	Breakthrough /Exhaustion Capacity (mg/g)	Reference
Pecan nut Shell Anionic Dye	Simulated	2.5	13	8	100	3	0.011-0.168 (q_{Thomas})	Aguayo-Villarreal *et al*. (2013)
Coconut Shell Pb (II)	Simulated	4		60	20-60	4-16 m/h	0.754-2.01 ($q_{0.5}$)	Dwivedi *et al*. (2008)
Peanut Husk	Simulated	2	43	1.5-5.4	50-100	1.8-5.4	6.23-15.23 ($q_{0.5}$)	Noreen *et al*. (2013)
Oil Palm Shell Trichloro-phenol	Simulated	1.2	19.5	1.5-3	25-50	15-20	5.31-9.05 ($q_{0.9}$)	Tan *et al*. (2009)
Peanut Husk Methylene Blue	Simulated	1	25	6-10.5	40-80	7.5-10	41-75 (q_{Thomas})	Song *et al*. (2011)
Wheat Straw Methylene Blue	Simulated	1.28	20	2.6-10.5	1,400	0.65-1.92	66-288.8 (q_{exp})	Zhang *et al*. (2011b)
Peanut Husk Indosol Yellow Dye	Simulated	2	43	2-4	50-100	1.8-5.4	15.6-25.92 (q_{Thomas})	Sadaf and Bhatt (2013)

Table 2.4: Review of Activated Carbon Production Processes

Precausor	Modification Process	Surface Area (m^2/g)	Pore Diameter (nm)	Pore Volume (cm^3/g)	References
Rice Husk	-NaOH activation	116	65.1		Chakraborty *et al.* (2011)
Rice Husk	-Carbonization at 400^oC	50.14	14.49	0.182	Mahvi *et al.* (2004)
Rice Husk	-H_3PO_4 activation -Carbonization at 300-600^oC	634-1820	1.3-11	0.63-2.01	Li *et al.* (2011b)
Rice Husk	-Carbonization at 400oC -H_3PO_4 activation -Heating at 700-900^oC	180-298	1.6-2.5	0.08-0.1 (micro)	Somasundaram *et al.* (2013)
Rice Husk	-$H_3PO_4/ZnCl_2$ activation -Carbonization at 400-700^oC -HCl acid washing	292-2434	2.06-3.02	0.116-0.59 (micro)	Liou and Wu (2009)
Rice Husk	-H_3PO_4/NaOH activation -CO_2 activation at 400-800^oC	9-91			Kalderis *et al.* (2008a)
Rice Husk	-Carbonization at 600-700^oC -CO_2 activation at 600-700^oC	162-166			Kalderis *et al.* (2008a)
Rice Husk	-Carbonization at 500-550^oC	44.7-139.7			Liu *et al.* (2011)

Table 2.4: Review of Activated Carbon Production Processes *(Cont'n)*

Precausor	Modification Process	Surface Area (m^2/g)	Pore Diameter (nm)	Pore Volume (cm^3/g)	References
Rice Straw	-KOH activation -Carbonization at 800^oC	420-866	0.66-0.9	0.15-0.32 (micro)	Basta *et al*. (2009)
Rice Straw	-Carbonization at 800^oC -KOH activation -Heating at 800^oC	1393-1917	0.84-1.14	0.53-0.73 (micro)	Basta *et al*. (2009)
Rice Husk	-Carbonization at 400^oC -H_3PO_4 activation -Heating at 700-900^oC	344.7-438.9	0.111-0.118	3.5-3.8 (micro)	Kennedy *et al*. (2007)
Rice Husk	-Carbonization at 600^oC -NaOH activation -Heating at 600-900^oC	1745-2841	1.07-1.4	0.59-0.85 (micro)	Song *et al*., 2013
Rice Husk	-Carbonization at 500-700^oC -H_2O activation at 550-750^oC	147-244		0.0566-0.1 (micro)	Zhang *et al*. (2011a)
Rice Husk	-H_2SO_4 activation -Carbonization at 200-800^oC	17		0.006 (micro)	Mohan *et al*. (2008)
Rice Husk	-Carbonization at 400^oC -CO_2 activation at 800-900^oC	227-334	1.22-1.4	0.157-0.212	Kumagai *et al*. (2009)
Rice Husk	-Carbonization at 600-800^oC -H_2O activation at 650-850^oC	168.8-231.7			Zhu *et al*. (2012)

Table 2.4: Review of Activated Carbon Production Processes *(Cont'n)*

Precausor	Modification Process	Surface Area (m^2/g)	Pore Diameter (nm)	Pore Volume (cm^3/g)	References
Rice Husk	-Carbonization at 300-500^oC	20.26-50.14	4.2-15.16	0.042-0.182	Kermani *et al*. (2006)
Coconut Shell	-H_2SO_4 activation -Carbonization at 200-800^oC	380		0.12	Singh *et al*. (2008)
Rice Husk Ash	-Carbonization at 300-800^oC -H_2O/ CO_2 activation 800^oC	39-74	2.89-3.14	0.0173-0.0326	Aworn *et al*. (2008)
Soyabean Oil Cake	-KOH activation -Carbonization at 600-800^oC	600-618.5	0.941-0.998	0.143-0.213	Tay *et al*. (2009)
Corn cob	-Carbonization at 500^oC -KOH activation -Carbonization at 500-700^oC	105-1320			Bagheri and Abedi (2009)
Durian Shell	-KOH activation -Carbonization at 673-923K	467-992		0.13-0.368 (micro)	Chandra *et al*. (2009)
Cotton Stalks	-$ZnCl_2$ activation -Carbonization at 750-900^oC -CO_2 activation at 850-900^oC	683-2053		0.044-0.413	Ozdemir *et al*. (2011)
Orange Peel	-Carbonization at 700^oC -K_2CO_3 activation (microwave oven)	1104.45-1661.04	2.23	0.247 (micro)	Foo and Hameed (2012)

Table 2.4: Review of Activated Carbon Production Processes *(Cont'n)*

Precausor	Modification Process	Surface Area (m^2/g)	Pore Diameter (nm)	Pore Volume (cm^3/g)	References
Tea Waste	-ZnCl activation -Carbonization at 700^oC	35.2-1141	2.09-2.83	0.13-0.337 (micro)	Ahmad *et al*. (2013)
Coconut Shell	-Carbonization at 800^oC -CO_2 activation at 850^oC -HCl activation	368-1400	2.19-2.51	0.21-0.51 (micro)	Gundogdu *et al*. (2013)
Cotton Stalk	-H_2PO_4 activation -Carbonization at 500-800^oC	330-1720		0.15-0.71	Nahil and Williams (2012)
Date Palm Pit	- H_2PO_4 activation -Carbonization at 400^oC	725	2.91		Reddy *et al*. (2012)
Date Palm Stem	- H_2PO_4 /KOH activation -Carbonization at 400-600^oC	278-1100	3.6-5	0.372-0.852	Jibril *et al*. (2008)
Cotton Stalk	- H_2PO_4 activation -Carbonization at 420^oC	594-838	0.98-1.19	0.28-0.4 (micro)	Girgis *et al*. (2009)
Acorn Shell	-$ZnCl_2$ activation -Carbonization at 300-600^oC	98-1289	2-3	0.061-0.256 (micro)	Saka (2012)

CHAPTER THREE

MATERIALS AND METHOD

3.1 Materials and Sample Collection

3.1.1 Materials/reagents

The materials used during the experimentation include furnace, ceramic flat surface, oven drier, de-ionized water, burette, measuring cylinder, pH meter, digital weighing balance, standard flask, conical flask, pipette, retort stand and clamp, magnetic stirrer (Jenway 1000 Hotplate and Stirrer), glass funnel, micro filter (0.2 µm), 5ml and 50ml syringe, centrifuge (Horizon Clinispin 842VES), UV spectrophotometer (Jenway 6404UV), quartz cuvettes, glass column, glass wool, connecting pipe and valve, thermal analyzer (TGA 4000 Perkin-Elmer), scanning electron microscope (Phenom ProX), fourier transform infrared spectrometer (Shimadzu 8400s), gas sorption analyzer (NOVA 4200e Quantachrome) and Design Expert software (version 8). The agricultural material used in this study was rice husk and the reagents used were phosphoric acid, nitric acid, sodium hydroxide and phenol, all of which were of analytical grade.

3.1.2 Sample collection/processing

Rice husk was the agricultural material used in the preparation of activated carbon and it is available as shown in Fig 3.1 and 3.2. The rice husk was collected in dry season from the rice mill of National Cereal Research Institute (NCRI), Badeggi in Niger State. After collection, it was washed with distilled water to remove dirt and surface impurity, then oven-dried at 100 ^{o}C for 24 hours as stated in literature (El Shafey, 2007; Dada *et al*., 2012; Kudaybergenov *et al.*, 2012).



Fig. 3.1: Availability of Rice Husk



Fig. 3.2: Dry Rice Husk

3.2 Production of Activated Carbon

3.2.1 Thermal pretreatment

The rice husk was placed on a ceramic flat surface, charged into a furnace and heated to a temperature of 300 ^{o}C at a heating rate of 20-25 ^{o}C/min and residence time of 1 hour (Daffalla *et al*., n.d). The charred residue was collected and cooled at room temperature. The procedure above was repeated for 400 ^{o}C and 500 ^{o}C. The thermal pretreated rice husks (carbonized rice husks) were labeled C300, C400 and C500 representing carbonization temperature of the rice husk at 300, 400 and 500 ^{o}C.

3.2.2 Chemical pretreatment

Each of the carbonized rice husks was activated with 1M phosphoric acid (H_3PO_4) for 3 hours at impregnation ratio of 2:1 (volume of acid : mass of rice husk) and later oven-dried overnight at 200 ^{o}C to ensure proper drying (Dim and Okafor, 2012; Amuda *et al.*, 2012). The material was then removed from the oven, cooled for 2 hours and then washed with distilled water to bring the pH to 7.0 and again oven-dried overnight at 100 ^{o}C (Amuda *et al.*, 2012). The combined thermal and chemical pretreated rice husks were labeled RH300, RH400, and RH500.

3.3 Batch Adsorption

3.3.1 Preparation of simulated wastewater

Stock phenol solution was prepared by diluting 1g of phenol to 1000 ml using de-ionized water to obtain 1 g/l of phenol solution. Intermediate solution was prepared by diluting 25 ml of stock solution to 250 ml using de-ionized water to obtain 100 mg/l of phenol

solution. Standard solutions were prepared by diluting 10, 20, 30, 40 and 50 ml of intermediate solution to 100 ml using de-ionized water to obtain 10, 20, 30, 40 and 50 mg/l of phenol solution respectively.

3.3.2 Batch experiment

2 g of the adsorbent was added to 100 ml of different phenol initial concentration (10, 20, 30, 40 and 50 mg/l) in 250 ml conical flask. The mixture in the flask was placed on magnetic stirrer and stirred at 150 rpm (Belgin *et al.*, 2008; Agarry and Aremu, 2012b) for 90 min at ambient temperature. Using a 5 ml syringe, 3-4 ml of samples were withdrawn at different time interval (10, 20, 30, 60 and 90 min) and centrifuged at 3000 rpm for 20 min. The supernatant solution was collected from the centrifuge by decantation and filtered using a micro filter (0.2 µm) attached to a 5 ml syringe. The micro filter was backwashed after each use with de-ionized water using a 50 ml syringe. The procedure above was repeated for 3 and 4 g of adsorbents.

The procedure above was also carried out at pH of 2, 4, 6, 8 and 10 under the optimum operating conditions developed from this study. The solution pH was adjusted by adding a few drops of HNO_3 or NaOH (Farajzadeh and Mohammad, 2005; Hameed and Rahman, 2008). The procedure above was also carried out at adsorption process temperature of 30, 40 and 50 ^{o}C, under the optimum operating conditions developed from this study. Subsequently, under the same optimum operating conditions, the procedure was carried out using thermal pretreated rice husk activated carbon so as to obtain the relative performance of the combined thermal and chemical pretreated rice husk activated carbon.

3.3.3 Determination of unadsorbed phenol

The analysis of phenol in each sample filtrate was carried out using UV spectrophotometer. The maximum absorbance for phenol using scanning spectrophotometry was found to be at a wavelength of 270 nm. This is in agreement with literature finding as observed by Belgin *et al*. (2008); Kamble *et al*. (2008); Girods *et al*. (2009); Nabais *et al*. (2009); Beker *et al*. (2010); Lazo-Cannata *et al*. (2011); Djebbar *et al*. (2012); Shri and Vijayababu (2013). Before the analysis, a technical calibration curve was prepared and it was linear over the concentration range used. Therefore, unadsorbed phenol concentration in the filtrate was determined by interpolation using the calibration curve.

3.3.4 Determination of adsorption capacities and removal efficiency

A. Determination of Adsorption Capacities

The adsorption capacities (q_t) at any given time (t) for each sample were computed using equ (3.1) proposed by Wang *et al*. (2010); Li *et al*. (2013):

$$q_t = \frac{(C_o - C_t)\,V}{m} \tag{3.1}$$

For each of the batch experiment, adsorption capacity q_e at equilibrium was computed using equ (3.2) as proposed by Karaca *et al*. (2008) and Demibras *et al*. (2009):

$$q_e = \frac{(C_o - C_e)\,V}{m} \tag{3.2}$$

B. Determination of Adsorption Removal Efficiency

Adsorption removal efficiency was computed using equ (3.3) as proposed by Garg *et al*. (2008); Saad *et al*. (2010); Lo *et al*. (2012):

$$RE = \frac{(C_o - C_e)}{C_o} \times 100 \tag{3.3}$$

Where:

q_e = adsorption capacity at equilibrium (mg/g)

q_t = adsorption capacity at time *t* (mg/g)

C_o = initial concentration of solute (mg/L)

C_e = equilibrium concentration of solute (mg/L)

C_t = concentration of solute at time *t* (mg/L)

V = volume of solution (L)

m = mass of activated carbon used (g)

RE = removal efficiency (%)

3.3.5 Adsorption equilibrium isotherm study

For the equilibrium isotherm study, the isotherm models discussed in the literature were used to analyze the experimental data.

A. Langmuir Isotherm Parameters

The linearized form of Langmuir isotherm model given below was used by plotting $\frac{C_e}{q_e}$ against C_e. Equilibrium isotherm parameters for the model were obtained from the slope and intercept of the plot (Amin, 2008; Homagai *et al*., 2010) using equ (3.4):

$$\frac{C_e}{q_e} = \frac{1}{bQ_m} + \frac{C_e}{Q_m} \quad (3.4)$$

Where:

q_e = adsorption capacity at equilibrium (mg/g)

C_e = equilibrium concentration of solute (mg/L)

Q_m = maximum monolayer adsorption capacity (mg/g)

b = Langmuir isotherm constant (dm^3/mg)

B. Freundlinch Isotherm Parameters

The linearized form of Freundlich isotherm model given below was used by plotting $\log q_e$ against $\log C_e$. Equilibrium isotherm parameters for the model were obtained from the slope and intercept of the plot (Demiral and Gunduzoglu, 2010; Krishnan *et al*., 2011) of equ (3.5):

$$\log q_e = \log K_f + \frac{1}{n} \log C_e \quad (3.5)$$

Where:

q_e = adsorption capacity at equilibrium (mg/g)

C_e = equilibrium concentration of solute (mg/L)

K_f = Freundlich isotherm constant (mg/g)

n = adsorption intensity

3.3.6 Adsorption kinetic study

For the adsorption kinetic study, the following kinetic models discussed in the literature were used to analyze the experimental data.

A. Pseudo-Second-Order Kinetic Parameter

The linearized form of pseudo-second-order kinetic model given below was used by plotting $\frac{t}{q_t}$ against *t.* Kinetic parameters for the model was obtained from the slope and intercept of the plot (Theydan and Ahmed, 2012; Kaouah *et al*., 2013) of equ (3.6):

$$\frac{t}{q_t} = \frac{1}{k_2 q_e^2} + \frac{1}{q_e} t \quad (3.6)$$

Where:

q_t = adsorption capacity at time *t* (mg/g)

q_e = adsorption capacity at equilibrium (mg/g)

t = time (min)

k_2 = kinetic rate constant (g mg^{-1} min^{-1})

B. Intra-Particle Diffusion Kinetic Parameter

The linearized form of intra-particle diffusion model (Weber Morris equation) given below was used by plotting q_t against $t^{1/2}$. Kinetic parameters for the model were obtained from the slope and intercept of the plot of equ (3.7) (Karagoz *et al*., 2008; Tan *et al*., 2008a):

$$q_t = k_{id} t^{1/2} + I \quad (3.7)$$

Where:

q_t = adsorption capacity at time *t* (mg/g)

t = time (min)

k_{id} = Intra-particle diffusion rate constant (mg/g$min^{1/2}$)

I = boundary layer constant (mg/g)

3.3.7 Adsorption thermodynamic study

For the adsorption thermodynamic study, the thermodynamic model discussed in the literature was used to analyze the experimental data.

Thermodynamic Model

The thermodynamic model (Van't Hoff equation) given below was used by plotting $\ln k_c$ against $^1/_T$. Thermodynamic parameters for the model were obtained from the slope and intercept of the plot (Wang, 2012; Baccar *et al*., 2013) using equ (3.8):

$$\ln k_c = \frac{\Delta S^o}{R} - \frac{\Delta H^o}{RT} \quad (3.8)$$

And the Gibbs free energy was determined from equ (3.9) (Lataye *et al*., 2008; Ghaedi *et al*., 2013):

$$\Delta G^o = \Delta H^o - T\Delta S^o \quad (3.9)$$

Where:

k_c = thermodynamic equilibrium constant (but $k_c = \frac{q_e}{C_e}$)

q_e = adsorption capacity at equilibrium (mg/g)

C_e = equilibrium concentration of solute (mg/L)

T = absolute temperature (K)

R = gas constant (8.314 J/mol K)

3.4 Modeling and Optimization

3.4.1 Experimental design

The Central Composite Design (CCD) was used in this study in the modeling and optimization of the interaction of process variables involved in the preparation of rice husk activated carbon as well as batch adsorption of phenol using the activated carbon prepared. The CCD is widely used for modeling and optimization and it requires only a minimum number of experiments. Generally, the CCD consists of three kinds of runs; they are factorial runs (2^n), axial runs ($2n$) and center runs (n_c) (Nasehir-Khan *et al*., 2010a; Cronje

et al., 2011). These designs consist of a 2^n factorial (coded to the usual ± 1 notation) augmented by 2*n* axial points ($\pm\alpha$,0,0), (0,$\pm\alpha$,0), (0,0,$\pm\alpha$), and n_c center points (0,0,0) (Sahu *et al*., 2009a; Sugashini and Meera, 2013) where α is the distance of the axial point from the center (Ahmad and Hammed, 2010). The center points are used to determine the experimental error and reproducibility of the data (Khodadoust *et al*., 2013; Hesas *et al*., 2013) and the axial points are chosen such that they allow rotatability which ensures that the variance of the model prediction is constant at all points equidistant from the design center (Sahu *et al*., 2010). Therefore, according to Arulkumar *et al*. (2011); Abbas (2013), the number of experimental runs required is given by equ (3.10):

$$N = 2^n + 2n + n_c \tag{3.10}$$

Where:

N = total number of experimental runs

n = number of independent variables (factors)

n_c = number of center points

Three variables (factors) were considered in this study, they are:

(i) Pretreatment temperature "A", a rice husk activated carbon preparation variable,

(ii) Initial phenol concentration "B", a batch adsorption process variable and

(iii) Adsorbent dosage "C", a batch adsorption process variable.

For the three variables, the number of center run was six, therefore number of experimental runs required was obtained as:

$$N = 2^n + 2n + n_c = 2^3 + 2(3) + 6 = 8 + 6 + 6 = 20$$

This implied that 20 experimental runs consisting of 8 factorial runs, 6 axial runs and 6 center runs was required.

The two response variables considered in this study were:

(i) Removal efficiency (Y_1) and

(ii) Adsorption capacity (Y_2)

3.4.2 Regression model

Each response was used to develop an empirical model that correlate the response to the three factors that is, rice husk activated carbon preparation variable (A) and batch adsorption process variables (B, C), using second-order polynomial (Amini *et al*., 2009; Manase, 2012; Das *et al.*, 2012) as in equ (3.11):

$$Y = b_o + \sum_{i=1}^{n} b_i X_i + \sum_{i=1}^{n} b_{ii} X_i^2 + \sum_{i=1}^{n-1} \sum_{j=i+1}^{n} b_{ij} X_i X_{j,} \quad (3.11)$$

Where Y is the predicted response, b_o is the constant coefficient, b_i is the linear coefficient, b_{ij} is the interaction coefficient, b_{ii} is the quadratic coefficient and X_i, X_j are the coded values for the factors.

3.4.3 Statistical and graphical analysis

Significance of the model equations and their terms were evaluated using statistical tools such as standard deviation, coefficient of determination (R-squared), Fisher value (F-value), probability (P-value) and residual (Lima *et al*., 2011; Roy *et al*., 2013; Hassani *et al*., 2013). Graphs were employed to analyze the combined effect of factors on responses using 3D plots and to also analyze the predicted versus actual value plots of the response variables.

3.4.4 Optimization

Optimization technique was employed to determine the optimum operating conditions for the process variables under consideration. To achieve this, goals were set with constraints. For each of the factors, goal was set "in range" with constraint 300-500, 10-50 and 2-4 of lower-upper level for factor A (pretreatment temperature), B (initial phenol concentration) and C (adsorbent dosage) respectively. For the response surface, the goal for Y_2 was also set "in range" with constraint 0.18-2.393 as lower-upper levels, while the goal for Y_1 was set "maximize" at 100. Therefore, removal efficiency becomes the objective function or performance index.

3.4.5 Model validation

Model validation was carried out by conducting batch experiment under optimum operating conditions. In order to evaluate the validity of the model, experimental values obtained were compared with the model predicted values.

3.4.6 Software application

Design Expert Software (version 8) was used for the design of experiment, regression, statistical analysis, optimization and graphical analysis.

3.5 Characterization of Activated Carbon

3.5.1 Thermogravimetric analysis (TGA)

The thermogravimetric analysis (TGA) was employed to study the thermal behavior of samples using a thermal analyzer (TGA 4000 Perkin-Elmer). The thermobalance automatically measures the weight loss of the sample as a function of temperature and time. The samples were subjected to pyrolysis under N_2 flow (35 ml/min) with heating rate of 20 ^{o}C/min. (Kalderis *et al*., 2008a; Hu *et al*., 2008; Basta *et al*., 2009; Liou, 2010).

3.5.2 Scanning electron microscopy (SEM) analysis

The surface morphology of the produced activated carbon was obtained using Scanning Electron Microscope (Phenom ProX) working at a high voltage of 15 kV. The samples were coated with gold by a gold sputtering device for clear visibility and conductivity. Thereafter, the coated sample was placed on the sample holder for analysis (Rosas *et al*., 2009; Somasundaram *et al*., 2013).

3.5.3 Fourier transform infrared (FTIR) spectroscopy analysis

The surface functional groups of the samples were estimated by Fourier Transform Infrared (FTIR) spectroscopy analysis using a spectrometer (Shimadzu 8400s). The pellet for infrared studies was prepared by mixing a given sample with potassium bromide (KBr) crystals and pressed into a pellet. The pellet which is homogeneous in appearance was inserted into the IR sample holder for the analysis. FTIR spectra of different samples were recorded within 400-4000 cm^{-1} at a resolution of 2 cm^{-1} (Liu *et al*., 2011; Wang *et al*., 2011b; Saka, 2012; Somasundaram *et al*., 2013).

3.5.4 Surface area and pore size analysis

The surface area and average pore size of samples were determined using a gas sorption analyzer (NOVA 4200e Quantachrome and the Quantachrome NovaWin software). The samples were degassed in a vacuum at 200 ^{o}C for 3 hours prior to measurement. The nitrogen adsorption-desorption data were recorded at liquid nitrogen temperature of 77.35 K. The adsorption equilibrium time was set at 60 s. The Brunauer-Emmett-Teller (BET) method was used to calculate the surface area, using the data obtained from the N_2 adsorption isotherm within the P/P_o range of 0.05-0.3, where P is the system pressure and P_o is the initial pressure at 1 bar. The micropore volume (V_{mic}) and the average pore diameter (d_p) were derived from the Dubinin-Radushkevich (DR) method (Jibril *et al*., 2008; Patnukao and Pavasant, 2008; Li *et al*., 2010; Reddy *et al*., 2012; Saka, 2012; Ang *et al*., 2013).

3.6 Column Adsorption

The optimum condition developed in the batch adsorption studies was applied in the column experiment. That is rice husk activated carbon was produced at optimum temperature of 441.46 ^{o}C and was used throughout the column experiment.

3.6.1 Adsorption of phenol from refinery wastewater

Column adsorption experiment was carried out in two modes as reported by Nhapi *et al*. (2011). That is Rapid Small Scale Column Test and Large Scale Column Test. The column experimental set-up is as shown in Fig. 3.3.

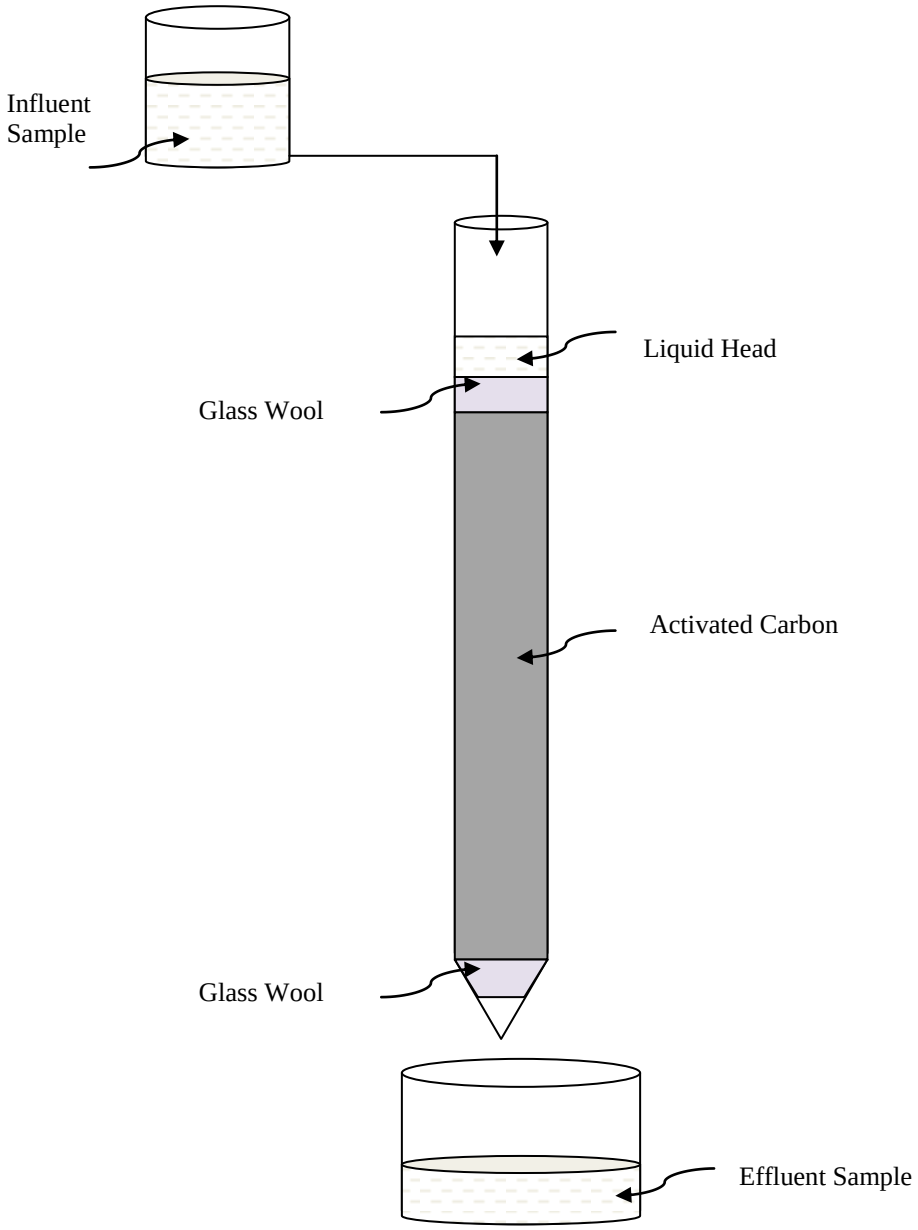


Fig. 3.3: Sketch of the Column Experimental Set-up

A. Rapid Small Scale Column Test (RSSCT)

In RSSCT, the optimum dosage of 4 g was the basis for the establishment of the bed height/depth of 6 cm. The column experiment was conducted using a glass column of 12 cm length, 2 cm internal diameter, 3.142 cm^2 surface area and 37.7 cm^3 empty bed volume. The column was packed with a known quantity of rice husk activated carbon to yield the desired bed depth/height. Glass wool was placed at the bottom as a support and also at the top to prevent flotation of rice husk activated carbon in excess wastewater (Sugashini and Meera, 2013) and a liquid head of at least 2 cm was sustained in order to prevent air voids (Shri and Vijayababu, 2013). Process wastewater, which is the wastewater generated from various unit processes/operations, was collected from Kaduna Refinery and Petrochemical Company before treatment. Phenol composition of the process wastewater was analyzed and found to be 51.32 mg/l. This initial concentration was used throughout the experiment. The wastewater was fed to the column in a downward flow mode through a pipe having a valve as the flow regulator. The effluent wastewater was collected from the column outlet at predetermined time interval for analysis of unadsorbed phenol concentration.

The effect of the following variables on the column performance was investigated:

(i) Bed depth: 7.5 cm (5 g), 6 cm (4 g), 4.5 cm (3 g); keeping the flow rate constant at 3 ml/min

(ii) Flow rate: 3 ml/min, 4.5 ml/min; keeping the bed depth constant at 6 cm (4 g).

B. Large Scale Column Test (LSCT) and Design Consideration

For the LSCT, the design criteria as described by "*Activated Carbon*", (n.d) were considered. Therefore, to avoid channeling the column diameter was chosen to be at least 50 times the effective particle size. The effective particle size of the rice husk activated

carbon was found to be 0.055 mm; hence the column diameter was taken as 6 cm. Also, the ratio of activated carbon bed to column diameter should be ~10, therefore activated carbon bed depth was taken as 60 cm. For the volumetric flow rate, the column linear velocity was taken as 2 cm/min, therefore the volumetric flow rate becomes:

$$Linear\ velocity = \frac{Flow\ rate}{Surface\ Area}$$

$$But,\ Surface\ Area = \frac{\pi d^2}{4} = 28.29\ cm^2\ and\ linear\ velocity = 2\ cm/min$$

$$Flow\ rate = 56.58\ ml/min$$

The activated carbon volume was obtained as:

$$Carbon\ volume = Surface\ Area\ \times Carbon\ depth = 28.29 \times 60 = 1697.4\ cm^3$$

Therefore, Empty bed contact time was obtained as:

$$EBCT = \frac{Carbon\ volume}{Flow\ rate} = \frac{1697.4}{56.58} = 30\ mins$$

And the mass of carbon required was found as:

$$Carbon\ mass = Density \times Carbon\ volume = 0.212 \times 1697.4 = 359.84\ g$$

3.6.2 Breakthrough curve

The breakthrough curves for different bed depths and flow rates were generated by plotting C_B/C_o against t. The breakthrough characteristics for each point were thereafter obtained from the curves.

A. Breakthrough Capacity q_B

Breakthrough capacity was determined using the equ (3.12) as expressed by Dwivedi *et al*. (2008):

$$q_B = \frac{t_B f C_o}{m} \quad (3.12)$$

B. Volume of Effluent Treated V_{eff}

The volume of effluent treated was determined using equ (3.13) as expressed by Sadaf and Bhatti (2013):

$$V_{eff} = t_B f \quad (3.13)$$

Where:

q_B = breakthrough adsorption capacity (mg/g)

V_{eff} = volume of effluent (L)

C_B, C_t = effluent concentration of solute at breakthrough or time *t* (mg/L)

t_B *or* t = breakthrough time or time (min)

C_o = influent concentration of solute (mg/L)

f = volumetric flow rate (ml/min)

m = mass of activated carbon (g)

3.6.3 Column adsorption models

For the column adsorption study, the column (kinetics) models discussed in the literature were used to analyze the experimental data.

A. Bed Depth Service Time (BDST) or Adam Bohart Model

The BDST model equation given below was used by plotting service time *t* against bed depth *z*. Model parameters were obtained from the slope and intercept of the plot of equ (3.14) (Kumar and Bandyopadhyay, 2005; Luo *et al*., 2011):

$$t = \frac{N_o}{C_o F} Z - \frac{1}{C_o k_a} \ln\left(\frac{C_o}{C_B} - 1\right) \quad (3.14)$$

K_a = adsorption rate constant (L mg^{-1} min^{-1})

F = linear flow velocity to bed (m/min)

C_B = effluent concentration of solute at breakthrough (mg/L)

C_o = influent concentration of solute (mg/L)

N_o = adsorption capacity (mg/L)

Z= bed depth (m)

t = time (min)

According to Kumar and Bandyopadhyay (2005); Han *et al*. (2006), equ (3.14) can be written as equ (3.15):

$$t = aZ - b \tag{3.15}$$

Where:

$$a = slope = \frac{N_o}{C_o F}$$

$$b = intercept = \frac{1}{C_o k_a} \ln\left(\frac{C_o}{C_B} - 1\right)$$

B. Thomas Model

The Thomas model equation given below was used to analyze the column experimental data by plotting $\ln\frac{C_o}{C_B} - 1$ against t. Model parameters were obtained from the slope and intercept of the plot using equ (3.16) as reported by Ozturk and Kavak (2005):

$$\ln\left(\frac{C_o}{C_B} - 1\right) = \frac{k_{Th} q_o m}{f} - k_{Th} C_o t \tag{3.16}$$

Where:

K_{Th} = Thomas rate constant (L/(min . mg))

f = volumetric flow rate (L/min)

C_B = effluent concentration of solute at breakthrough (mg/L)

C_o = influent concentration of solute (mg/L)

q_o = adsorption capacity (mg/g)

m= mass of the adsorbent (g)

t = time (min)

C. Yoon Nelson Model

The Yoon Nelson model equation given below was also used to analyze the column experimental data by plotting $\ln\frac{C_B}{C_o-C_B}$ against t. Model parameters were obtained from the slope and intercept of the plot using equ (3.17) (Chowdhury *et al*., 2013):

$$\ln\left(\frac{C_B}{C_o-C_B}\right) = k_{YN}t - k_{YN}\tau \quad (3.17)$$

Where:

K_{YN} = Yoon Nelson rate constant

C_B = effluent concentration of solute at breakthrough (mg/L)

C_o = influent concentration of solute (mg/L)

τ = breakthrough time at 50% (min)

t = time (min)

3.6.4 Treatment of raw water from samaru stream

Raw water samples were collected at three different sampling points (point 1, 2 and 3) from Samaru stream flowing into Ahmadu Bello University, Zaria. The raw water samples were analyzed for general characterization to determine the values of the following parameters before treatment: pH, Electrical Conductivity, Total Dissolved Solid,

Biochemical Oxygen Demand, Chemical Oxygen Demand, Ammonium, Nitrate, Chloride, Iron (III), Copper (II) and Zinc (II). For treatment of the raw water, the samples were fed to the column in a downward flow mode through a pipe having a valve as the flow regulator. The column was packed with a known quantity of rice husk activated carbon (4 g) to yield a bed depth/height of 6 cm. Glass wool was placed at the bottom as a support and also at the top to prevent flotation of rice husk activated carbon in excess raw water (Sugashini and Meera, 2013). The effluents were collected from the column outlet for determination of the treated raw water parameters.

3.6.5 Determination of influent and effluent stream water parameters

Electrical Conductivity and Total Dissolved Solid concentrations were determined using EC/TDS Auto Ranging meter (Hanna Instrument HI 9835). Biochemical Oxygen Demand at 5 days was determined by Azide modification of the Winker method as stated in standard method for water and wastewater analysis. Chemical Oxygen Demand was determined by refluxing based on Standard Methods for the Examination of Water and Wastewater (APHA, 1998). Ammonium concentrations were determined using Lovibond 1000 comparator with ammonia disc, nitrate concentrations were determined using multiparameter bench photometer (Hanna Instrument HI 83200) and chloride concentrations were determined by titration which is based on the Standard Methods for the Examination of Water and Wastewater (APHA, 1998). Iron (III), Copper (II), Zinc (II) and Lead (II) concentrations were determined using Atomic Absorption Spectrometer (Varian AA240FS) as described in standard methods.

CHAPTER FOUR

RESULTS AND DISCUSSION

4.1 Batch Adsorption Capacity and Removal Efficiency of Phenol

300 ^{o}C Pretreatment Temperature (RH300)

Table 4.1 presents the 300 ^{o}C pretreatment temperature results of adsorption capacity and removal efficiency as influenced by adsorbent dosage and initial concentration of phenol during the batch adsorbtion process. From the results, it was observed that the highest removal efficiency of 94.175 % was obtained at 4 g adsorbent dosage and 50 mg/l initial concentration of phenol. This was followed by the removal efficiency of 92.982 % obtained at 4 g adsorbent dosage and 40 mg/l initial phenol concentration, while the least removal efficiency of 56.491 % was obtained at 2 g adsorbent dosage and initial phenol concentration of 10 mg/l. In terms of adsorption capacity, the highest value of 2.208 mg/g was obtained at 2 g adsorbent dosage and 50 mg/l initial phenol concentration. This was followed by adsorption capacity of 1.719 mg/g obtained at 2 g dosage and 40 mg/l initial concentration, while the least adsorption capacity of 0.18 mg/g was obtained at 4 g adsorbent dosage and initial concentration of 10 mg/l. This trend indicates that adsorbent dosage and initial concentration have influence on adsorption capacity and removal efficiency of phenol in the batch adsorption process at 300 ^{o}C pretreatment temperature.

The highest adsorption capacity and removal efficiency were observed to occur at different adsorbent dosage but same initial concentration of phenol. This is because, while adsorption capacity is a performance index that is measured as a ratio of amount of solute removed to dose of adsorbent, removal efficiency measures amount of solute removal in relation to initial concentration of solute. This explains therefore, why 2 g adsorbent

dosage with 50 mg/l initial phenol concentration gave 2.2 mg/g adsorption capacity and removal efficiency of 88.316 %. But as the adsorbent dosage increased from 2 to 4 g and the initial concentration remain unchanged, the removal efficiency increased from 88.316 to 94.175 %. This is most likely due to increased amount of adsorbent at same initial concentration which translates to additional amount of solute removal from solution. On the other hand, adsorption capacity decreased from 2.208 to 0.18 mg/g because same amount of solute in solution was contacted with increased amount of adsorbent thereby decreasing what a unit mass of adsorbent can adsorb (Table 4.1).

Under a fixed initial phenol concentration of 50 mg/l, the adsorption capacity and removal efficiency at 300 ^{o}C pretreatment temperature were found to vary in relation to time as expressed in Table 4.2. From this table, the highest removal efficiency of 94.386 % was observed at adsorbent dosage of 4 g but at variable times first at 10 min which decreased with increasing time before increasing after 30 min to peak at 60 min. A careful examination shows that the minimum removal efficiency of 84.38 % was obtained at 2 g adsorbent dosage at 10 min. For adsorption capacity, the highest value of 2.263 mg/g was observed at adsorbent dosage of 2 g at 90 min. This was followed by 2.246 mg/g at 2 g adsorbent dosage at 20 min while the minimum adsorption capacity of 1.175 mg/g was obtained at both 4 g adsorbent dosage at the initial 20 min and 90 min. Thus the observed adsorption capacities and removal efficiencies did not show constant pattern in variation with time at all the adsorbent dosages, that is, it was oscillating between increase and decrease with increasing time.

Table 4.1: Adsorption capacity and Removal efficiency as a function of adsorbent dosage and initial concentration of phenol *(RH300)*

m(g)	C_o (mg/l)	C_e (mg/l)	q_e (mg/g)	RE (%)
2	10	4.351	0.282	56.491
2	20	5.175	0.741	74.123
2	30	5.298	1.235	82.339
2	40	5.614	1.719	85.965
2	50	5.842	2.208	88.316
3	10	3.789	0.207	62.105
3	20	4.474	0.518	77.632
3	30	5.228	0.826	82.573
3	40	6.140	1.129	84.649
3	50	3.561	1.548	92.877
4	10	2.807	0.180	71.930
4	20	2.105	0.447	89.474
4	30	2.426	0.689	91.912
4	40	2.807	0.930	92.982
4	50	2.912	1.177	94.175

Table 4.2: Adsorption capacity and Removal efficiency as a function of Contact time at a Fixed Initial Phenol concentration (C_o=50mg/l, RH300)

m (g)	t (min)	q_t (mg/g)	RE (%)
2	10	2.110	84.386
2	20	2.246	89.825
2	30	2.232	89.298
2	60	2.189	87.544
2	90	2.263	90.526
3	10	1.547	92.807
3	20	1.544	92.632
3	30	1.558	93.509
3	60	1.550	92.982
3	90	1.541	92.456
4	10	1.180	94.386
4	20	1.175	94.035
4	30	1.175	94.035
4	60	1.180	94.386
4	90	1.175	94.035

400 ^{o}C Pretreatment Temperature (RH400)

Results of adsorption capacity and removal efficiency in relation to adsorbent dosage and initial concentration of phenol for 400 ^{o}C pretreatment temperature are presented in Table 4.3. From this table, the highest removal efficiency of 95.263 % was obtained at 4 g adsorbent dosage and 50 mg/l initial concentration of phenol. This was followed by the removal efficiency of 95.175 % obtained at 4 g adsorbent dosage and 40 mg/l initial phenol concentration while the least removal efficiency of 67.895 % was obtained at 2 g adsorbent dosage and initial phenol concentration of 10 mg/l. For adsorption capacity, the highest value of 2.354 mg/g was obtained at 2 g adsorbent dosage and 50 mg/l initial phenol concentration. This was followed by adsorption capacity of 1.825 mg/g obtained at 2 g dosage and 40 mg/l initial concentration while the minimum adsorption capacity of 0.207 mg/g was obtained at 4 g adsorbent dosage and initial concentration of 10 mg/l. This trend is similar to that of 300 ^{o}C and also indicates that adsorbent dosage and initial concentration have influence on the adsorption capacity and removal efficiency of phenol in the batch adsorption process at 400 ^{o}C pretreatment temperature.

For 400 ^{o}C pretreatment temperature, under a fixed initial phenol concentration of 50 mg/l, results in Table 4.4 shows that the highest adsorption capacity of 2.368 mg/g was observed at adsorbent dosage of 2 g at 60 min. This was followed by adsorption capacity of 2.36 mg/g at 2 g adsorbent dosage at 20 min while minimum adsorption capacity of 1.173 mg/g was obtained at 4 g adsorbent dosage at 20 min. In terms of removal efficiency, the highest value of 96.316 % was observed at 4 g adsorbent dosage of at 60 min. This was followed by 96.14 % at 4 g adsorbent dosage at 10 min, while minimum removal efficiency of 92.982 % was obtained at 3 g adsorbent dosage at 10 min. Similar to that of 300 ^{o}C

pretreatment temperature, the observed adsorption capacity and removal efficiency did not show constant pattern in variation with time. At all the adsorbent dosages, the values were oscillating between increase and decrease with increasing time.

Table 4.3: Adsorption capacity and Removal efficiency as a function of adsorbent dosage and initial concentration *(RH400)*

m(g)	C_o (mg/l)	C_e (mg/l)	q_e (mg/g)	RE (%)
2	10	3.211	0.339	67.895
2	20	3.333	0.833	83.333
2	30	3.474	1.326	88.421
2	40	3.509	1.825	91.228
2	50	2.912	2.354	94.175
3	10	2.421	0.253	75.789
3	20	2.456	0.585	87.719
3	30	2.860	0.905	90.468
3	40	2.895	1.237	92.763
3	50	3.263	1.558	93.474
4	10	1.737	0.207	82.632
4	20	1.842	0.454	90.789
4	30	1.895	0.703	93.684
4	40	1.930	0.952	95.175
4	50	2.368	1.191	95.263

Table 4.4: Adsorption capacity and Removal efficiency as a function of Contact time at a Fixed Initial Phenol concentration (C_o=50mg/l, RH400))

m (g)	t (min)	q_t (mg/g)	RE (%)
2	10	2.351	94.035
2	20	2.360	94.386
2	30	2.355	94.211
2	60	2.368	94.737
2	90	2.338	93.509
3	10	1.550	92.982
3	20	1.558	93.509
3	30	1.553	93.158
3	60	1.564	93.860
3	90	1.564	93.860
4	10	1.202	96.140
4	20	1.173	93.860
4	30	1.182	94.561
4	60	1.204	96.316
4	90	1.193	95.439

500 ^{o}C Pretreatment Temperature (RH500)

Table 4.5 shows the 500 ^{o}C pretreatment temperature result of adsorption capacity and removal efficiency against adsorbent dosage and initial concentration of phenol. Also observed was that the highest removal efficiency of 96.316 % was obtained at 3 g adsorbent dosge and 50 mg/l initial concentration of phenol and this was followed by the removal efficiency of 95.719 % obtained at 2 g adsorbent dosage and 50 mg/l initial phenol concentration while the least removal efficiency of 78.246 % was obtained at 2 g adsorbent dosage and initial phenol concentration of 10 mg/l. In terms of adsorption capacity, the highest value of 2.393 mg/g was obtained at 2 g adsorbent dosage and 50 mg/l initial phenol concentration and this was followed by the adsorption capacity of 1.895 mg/g obtained at 2 g dosage and 40 mg/l initial concentration, while the least adsorption capacity of 0.214 mg/g was obtained at 4 g adsorbent dosage and initial concentration of 10 mg/l. This trend could also indicate that adsorbent dosage and initial concentration have influence on adsorption capacity and removal efficiency of phenol in the batch adsorption process at 500 ^{o}C pretreatment temperature.

As presented in Table 4.6 under a fixed initial phenol concentration of 50 mg/l, it was found that for 500 ^{o}C pretreatment temperature, the highest adsorption capacity of 2.434 mg/g was observed at adsorbent dosage of 2 g at 60 min. This was followed by adsorption capacity of 2.43 mg/g at 2 g adsorbent dosage at 90 min, while the minimum adsorption capacity of 1.175 mg/g was obtained at 4 g adsorbent dosage at 20 min. For the removal efficiency, the highest value of 97.368 % was observed at adsorbent dosage of 4 g at 60 min. This was followed by 97.193 % at 4 g adsorbent dosage at 90 min while the minimum removal efficiency of 92.982 % was obtained at 3 g adsorbent dosage at 10 min. Similarly,

the observed adsorption capacity and removal efficiency did not show constant pattern in variation with time at all the adsorbent dosages.

Table 4.5: Adsorption capacity and Removal efficiency as a function of adsorbent dosage and initial concentration *(RH500)*

m (g)	C_o (mg/l)	C_e (mg/l)	q_e (mg/g)	RE (%)
2	10	2.175	0.391	78.246
2	20	1.930	0.904	90.351
2	30	2.088	1.396	93.041
2	40	2.105	1.895	94.737
2	50	2.140	2.393	95.719
3	10	1.579	0.281	84.211
3	20	1.754	0.608	91.228
3	30	1.842	0.939	93.860
3	40	2.105	1.263	94.737
3	50	1.842	1.605	96.316
4	10	1.421	0.214	85.789
4	20	1.754	0.456	91.228
4	30	2.123	0.697	92.924
4	40	2.193	0.945	94.518
4	50	2.649	1.184	94.702

Table 4.6: Adsorption capacity and Removal efficiency as a function of Contact time at a Fixed Initial Phenol concentration (C_o=50mg/l, RH500)

m (g)	t (min)	q_t (mg/g)	RE (%)
2	10	2.377	95.088
2	20	2.395	95.789
2	30	2.329	93.158
2	60	2.434	97.368
2	90	2.430	97.193
3	10	1.611	96.667
3	20	1.605	96.316
3	30	1.605	96.316
3	60	1.620	97.192
3	90	1.585	95.088
4	10	1.149	91.930
4	20	1.206	96.491
4	30	1.178	94.211
4	60	1.206	96.491
4	90	1.180	94.386

For all the pretreatment temperatures under consideration, it was observed that adsorption of phenol onto rice husk activated carbon attained equilibrium adsorption capacity of 2.354 mg/g at a dosage of 2 g, initial concentration of 50 mg/l and carbonization temperature of 400 ^{o}C (Table 4.3) and also 2.393 mg/g at a dosage of 2 g with initial concentration of 50 mg/l and carbonization temperature of 500 ^{o}C (Table 4.5). Removal efficiency of 96.316 % was attained at a dosage of 3 g, initial concentration of 50 mg/l and carbonization temperature of 500 ^{o}C (Table 4.5).

4.2 Effect of Process Variables on Phenol Adsorption

4.2.1 Effect of initial concentration

Effect of Initial Concentration on Adsorption Capacity

Effect of initial phenol concentration on adsorption capacity was studied as presented in Fig. 4.1, 4.2 and 4.3. It was observed in Fig 4.1 (RH300) that when initial concentration was increased from 10 to 50 mg/l, the adsorption capacity increased from 0.282 to 2.208 mg/g, 0.207 to 1.548 mg/g and 0.18 to 1.177 mg/g for 2 g, 3 g and 4 g of adsorbent dosage respectively. The straight line pattern in the graph implies that a change in the initial concentration of phenol results in a uniform change pattern in the amount of phenol uptake per unit of rice husk activated carbon. It was also observed that increasing the initial concentration of the phenol in solution increases the adsorption capacity. This is due to the fact that the initial concentration of solute in solution provides an important driving force to overcome all mass transfer resistance of solutes between the liquid and solid phase. Therefore, increasing the initial phenol concentration provides an important driving force for which phenol molecules pass from the bulk solution to the surface of the rice husk

activated thereby resulting in higher adsorption capacity. This is in agreement with observations reported by Krishnan and Anirudhan (2003); Ho and McKay (2004); Mahvi *et al*. (2004); Kermani *et al*. (2006); Alzaydien and Waleed (2009); Mina *et al.* (2011). According to Alzaydien and Waleed (2009), increase in adsorption capacity resulting from increase in initial concentration could be due to higher probability of collision between solute and adsorbent surface as the amount of solute increases.

For RH400, Fig 4.2 shows that increase in initial concentration from 10 to 50 mg/l resulted in increase in adsorption capacity of 0.339 to 2.354 mg/g, 0.253 to 1.558 mg/g and 0.207 to 1.191 mg/g for 2 g, 3 g and 4 g adsorbent dosage respectively. The observed trend is similar to that of RH300. It was also observed in Fig 4.3 that for RH500 adsorption capacity increased from 0.391 to 2.393 mg/g, 0.281 to 1.605 mg/g and 0.214 to 1.184 mg/g for 2 g, 3 g and 4 g adsorbent dosage respectively as initial concentration increased from 10 to 50 mg/l. The trend observed in the figure is similar to those of RH300 and RH400 due to same reasons as in RH300.

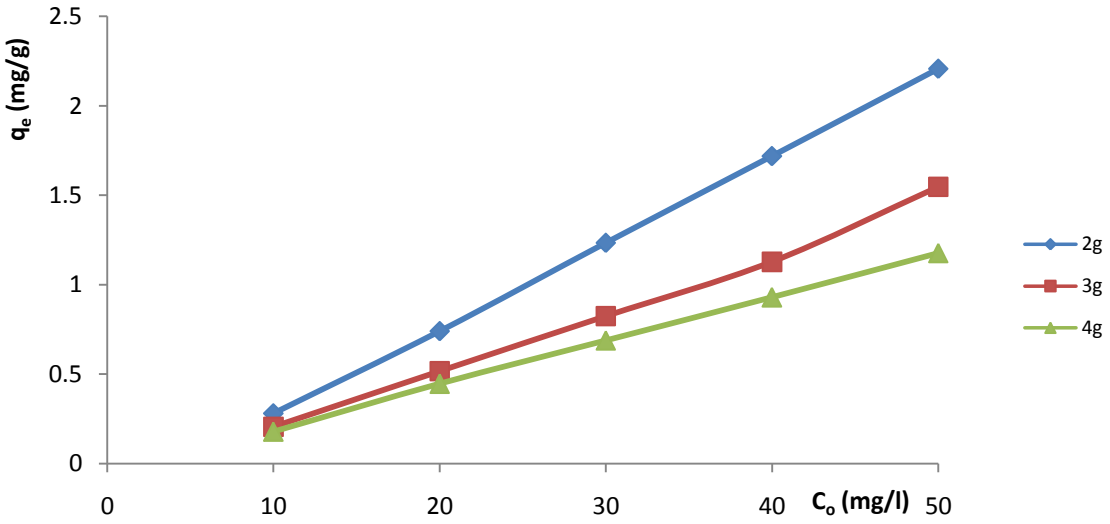


Fig 4.1: Effect of Initial concentration on Adsorption Capacity *(RH300)*

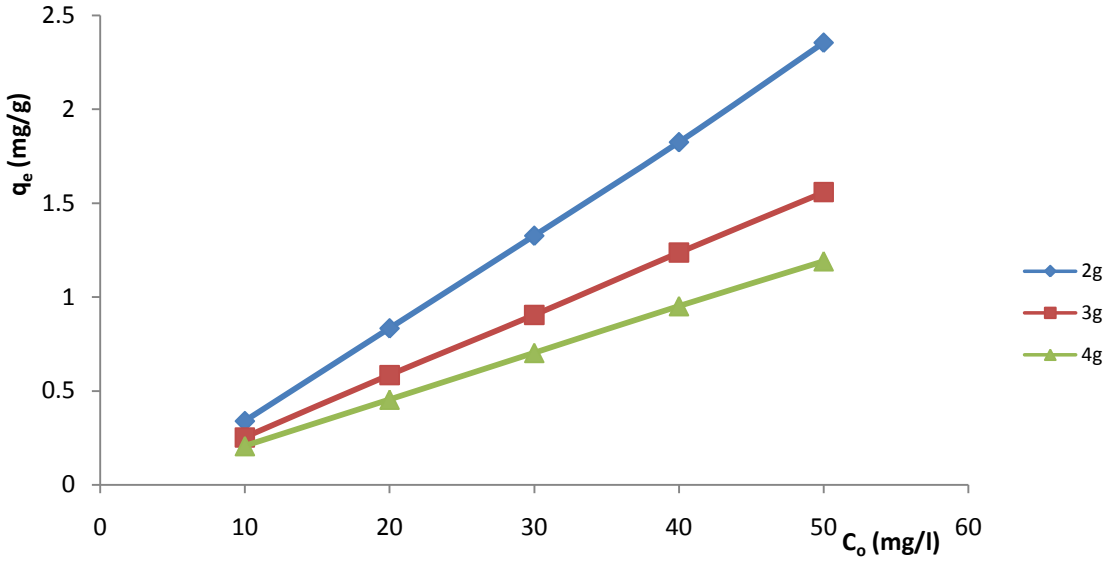


Fig 4.2: Effect of initial concentration on Adsorption Capacity *(RH400)*

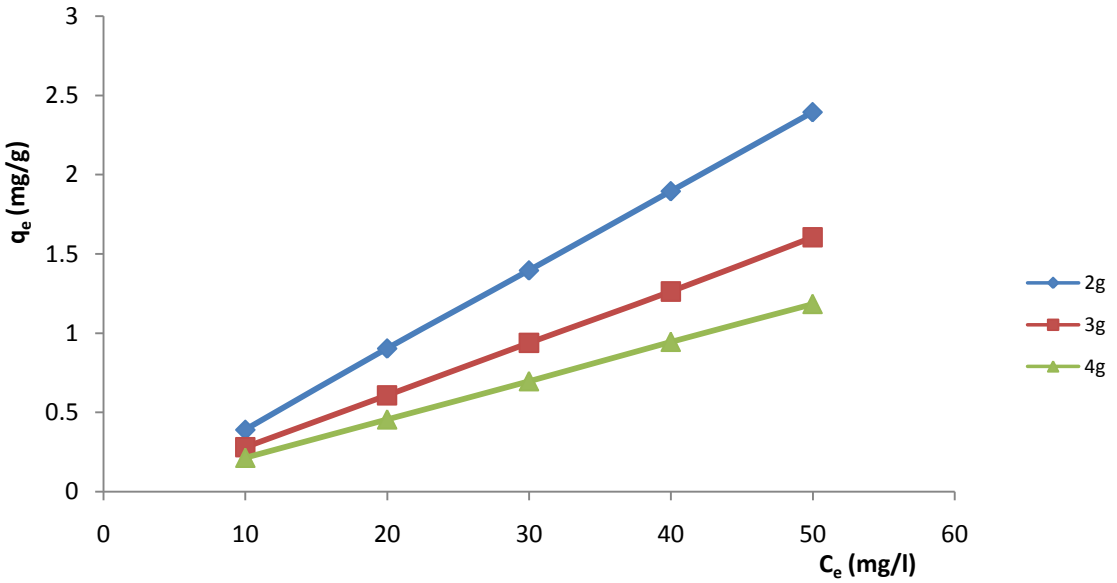


Fig 4.3: Effect of Initial concentration on Adsorption Capacity *(RH500)*

Effect of Initial Concentration on Removal Efficiency

Also studied was the effect of initial concentration of phenol on removal efficiency and this was presented in Fig. 4.4, 4.5 and 4.6. It was observed in Fig 4.4 for RH300 that removal efficiency increased from 56.49 to 88.32 %, 62.12 to 92.88 % and 71.93 to 94.18 % for 2 g, 3 g and 4 g adsorbent dosage respectively as initial concentration increased from 10 to 50 mg/l. The curve pattern in the graph signifies that at low values of initial concentration, change in the initial concentration of phenol molecules results in a steep increase in removal efficiency. While at high values of initial concentration, change in the initial concentration of phenol molecules results in a lesser or no change (at extremes of concentration) in removal efficiency, indicating an approach to saturation. Increasing the initial concentration was also observed to increase the percentage removal efficiency. Though this did not conform to the normal trend, it could suggest physical adsorption characterized by multilayer phenomenon. This is because for an increasing initial concentration at fixed adsorbent dosage with a monolayer surface adsorption, the amount of solute attached to the surface of the adsorbent in relation to the initial amount of solute in solution will be observed to be decreasing, hence this result in decreasing removal efficiency. While for an increasing initial concentration at fixed adsorbent dosage with a multilayer surface adsorption, the amount of solute attached to the surface of the adsorbent in relation to the initial amount of solute in solution will be observed to be increasing, hence this result in increasing removal efficiency.

In Fig 4.5 (RH400), it could be observed that when initial concentration was increased from 10 to 50 mg/l, the removal efficiency increased from 67.9 to 94.18 %, 75.79 to 93.48 % and 82.63 to 95.26 % for 2 g, 3 g and 4 g dosage respectively. The trend is similar to the

prevailing observations of RH300. For RH500 (Fig 4.6), the increase in initial concentration from 10 to 50 mg/l resulted in 78.25 to 95.72 %, 84.21 to 96.32 % and 85.79 to 94.7 % increase in removal efficiency for 2 g, 3 g and 4 g adsorbent dosage respectively. The figure shows a similar trend to that of RH300 and RH400 and based on likely similar reasons.

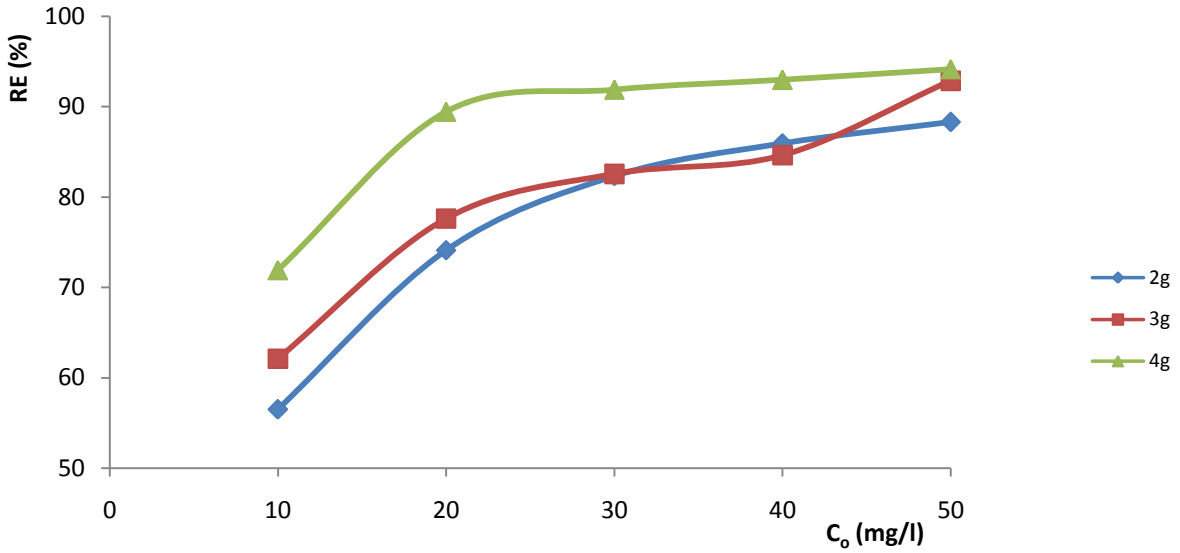


Fig 4.4: Effect of Initial concentration on Removal Efficiency *(RH300)*

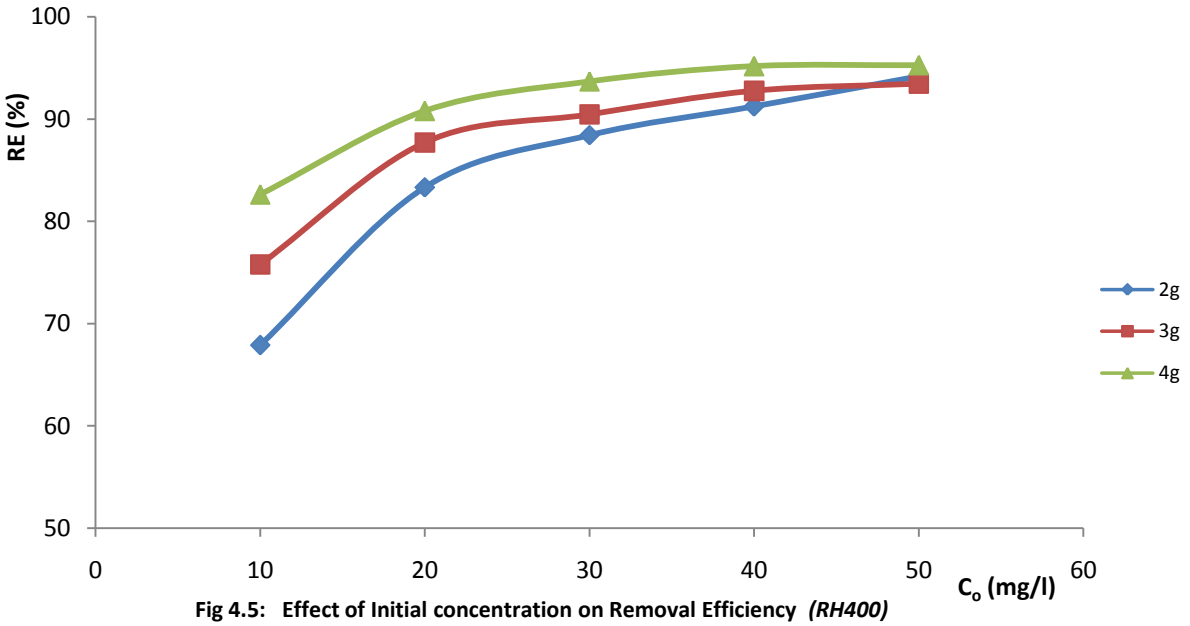


Fig 4.5: Effect of Initial concentration on Removal Efficiency *(RH400)*

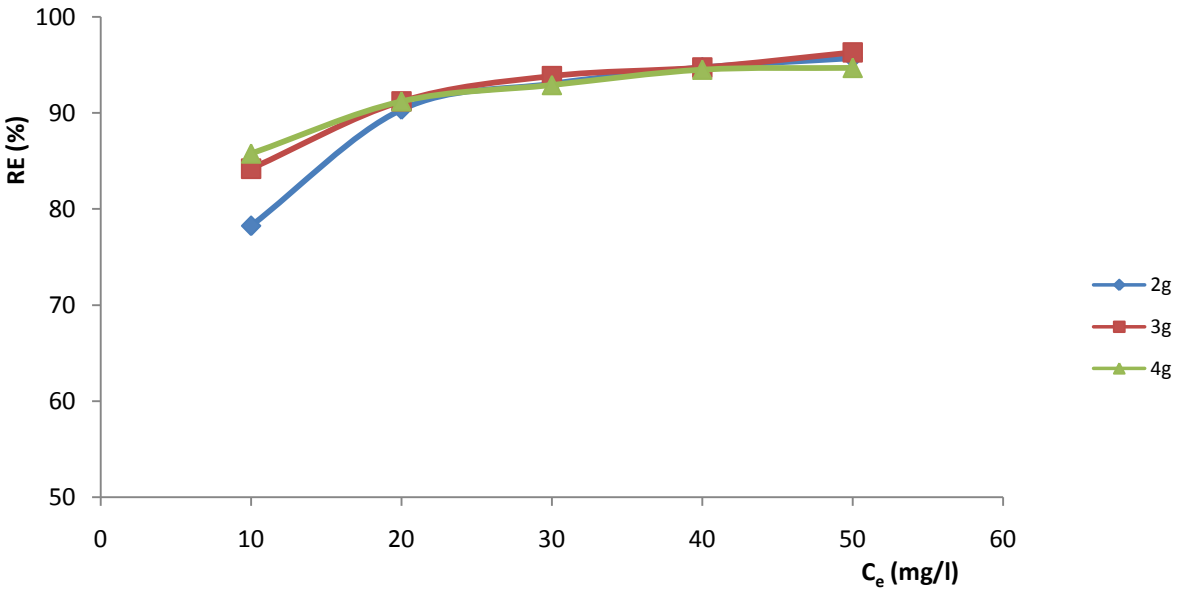


Fig 4.6: Effect of Initial concentration on Removal Efficiency *(RH500)*

4.2.2 Effect of adsorbent dosage

Effect of Adsorbent Dosage on Adsorption Capacity

Effect of adsorbent dosage of rice husk activated carbon on adsorption capacity was studied as presented in Fig. 4.7, 4.8 and 4.9. It was observed in Fig 4.7 (RH300) that when adsorbent dosage was increased from 2 to 4 g, the adsorption capacity decreased from 0.282 to 0.18 mg/g, 1.235 to 0.689 mg/g and 2.208 to 1.177 mg/g for 10 mg/l, 30 mg/l and 50 mg/l initial concentration respectively. The figure shows that adsorption capacity decreases with increase in adsorbent dosage. This could be attributed to the fact that at high adsorbent dosage the available phenol molecules are not able to cover all the exchangeable sites on the activated carbon resulting in low phenol uptake. Because the initial solute amount in solution remains unchanged, increase in adsorbent dosage provides more sorption sites thereby decreasing the ratio of solute uptake to sorption site, hence a decreasing adsorption capacity will be observed. This is similar to the observations of Ho and McKay (2004); Abdelwahab (2007); Vijayakumar *et al*. (2012).

For RH400, Fig 4.8 shows that increase in adsorbent dosage from 2 to 4 g resulted in decrease in adsorption capacity from 0.339 to 0.207 mg/g, 1.326 to 0.703 mg/g and 2.354 to1.191 mg/g for 10 mg/l, 30 mg/l and 50 mg/l of initial concentration respectively. The observed trend is similar to that of RH300. It was also observed in Fig 4.9 for RH500 that adsorption capacity decreased from 0.391 to 0.214 mg/g, 1.396 to 0.697 mg/g and 2.393 to 1.184 mg/g for 10 mg/l, 30 mg/l and 50 mg/l initial concentration respectively as adsorbent dosage increased from 2 to 4 g. The condition shows a similar trend to that of RH300 and RH400.

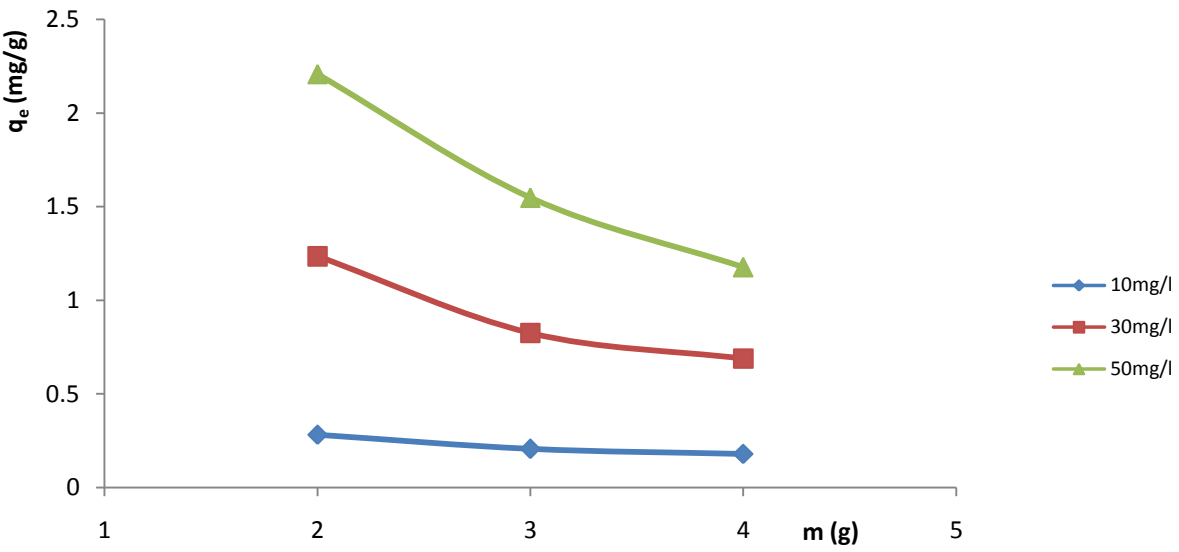


Fig 4.7: Effect of Adsorbent dosage on Adsorption Capacity *(RH300)*

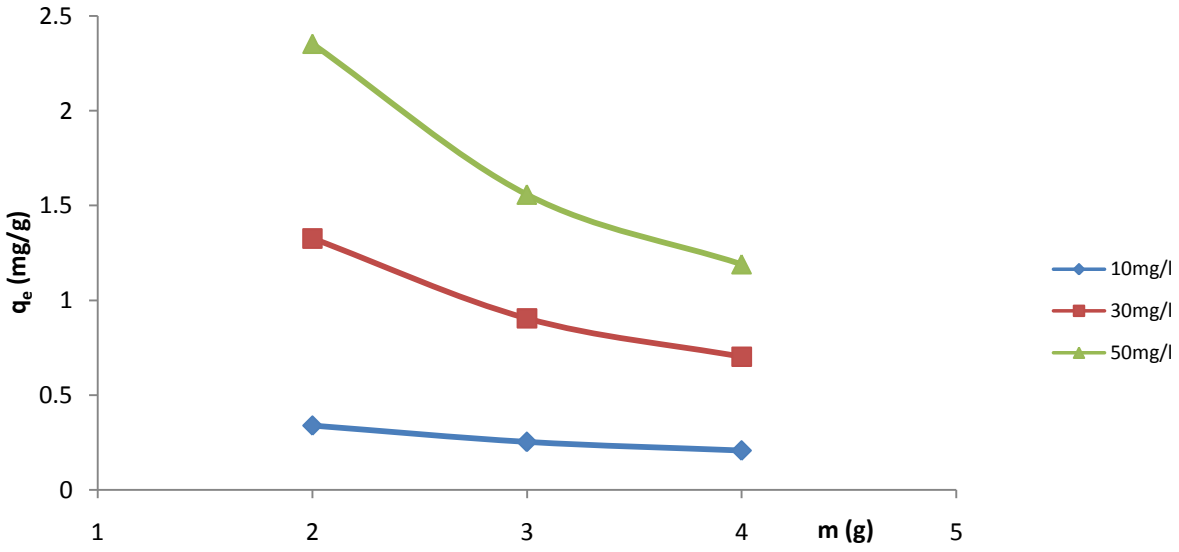


Fig 4.8: Effect of Adsorbent Dosage on Adsorption Capacity *(RH400)*

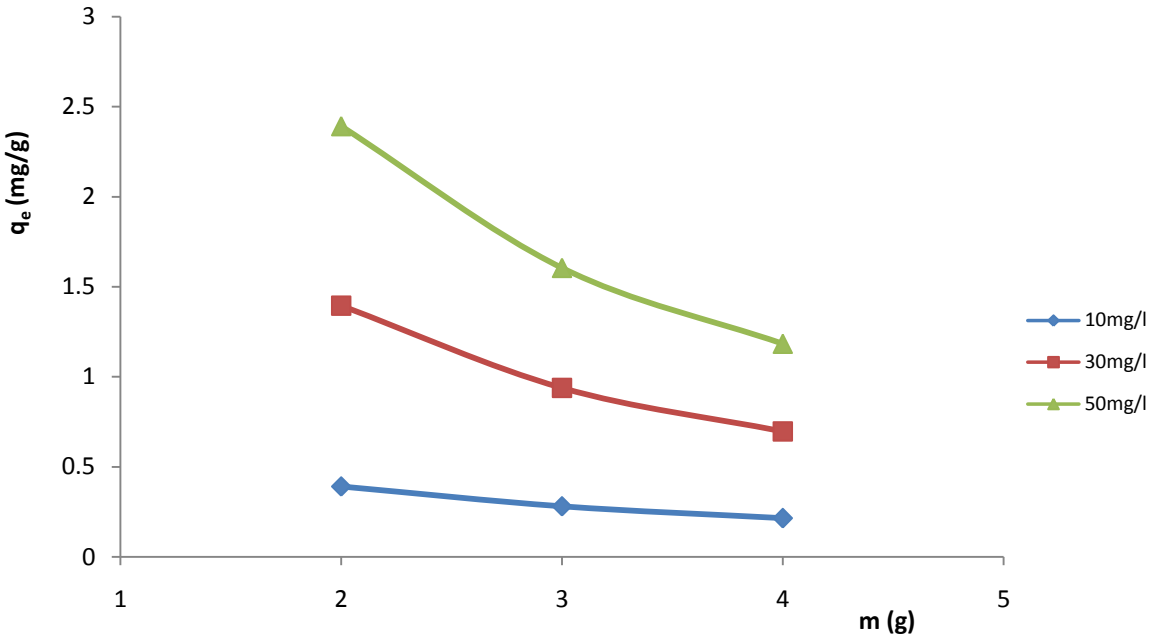


Fig 4.9: Effect of Adsorbent Dosage on Adsorption Capacity *(RH500)*

Effect of Adsorbent Dosage on Removal Efficiency

Effect of adsorbent dosage of rice husk activated carbon on removal efficiency was assessed as presented in Fig. 4.10, 4.11 and 4.12. It was observed in Fig 4.10 for RH300 that removal efficiency increased from 56.49 to 71.93 %, 82.34 to 91.91 % and 88.32 to 94.18 % for 10 mg/l, 30 mg/l and 50 mg/l initial concentration respectively as adsorbent dosage increased from 2 to 4 g. The figure indicates that at low values of initial concentration, change in percentage removal efficiency resulting from a change in adsorbent dosage is larger than at high values of initial concentration. This change manifests such that the percentage removal efficiency increases with increase in adsorbent dosage. Increase in removal efficiency as a result of increase in adsorbent dosage is due to increased number of sites available for solute-sorbent interaction as more adsorbents are added. This means that as the number of sites available for adsorption increases while the initial amount of solute in solution remains unchanged, the amount of solute uptake on the sorption sites will be observed to increase. This is similar to observations of Al-Anber and Mohammed (2008); Awala and El Jamal (2011); Daffalla *et al*. (2012); Omar (2012).

It was also observed in Fig 4.11 (RH400) that when adsorbent dosage was increased from 2 to 4 g, the removal efficiency increased from 67.9 to 82.63 %, 88.42 to 93.68 % and 94.18 to 95.26 % for 10 mg/l, 30 mg/l and 50 mg/l of initial concentration respectively. The figure shows similar trend with that of RH400. For RH500, Fig 4.12 shows that increase in adsorbent dosage from 2 to 4 g resulted in 78.25 to 85.79 % increase in removal efficiency for 10 mg/l and 93.04 to 92.92 % and 95.72 to 94.7 % decrease in removal efficiency for 30 mg/l and 50 mg/l initial concentration respectively. The trend was observed to be simiar to that of RH300 and RH400.

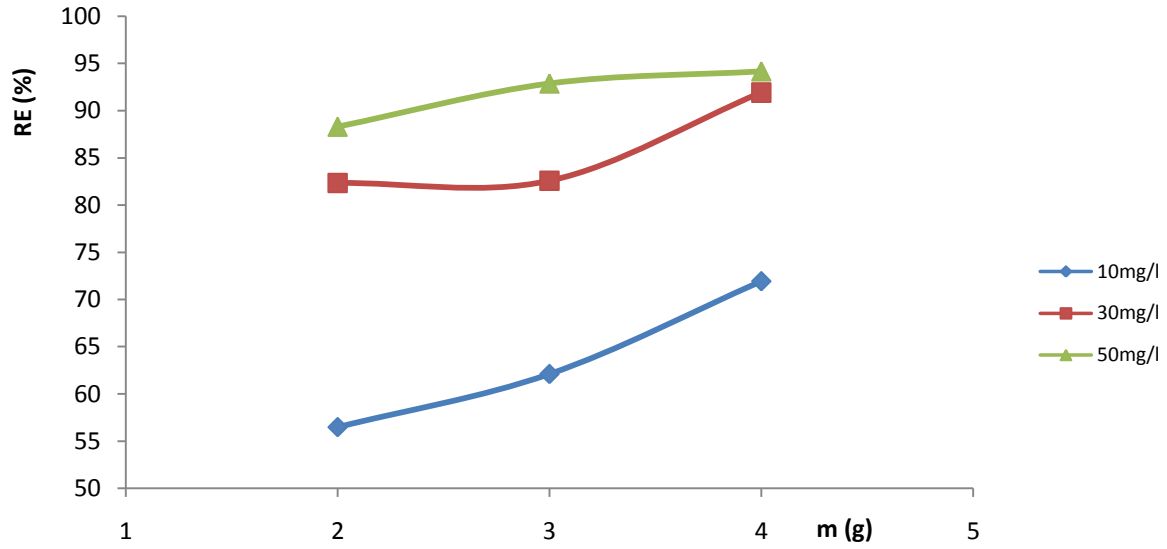


Fig 4.10: Effect of Adsoebent dosage on Removal Efficiency *(RH300)*

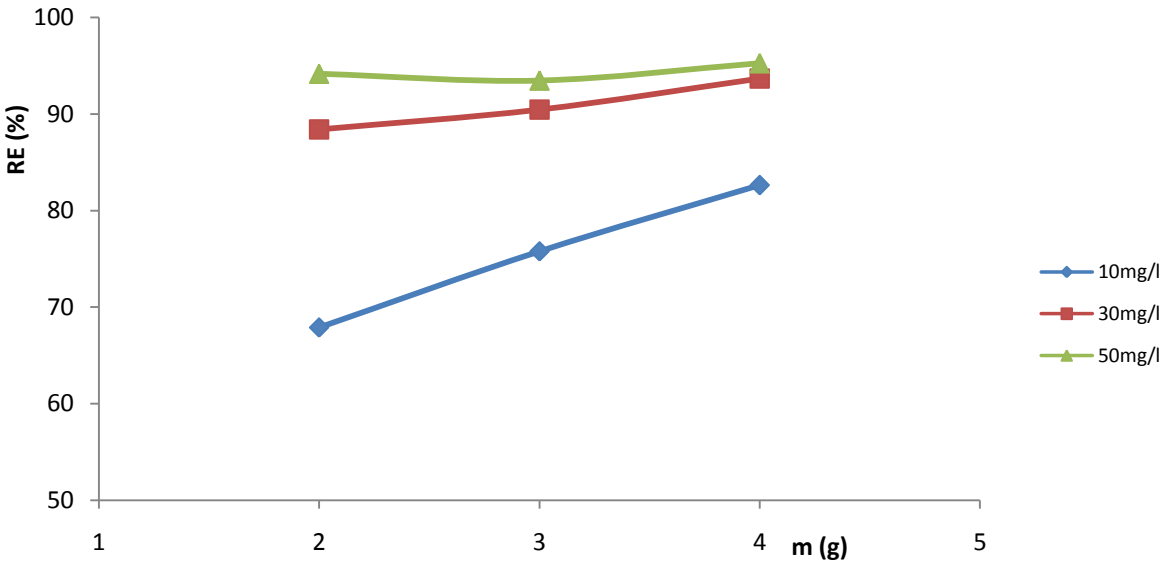


Fig 4.11: Effect of Adsorbent Dosage on Removal Efficiency *(RH400)*

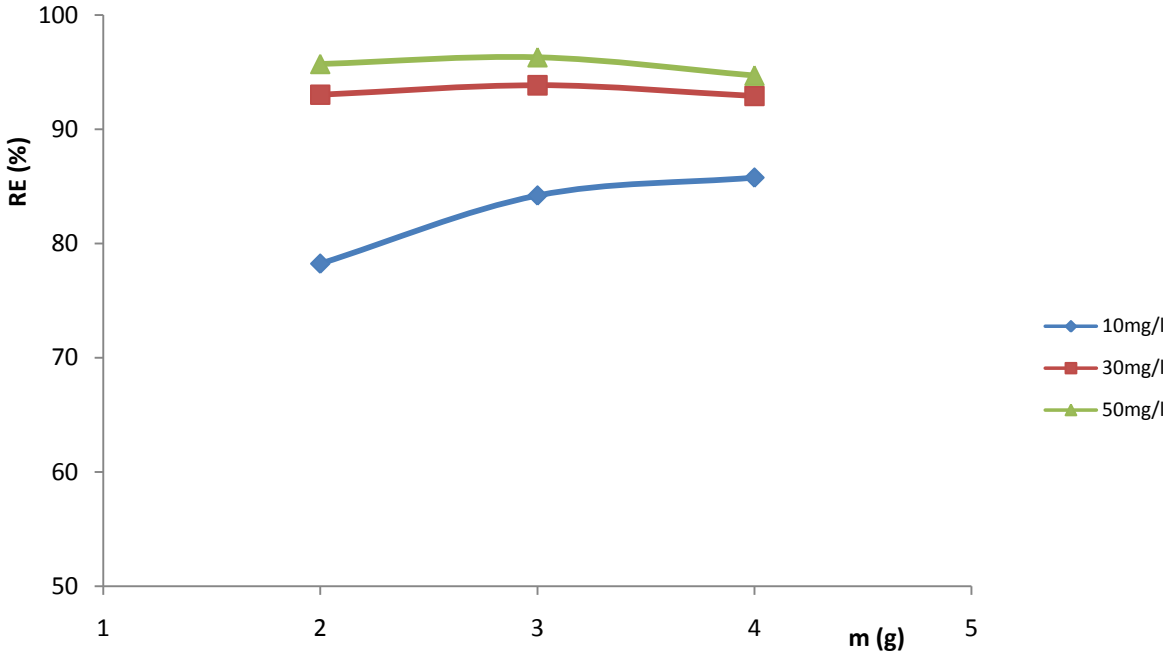


Fig 4.12: Effect of Adsorbent Dosage on Removal Efficiency *(RH500)*

4.2.3 Effect of contact time

Effect of contact time on adsorption capacity and removal efficiency was studied for the different pretreatment temeratures of 300, 400 and 500 ^{o}C and presented in Fig 4.13, 4.14, 4.15, 4.16, 4.17 and 4.18. It was observed in Fig 4.13 and 4.14 that for RH300, adsorption capacity and removal efficiency of 2.25 mg/g and 94.38 % were attained within 10 to 20 mins of contact time. It was also observed that large amount of phenol was adsorbed in the first 10-20 minutes of contact time. This initial fast rate of adsorption may be a consequence of the availability of several binding sites for solute uptake. The large amount of phenol removal in the first few minutes of contact time between solute and adsorbent may be due to increased surface area resulting from the influence of thermal pretreatment and improved (special) surface reactivity resulting from the influence of chemical pretreatment. Similar observation of large removal in less than 20 minutes was reported by Abdelwahab (2007); Potgieter *et al*. (2009); Awala and El Jamal (2011); Chowdhury *et al*. (2011); Galleti *et al*. (2012). Recent studies on the utilization of rice husk for adsorption of phenol by Mahvi *et al.* (2004); Kermani, *et al*. (2006); Kennedy *et al*. (2007); Daffalla *et al*., (n.d) show that the residence time observed for large removal was not less than 120 min. Mohd-Din *et al*. (2009) reported that rapid solute removal and immediate attainment of equilibrium signifies the efficiency of an adsorbent for wastewater treatment. In a batch adsorption process, agitation which is associated with energy and cost is a function of solute-sorbent residence time. A smaller residence time will require less agitation period than a larger residence time and this entails comparative energy/cost savings advantage. In Fig 4.13, percentage removal efficiency was observed to be unstable, though the change was not significant. Similarly, in Fig. 4.14, adsorption capacity was also observed to be

unstable. This instability could be as a result of simultaneous adsorption/desorption as was also observed by Abdelwahab *et al*. (2005); Belgin *et al*. (2008); Kalalagh *et al*. (2011); Galleti *et al*. (2012); Khdeem (2013).

Fig 4.15 and 4.16 also shows that, for RH400 adsorption capacity and removal efficiency of 2.36 mg/g and 96.14 % were attained within 10 to 20 mins of contact time. The figures shows similar trend to that of RH300. For RH500, it was observed in Fig 4.17 and 4.18 that adsorption capacity and removal efficiency of 2.4 mg/g and 96.49 % were attained within 10 to 20 mins of contact time. The figures show similar trend to that of RH300 and RH400.

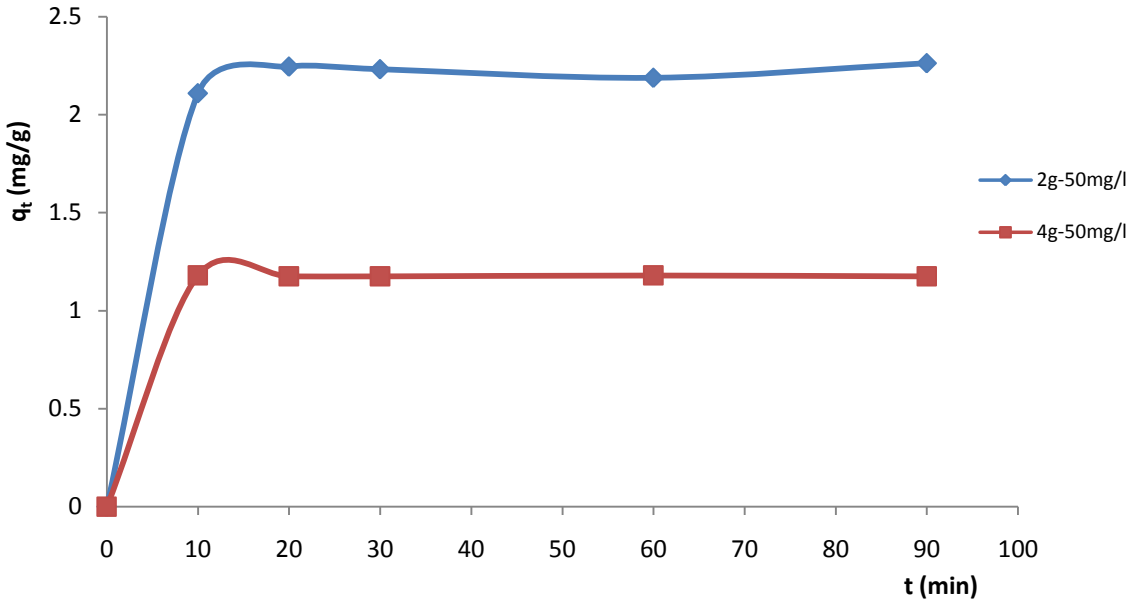


Fig 4.13: Effect of Contact time on Adsorption Capacity *(RH300)*

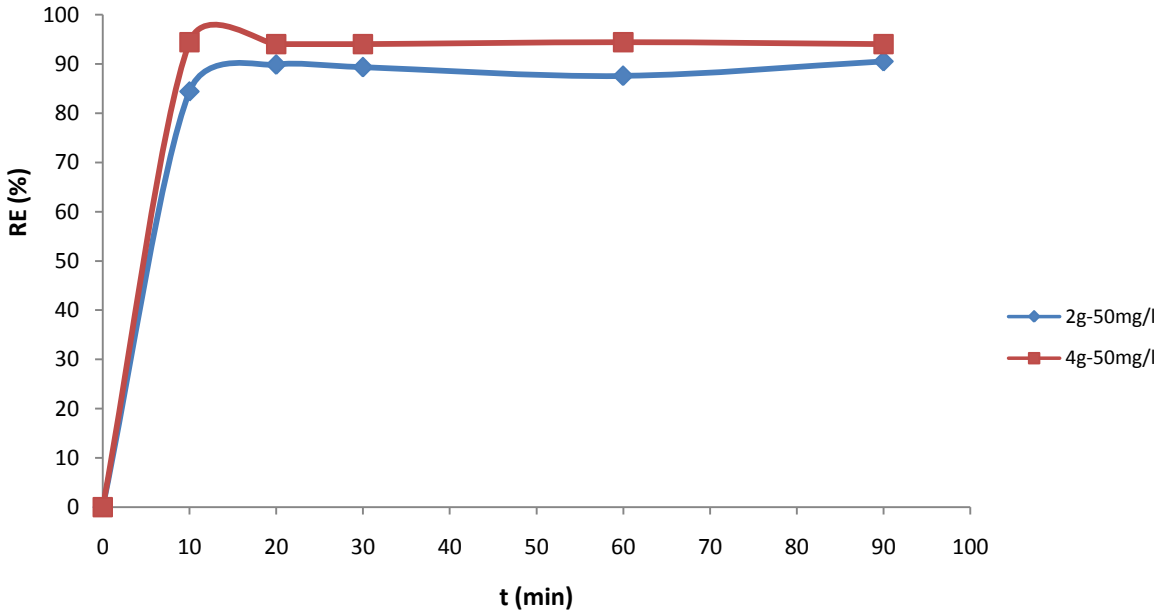


Fig 4.14: Effect of Contact time on Removal Efficiency *(RH300)*

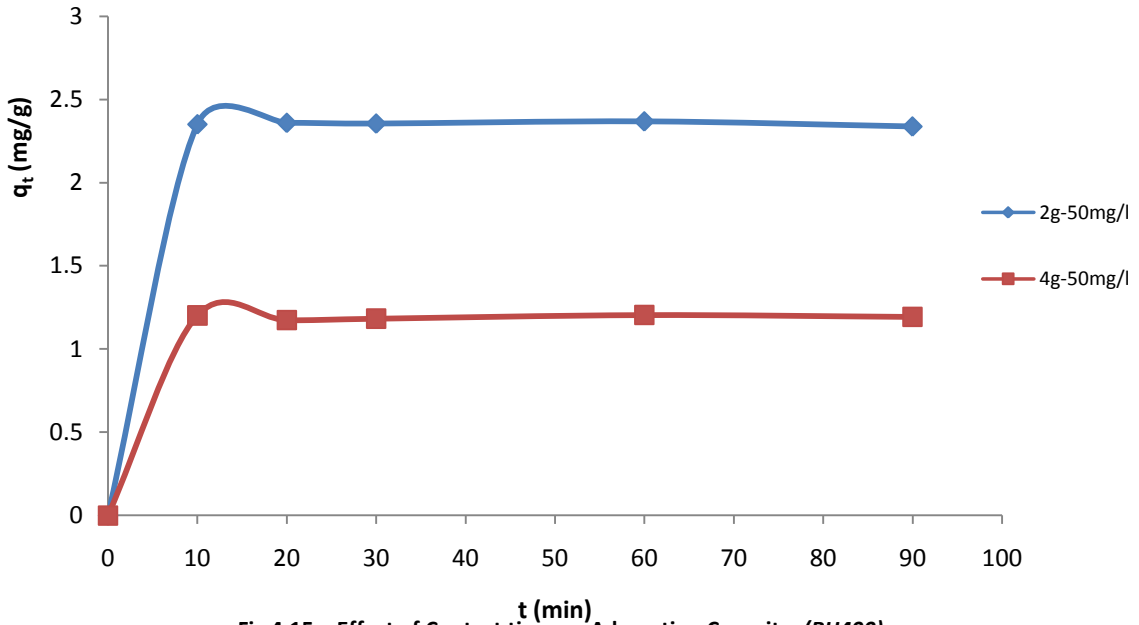


Fig 4.15: Effect of Contact time on Adsorption Capacity *(RH400)*

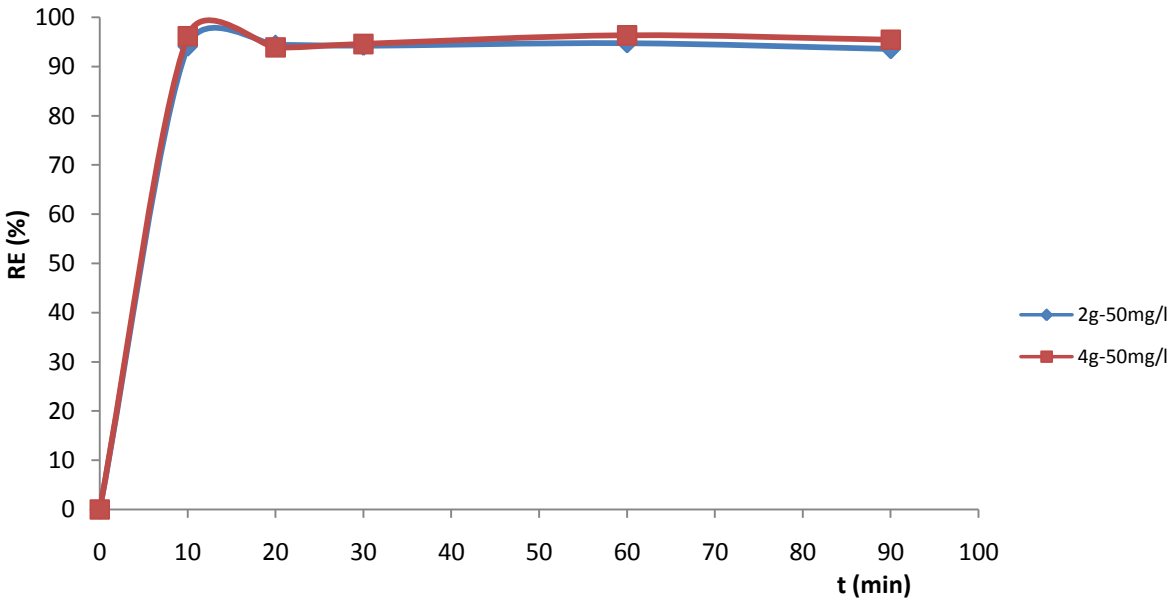


Fig 4.16: Effect of Contact time on Removal Efficiency *(RH400)*

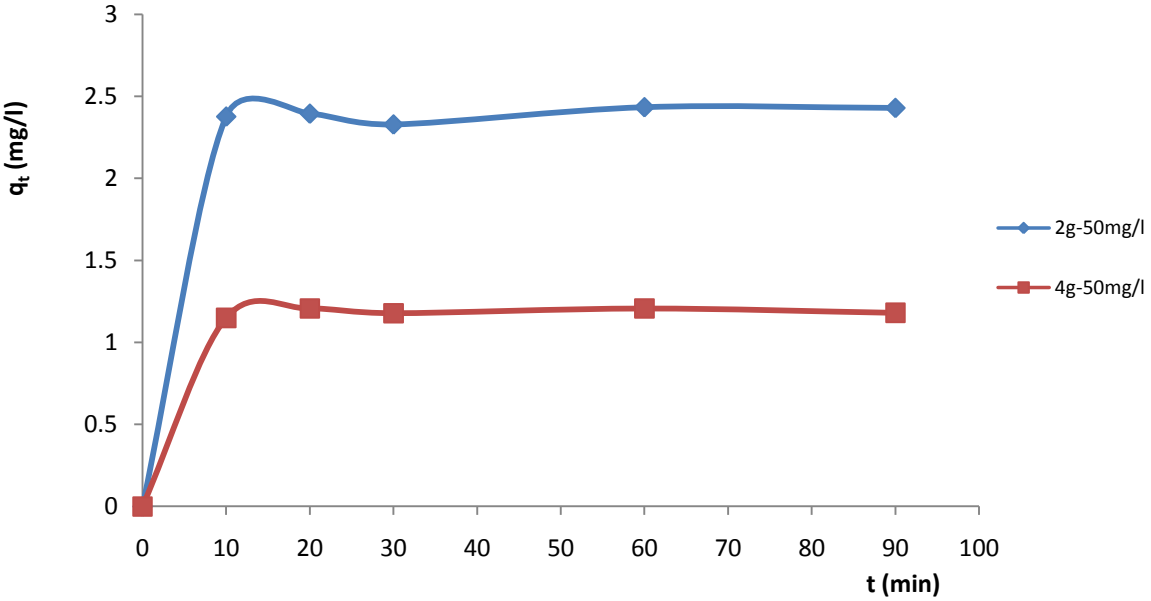


Fig 4.17: Effect of Contact time on Adsorption Capacity *(RH500)*

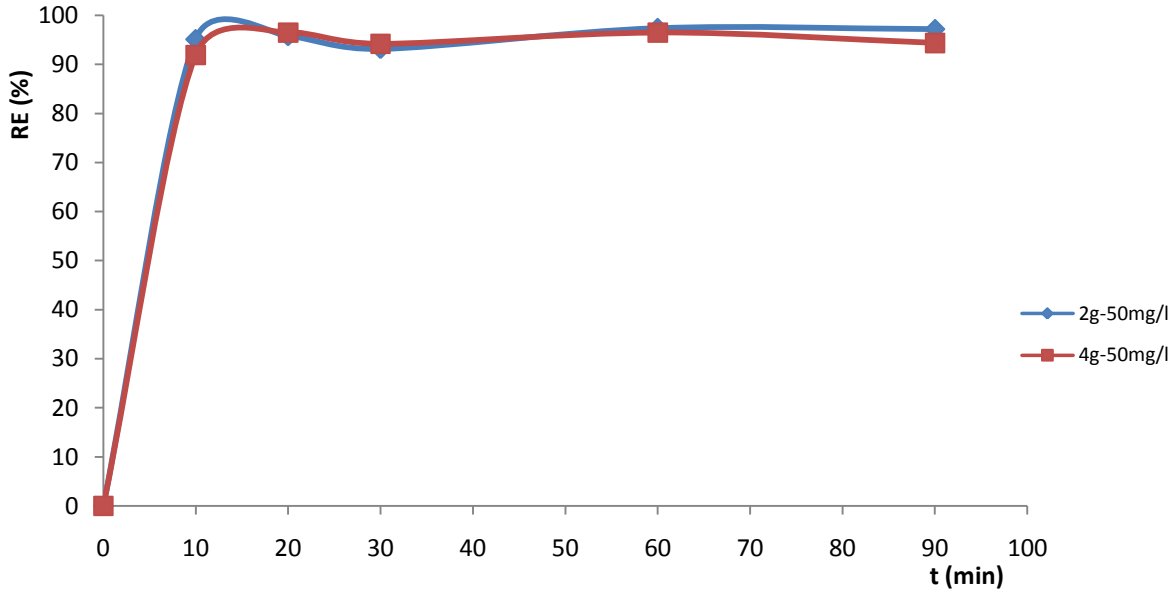


Fig 4.18: Effect of Contact time on Removal Efficiency *(RH500)*

4.2.4 Effect of pre-treatment (carbonization) temperature

Influence of rice husk activated carbon pretreatment temperature on the adsorption of phenol was studied as presented in Fig 4.19, 4.20, 4.21 and 4.22. It was observed in Fig 4.19 that at initial concentration of 10 mg/l, removal efficiency increased from 56.49 to 78.25 % when carbonization temperature was increased from 300 to 500 ^{o}C, but the increase in removal efficiency was observed to be lower as initial concentration was increased to 50 mg/l. This increase could be as a result of the availability of more binding sites resulting from improved surface area at higher carbonization temperature. While Fig. 4.20 shows that as the adsorbent dosage was increased to 4 g, increasing carbonization temperature from 300 to 500 ^{o}C resulted in increase in removal efficiency from 71.93 to 85.79 % for initial concentrations of 10 mg/l. Thereafter, it was also observed that, as the initial concentration was increased from 20 to 50 mg/l, carbonization temperature has little or no significant influence on removal efficiency.

Fig. 4.21 shows that at adsorbent dosage of 2 g, adsorption capacity is slightly dependent on carbonization temperature, while Fig. 4.22 shows that at adsorbent dosage of 4 g, adsorption capacity is relatively independent of the carbonization temperature.

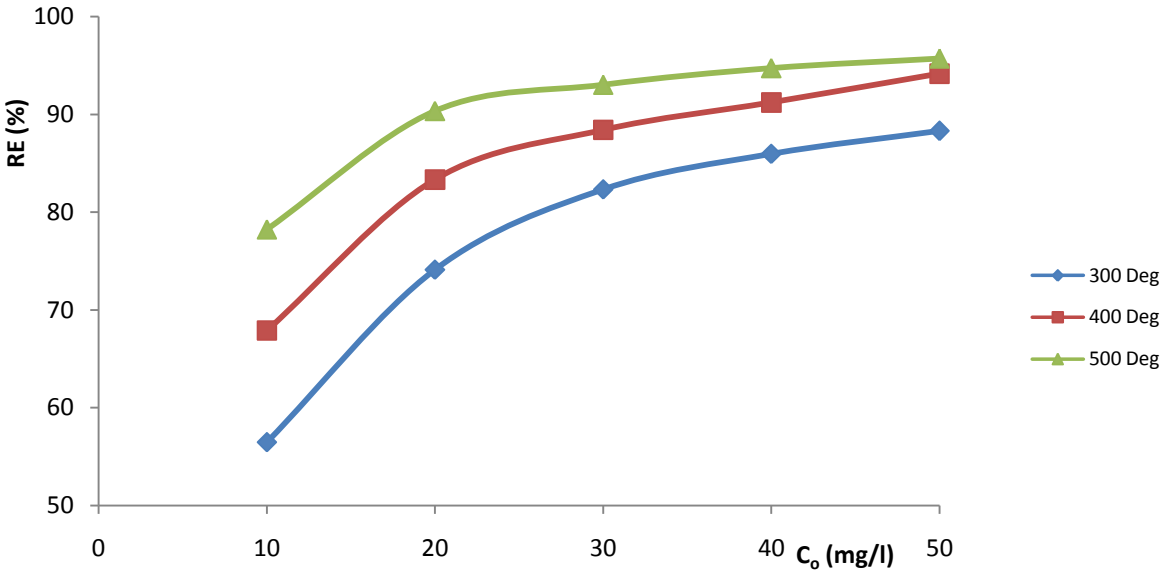


Fig 4.19: Effect of Pretreatment Temperature on Removal Efficiency, m=2g

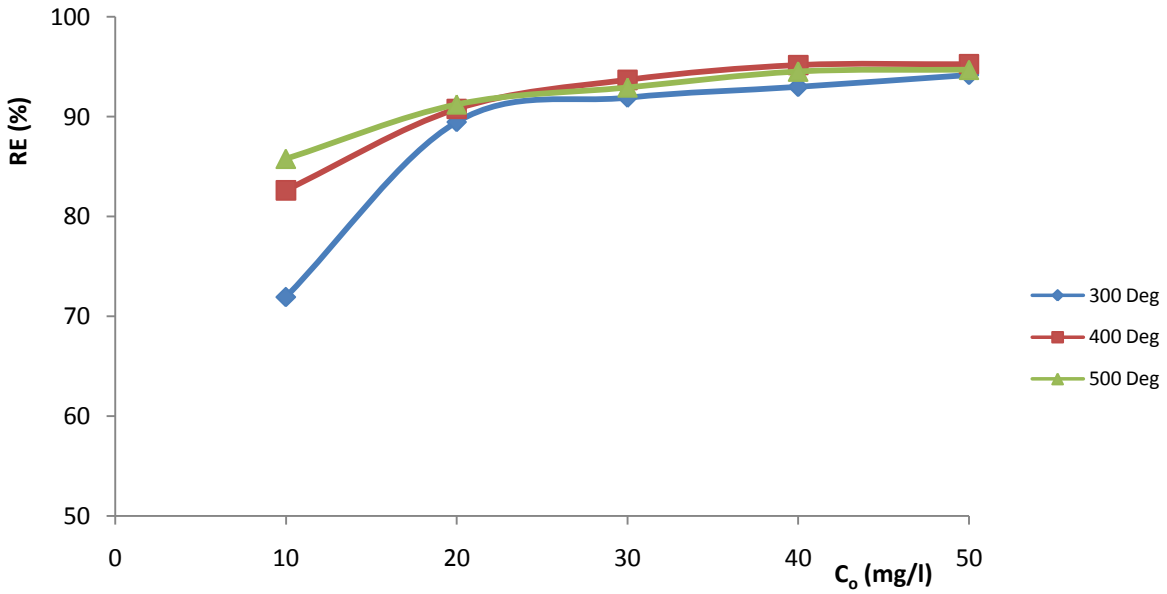


Fig 4.20: Effect of Pretreatment Temperature on Removal Efficiency, m=4g

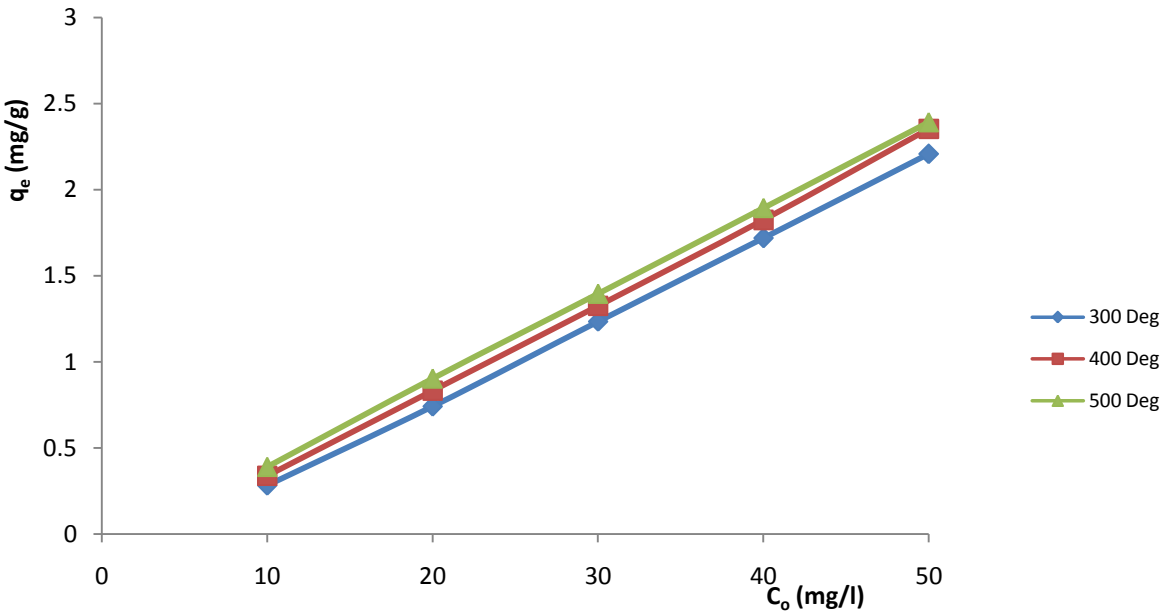


Fig 4.21: Effect of Pretreatment Temperature on Adsorption Capacity, m=2g

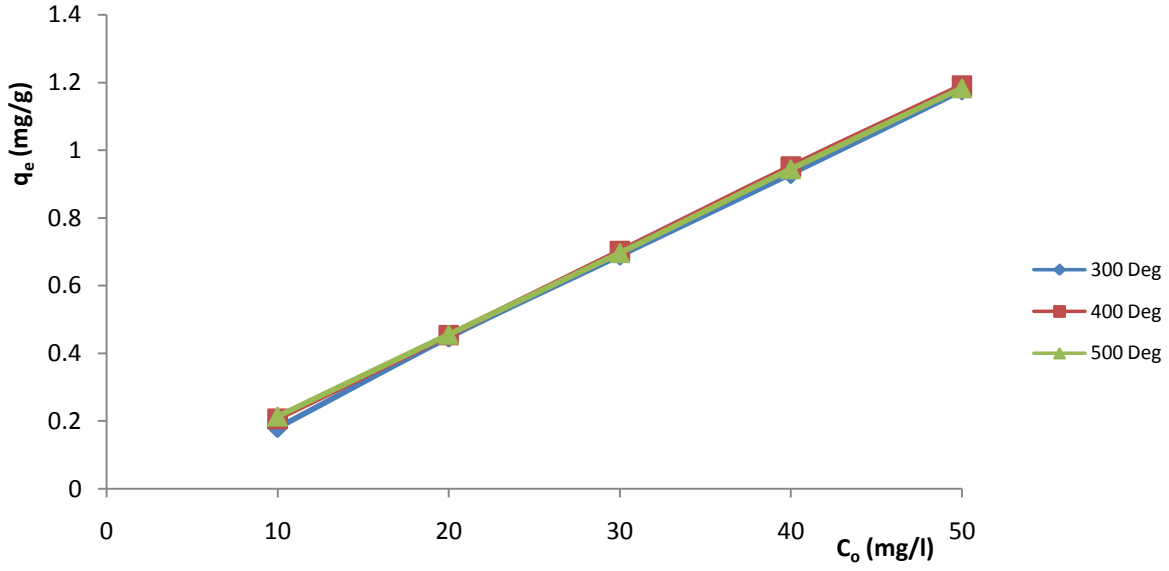


Fig 4.22: Effect of Pretreatment Temperature on Adsorption Capacity, m=4g

4.2.5 Effect of solution pH

It was observed in Fig. 4.23 that when pH was increased from 2 to 4, adsorption capacity increased from 0.960 to 0.965 mg/g, and thereafter adsorption capacity was observed to decrease progressively. Fig 4.24 shows that removal efficiency increased from 94.6 to 95.03 % as pH increased from 2 to 4, and thereafter removal efficiency was also observed to decrease progressively. Therefore, the optimum pH for phenol adsorption was taken as 4.

The pKa of phenol, a weak acid is 9.89 and as a result, phenol is usually dissociated at pH>pKa. In a phenol solution, when pH<pKa of phenol, the molecular form of phenol is the predominating specie which are either neutral or positively charged. Therefore, maximum adsorption performance is observed at low pH because phenol is not dissociated and the driving force for adsorption is dispersion interaction (Busca *et al*., 2008; Hameed and Rahman, 2008; Nabais *et al*., 2009; Soto *et al*., 2011). But when pH>pKa, the ionic form, which is a consequence of the aromatic ring being partially negatively charged by means of the hydroxyl group ionization (equ 4.1), is the predominating specie. This leads to electrostatic repulsion between phenolate ions and negatively charged activated carbon surfaces consequent upon which a significant decrease in adsorption is observed (Nabais *et al*., 2009). According to Busca *et al*. (2008), these phenolate ions are more soluble in aqueous solution and the stronger adsorbate-water molecule must be overcome before adsorption takes place. Similar trend was also reported by Kennedy *et al*. (2007).

$$C_6H_5OH + H_2O \Longleftrightarrow C_6H_5O^- + H_3O^+ \qquad (4.1)$$

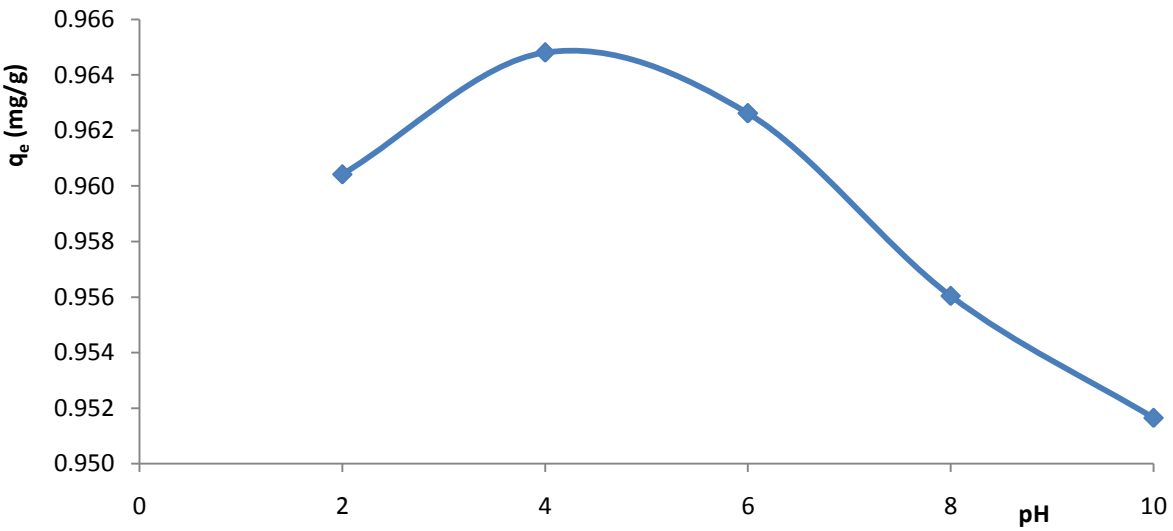


Fig. 4.23: Effect of pH on Adsorption Capacity

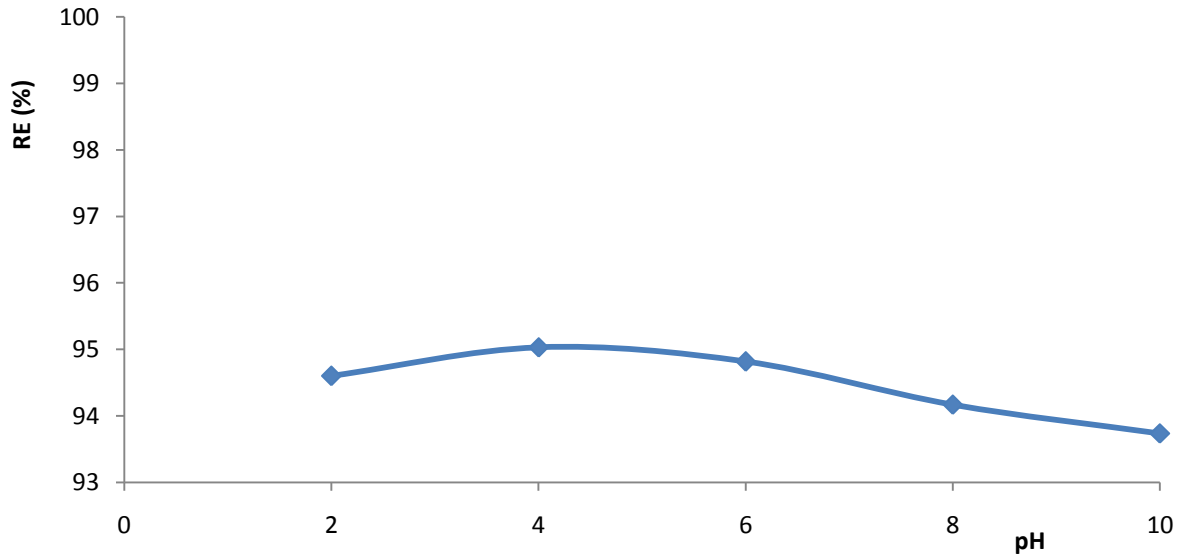


Fig. 4.24: Effect of pH on Removal efficiency

4.2.6 Effect of solution temperature

It was observed in Fig. 4.25 that when temperature was increased from 30 to 50 ^{o}C adsorption capacity decreased from 0.958 to 0.948 mg/g. Fig 4.26 shows that removal efficiency also decreased from 94.38 to 93.52 % as the temperature increased from 30 to 50 ^{o}C. Therefore, it implies that low temperatures favour higher adsorption capacity and removal efficiency most probably because adsorption process is exothermic. This observation is in agreement with the trend reported by Ozturk and Kavak (2005); Kennedy *et al*. (2007); Daffalla *et al*. (n.d).

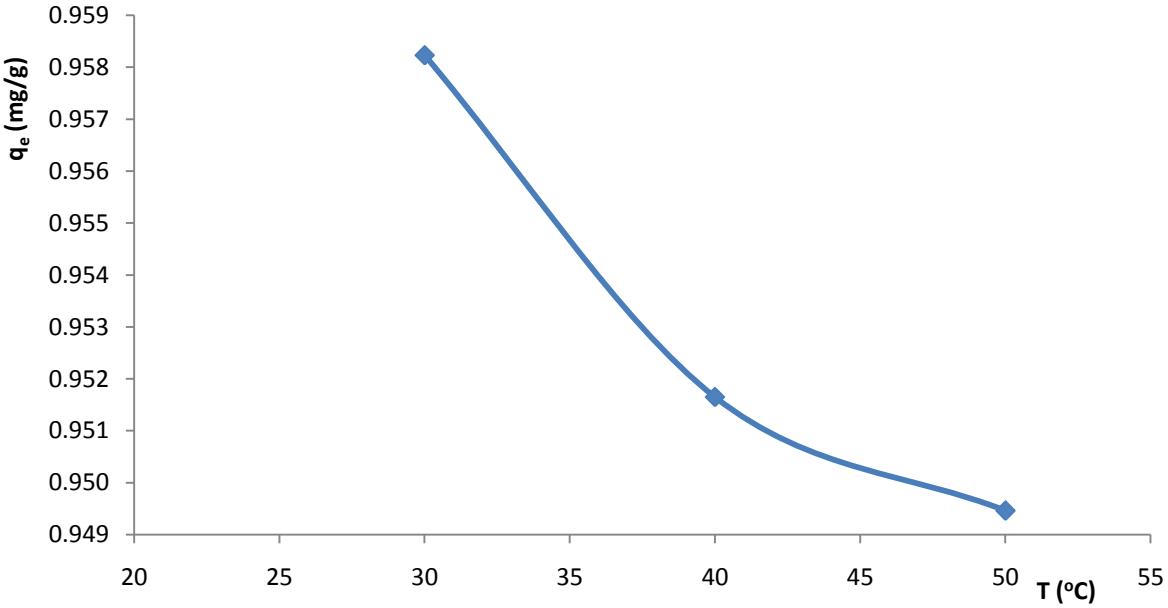


Fig. 4.25: Effect of Temperature on Adsorption Capacity

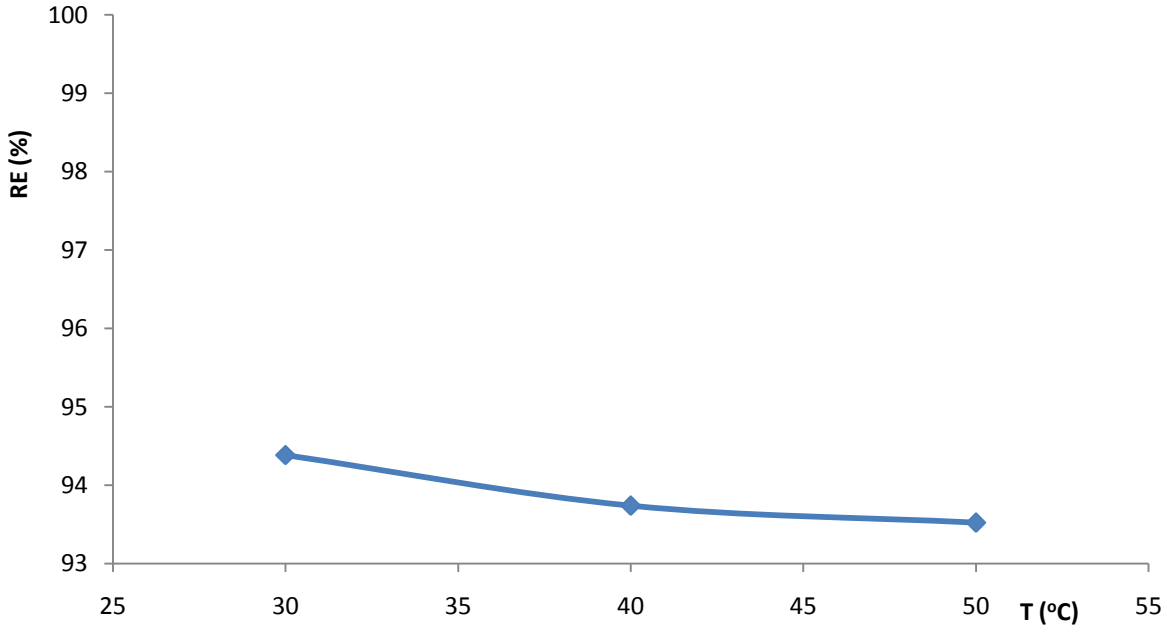


Fig. 4.26: Effect of Temperature on Removal Efficiency

4.3 Adsorption Isotherm, Kinetics and Thermodynamic Models

4.3.1 Adsorption isotherms

A. Langmuir Isotherm

Parameters for Langmuir isotherm are presented in Table 4.7, 4.8 and 4.9. It was observed in Table 4.7 that for RH300, maximum monolayer adsorption capacity (q_m) of 0.112 mg/g, 0.198 mg/g and 0.398 mg/g were obtained for 2 g, 3 g and 4 g adsorbent dosage respectively and these are less than the corresponding experimental adsorption capacity ($q_{e,exp}$). Therefore, the obtained maximum monolayer adsorption capacity (q_m) from the experimental data deduced from the Langmuir isotherm model were less than the experimental adsorption capacity indicating that the maximum amount of phenol monolayer coverage on a unit of rice husk activated carbon was exceeded by the experimental value ($q_{e,exp}$); hence the adsorption process is inconsistent with the Langmuir assumption. This trend suggests the existence of multilayer adsorption phenomenon meaning that phenol molecules deposit on not only the free surface of the rice husk activated carbon but also on already adsorbed ones, that is sorption sites accommodate more than one phenol molecules. This could be the reason for the earlier observation of increase in removal efficiency as the initial concentration increases.

For RH400, Table 4.8 shows that maximum monolayer adsorption capacity of 0.042 mg/g, 0.375 mg/g and 0.03 mg/g were obtained for 2 g, 3 g and 4 g adsorbent dosage and these are also less than the corresponding experimental adsorption capacity. This observation is similar to that of RH300. It was also observed in Table 4.9 that for RH500, maximum monolayer adsorption capacity of 0.177 mg/g, 0.140 mg/g and 0.197 mg/g were obtained

for 2 g, 3 g and 4 g adsorbent dosage and these are less than the corresponding experimental adsorption capacity. This observation is similar to that of RH300 and RH400.

Table 4.7: Langmuir Adsorption Isotherm Data *(RH300)*

m (g)	C_o (mg/l)	C_e (mg/l)	C_e/q_e (g/l)	$q_{e, exp}$ (mg/g)	-b	q_m (mg/g)	R^2	$q_{e, cal}$ (mg/g)
2	10	4.351	15.404	0.282	0.167	0.112	0.945	0.298
2	20	5.175	6.982	0.741	0.167	0.112	0.945	0.716
2	30	5.298	4.290	1.235	0.167	0.112	0.945	0.864
2	40	5.614	3.265	1.719	0.167	0.112	0.945	1.694
2	50	5.842	2.646	2.208	0.167	0.112	0.945	4.576
3	10	3.789	18.305	0.207	0.147	0.198	0.749	0.247
3	20	4.474	8.644	0.518	0.147	0.198	0.749	0.377
3	30	5.228	6.331	0.826	0.147	0.198	0.749	0.649
3	40	6.140	5.440	1.129	0.147	0.198	0.749	1.783
3	50	3.561	2.301	1.548	0.147	0.198	0.749	0.216
4	10	2.807	15.610	0.180	0.255	0.398	0.950	0.997
4	20	2.105	4.706	0.447	0.255	0.398	0.950	0.460
4	30	2.426	3.520	0.689	0.255	0.398	0.950	0.643
4	40	2.807	3.019	0.930	0.255	0.398	0.950	0.997
4	50	2.912	2.474	1.177	0.255	0.398	0.950	1.142

Table 4.8: Langmuir Adsorption Isotherm Data *(RH400)*

m (g)	C_o (mg/l)	C_e (mg/l)	C_e/q_e (g/l)	$q_{e, exp}$ (mg/g)	-b	q_m (mg/g)	R^2	$q_{e, cal}$ (mg/g)
2	10	3.211	9.457	0.339	0.280	0.042	0.891	0.376
2	20	3.333	4.000	0.833	0.280	0.042	0.891	0.591
2	30	3.474	2.619	1.326	0.280	0.042	0.891	1.488
2	40	3.509	1.923	1.825	0.280	0.042	0.891	2.326
2	50	2.912	1.237	2.354	0.280	0.042	0.891	0.187
3	10	2.421	9.583	0.253	0.252	0.375	0.857	0.585
3	20	2.456	4.200	0.585	0.252	0.375	0.857	0.608
3	30	2.860	3.161	0.905	0.252	0.375	0.857	0.964
3	40	2.895	2.340	1.237	0.252	0.375	0.857	1.008
3	50	3.263	2.095	1.558	0.252	0.375	0.857	1.726
4	10	1.737	8.408	0.207	0.508	0.030	0.978	0.222
4	20	1.842	4.058	0.454	0.508	0.030	0.978	0.429
4	30	1.895	2.697	0.703	0.508	0.030	0.978	0.752
4	40	1.930	2.028	0.952	0.508	0.030	0.978	1.445
4	50	2.368	1.989	1.191	0.508	0.030	0.978	0.176

Table 4.9: Langmuir Adsorption Isotherm Data *(RH500)*

m (g)	C_o (mg/l)	C_e (mg/l)	C_e/q_e (g/l)	$q_{e, exp}$ (mg/g)	-b	q_m (mg/g)	R^2	$q_{e, cal}$ (mg/g)
2	10	2.175	5.561	0.391	0.432	0.177	0.932	2.764
2	20	1.930	2.136	0.904	0.432	0.177	0.932	0.889
2	30	2.088	1.496	1.396	0.432	0.177	0.932	1.629
2	40	2.105	1.111	1.895	0.432	0.177	0.932	1.780
2	50	2.140	0.894	2.393	0.432	0.177	0.932	2.173
3	10	1.579	5.625	0.281	0.445	0.140	0.751	0.332
3	20	1.754	2.885	0.608	0.445	0.140	0.751	0.501
3	30	1.842	1.963	0.939	0.445	0.140	0.751	0.640
3	40	2.105	1.667	1.263	0.445	0.140	0.751	2.098
3	50	1.842	1.148	1.605	0.445	0.140	0.751	0.640
4	10	1.421	6.626	0.214	0.377	0.197	0.927	0.227
4	20	1.754	3.846	0.456	0.377	0.197	0.927	0.385
4	30	2.123	3.046	0.697	0.377	0.197	0.927	0.790
4	40	2.193	2.320	0.945	0.377	0.197	0.927	0.941
4	50	2.649	2.238	1.184	0.377	0.197	0.927	168.715

B. Freundlich Isotherm

Parameters for Freundlich isotherm are presented in Tables 4.10, 4.11 and 4.12. It was observed in Table 4.10 that for RH300, adsorption intensity of 7.09, 3.47 and 2.79 were obtained for 2 g, 3 g and 4 g adsorbent dosage respectively. It could also be observed from the table that adsorption intensity is greater than one, indicating co-operative or physical adsorption and this is supportive of the earlier multilayer physical adsorption process. The greater the value of $^{1}/n$, the less heterogeneous is the surface of the activated carbon but with high affinity between solute and adsorbent.

For RH400, Table 4.11 shows that adsorption intensity of 17.7, 3.51 and 14.39 were obtained for 2 g, 3 g and 4 g adsorbent dosages respectively. This observation is similar to that of RH300. It was also observed in Tables 4.12 that for RH500, adsorption intensity of 8.62, 5.23 and 3.18 were obtained for 2 g, 3 g and 4 g adsorbent dosage respectively. This observation shows a similar trend to that of RH300 and RH400.

This is in agreement with Potgieter *et al*. (2009); Gayatri and Ahmaruzzaman (2010); Hameed and Foo (2010); Dada *et al*. (2012). Similar trends of 1/n value greater than one were also observed by Maximova and Koumanova (2008); Awala and El-Jamal (2011); Nhapi *et al*. (2011); Moyo *et al*. (2012); Mallikarjun and Mise (2012); Khdeem *et al*. (2013). This possibility of a multilayer physical adsorption process is further supported by the relative goodness of fit of the experimental data to Freundlich than Langmuir isotherm.

Table 4.10: Freundlich Adsorption Isotherm Data *(RH300)*

m(g)	C_o (mg/l)	C_e (mg/l)	log q_e (mg/g)	log C_e (mg/l)	$q_{e,\,exp}$ (mg/g)	1/n	$10^{-3}\,k_f$	R^2	$q_{e,\,cal}$ (mg/g)
2	10	4.351	-0.549	0.639	0.282	7.091	0.008	0.974	0.271
2	20	5.175	-0.130	0.714	0.741	7.091	0.008	0.974	0.928
2	30	5.298	0.092	0.724	1.235	7.091	0.008	0.974	1.096
2	40	5.614	0.235	0.749	1.719	7.091	0.008	0.974	1.652
2	50	5.842	0.344	0.767	2.208	7.091	0.008	0.974	2.192
3	10	3.789	-0.684	0.579	0.207	3.471	2.377	0.945	0.242
3	20	4.474	-0.286	0.651	0.518	3.471	2.377	0.945	0.431
3	30	5.228	-0.083	0.718	0.826	3.471	2.377	0.945	0.740
3	40	6.140	0.053	0.788	1.129	3.471	2.377	0.945	1.294
3	50	3.561	0.190	0.552	1.548	3.471	2.377	0.945	0.195
4	10	2.807	-0.745	0.448	0.180	2.785	56.754	0.98	1.005
4	20	2.105	-0.349	0.323	0.447	2.785	56.754	0.98	0.451
4	30	2.426	-0.162	0.385	0.689	2.785	56.754	0.98	0.670
4	40	2.807	-0.032	0.448	0.930	2.785	56.754	0.98	1.005
4	50	2.912	0.071	0.464	1.177	2.785	56.754	0.98	1.114

Table 4.11: Freundlich Adsorption Isotherm Data *(RH400)*

m (g)	C_o (mg/l)	C_e (mg/l)	log q_e (mg/g)	log C_e (mg/l)	$q_{e, exp}$ (mg/g)	1/n	10^{-3} k_f	R^2	$q_{e, cal}$ (mg/g)
2	10	3.211	-0.469	0.507	0.339	17.7	3.945E-07	0.973	0.365
2	20	3.333	-0.079	0.523	0.833	17.7	3.945E-07	0.973	0.710
2	30	3.474	0.123	0.541	1.326	17.7	3.945E-07	0.973	1.472
2	40	3.509	0.261	0.545	1.825	17.7	3.945E-07	0.973	1.759
2	50	2.912	0.372	0.464	2.354	17.7	3.945E-07	0.973	0.065
3	10	2.421	-0.598	0.384	0.253	3.508	25.410	0.928	0.565
3	20	2.456	-0.233	0.390	0.585	3.508	25.410	0.928	0.594
3	30	2.860	-0.044	0.456	0.905	3.508	25.410	0.928	1.013
3	40	2.895	0.092	0.462	1.237	3.508	25.410	0.928	1.058
3	50	3.263	0.193	0.514	1.558	3.508	25.410	0.928	1.610
4	10	1.737	-0.685	0.240	0.207	14.39	0.072	0.997	0.202
4	20	1.842	-0.343	0.265	0.454	14.39	0.072	0.997	0.471
4	30	1.895	-0.153	0.278	0.703	14.39	0.072	0.997	0.706
4	40	1.930	-0.021	0.286	0.952	14.39	0.072	0.997	0.920
4	50	2.368	0.076	0.374	1.191	14.39	0.072	0.997	17.517

Table 4.12: Freundlich Adsorption Isotherm Data *(RH500)*

m (g)	C_o (mg/l)	C_e (mg/l)	log q_e (mg/g)	log C_e (mg/l)	$q_{e,\,exp}$ (mg/g)	1/n	$10^{-3}\,k_f$	R^2	$q_{e,\,cal}$ (mg/g)
2	10	2.175	-0.408	0.338	0.391	8.621	2.992	0.889	2.432
2	20	1.930	-0.044	0.286	0.904	8.621	2.992	0.889	0.866
2	30	2.088	0.145	0.320	1.396	8.621	2.992	0.889	1.706
2	40	2.105	0.278	0.323	1.895	8.621	2.992	0.889	1.833
2	50	2.140	0.379	0.330	2.393	8.621	2.992	0.889	2.114
3	10	1.579	-0.552	0.198	0.281	5.227	30.130	0.911	0.328
3	20	1.754	-0.216	0.244	0.608	5.227	30.130	0.911	0.569
3	30	1.842	-0.028	0.265	0.939	5.227	30.130	0.911	0.734
3	40	2.105	0.101	0.323	1.263	5.227	30.130	0.911	1.475
3	50	1.842	0.206	0.265	1.605	5.227	30.130	0.911	0.734
4	10	1.421	-0.669	0.153	0.214	3.179	71.945	0.979	0.220
4	20	1.754	-0.341	0.244	0.456	3.179	71.945	0.979	0.430
4	30	2.123	-0.157	0.327	0.697	3.179	71.945	0.979	0.787
4	40	2.193	-0.024	0.341	0.945	3.179	71.945	0.979	0.873
4	50	2.649	0.073	0.423	1.184	3.179	71.945	0.979	1.592

4.3.2 Adsorption kinetics

A. Pseudo-Second-Order Kinetics

Kinetics parameters are presented in Table 4.13, 4.14 and 4.15. It was observed in Table 4.13 that for RH300, theoretical equilibrium adsorption capacity of 2.263 mg/g, 1.54 mg/g and 1.18 mg/g were obtained for 2 g, 3 g and 4 g adsorbent dosages and this reasonably predicts the corresponding experimental equilibrium adsorption capacity. It was also observed that adsorption experimental data correlate very well with pseudo-second order rate model with correlation co-efficient of 0.9 to 1. Similar observation was also reported by El Shafey (2010).

For RH400, Table 4.14 shows that theoretical equilibrium adsorption capacity of 2.34 mg/g, 1.57 mg/g and 1.2 mg/g were obtained for 2 g, 3 g and 4 g adsorbent dosages and this also reasonably predicts the corresponding experimental equilibrium adsorption capacity. This observation is similar to that of RH300. It was also observed in Table 4.15 that for RH500, theoretical equilibrium adsorption capacity of 2.45 mg/g, 1.59 mg/g and 1.19 mg/g were obtained for 2 g, 3 g and 4 g adsorbent dosage and this reasonably predicts the corresponding experimental equilibrium adsorption capacity. This observation is similar to that of RH300 and RH400.

Table 4.13: Pseudo-Second-Order Kinetics Data *(C_o=50mg/l, RH300)*

m (g)	t (min)	$q_{t,\,exp}$ (mg/g)	t/q_t (gmin/mg)	q_e (mg/g)	k	R^2	$q_{t,\,cal}$ (mg/g)
2	10	2.110	4.740	2.262	8.278	0.999	2.235
2	20	2.246	8.906	2.262	8.278	0.999	2.249
2	30	2.232	13.438	2.262	8.278	0.999	2.253
2	60	2.189	27.415	2.262	8.278	0.999	2.258
2	90	2.263	39.767	2.262	8.278	0.999	2.259
3	10	1.547	6.465	1.541	15.876	1.000	1.531
3	20	1.544	12.955	1.541	15.876	1.000	1.536
3	30	1.558	19.250	1.541	15.876	1.000	1.538
3	60	1.550	38.717	1.541	15.876	1.000	1.539
3	90	1.541	58.406	1.541	15.876	1.000	1.540
4	10	1.180	8.476	1.176	59.000	1.000	1.174
4	20	1.175	17.015	1.176	59.000	1.000	1.175
4	30	1.175	25.522	1.176	59.000	1.000	1.176
4	60	1.180	50.855	1.176	59.000	1.000	1.176
4	90	1.175	76.567	1.176	59.000	1.000	1.176

Table 4.14: Pseudo-Second-Order Kinetics Data *(C_o=50mg/l, RH400)*

m (g)	t (min)	$q_{t,\ exp}$ (mg/g)	t/q_t (gmin/mg)	q_e (mg/g)	k	R^2	$q_{t,\ cal}$ (mg/g)
2	10	2.351	4.254	2.342	28.216	0.999	2.334
2	20	2.360	8.476	2.342	28.216	0.999	2.338
2	30	2.355	12.737	2.342	28.216	0.999	2.339
2	60	2.368	25.333	2.342	28.216	0.999	2.341
2	90	2.338	38.499	2.342	28.216	0.999	2.341
3	10	1.550	6.453	1.567	16.327	1.000	1.558
3	20	1.558	12.833	1.567	16.327	1.000	1.563
3	30	1.553	19.322	1.567	16.327	1.000	1.564
3	60	1.564	38.355	1.567	16.327	1.000	1.566
3	90	1.564	57.533	1.567	16.327	1.000	1.566
4	10	1.202	8.321	1.199	8.047	0.999	1.184
4	20	1.173	17.047	1.199	8.047	0.999	1.192
4	30	1.182	25.380	1.199	8.047	0.999	1.194
4	60	1.204	49.836	1.199	8.047	0.999	1.197
4	90	1.193	75.441	1.199	8.047	0.999	1.197

Table 4.15: Pseudo-Second-Order Kinetics Data *(C_o=50mg/l, RH500)*

m (g)	t (min)	$q_{t,\ exp}$ (mg/g)	t/q_t (gmin/mg)	q_e (mg/g)	k	R^2	$q_{t,\ cal}$ (mg/g)
2	10	2.377	4.207	2.451	9.249	0.999	2.425
2	20	2.395	8.352	2.451	9.249	0.999	2.438
2	30	2.329	12.881	2.451	9.249	0.999	2.442
2	60	2.434	24.649	2.451	9.249	0.999	2.447
2	90	2.430	37.040	2.451	9.249	0.999	2.448
3	10	1.611	6.207	1.590	7.395	0.999	1.569
3	20	1.605	12.459	1.590	7.395	0.999	1.579
3	30	1.605	18.689	1.590	7.395	0.999	1.583
3	60	1.620	37.040	1.590	7.395	0.999	1.586
3	90	1.585	56.790	1.590	7.395	0.999	1.587
4	10	1.149	8.702	1.186	24.713	0.999	1.181
4	20	1.206	16.582	1.186	24.713	0.999	1.184
4	30	1.178	25.475	1.186	24.713	0.999	1.185
4	60	1.206	49.745	1.186	24.713	0.999	1.185
4	90	1.180	76.283	1.186	24.713	0.999	1.186

B. Intra-Particle Diffusion Mechanism

Analysis of Intra-particle diffusion mechanism in Fig. 4.27, 4.28 and 4.29 shows that the plots did not pass through the origin and they are not linear; hence intra-particle diffusion (the rate at which solutes migrate from the external surface into the pores of the activated carbon), is not the only rate-limiting step. This implies that the mechanism of adsorption is also controlled by the transport of phenol molecules from bulk solution to the external surface of the rice husk activated carbon. In a solid-liquid adsorption process, the solute transfer is usually characterized by either external mass transfer or intraparticle diffusion or both. The initial step portion in the plot is due to the adsorption on the external surface and the second step is the gradual adsorption stage where intra-particle diffusion is rate controlling (Gottipati, 2012; Shih, 2012; Suteu and Malutan, 2013).

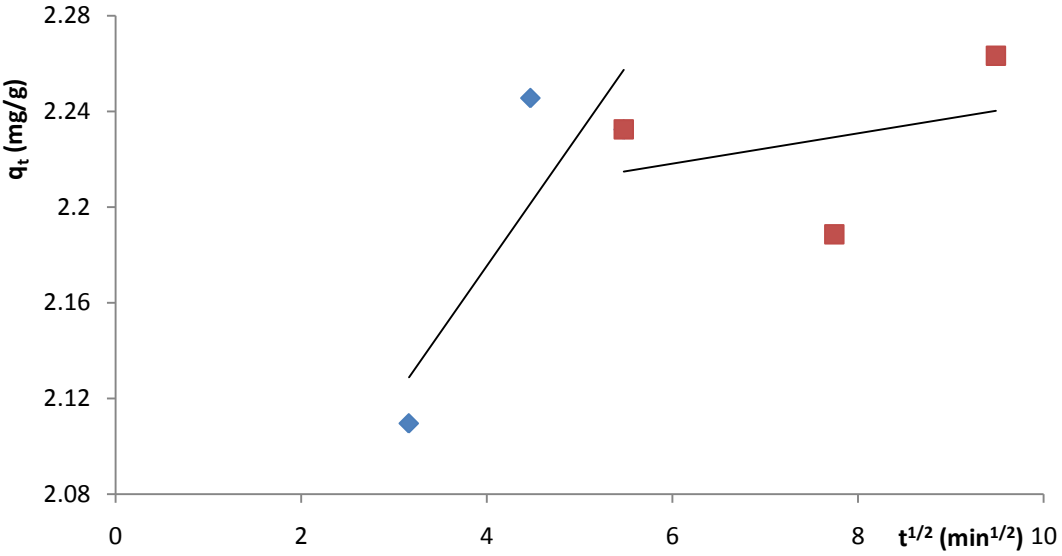


Fig 4.27: Intra-particle Diffusion Plot *(RH300)*

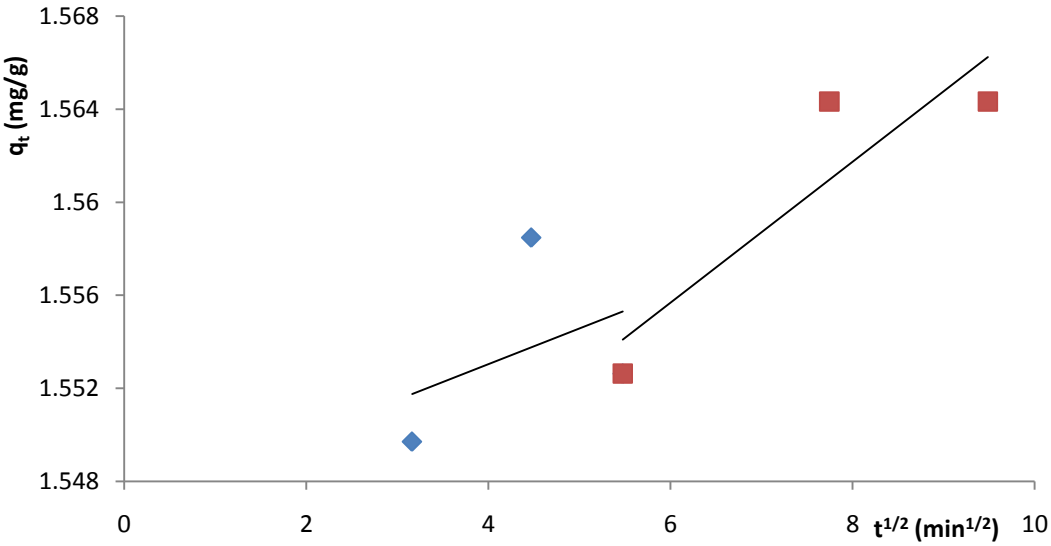


Fig 4.28: Intra-particle Diffusion Plot *(RH400)*

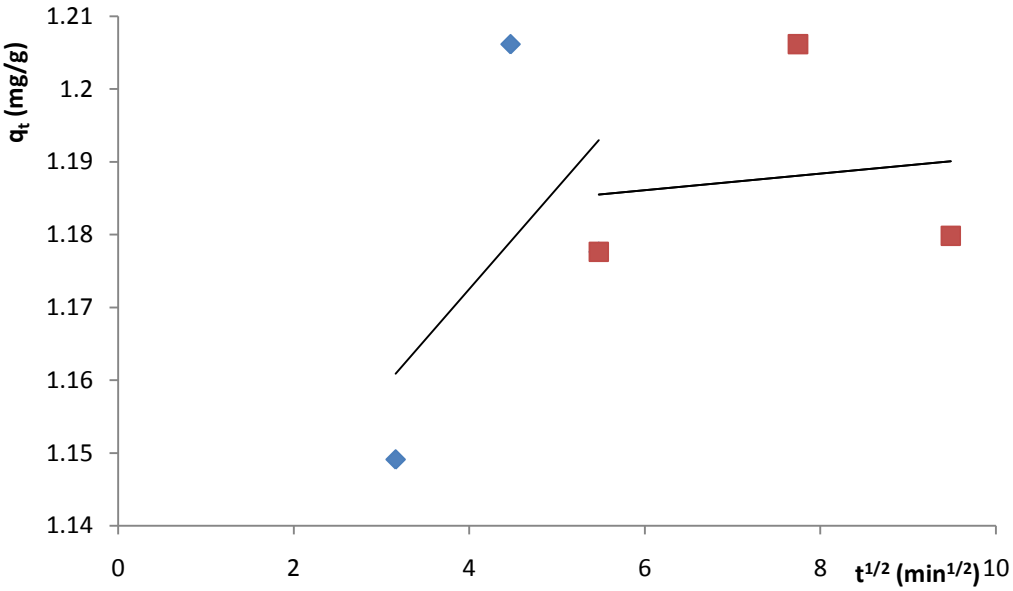


Fig 4.29: Intra-particle Diffusion Plot *(RH500)*

4.3.3 Adsorption thermodynamics

Thermodynamics parameters are presented in Table 4.16. It was observed from the table that the change in enthalpy of the adsorption process has negative value of -6.229 kJ/mol, this indicates that the adsorption process is exothermic. As it has been reported in literature, low negative value of change in enthalpy is an indication that physical adsorption is among the mechanism of the adsorption process (Khalir *et al*., 2012). The change in entropy was also observed to have negative value of -0.028 kJ/mol. According to Sadaf and Bhatti (2013), neagative values imply a decrease in disorder at the sorbent/solution interface. The Gibbs free energy was observed to have positive value and this value increased from 2.216 to 2.773 kJ/mol as the temperature was increased from 30 to 50 ^{o}C. Though this indicates that the process is not spontaneous, the weak positive values indicate that the process is feasible and the weaker values at lower temperatures imply that adsorption is favored at lower temperatures. This observation is in agreement with the earlier discussion on effect of temperature.

4.4 Comparative Study

Table 4.17 presents the results of the relative performance of the combined thermal and chemical pretreated rice husk activated carbon to thermal pretreated rice husk activated carbon. The table shows that combined pretreatment of rice husk yielded adsorption capacity and removal efficiency of 0.969 mg/g and 95.56 % while thermal pretreatment yielded adsorption capacity and removal efficiency of 0.559 mg/g and 58.96 % respectively. This implies that combined thermal and chemical pretreatment has higher influence on the adsorption of phenol in comparison to thermal pretreatment only.

Table 4.16: Adsorption Thermodynamics Data

T (k)	Ink (g/l)	1/T (k^{-1})	ΔG (kJ/mol)	ΔS (kJ/mol)	ΔH (kJ/mol)
303	-0.867	0.00330	2.216	-0.028	-6.229
313	-0.983	0.00319	2.495	-0.028	-6.229
323	-1.019	0.00310	2.773	-0.028	-6.229

Table 4.17: Comparison of Thermal and Combined Pre-Treatment

Pre-treatment Type	Temp (^oC)	m (g)	C_o (mg/l)	C_e (mg/l)	q_e (mg/g)	RE (%)
$RH_{TC(Thermal \& Chemical)}$	441.46	4	40.61	1.842	0.969	95.464
$RH_{T(Thermal)}$	441.46	4	40.61	16.667	0.599	58.959

4.5 Modeling and Optimization

4.5.1 Design of experiment

Table 4.18 shows the design matrix consisting of types of run, coded and actual factors as randomized by the Design Expert software (version 8) and the respective response obtained from the experiment.

Table 4.18: Design Matrix for the Factors and Respective Response from Experiment

		Coded Factors			Uncoded (Actual) Factors			Responses	
Run	**Type**	**A (^oC)**	**B (mg/l)**	**C (g)**	**A (^oC)**	**B (mg/l)**	**C (g)**	**Y_1 (%)**	**Y_2 (mg/g)**
1	Factorial	-1	1	-1	300	50	2	88.32	2.21
2	Factorial	1	1	1	500	50	4	94.70	1.18
3	Factorial	1	1	-1	500	50	2	95.72	2.39
4	Axial	1	0	0	500	30	3	93.86	0.94
5	Center	0	0	0	400	30	3	90.47	0.91
6	Axial	-1	0	0	300	30	3	82.57	0.83
7	Center	0	0	0	400	30	3	90.47	0.91
8	Factorial	-1	1	1	300	50	4	94.17	1.18
9	Axial	0	1	0	400	50	3	93.47	1.56
10	Center	0	0	0	400	30	3	90.47	0.91
11	Axial	0	-1	0	400	10	3	75.79	0.25
12	Axial	0	0	1	400	30	4	93.68	0.70
13	Factorial	-1	-1	-1	300	10	2	56.49	0.28
14	Factorial	1	-1	-1	500	10	2	78.25	0.39
15	Center	0	0	0	400	30	3	90.47	0.91
16	Factorial	-1	-1	1	300	10	4	71.93	0.18
17	Center	0	0	0	400	30	3	90.47	0.91
18	Center	0	0	0	400	30	3	90.47	0.91
19	Axial	0	0	-1	400	30	2	88.42	1.33
20	Factorial	1	-1	1	500	10	4	85.79	0.21

4.5.2 Development of model equations

Correlation between the response surface and factors were developed using Central Composite Design (CCD) of the Design Expert software. According to sequential model sum of squares, the models were selected based on the highest order polynomials where the additional terms were significant and the models were not aliased. Correlation coefficient (R^2) and standard deviation were used to evaluate the fitness of the models developed. The closer the R^2 value is to unity and the smaller the standard deviation, the better the model in predicting the response (Tan *et al.*, 2008b; Alam *et al*., 2009; Chaudhary and Balomajumder, 2013).

Table 4.19 shows that the quadratic model for response Y_1 was not aliased. It was also observed in the table that the quadratic model has relatively small standard deviation of 0.61 and relatively high R^2 value of 0.9979 with predicted R^2 (0.9960) in reasonable agreement with adjusted R^2 (0.9826). This implies that the quadratic model can most suitably be employed to describe the relationship between response Y_1 and the interacting variables. Table 4.20 shows that the quadratic model for response Y_2 was not aliased. It was also observed in the table that the quadratic model has relatively small standard deviation of 0.036 and relatively high R^2 value of 0.9981 with predicted R^2 (0.9819) in reasonable agreement with adjusted R^2 (0.9963). This implies that the quadratic model can most suitably describe the relationship between response Y_2 and the interacting variables.

The R^2 values of 0.9979 and 0.9981 implied that 99.79 % and 99.81 % of the variation in removal efficiency and adsorption capacity respectively can be attributed to the three factors considered (A-pretreatment temperature; B-initial phenol concentration and C-

adsorbent dosage). Therefore, the quadratic models were selected as deduced by the software and the response surface model equations in their actual values are as in equ (4.2) and equ (4.3):

$$Y_1 = 0.000217641A^2 - 0.014404B^2 + 0.65959C^2 - 0.00173025AB - 0.018465AC - 0.1137BC + 0.33625A + 2.38714B + 10.1384C - 51.11583 \quad (4.2)$$

$$Y_2 = -0.00000184545A^2 + 0.0000113636B^2 + 0.11355C^2 + 0.0000030625AB - 0.00031625AC - 0.012256BC + 0.00278124A + 0.070862B - 0.50129C - 0.12217 \quad (4.3)$$

Table 4.19: Model Summary Statistics for Response Y_1 (Removal Efficiency)

Source	Standard Deviation	R^2	Adjusted R^2	Predicted R^2	Comment
Linear	5.02	0.7729	0.7303	0.5487	
2FI	4.29	0.8653	0.8031	0.1189	
Quadratic	0.61	0.9979	0.9960	0.9826	Suggested
Cubic	0.056	1.0000	1.0000	0.9871	Aliased

Table 4.20: Model Summary Statistics for Response Y_2 (Adsorption Capacity)

Source	Standard Deviation	R^2	Adjusted R^2	Predicted R^2	Comment
Linear	0.19	0.9173	0.9018	0.8114	
2FI	0.073	0.9897	0.9850	0.9442	
Quadratic	0.036	0.9981	0.9963	0.9819	Suggested
Cubic	3.00E-03	1.0000	1.0000	0.9902	Aliased

Statistical Analysis

The model equations selected were further evaluated using ANOVA component of the software. From Table 4.21, response surface quadratic model for removal efficiency has F-value of 529.68 indicating that the model is significant. For the model terms, P-value less than 0.05 implies that model term is significant (Nasehir-Khan *et al*., 2010b; Rusly and Shaliza, 2010; Saadat and Karimi, 2011; Basu *et al*., 2012; Gottipati and Mishra, 2012) and largest F-value signifies the model term having the most significant effect on the response (Tan *et al.*, 2008b; Kalavathy *et al*., 2009). In this case, the significant model terms are A, B, C, AB, AC, BC, A^2 and B^2 while C^2 is the insignificant model term. The model term having the most significant effect on the response is B with F-value of 2589.51 and the significance of the effect is in the order B>A>C>AB>B2>BC>AC>A^2. Table 4.22 shows that response surface quadratic model for adsorption capacity has F-value of 570.02 indicating that the model is significant. In this case, the significant model terms are A, B, C, AC, BC and C^2 while AB, A^2 and B^2 are the insignificant model terms. The model term having the most significant effect on the response is B with F-value of 3947.85 and the effect is in the order B>C>BC>C2>A>AC.

After removing the insignificant model terms (model reduction) from equ (4.2) and equ (4.3), the quadratic models for the responses were reduced to equ (4.4) and equ (4.5):

$$Y_1 = -0.000217641A^2 - 0.014404B^2 - 0.00173025AB - 0.018465AC - 0.1137BC + 0.33625A + 2.38714B + 10.1384C - 51.11583 \quad (4.4)$$

$$Y_2 = 0.11355C^2 - 0.00031625AC - 0.012256BC + 0.00278124A + 0.070862B - 0.50129C - 0.12217 \quad (4.5)$$

Table 4.21: Model ANOVA for Response Y_1 (Removal Efficiency)

Source	Sum of Squares	df	Mean Square	F-value	P-value	Comment
Model	1773.14	9	197.02	529.63	<0.0001	Significant
A	300.64	1	300.64	808.29	<0.0001	Significant
B	963.17	1	963.17	2589.51	<0.0001	Significant
C	109.47	1	109.47	294.33	<0.0001	Significant
AB	95.8	1	95.8	257.56	<0.0001	Significant
AC	27.28	1	27.28	73.33	<0.0001	Significant
BC	41.13	1	41.13	110.59	<0.0001	Significant
A^2	13.07	1	13.07	35.02	0.0001	Significant
B^2	91.28	1	91.28	245.42	<0.0001	Significant
C^2	1.2	1	1.2	3.22	0.1031	
Residual	3.72	10	0.37			

Table 4.22: Model ANOVA for Response Y_2 (Adsorption Capacity)

Source	Sum of Squares	df	Mean Square	F-value	P-value	Comment
Model	6.74	9	0.75	570.02	<0.0001	Significant
A	0.02	1	0.02	15.28	0.0029	Significant
B	5.18	1	5.18	3947.56	<0.0001	Significant
C	0.99	1	0.99	751.81	<0.0001	Significant
AB	3.00E-04	1	3.00E-04	0.23	0.6429	
AC	8.00E-03	1	8.00E-03	6.09	0.0332	Significant
BC	0.48	1	0.48	366.07	<0.0001	Significant
A^2	9.37E-04	1	9.37E-04	0.71	0.4181	
B^2	5.68E-05	1	5.68E-05	0.043	0.8394	
C^2	0.035	1	0.035	27	0.0004	Significant
Residual	0.013	10	1.31E-03			

4.5.3 Comparison of actual (experimental) and predicted values

The plots of actual vs. predicted values for response Y_1 (removal efficiency) as observed in Fig. 4.30 shows very minimal divergence of points from the diagonal indicating that these response surface model equations can be used to adequately represent the interaction of the three factors. The plots of actual vs. predicted values for response Y_2 (adsorption capacity) as observed in Fig. 4.31 also shows very minimal divergence of points from the diagonal. This observation is similar to that of Y_1.

Model Residual

The residual of the response surface models presented in Table 4.23 shows that the highest-lowest error for response Y_1 and Y_2 are 1.02-0.03 and 0.07-0.0002727 respectively. This also signifies the quality of the models in terms of predicting the responses.

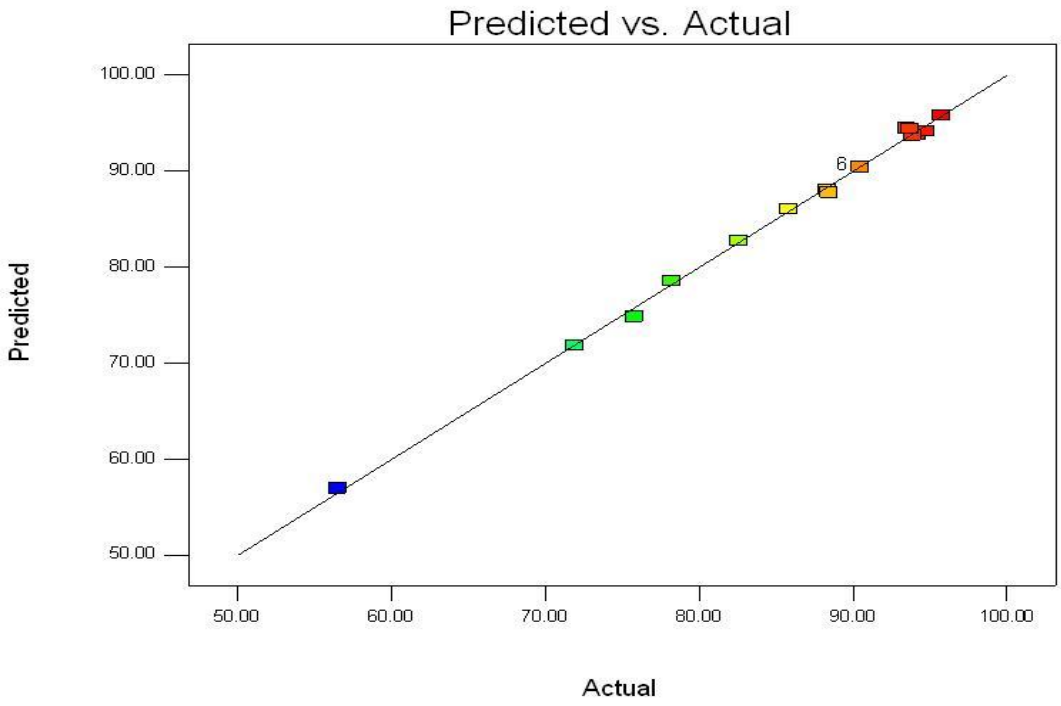


Fig 4.30: Predicted-Actual Plot for Response Y_1

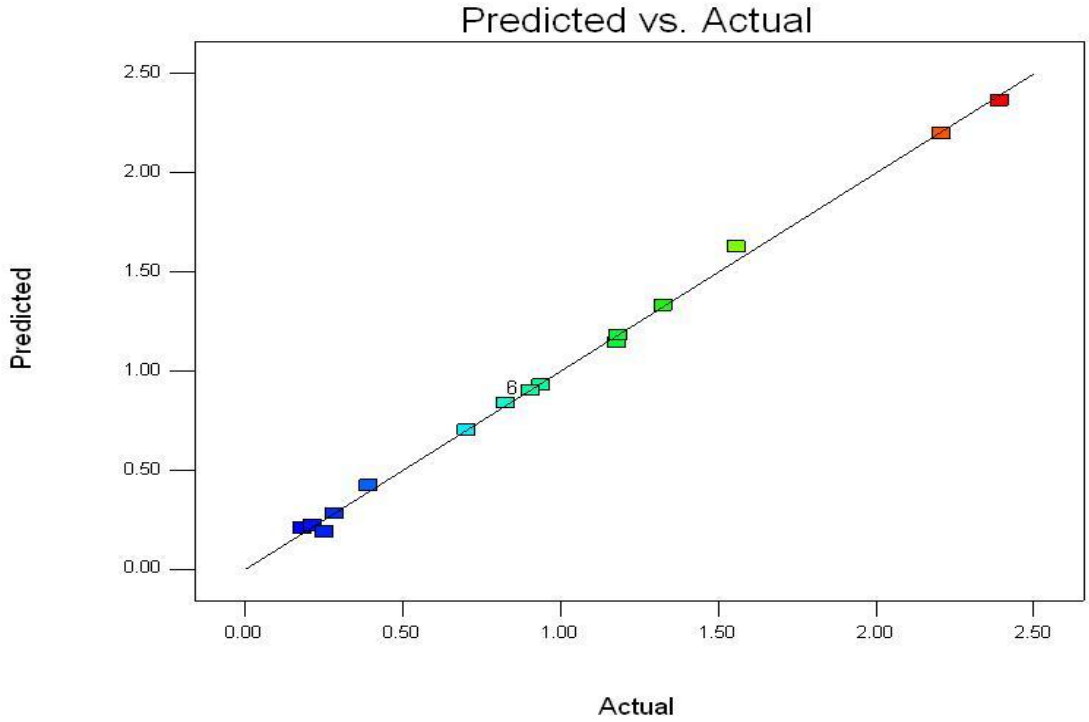


Fig 4.31: Predicted-Actual Plot for Response Y_2

Table 4.23: Actual-Predicted Values and Residual

		Uncoded (Actual) Factors			Response Y_1 (%)			Response Y_2 (mg/g)		
Run	**Type**	**A(^{o}C)**	**B (mg/l)**	**C(g)**	**Actual**	**Predicted**	**Residual**	**Actual**	**Predicted**	**Residual**
1	Factorial	300	50	2	88.32	88.06	0.25	2.21	2.20	8.21E-03
2	Factorial	500	50	4	94.70	94.19	0.51	1.18	1.18	1.01E-03
3	Factorial	500	50	2	95.72	95.8	0.083	2.39	2.36	0.028
4	Axial	500	30	3	93.86	93.74	0.12	0.94	0.93	9.27E-03
5	Center	400	30	3	90.47	90.44	0.03	0.91	0.90	1.62E-03
6	Axial	300	30	3	82.57	82.78	0.21	0.83	0.84	0.014
7	Center	400	30	3	90.47	90.44	0.03	0.91	0.90	1.62E-03
8	Factorial	300	50	4	94.17	93.84	0.34	1.18	1.14	0.033
9	Axial	400	50	3	93.47	94.49	1.02	1.56	1.63	0.07
10	Center	400	30	3	90.47	90.44	0.03	0.91	0.90	1.62E-03
11	Axial	400	10	3	75.79	74.86	0.93	0.25	0.19	0.065
12	Axial	400	30	4	93.68	94.41	0.72	0.70	0.70	2.73E-04
13	Factorial	300	10	2	56.49	56.98	0.49	0.28	0.28	2.07E-04
14	Factorial	500	10	2	78.25	78.56	0.31	0.39	0.42	0.03
15	Center	400	30	3	90.47	90.44	0.03	0.91	0.90	1.62E-03
16	Factorial	300	10	4	71.93	71.82	0.11	0.18	0.21	0.027
17	Center	400	30	3	90.47	90.44	0.03	0.91	0.90	1.62E-03
18	Center	400	30	3	90.47	90.44	0.03	0.91	0.90	1.62E-03
19	Axial	400	30	2	88.42	87.79	0.63	1.33	1.33	5.13E-03
20	Factorial	500	10	4	85.79	86.02	0.23	0.21	0.22	6.99E-03

4.5.4 Combined effect of factors on response

Combined Effect of Temperature and Initial Concentration at Constant Adsorbent Dosage

Fig 4.32 shows the combined effect of temperature and initial concentration on removal efficiency. It was observed that the two factors have significant combined effect on removal efficiency and increase in any of the factors reasonably increases the removal efficiency. The combined effect was observed to be greater at higher values of the two factors.

The combined effect of temperature and initial concentration on adsorption capacity is as shown in Fig 4.33. The figure shows that the combined effect is almost completely as a result of the singular effect of initial concentration with temperature having very small effect. It was also observed that adsorption capacity is significantly increased with increase in initial concentration whereas increase in temperature results in relatively insignificant increase in adsorption capacity.

Combined Effect of Temperature and Adsorbent Dosage at Constant Initial Concentration

Fig 4.34 shows that temperature and adsorbent dosage have relatively low combined effect on removal efficiency. It was observed that the effect of temperature is relatively higher than that of adsorbent dosage and increase in any of the two factors increases the removal efficiency.

Fig 4.35 shows the combined effect of temperature and adsorbent dosage on adsorption capacity. It was noted that adsorbent dosage controls the combined effect of the two factors

with temperature having lower effect. It was also observed that increasing the adsorbent dosage decreases the adsorption capacity.

Combined Effect of Initial Concentration and Adsorbent Dosage at Constant Temperature

Fig 4.36 shows that initial concentration and adsorbent dosage have significant combined effect on removal efficiency, with initial concentration exhibiting the greatest effect, though adsorbent dosage shows reasonable effect too. The combined effect was observed to be greater at higher values of the two factors. It was also noted that increasing any of the factors increases the removal efficiency.

Fig 4.37 shows that the two factors have significant combined effect on adsorption capacity. It was observed that at higher initial concentration, increase in adsorbent dosage greatly decreases the adsorption capacity than at lower initial concentrations. Increase in initial concentration was also observed to increase the adsorption capacity but with much effect at lower adsorbent dosage.

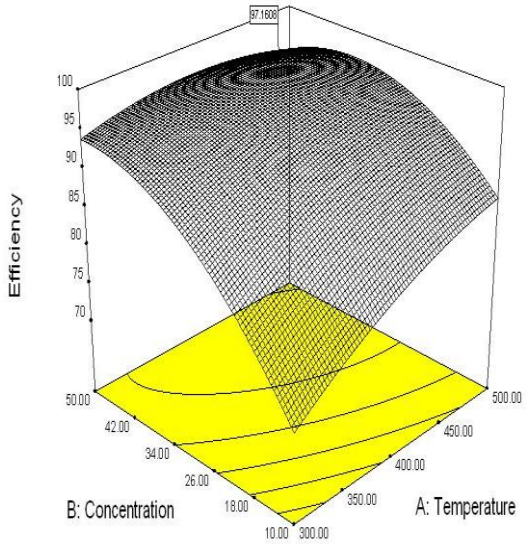


Fig 4.32: Combined Effect of Factors A-B on Y_1

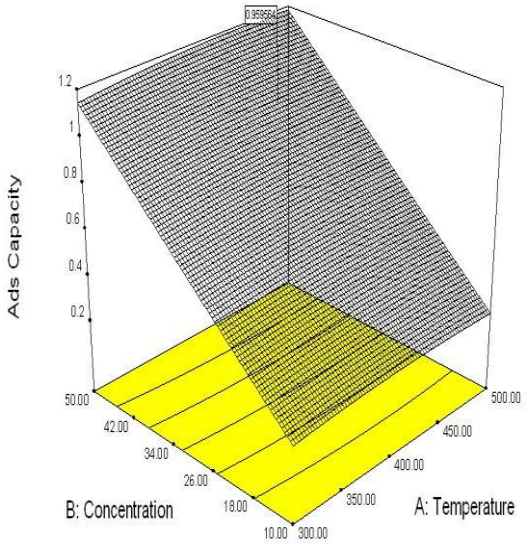


Fig 4.33: Combined Effect of Factors A-B on Y_2

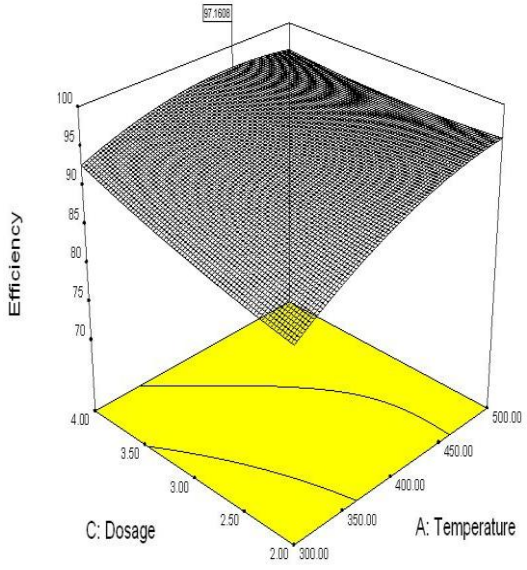


Fig 4.34: Combined Effect of Factors A-C on Y_1

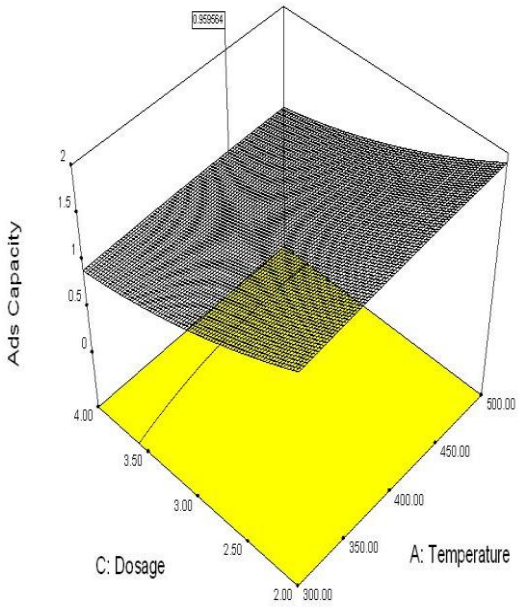


Fig 4.35: Combined Effect of Factors A-C on Y_2

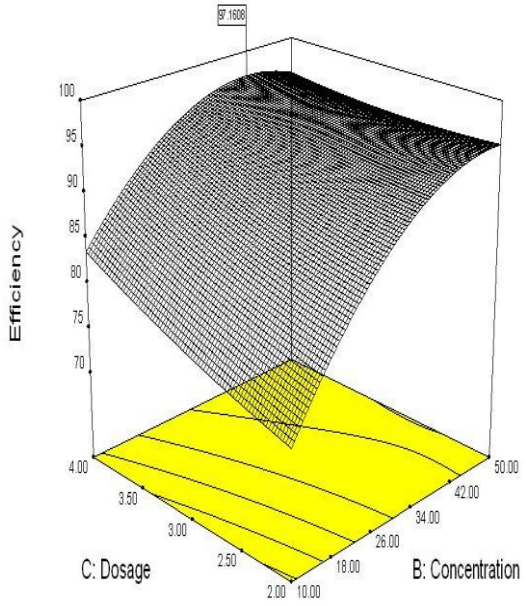


Fig 4.36: Combined Effect of Factors A-C on Y_1

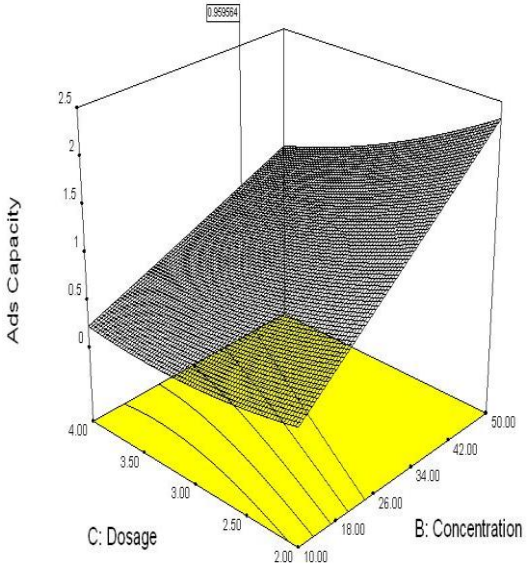


Fig 4.37: Combined Effect of Factors A-C on Y_2

4.5.5 Optimization

Optimization of the two responses under the same condition was difficult because the interest regions of factors are different. When Y_1 increases, Y_2 decreases and vice versa. Therefore the function of desirability was applied and the operating condition with the highest desirability was considered as selected by the software in Table 4.24. Hence, the optimum operating conditions for the preparation of rice husk activated carbon and batch adsorption of phenol using the rice husk activated carbon are:

Factors

A-Temperature of pretreatment of rice husk = 441.46 ^{o}C

B-Initial phenol concentration = 40.61 mg/l

C-Activated carbon dosage = 4 g

Response

Y_1-Removal efficiency = 97.1608 %

Y_2-Adsorption capacity = 0.959522 mg/g

4.5.6 Model validation

Table 4.25 compares the results of experimental values with predicted values under optimum operating condition. It can be seen from the table that the percentage error for adsorption capacity and removal efficiency are 1 % and 1.777 % respectively. Therefore, this shows that the models and optimum operating condition developed for the factors are valid and applicable in predicting the response variables.

Table 4.24: Desirability for Optimum Operating Conditions

No	A (^oC)	B (mg/l)	C (g)	Y_1 (%)	Y_2 (mg/g)	Desirability	*Comment*
1	441.46	40.61	4.00	97.1608	0.959522	0.935	*Selected*
2	439.43	40.82	4.00	97.1600	0.964681	0.935	
3	439.54	40.97	4.00	97.1594	0.968167	0.935	
4	444.96	40.35	4.00	97.1586	0.953393	0.935	
5	446.93	40.21	4.00	97.1555	0.949848	0.935	
6	434.77	41.06	4.00	97.1536	0.970199	0.935	
7	449.51	40.18	4.00	97.1479	0.94922	0.934	
8	441.92	39.34	4.00	97.1385	0.928925	0.934	
9	429.18	41.80	4.00	97.1332	0.987812	0.934	
10	459.95	39.80	4.00	97.1022	0.939501	0.933	
11	464.28	42.45	4.00	96.9252	1.00336	0.929	
12	389.90	42.76	4.00	96.7094	1.00576	0.924	
13	499.99	44.94	2.00	96.1671	2.11701	0.912	
14	500.00	45.38	2.00	96.1585	2.13585	0.912	
15	497.71	45.54	2.00	96.1545	2.14569	0.912	
16	500.00	45.13	2.01	96.1519	2.11912	0.912	
17	492.80	44.73	2.00	96.1241	2.10346	0.911	

Table 4.25: Model Validation

				Experimental		Theoretical		% Error	
T (^oC)	m(g)	C_o(mg/l)	C_e(mg/l)	q_e (mg/g)	RE (%)	q_e (mg/g)	RE (%)	q_e	RE
441.46	4	40.61	1.842	0.969	95.464	0.960	97.160	1.000	1.777

4.6 Characterization of Activated Carbon

4.6.1 Themo-gravimetric analysis (TGA) profiles

The TGA profiles (Fig. 4.38 and 4.39) shows three-step weight loss. The first was observed at less than 150 ^{o}C (initial 6mins of residence time) amounting to 5 % of the weight loss. This largely account for the removal of water molecules present in the sample. The sample was observed to be virtually stable at temperature range of 150-300 ^{o}C (Fig. 4.38) corresponding to residence time of 5-14 mins (Fig. 4.39) and representing about 5 % weight loss. Thereafter, significant weight loss was observed between 300-415 ^{o}C (Fig. 4.38) occurring between 14-20 mins of residence time (Fig. 4.39) and this represent about 50 % of the weight loss. This is usually due to hemicelluloses and cellulose decomposition. From 415 ^{o}C (Fig. 4.38), percentage weight loss was observed to be relatively low which is due to the decomposition of lignin component that degrades slowly over a wide range of temperature, hence yield was observed to be almost stable. Fig. 4.39 shows that at 40 mins of residence time, temperature of 441. 46 ^{o}C gave higher yield of 34.9 % compared to 30.6 % obtained from temperature of 800 ^{o}C. It was also observed that increasing the residence time from 40 to 80 mins while maintaining the temperature at 441.46 ^{o}C did not significantly decrease the yield as it only amount to 34.01 % yield. These observations are in agreement with findings in literature (Rosas *et al*., 2009; Mohammad *et al*., 2012).

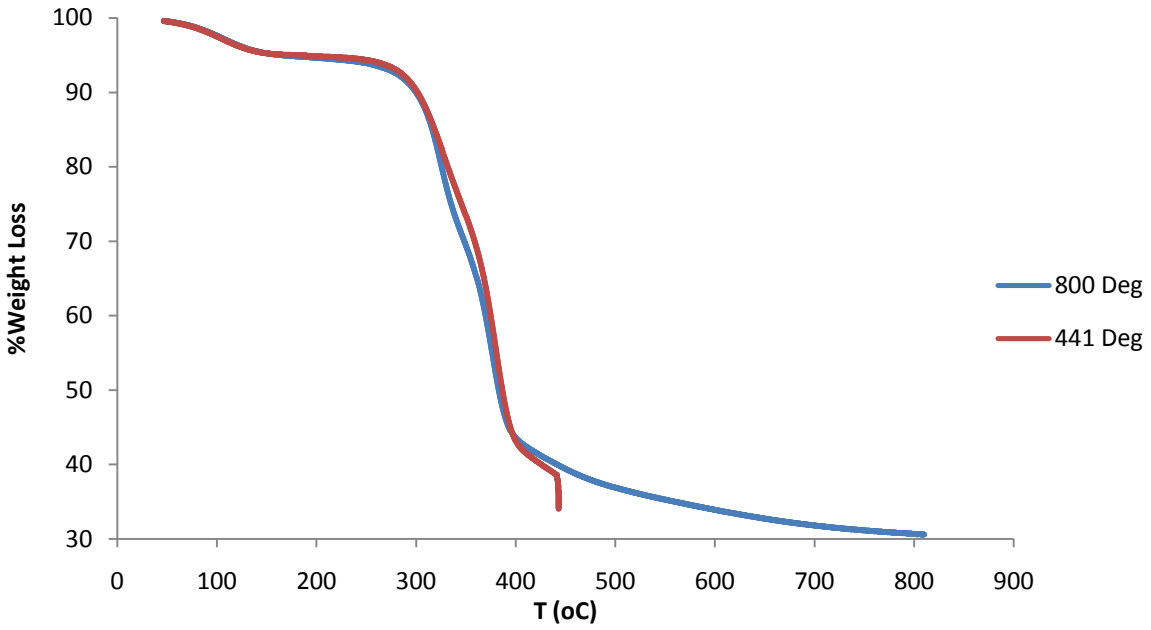


Fig 4.38: TGA profile for percentage weight loss against temperature

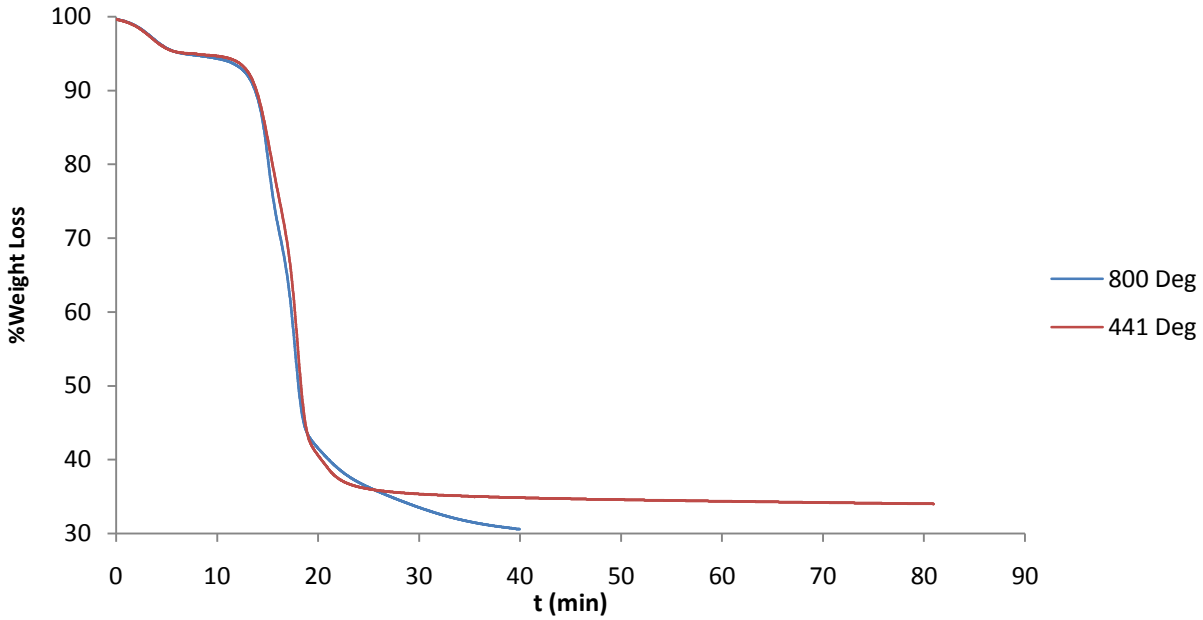


Fig 4.39: TGA profile for percentage weight loss against time

4.6.2 Fourier transformed infrared spectroscopy (FTIR) spectrum

The FTIR spectrum of the charred residue obtained from thermal pretreatment is as presented in Fig. 4.40 and that of the phosphoric acid modification of the charred residue is as presented in Fig. 4.41. Girgis *et al*. (2009); Liou and Wu (2009); Shi *et al*. (2010); Nahil and Williams (2012) reported that the band in the region of 1300-900 cm^{-1} could be caused by phosphorous-oxy-containing functional groups for the FTIR spectrum of carbon prepared by phosphoric acid activation,. Therefore, in comparison the shift in broad band to 1095.6 cm^{-1} observed in Fig. 4.41 could be attributed to P=O in organic phosphates, O-C bond in P-O-C linkage or P=OOH bond. This indicates the presence of phosphorous-oxy-containing group in the activated carbon implying that traces of phosphates remain in the carbon even after repeated washing. The appearance of the broad band in the region 720-590 cm^{-1} in Fig. 4.41 which could be assigned to O-H (out of plane bend) could indicate the introduction of oxy-containing functional groups resulting from phosphoric acid modification. These oxy-containing functional groups on the activated carbon surface contribute in enhancing phenol adsorption (Liu *et al*., 2011).

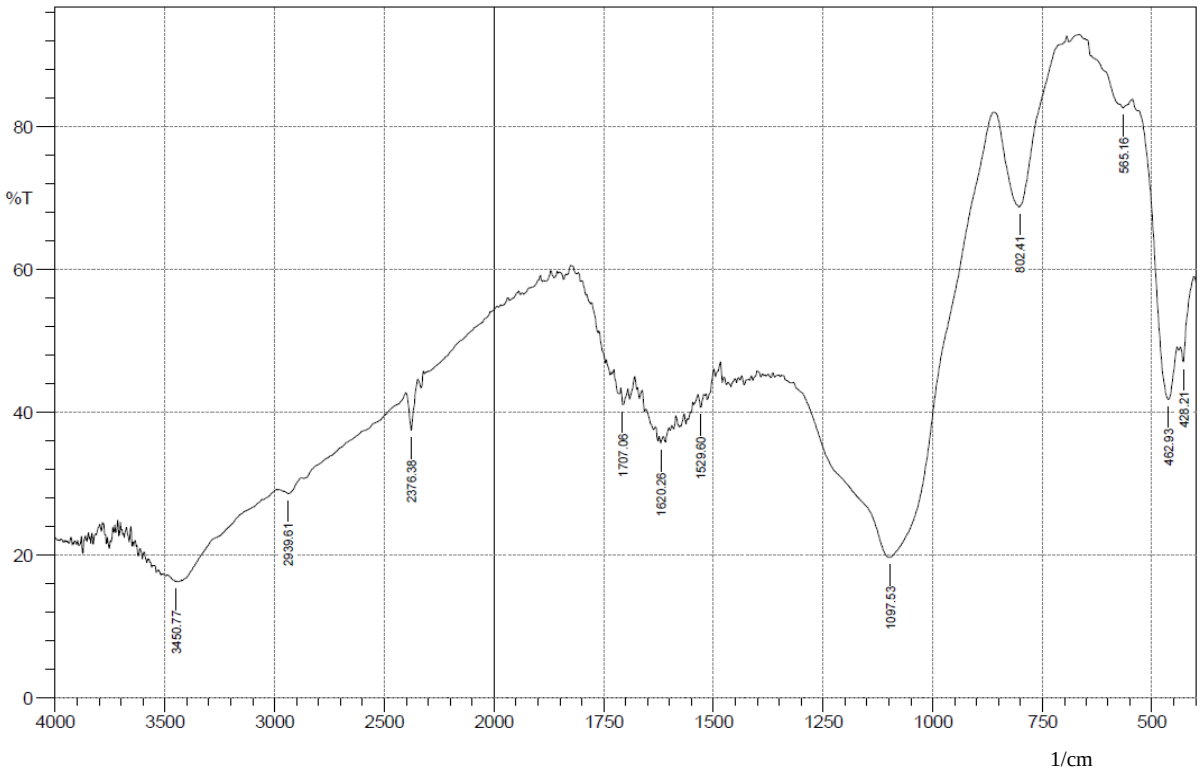


Fig. 4.40: FTIR spectrum before phosphoric acid modification

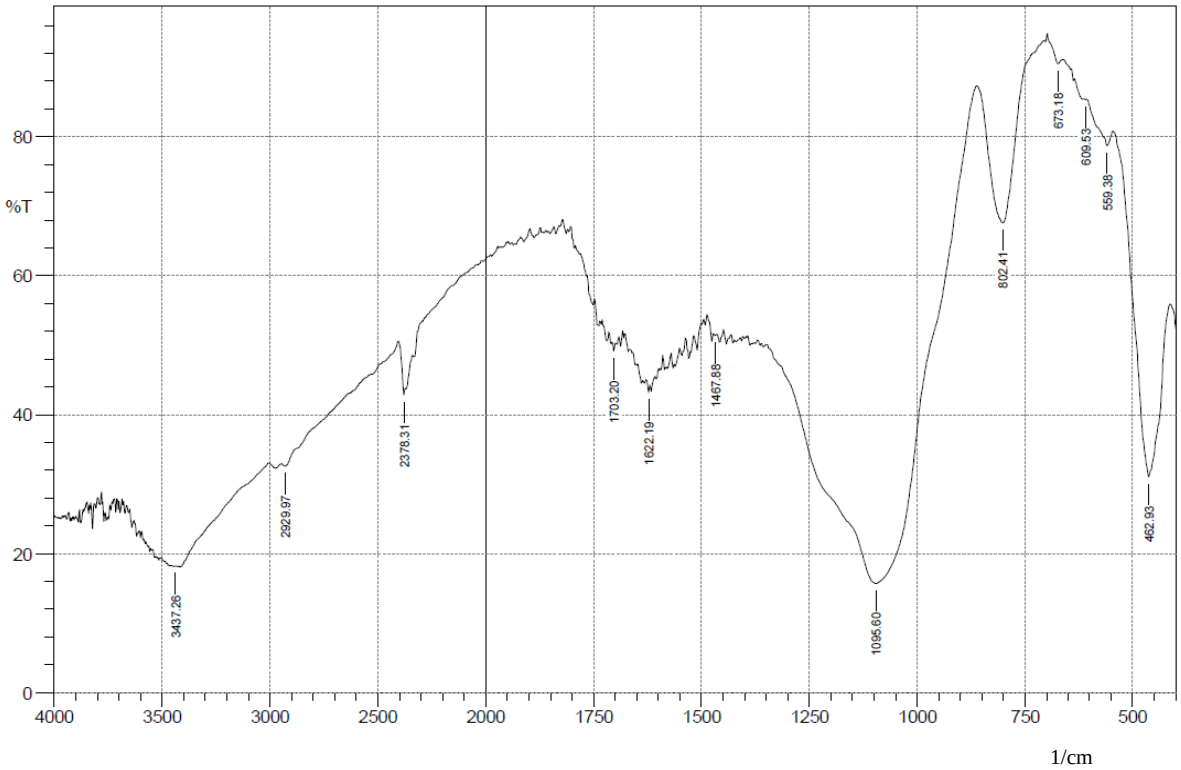


Fig. 4.41: FTIR spectrum after phosphoric acid modification

4.6.3 Scanning electron microscopy (SEM) micrograph

The micrographs in Fig. 4.42 and 4.43 revealed the morphology of the charred residue obtained from thermal pretreatment and the phosphoric acid modified charred residue. Fig. 4.42 shows that the charred residue obtained from thermal pretreatment is characterized by heterogeneous surface. In comparison, phosphoric acid modification of the charred residue as observed in Fig. 4.43 shows that the surface heterogeneity of the activated carbon was significantly reduced. Further comparison of the micrographs confirms that the micrograph in Fig. 4.43 revealed relative improvement in the surface area and pore development.

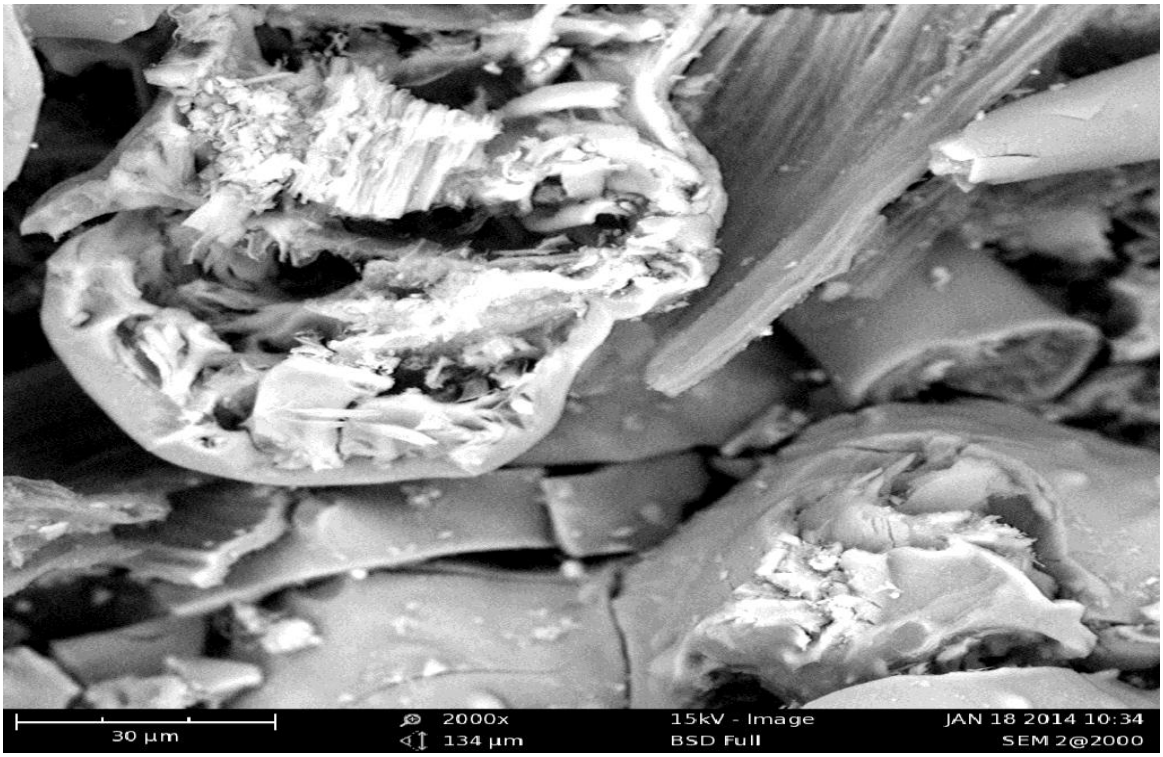


Fig. 4.42: SEM Micrographs before phosphoric acid modification

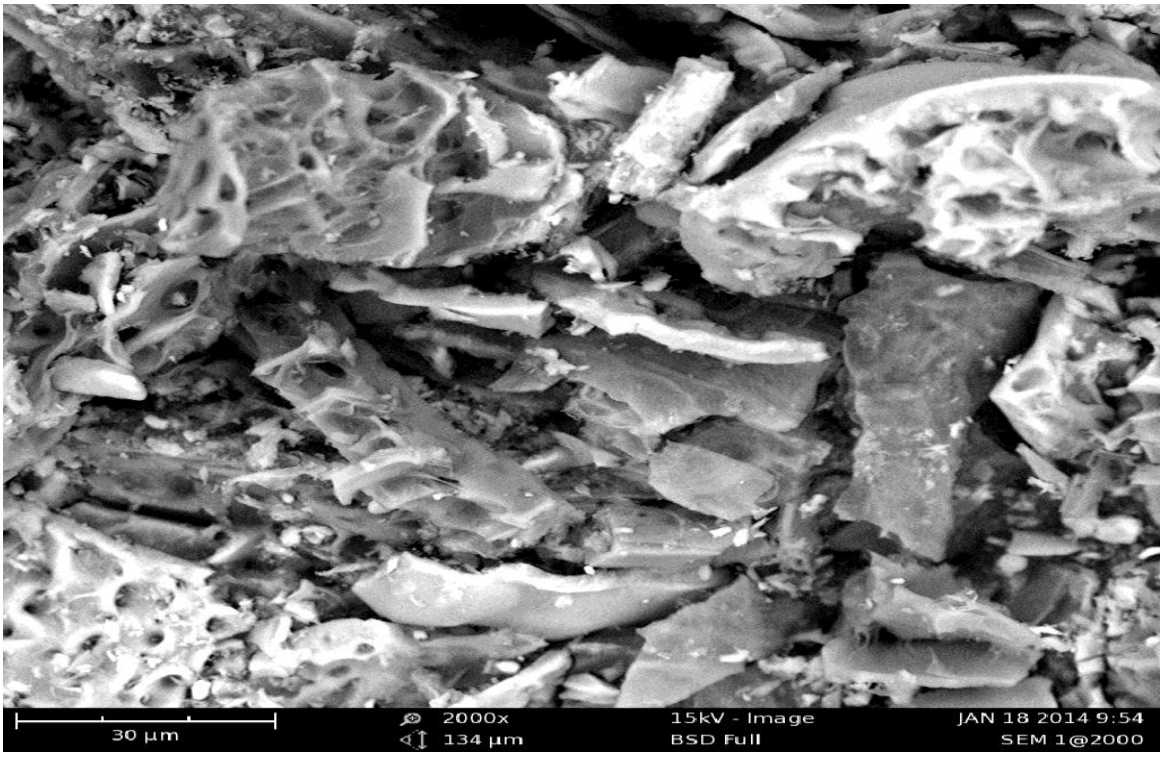


Fig. 4.43: SEM Micrographs after phosphoric acid modification

4.6.4 Surface area and pore size

Surface Area

The surface area of the activated carbon was determined using Langmuir and BET model. Table 4.26 shows that the charred residue obtained from thermal pretreatment revealed Langmuir, BET (single point) and BET (multipoint) surface area of 12.47, 9.553 and 9.071 m^2/g respectively. Also noted was that the phosphoric acid modification of the charred residue increased the surface area of the rice husk activated carbon to 102.4, 64.7 and 66.13 m^2/g for Langmuir, BET (single point) and BET (multipoint) respectively. This observation is probably due to the fact that activated carbon produced from rice husk by physical (thermal) pretreatment shows relatively low specific surface area because of high silica content. Also, the increase in surface area could be attributed to the phosphoric acid impregnation and washing which lead to the removal of unorganized carbon or residual tars materials at low temperatures thereby opening the closed pores or the removal of soluble phosphates formed from the reaction of phosphoric acid and silica deposited into pores. This is in agreement with the findings of Liou and Wu (2009); Rosas *et al*. (2009); Rosas *et al*. (2010); Chen *et al*. (2011b); Li *et al*. (2011b); Somasundaram *et al*. (2013). Improvement in surface area resulting from the effect of activating agent was also reported by Gundogdu *et al*. (2013).

Pore Size

The micropore volume was determined using the DR method. Table 4.26 shows that the charred residue has micropore volume of 0.0052 cm^3/g while phosphoric acid enhanced the micropore volume to 0.034 cm^3/g. Therefore, the microporosity of the rice husk activated

carbon was increased in volume from 0.0052 to 0.034 cm^3/g as a result of the phosphoric acid modification. This was found to be similar to the observations of Foo and Hameed (2012) that acid modification led to enhancement in pore volume from 0.008 to 0.247 cm^3/g.

It was also observed that prior to the phosphoric acid modification; the charred residue had an average pore diameter of 2.4 nm. Thereafter, development of micropores was improved via acid modification resulting in average pore diameter of 1.82 nm. Modification was also observed by Foo and Hameed (2012) to enhance pore diameter from 2.48 to 2.23 nm. This could be as a result of the introduction of functional groups on the surface of the smaller mesorepores thereby shrinking them to micropores.

Table 4.26: Surface Area and Pore Size before and after Phosphoric Acid Modification

Sample	S_L (m^2/g)	S_{BET1} (m^2/g)	S_{BET2} (m^2/g)	V_{mic} (cm^3/g)	D_p (nm)
Before acid modification	12.47	9.553	9.071	0.0052	2.48
After acid modification	102.4	64.7	66.13	0.034	1.82

4.7 Column Adsorption

4.7.1 Adsorption of phenol from refinery wastewater *(RSSCT mode)*

It was observed in Table 4.27 that as the column adsorption proceeds with time, the adsorption capacity increases while the removal efficiency decreases. This could be due to the fact that as the influent stream pass through the bed, more solute molecule are captured and retained by the activated carbon and this continuously increases the adsorption capacity until the bed becomes saturated. But as this continues with time, the amount of solute captured from the stream and retained by the activated carbon decreases and this result in an increase in the amount of solute concentration in the effluent stream, hence removal efficiency will be observed to be decreasing subsequently. The table also shows that adsorption capacity obtained from column study is higher than that of batch study and it also shows that at breakthrough point of 0.5 (Fig 4.44), the bed adsorption capacity is 28 mg/g.

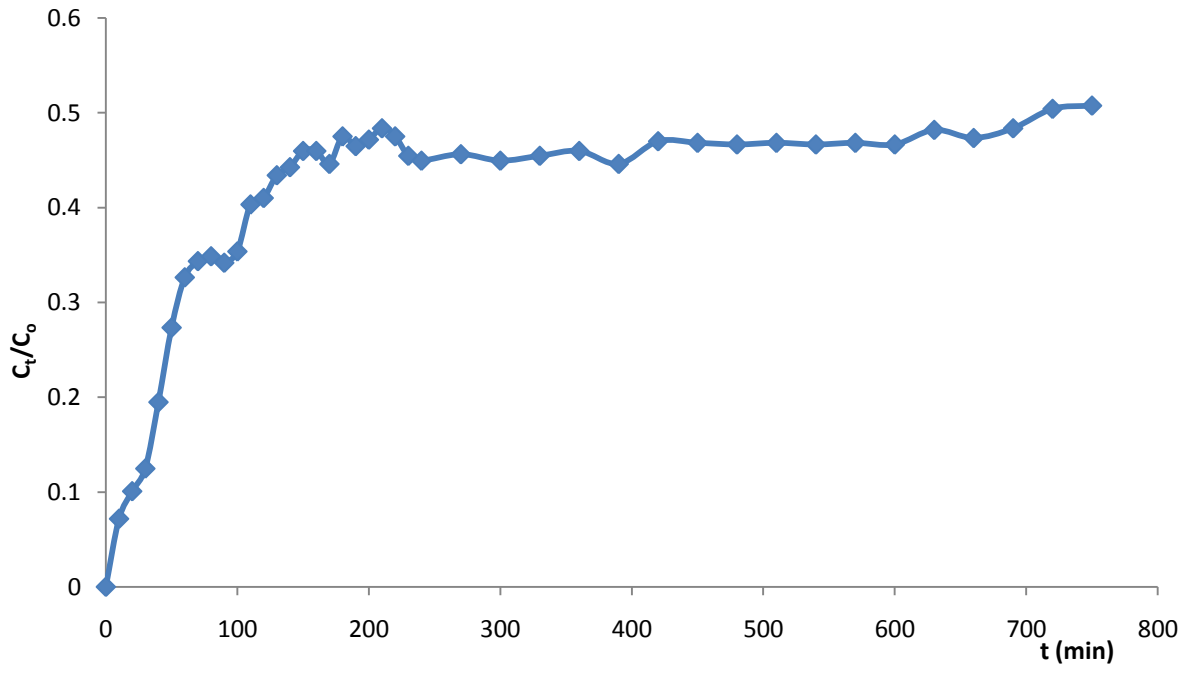


Fig 4.44: Breakthrough Curve for bed Depth, 6cm (4g) and Flow rate, 4.5ml/min

Table 4.27: Breakthrough Curve data for *z=6cm, f=4.5ml/min, C_o=51.32mg/l*

t (min)	C_t (mg/l)	q_B (mg/g)	RE (%)	C_t/C_o
10	3.684	0.385	92.821	0.072
20	5.175	0.770	89.915	0.101
30	6.404	1.155	87.522	0.125
40	10.000	1.540	80.514	0.195
50	14.035	1.925	72.652	0.273
60	16.754	2.309	67.353	0.326
70	17.632	2.694	65.644	0.344
80	17.895	3.079	65.131	0.349
90	17.544	3.464	65.815	0.342
100	18.158	3.849	64.618	0.354
110	20.702	4.234	59.661	0.403
120	21.053	4.619	58.978	0.410
130	22.281	5.004	56.585	0.434
140	22.719	5.389	55.730	0.443
150	23.596	5.774	54.021	0.460
160	23.596	6.158	54.021	0.460
170	22.895	6.543	55.388	0.446
180	24.386	6.928	52.483	0.475
190	23.860	7.313	53.508	0.465
200	24.211	7.698	52.824	0.472
210	24.825	8.083	51.628	0.484
220	24.386	8.468	52.483	0.475
230	23.333	8.853	54.534	0.455
240	23.070	9.238	55.046	0.450
270	23.421	10.392	54.363	0.456
300	23.070	11.547	55.046	0.450
330	23.333	12.702	54.534	0.455
360	23.596	13.856	54.021	0.460
390	22.895	15.011	55.388	0.446
420	24.123	16.166	52.995	0.470
450	24.035	17.321	53.166	0.468
480	23.947	18.475	53.337	0.467
510	24.035	19.630	53.166	0.468
540	23.947	20.785	53.337	0.467
570	24.035	21.939	53.166	0.468
600	23.947	23.094	53.337	0.467
630	24.737	24.249	51.799	0.482
660	24.298	25.403	52.653	0.473
690	24.825	26.558	51.628	0.484
720	25.877	27.713	49.577	0.504
750	26.053	28.868	49.235	0.508

4.7.2 Effect of bed depth and flow rate

A. Effect of Bed Depth

It was observed in Fig. 4.45 that at the same breakthrough point, the breakthrough time increases with increase in bed depth. This observation is due to increased surface area and availability of more binding sites for sorption as the bed depth increases thereby resulting in a broadened mass transfer zone. This means that as the bed depth is increased the length of the bed which the wastewater passes through also increases. This observation is similar to those of Kalavathy *et al.* (2010); Zhang *et al.* (2011b); Ji *et al.* (2013). Table 4.28 shows the breakthrough characteristics with respect to increase in bed depth. It was observed that at any breakthrough point, the corresponding breakthrough time, capacity and volume of wastewater treated increases with increase in bed depth. It was also observed that the longer the breakthrough time, the higher the breakthrough capacity of the column. This could be as a result of the fact that increase in bed depth provides the solute (phenol) molecule with more time to get adsorbed into the broadened mass transfer zone and this also results in treating more volume of effluent (Luo *et al*., 2011; Sadaf and Bhatti, 2013). Therefore, a decrease in the phenol composition of the effluent can be achieved in a column design approach by increasing the bed depth at the same time (Han *et al*., 2006; Song *et al*., 2011). Hence, higher bed depth favours better column performance.

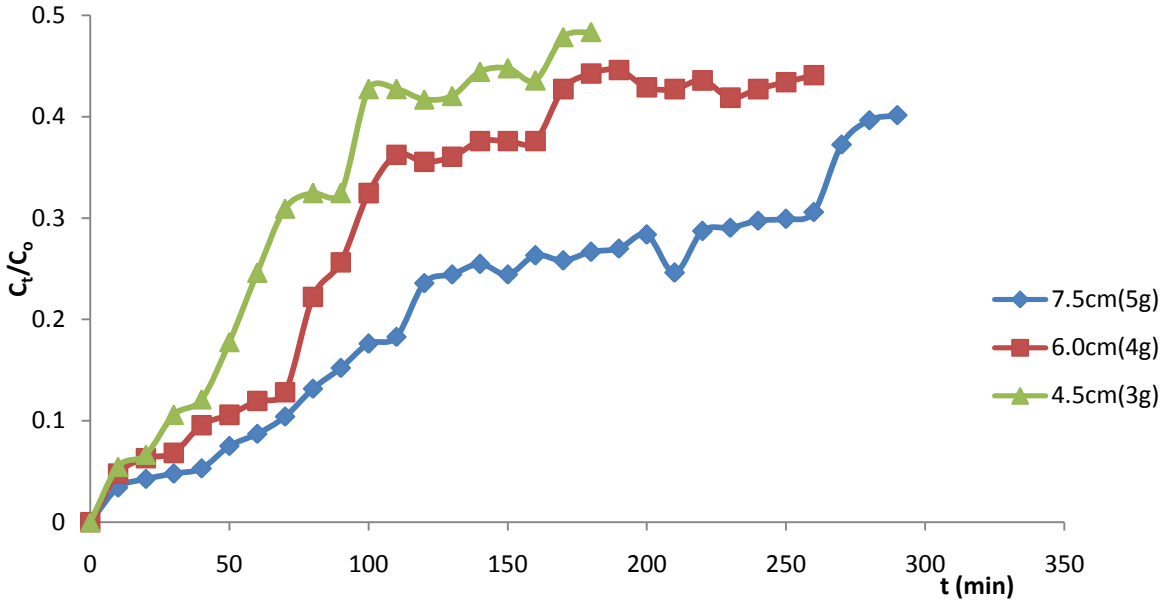


Fig 4.45: Breakthrough Curve for different Bed Depths

Table 4.28: Breakthrough Characteristics

Breakthrough points (b.p)		0.1			0.2			0.4		
Z (cm)	f (ml/min)	t_B (min)	V_{eff} (ml)	q_B (mg/g)	t_B (min)	V_{eff} (ml)	q_B (mg/g)	t_B (min)	V_{eff} (ml)	q_B (mg/g)
4.5	3	23	69	1.180	54	162	2.771	97	291	4.978
6	3	44	132	1.694	77	231	2.974	165	495	6.351
7.5	3	69	207	2.125	103	309	3.172	290	870	8.930
6	4.5	21	94.5	1.212	42	189	2.425	110	484	6.210

B. Effect of Flow Rate

Fig 4.46 shows that at the same breakthrough point, the breakthrough time decreases with increase in flow rate. This observation is in agreement with the trend reported by Kundu and Gupta (2005); Zhang *et al*. (2011b). Table 4.28 shows the breakthrough characteristics with respect to increase in flow rate. The table also shows that relative breakthrough time, capacity and volume of wastewater treated at any breakthrough point decreases as the flow rate increases. This is because as the flow rate is increased, more volume of the wastewater is made to pass through the adsorption zone thereby providing insufficient residence time for the solute molecule to adequately transverse to the functional group-containing pores. This leads to the exit of solute in the wastewater from the column before the establishment of equilibrium and usually results in shorter breakthrough time and capacity. Hence, lower flow rate favours better column performance. These findings are in agreement with reports of Chen *et al.* (2011a); Sadaf and Bhatti (2013).

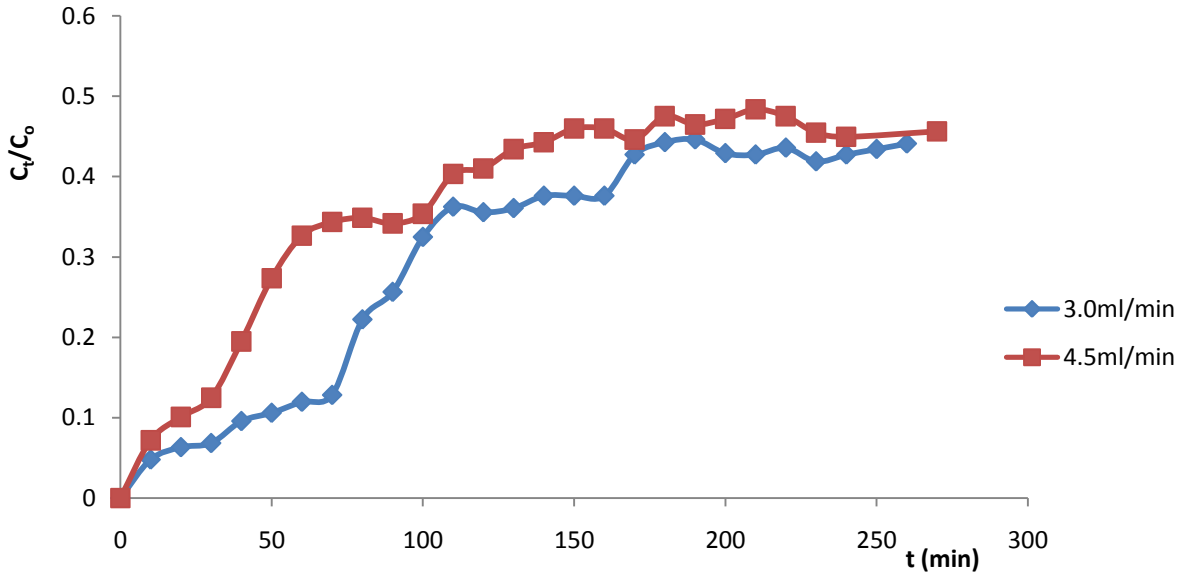


Fig 4.46: Breakthrough Curve for different Flow Rates

4.7.3 Bed Depth Service Time (BDST) model

The BDST model parameters were obtained from Fig. 4.47 and are presented in Table 4.29. The large value of co-efficient of determination (0.9717-0.9988) as observed in the table shows that the experimental data fit well to the model. Therefore BDST model could be employed in the adsorption of phenol onto rice husk activated carbon for the estimation of column design parameters such as bed depth and breakthrough time in the event of any change in flow rate, concentration and breakthrough point.

4.7.4 Thomas model

Thomas model parameters were obtained from the slope and intercept of Fig. 4.48 and are presented in Table 4.30. It was observed that the theoretical breakthrough capacity (q_o) increases as the bed depth increases and decreases as the flow rate increases. This trend is in agreement with the earlier discussion on the effect of bed depth and flow rate on breakthrough capacity and similar observation as was reported by Han *et al.* (2006); Noreen *et al*. (2013). Hence lower flow rate and higher bed depth favour better column performance. The table also shows that the theoretical breakthrough capacity obtained from Thomas model is close to the experimental breakthrough capacity indicating that Thomas model can be used to describe the column performance on the adsorption of phenol onto rice husk activated carbon.

Table 4.29: Bed Depth Service Time (BDST) model parameters

b.p	C_o/C_t -1	$\ln(C_o/C_t$ -1)	a	b	N_o (mg/l)	K_a	R^2
0.1	9	2.197	15.333	46.667	751.122	0.000917	0.9975
0.2	5	1.609	16.333	20	800.109	0.001568	0.9988
0.4	2.5	0.916	64.333	202	3151.498	8.84E-05	0.9717

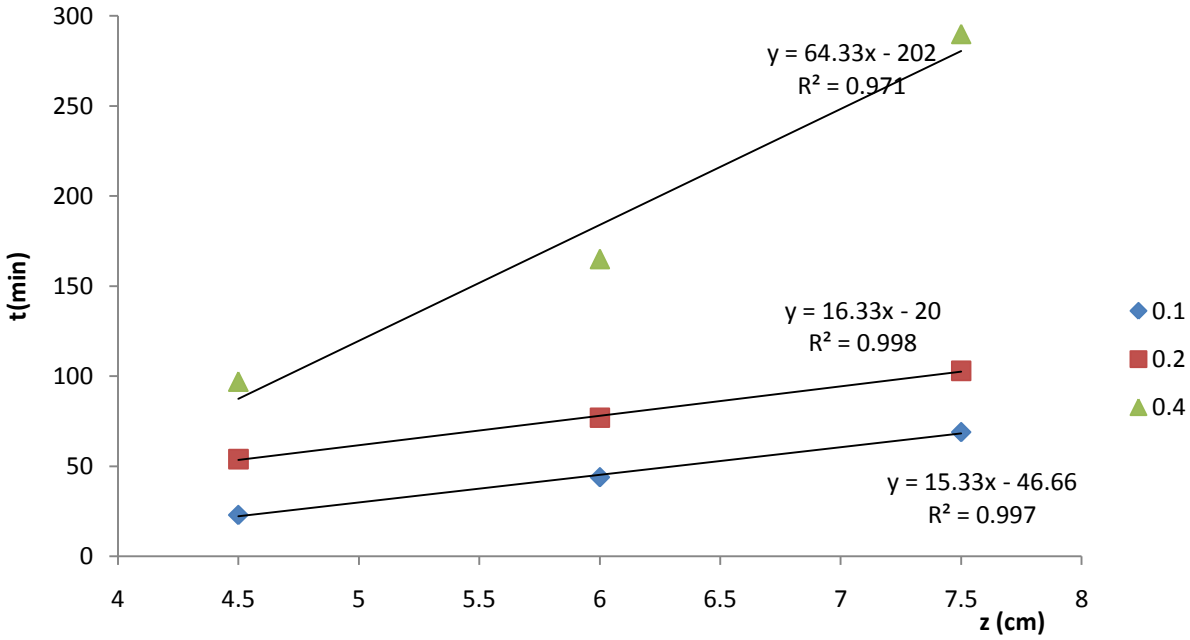


Fig 4.47: Bed Depth Service Time (BDST) Plot for different Breakthrough Points

Table 4.30: Thomas Model Parameters

Z (cm)	f (ml/min)	K_{Th}	q_o (mg/g)	$q_{(exp)}$ (mg/g)	R^2
4.5	3	0.00055924	5.468	5.132	0.9916
6	3	0.00034295	6.451	6.543	0.9725
7.5	3	0.00017732	9.554	8.930	0.9386
6	4.5	0.00040725	6.061	6.351	0.8422

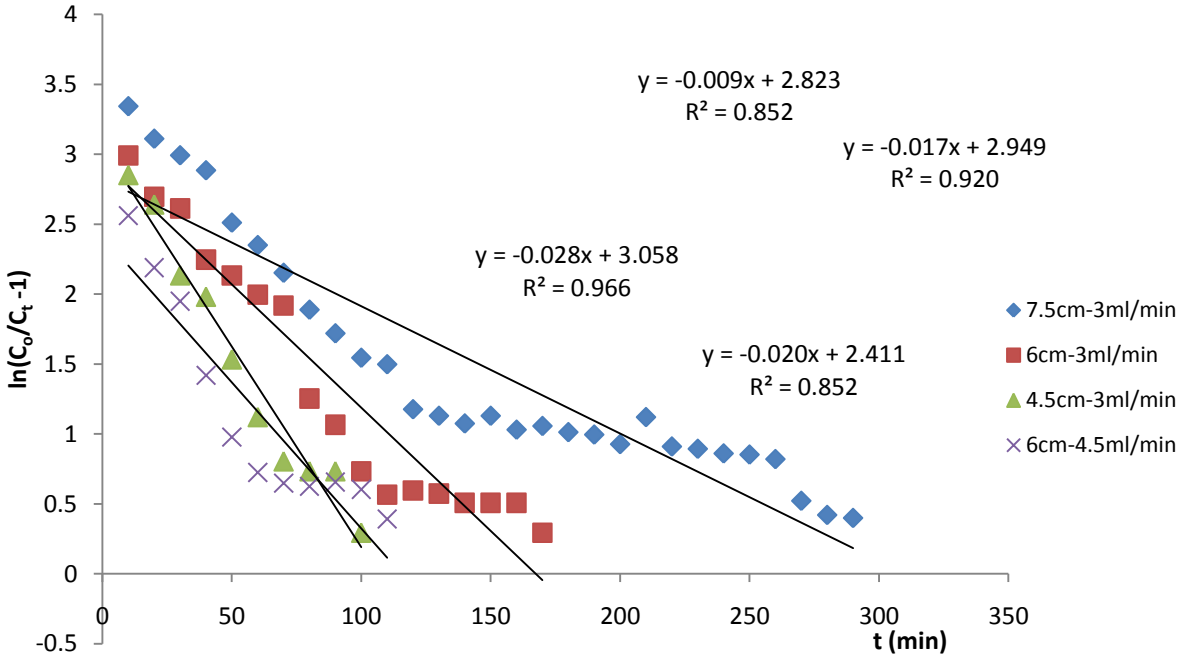


Fig 4.48: Thomas Model Plot

4.7.5 Yoon Nelson model

Yoon Nelson model parameters were obtained from the slope and intercept of the plots in Fig 4.49 and are presented in Table 4.31. The table shows that the theoretical breakthrough time at 50 % (τ) increases with increase in bed depth but decreases with increase in flow rate. This observation is in agreement with the earlier report on the effect of bed depth and flow rate on breakthrough time and similar trend as observed by Chowdhury *et al.* (2013). The 50 % breakthrough time obtained from Yoon Nelson model could be said to be very close to the experimental value as in each case, it was observed to be slightly more than the 40 % experimental breakthrough time.

Table 4.31: Yoon Nelson Model Parameters

Z (cm)	f (ml/min)	K_{YN}	τ (min)	$\tau_{(exp)}$ (min)	R^2
4.5	3	0.0287	106.554	>97	0.9916
6	3	0.0176	167.602	>165	0.9725
7.5	3	0.0091	310.275	>290	0.9386
6	4.5	0.0209	115.373	>110	0.8422

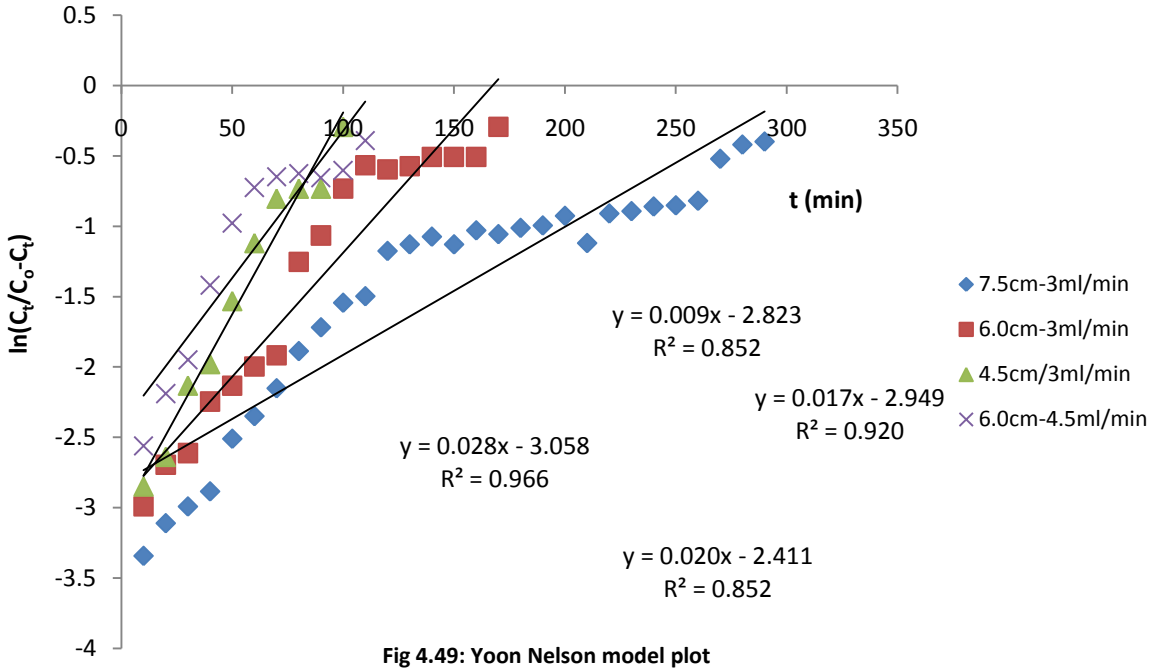


Fig 4.49: Yoon Nelson model plot

4.7.6 Adsorption of phenol from refinery wastewater *(LSCT mode)*

Table 4.32 show the breakthrough data for the large column adsorption test and the resulting breakthrough curve is presented in Fig. 4.50. It was observed in Table 4.6f that at breakthrough point of 0.1, the large column test attained adsorption capacity of 11.32 mg/g at breakthrough time of 920 mins. This indicates better column performance as compared to the adsorption capacity of 2.155 mg/g observed (Table 4.27) for Rapid Small Scale Column Test at the same breakthrough time. This could be as a result of increased bed depth which translates to broadened mass transfer zone. It was also observed in Table 4.32 that at exhaustion point (0.9), the large column test attained adsorption capacity of 55.106 mg/g at breakthrough time of 4480 mins. This may imply the peak or actual adsorption capacity of the rice husk activated carbon.

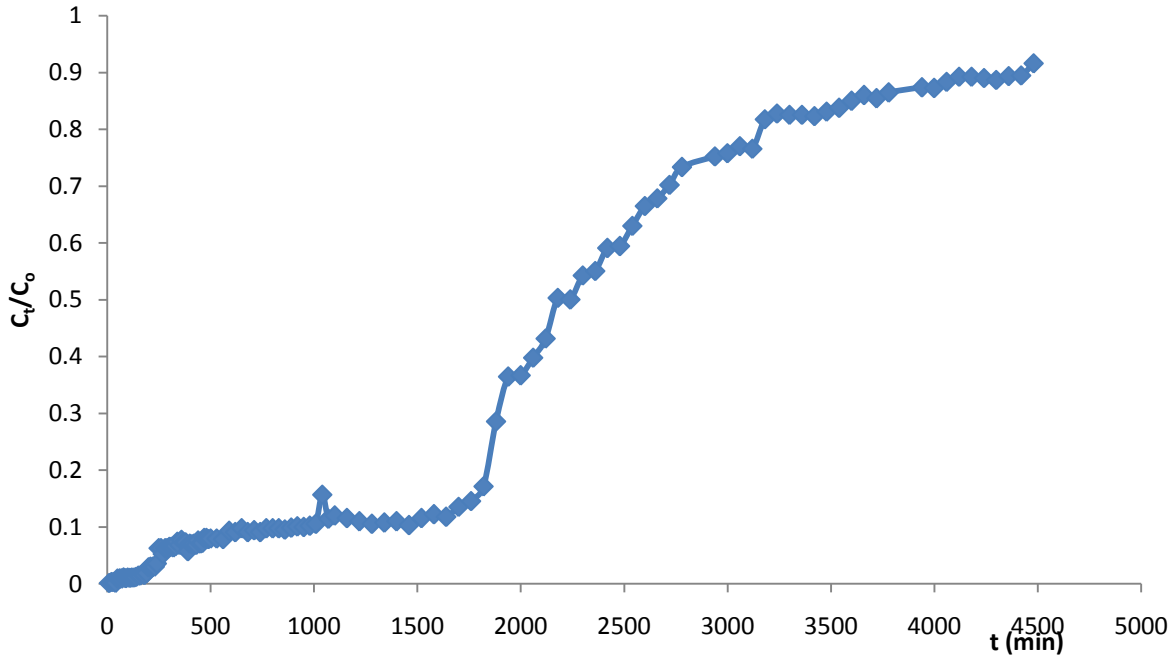


Fig 4.50: Breakthrough Curve for bed depth 60cm (359.84g)

Table 4.32: Breakthrough Curve data for *z=60cm (359.84g), f=56.58ml/min, C_o=78.32mg/l*

t (min)	C_t (mg/l)	C_t/C_o	q_B (mg/g)	RE (%)
10	0.105	0.001	0.123	99.865
20	0.237	0.003	0.246	99.697
30	0.238	0.003	0.369	99.696
40	0.140	0.002	0.492	99.821
50	0.724	0.009	0.615	99.075
60	0.711	0.009	0.738	99.092
70	0.711	0.009	0.861	99.092
80	0.842	0.011	0.984	98.924
90	0.789	0.010	1.107	98.991
100	0.860	0.011	1.230	98.901
110	0.807	0.010	1.353	98.968
120	0.860	0.011	1.476	98.901
130	0.851	0.011	1.599	98.912
140	0.965	0.012	1.722	98.767
150	1.140	0.015	1.845	98.542
160	1.140	0.015	1.968	98.542
170	1.316	0.017	2.091	98.318
180	1.228	0.016	2.214	98.430
190	1.491	0.019	2.337	98.094
200	2.281	0.029	2.460	97.085
210	2.368	0.030	2.583	96.972
220	2.368	0.030	2.706	96.972
230	2.368	0.030	2.829	96.972
240	2.807	0.036	2.952	96.412
250	4.912	0.063	3.075	93.721
260	4.912	0.063	3.198	93.721
270	4.123	0.053	3.321	94.730
280	4.912	0.063	3.444	93.721
290	4.912	0.063	3.567	93.721
300	5.088	0.065	3.690	93.496
310	5.088	0.065	3.813	93.496
320	5.000	0.064	3.936	93.609
330	5.175	0.066	4.059	93.384
340	5.789	0.074	4.182	92.599
350	5.351	0.068	4.305	93.160
360	6.053	0.077	4.428	92.263
370	5.702	0.073	4.551	92.712
380	5.702	0.073	4.674	92.712
390	4.474	0.057	4.797	94.281
400	5.526	0.071	4.920	92.936
410	5.439	0.070	5.043	93.048

Table 4.32: Breakthrough Curve data for *z=60cm (359.84g), f=56.58ml/min, C_o=78.32mg/l (Cont'n)*

t (min)	C_t (mg/l)	C_t/C_o	q_B (mg/g)	RE (%)
420	5.526	0.071	5.166	92.936
430	5.351	0.068	5.289	93.160
440	5.965	0.076	5.412	92.375
450	5.526	0.071	5.535	92.936
460	5.614	0.072	5.658	92.824
470	6.316	0.081	5.781	91.927
480	6.316	0.081	5.904	91.927
490	6.140	0.078	6.027	92.151
500	6.228	0.080	6.150	92.039
530	6.228	0.080	6.519	92.039
560	6.140	0.078	6.888	92.151
590	7.281	0.093	7.257	90.693
620	7.105	0.091	7.626	90.917
650	7.632	0.098	7.995	90.245
680	7.105	0.091	8.364	90.917
710	7.368	0.094	8.733	90.581
740	7.105	0.091	9.102	90.917
770	7.632	0.098	9.471	90.245
800	7.632	0.098	9.840	90.245
830	7.632	0.098	10.210	90.245
860	7.456	0.095	10.579	90.469
890	7.719	0.099	10.948	90.133
920	7.895	0.101	11.317	89.908
950	7.807	0.100	11.686	90.020
980	7.982	0.102	12.055	89.796
1010	8.246	0.105	12.424	89.460
1040	12.281	0.157	12.793	84.302
1070	8.947	0.114	13.162	88.563
1100	9.386	0.120	13.531	88.002
1160	9.035	0.115	14.269	88.451
1220	8.596	0.110	15.007	89.011
1280	8.246	0.105	15.745	89.460
1340	8.421	0.108	16.483	89.236
1400	8.596	0.110	17.221	89.011
1460	8.070	0.103	17.959	89.684
1520	9.035	0.115	18.697	88.451
1580	9.561	0.122	19.435	87.778
1640	9.211	0.118	20.173	88.226
1700	10.614	0.136	20.911	86.432
1760	11.404	0.146	21.649	85.423
1820	13.421	0.172	22.387	82.844
1880	22.368	0.286	23.125	71.407
1940	28.509	0.364	23.863	63.558

Table 4.32: Breakthrough Curve data for *z=60cm (359.84g), f=56.58ml/min, C_o=78.32mg/l (Cont'n)*

t (min)	C_t (mg/l)	C_t/C_o	q_B (mg/g)	RE (%)
2000	28.684	0.367	24.601	63.333
2060	31.140	0.398	25.339	60.194
2120	33.772	0.432	26.077	56.830
2180	39.386	0.503	26.815	49.654
2240	39.123	0.500	27.553	49.990
2300	42.456	0.543	28.291	45.729
2360	43.070	0.551	29.029	44.944
2420	46.228	0.591	29.767	40.907
2480	46.491	0.594	30.506	40.571
2540	49.298	0.630	31.244	36.983
2600	52.018	0.665	31.982	33.507
2660	53.070	0.678	32.720	32.161
2720	54.912	0.702	33.458	29.807
2780	57.368	0.733	34.196	26.667
2940	58.860	0.752	36.164	24.761
3000	59.298	0.758	36.902	24.200
3060	60.263	0.770	37.640	22.967
3120	59.912	0.766	38.378	23.415
3180	63.947	0.817	39.116	18.257
3240	64.737	0.828	39.854	17.248
3300	64.561	0.825	40.592	17.472
3360	64.561	0.825	41.330	17.472
3420	64.386	0.823	42.068	17.697
3480	65.000	0.831	42.806	16.912
3540	65.526	0.838	43.544	16.239
3600	66.491	0.850	44.282	15.005
3660	67.281	0.860	45.020	13.996
3720	66.842	0.854	45.758	14.557
3780	67.632	0.865	46.496	13.548
3940	68.333	0.873	48.464	12.651
4000	68.246	0.872	49.202	12.763
4060	69.123	0.884	49.940	11.642
4120	69.825	0.893	50.679	10.745
4180	69.825	0.893	51.417	10.745
4240	69.649	0.890	52.155	10.969
4300	69.386	0.887	52.893	11.305
4360	69.912	0.894	53.631	10.632
4420	70.000	0.895	54.369	10.520
4480	71.667	0.916	55.107	8.390
4540	72.982	0.933	55.845	6.708
4600	72.895	0.932	56.583	6.820
4660	72.719	0.930	57.321	7.044

4.7.7 Treatment of raw water from Samaru stream

The values of the raw water parameters collected at the three different sampling points of Samaru stream, their respective values after treatment and percentage removal efficiencies are as presented in Table 4.33. It was observed that pH neutrality of the samples was increased after treatment by 6.3 - 8.97 %. The Electrical Conductivities of the three samples were also observed to be reduced after treatment with sample point 2 having the highest removal efficiency of 47.59 %. Reduction in TDS was observed in all the three samples after treatment with sample point 2 attaining the highest removal efficiency of 53.61 %. After treatment, the COD of the three samples was also observed to be reduced and highest removal efficiency of 65.38 % was attained in sample point 1. Though BOD of the untreated samples was observed to be very low in all the raw water samples, reduction was achieved in all the three sample points after treatment and the highest removal efficiency of 75 % was attained in sample point 1.

The concentration of ammonium was also observed to be reduced after treatment in all the sample points and highest percentage removal of 90 % (sample point 2 & 3) was attained. In all the sample points, nitrate concentration was also observed to be reduced after treatment and highest percentage removal of 51.7 % was attained in sample point 2. For the chloride, concentration in the three samples was also observed to be reduced after treatment with sample point 1 showing the highest percentage removal (96.18 %). These observations imply that the low-cost adsorbent could be employed in the improvement of Samaru stream water quality.

For the heavy metals, the concentration of iron (III) was observed to be reduced after treatment in all the samples and considerable percentage removal of 91.76 % was attained in sample point 3. Copper (II) concentration was also observed to be reduced after treatment in all the samples with sample point 3 showing the highest percentage removal of 90.91 %. Concentration of lead (II) was also observed to show highest percentage removal of 52.9 % in sample point 3 and this was followed by 36.06 % in sample point 1. Concentration of zinc (II) was also observed to show highest percentage removal of 31.61 % in sample point 1 and this was followed by 22.36 % in sample point 2. Therefore, concentration of all the heavy metals considered in this study were observed to be reduced after treatment with the exception of zinc (II) in sample point 3 and lead (II) in sample point 2 and this could be attributed to experimental error. This study indicates that among the heavy metals considered, the low cost adsorbent has better adsorption affinity to iron (III) and copper (II) than lead (II) and zinc (II). These percentage removal efficiencies could be attributed to the effectiveness of the rice husk activated carbon resulting from its modification. Though low percentage removal efficiencies were observed in some sample parameters which may be as a result of bed saturation, such efficiencies could always be improved by employing higher bed depth or lower flow rates. Therefore, this modified rice husk activated carbon could be employed in multicomponent wastewater treatment.

Table 4.33: Values of Raw and Treated Sample Parameters Colleced at different Pionts of Samaru Stream

z=6cm, f=3ml/min, t=300min

Parameters	Point 1			Point 2			Point 3		
	Raw	**Treated**	**%Removal**	**Raw**	**Treated**	**%Removal**	**Raw**	**Treated**	**%Removal**
pH	7.8	7.1	8.97	7.8	7.1	8.97	7.9	7.4	6.33
E C (µS)	3.56	2.9	18.54	706	370	47.59	276.3	170.5	38.29
NH_4^+ (mg/l)	1.2	1.12	6.67	0.2	0.02	90.00	0.2	0.02	90.00
TDS (mg/l)	1.84	1.46	20.65	360	167	53.61	131.4	83.7	36.30
BOD (mg/l)	0.4	0.1	75.00	0.2	0.1	50.00	0.3	0.2	33.33
COD (mg/l)	260	90	65.38	230	100	56.52	210	160	23.81
NO_3^- (mg/l)	4.8	4.3	10.42	29.4	14.2	51.70	9.2	5.3	42.39
Cl^- (mg/l)	759.76	28.99	96.18	46.98	13.49	71.29	18.49	11.99	35.15
Fe (mg/l)	24.48	13.38	45.34	22.08	14.28	35.33	166.8	13.74	91.76
Cu (mg/l)	0.9	0.42	53.33	0.54	0.24	55.56	0.66	0.06	90.91
Zn (mg/l)	1.044	0.714	31.61	1.422	1.104	22.36	1.218	-	-
Pb (mg/l)	3.02	1.931	36.06	3.056	-	-	6.798	3.2	52.93

4.8 Important Outcome of this Study

Table 4.34, 4.35 and 4.36 presents the important outcome of this study as compared to related studies available in the literature.

Table 4.34: Outcome of Batch Adsorption

Adsorbent Adsorbate	Modification Techniques	Dosage (g)	Initial Conc. (mg/l)	Opti-mum pH	Equil. Contact time (min)	Adsorption Capacity (mg/g) Removal Efficiency (%)	Isotherm model Kinetic model Thermodynamic model	Optimiz-ation	Reference
Rice Husk Phenol	-Carbonization at 400-600^{o}C	1-10	10-1000	4	240	0.98-46.19	Freundlich	-	Daffalla *et al*. (n.d)
Rice husk Phenol	-H_2SO_4 activation -Carbonization at 850-900^{o}C			5.1	6h	75.15 (q_m)	-	-	Srihari and Das (2008)
Rice Husk Phenol	-Carbonization at 400^{o}C -H_3PO_4 activation -Heating at 700-900^{o}C			2.5	75	2.35x10^{-4}mol/g	Freundlich Second order Exothermic	-	Kennedy *et al*. (2007)
Rice Husk Phenol	-Carbonization at 600^{o}C -NaOH activation - Heating at 600-900^{o}C	0.05	1000			544.8	Freundlich Second order	-	Song *et al*. (2013)
Rice Husk Phenol	-$ZnCl_2$ activation -Carbonization at 700^{o}C	0.03-0.18	10 ppm		240	27.58		-	Kalderis *et al*. (2008b)
Rice Husk Phenol	-Carbonization at 400^{o}C			7	180	0.886 (q_{exp})	Freundlich First order	-	Mahvi *et al*. (2004)
Rice Husk Phenol	-Carbonization at 300-500^{o}C	1-10	10-300	4	300	0.951-1(q_{exp})	Freundlich	-	Kermani *et al*. (2006)
Rice Husk Phenol	-		10-70	8		1.23 (q_m)	Langmuir First order	-	SivaSubra-manian *et al*. (2012)
Rice Husk Phenol	-Carbonization at 300-500^{o}C -H_3PO_4 activation	2-4	10-50	4	20	2.4 (q_{exp})	Freundlich Second order Exothermic	441.46^{o}C (RSM)	This Study

Table 4.35: Outcome of Activated Carbon Modification

Precursor	Modification Process	Surface Area (m^2/g)	Pore Diameter (nm)	Pore Volume (cm^3/g)	Optimization	References
Rice Husk	-NaOH activation	116	65.1		-	Chakraborty *et al*. (2011)
Rice Husk	-Carbonization at 400^oC	50.14	14.49	0.182	-	Mahvi *et al*. (2004)
Rice Husk	-H_3PO_4 activation -Carbonization at 300-600^oC	634-1820	1.3-11	0.63-2.01 (ml/g)	-	Li *et al*. (2011b)
Rice Husk	-Carbonization at 400oC -H_3PO_4 activation -Heating at 700-900^oC	180-298	1.6-2.5	0.08-0.1 (micro)	-	Somasundaram *et al*. (2013)
Rice Husk	-H_3PO_4/$ZnCl_2$ activation -Carbonization at 400-700^oC -HCl acid washing	292-2434	2.06-3.02	0.116-0.59 (micro)	-	Liou and Wu (2009)
Rice Husk	-H_3PO_4/NaOH activation -CO_2 activation at 400-800^oC	9-91			-	Kalderis *et al*. (2008a)
Rice Husk	-Carbonization at 600-700^oC -CO_2 activation at 600-700^oC	162-166			-	Kalderis *et al*. (2008a)
Rice Husk	-Carbonization at 500-550^oC	44.7-139.7			-	Liu *et al*. (2011)
Rice Husk	-Carbonization at 400^oC -H_3PO_4 activation -Heating at 700-900^oC	344.7-438.9	0.111-0.118	3.5-3.8 (micro)	-	Kennedy *et al*. (2007)
Rice Husk	-Carbonization at 600^oC -NaOH activation -Heating at 600-900^oC	1745-2841	1.07-1.4	0.59-0.85 (micro)	-	Song *et al*. (2013)
Rice Husk	-Carbonization at 500-700^oC -H_2O activation at 550-750^oC	147-244		0.0566-0.1 (micro)	-	Zhang *et al*. (2011a)
Rice Husk	-H_2SO_4 activation -Carbonization at 200-800^oC	17		0.006 (micro)	-	Mohan *et al*. (2008)
Rice Husk	-Carbonization at 400^oC -CO_2 activation at 800-900^oC	227-334	1.22-1.4	0.157-0.212	-	Kumagai *et al*. (2009)
Rice Husk	-Carbonization at 600-800^oC -H_2O activation at 650-850^oC	168.8-231.7			-	Zhu *et al*. (2012)
Rice Husk	-Carbonization at 300-500^oC	20.26-50.14	4.2-15.16	0.042-0.182	-	Kermani *et al*. (2006)
Rice Husk	-Carbonization at 400-800^oC -$ZnCl_2$ activation -CO_2 activation -HCl acid washing	604.34	2.75	0.41	500^oC (Zn II)	Nasehir-khan *et al*. (2010b)
Rice Husk	-Carbonization at 300-500^oC -H_3PO_4 activation	64.7-102.4	1.82	0.034 (micro)	441.46^oC (Phenol)	This Study

Table 4.36: Outcome of Column Adsorption

Adsorbent Adsorbate	Type of Wastewater	Internal Diameter (cm)	Column Length (cm)	Carbon Depth (cm)	Initial Conc. (mg/l)	Flow Rate (ml/min)	Breakthrough /Exhaustion Capacity (mg/g)	Reference
Rice Husk Congo Red Dye	Simulated	1.2	50	12-30	18-42	3.6-5.6	2.47-3.08 (q_{Thomas})	Han *et al*. (2008)
Rice Husk Cu (II)	Simulated	3	30	3-9	10-50	5-15	1.4-6.33 ($q_{0.1}$)	Luo *et al*. (2011)
Rice Husk Cd (II)	Simulated	2	55	10-30	10-20	5-15	-	Kumar and Bandyopadh-yay (2005)
Rice Husk Cr (IV)	Simulated	1.5	40	15-25	100-300	25-50	1731-2535 (q_{Thomas})	Sugashini and Meera (2013)
Rice Husk Methylene Blue	Simulated	1.5	50	8.4-39	35-100	3.4-8.2	3.23-6.63 (q_{Thomas})	Han *et al*. (2006)
Rice Husk Cu (II)	Simulated	1.2	19.5	3-8	5-15	10-30	34.56	Nasehir-Khan *et al*. (2011)
Sugar Cane Bagasse Phenol	Simulated	3	55	16-32	20	33.3	12.02-12.34 ($q_{0.9}$)	Karunarathne and Amarasinghe (2013)
Date Stone Phenol	Simulated	1.1	50	5-25	50-150 ppm	23-141	-	Alhamed (2009)
Rice Husk Phenol	Petroleum Refinery	2-6	12-75	4.5-60	52.32-78.32	4.5-56.58	55.12 ($q_{0.9}$)	This study

CHAPTER FIVE

CONCLUSION AND RECOMMENDATIONS

5.1 Conclusion

This experimental study has led to the following conclusions:

1) Thermal and chemically pretreated rice husk activated carbon has been successfully used in the removal of phenol and treatment of Samaru stream water.
2) Adsorption capacity and removal efficiency of phenol onto rice husk activated carbon are dependent on the process variables studied (carbonizatiion temperature, initial phenol concentration, adsorbent dosage, contact time, solution temperature and pH).
3) The adsorption of phenol onto rice husk activated carbon is a multilayer and physical process. The adsorption process was found to be unspontaneous but feasible and exothermic.
4) The optimum temperature for the production of rice husk activated carbon for adsorption of phenol using response surface methodology is $441.46^{o}C$.
5) Modification of the thermally treated rice husk with phosphoric acid enhanced the characteristics and performance of the rice husk activated carbon in the adsorption of phenol.
6) The column experimental study has demonstrated the applicability of rice husk activated carbon in adsorption of phenol from real refinery wastewater.

5.2 Recommendations

1) Utilization of rice husk activated carbon has been demonstrated to have prospects in the treatment of phenolic wastewaters from refinery effluent and hence should be exploited in simultaneous adsorption of multi-component contaminants from the refinery wastewater.

2). Study should also be carried out to determine the pyrolytic volatile products (biofuel and biochemical) derivable from rice husk at the optimum carbonization temperature developed in this study.

3) Pilot scale study should also be carried out to investigate the viability of this bench scale study in industrial application.

4) Economic analysis of rice husk application in adsorption of phenol should be carried out in relation to other agricultural waste materials.

REFERENCES

Abbas, S.T. (2013). Modeling and optimization of adsorption of heavy metal ions onto local activated carbon. *Aquatic Science and Technology*, 1(2), 108-134

Abdelkreem, M. (2013). Adsorption of phenol from industrial wastewater using olive mill waste. *APCBEE Procedia*, 5, 349 – 357

Abdelwahab, O. (2007). Kinetic and isotherm studies of copper (II) removal from wastewater using various adsorbents. *Egyptian Journal of Aquatic Research*, 33(1), 125-143

Abdelwahab, O., Ahmed, E., Amany, E. and Azza K. (2005). Use of rice husk for adsorption of direct dyes from aqueous solution: A case study of Direct F. Scarlet. *Egyptian Journal of Aquatic Research*, 31(1), 1-11

Abechi, S.E., Gimba, C.E, Uzairu, A. and Dallatu, Y.A. (2013). Preparation and characterization of activated carbon from palm kernel shell by chemical activation. *Research Journal of Chemical Science*, 3(7), 54-61

Achmad, A., Jain, K., Tong, K.S., Rozaini, C.A. and Tan, L.S. (2012). Equilibrium, kinetic and thermodynamic studies on the adsorption of direct dye onto a novel green adsorbent developed from *Uncaria Gambir* extract. *Journal of Physical Science*, 23(1), 1–13

Activated Carbon Columns Plant Design (n.d). Retrieved June 20, 2014, from http://bibing.us.es/proyectos/abreproy/20087/fichero/CHAPTER+3.pdf

Adie, D.B., Olarinoye, N.A., Oke, I.A., Ismail, A., Lukman, S. and Otun, J.A. (2010). Removal of lead ions from aqueous solutions using powdered corn cobs. *The Canadian Journal of Chemical Engineering*, 88, 241-255

Agarry, S.E. and Aremu, M.O. (2012a). Batch equilibrium and kinetic studies of simultaneous adsorption and biodegradation of phenol by pineapple peels immobilized *Pseudomonas Aeruginosa* NCIB 950. *British Biotechnology Journal*, 2(1), 26-48

Agarry, S.E. and Aremu, M.O. (2012b) Batch Equilibrium and Kinetic Studies of Simultaneous Adsorption and Biodegradation of Naphthalene by Orange Peels Immobilized *Pseudomonas aeruginosa* NCIB 950, *Journal of Bioremediation and Biodegradion*, 3(2), 1-12

Aguayo-Villarreal, I.A., Ramirez-Montoyab, L.A., Hernandez-Montoyab, V., Bonilla-Petriciolet, A., Montes-Moranc, M.A. and Ramirez-Lopez, E.M. (2013). Sorption mechanism of anionic dyes on pecan nut shells (Carya illinoinensis) using batch and continuous systems. *Industrial Crops and Products*, 48, 89– 97

Ahmad, A.A. and Hameed, B.H. (2010). Effect of preparation conditions of activated carbon from bamboo waste for real textile wastewater. *Journal of Hazardous Materials*, 173, 487–493

Ahmad, A.A., Hameed, B.H. and Ahmad, A.L. (2009). Removal of disperse dye from aqueous solution using waste-derived activated carbon: Optimization study. *Journal of Hazardous Materials*, 170, 612–619

Ahmad, F., Wan Daud, W. M., Ahmad, M. A. and Radzi, R. (2013). The effects of acid leaching on porosity and surface functional groups of cocoa (Theobroma cacao)-shell based activated carbon. *Chemical Engineering Research and Design*, 91, 1028 −1038

Ahmad, M. and Alrozi, R. (2010). Optimization of preparation conditions for mangosteen peel-based activated carbons for the removal of Remazol Brilliant Blue R using response surface methodology. *Chemical Engineering Journal*, 165, 883–890

Ahmaruzzaman, M.D (2008). Adsorption of phenolic compounds on low-cost adsorbents: A review. *Advances in Colloid and Interface Science*, 143, 48–67

Aidan, G. (2012). Agricultural wastes and activated carbon from them for furfural removal from water solutions. *Life Science Journal*, 9(3), 2501-2505

Alam, M.D.Z., Ameem, E.S., Suleyman, A.M. and Nassereldeen, A.K. (2009). The factors affecting the performance of activated carbon prepared from oil palm empty fruit bunches for adsorption of phenol. *Chemical Engineering Journal*, 155, 191–198

Al-Anber, Z.A. and Mohammed A.S.A. (2008). Thermodynamics and kinetic studies of iron (III) adsorption by olive cake in a batch system. *J. Mex. Chem. Soc.*, 52(2), 108-115.

Albadarin, A.B., Yang, Z., Mangwandi, C., Glocheux, Y., Walker, G. and Ahmad, M.N.M. (2013). Experimental design and batch experiments for optimization of Cr (VI) removal from aqueous solutions by hydrous cerium oxide nanoparticles. *Chemical Engineering Research and Design*, http://dx.doi.org/10.1016/j.cherd.2013.10.015

Albanis, T.A., Hela, D.G., Sakellarides, T.M and Danis, T.G. (2000). Removal of dyes from aqueous solutions by adsorption on mixtures of fly ash and soil in batch and column techniques. *Global Nest: The Int. J.*, 2(3), 237-244

Alhamed, Y.A. (2009). Adsorption kinetics and performance of packed bed adsorber for phenol removal using activated carbon from dates' stones. *Journal of Hazardous Materials*, 170, 763–770

Ali, I., Asim, M. and Khan, T.A. (2012). Low cost adsorbents for the removal of organic pollutants from wastewater. *Journal of Environmental Management*, 113, 170-183

Alicia P.A. and Margarita T.M.M. (2012). Lignocellulosic precursors used in the elaboration of activated carbon, lignocellulosic precursors used in the synthesis of activated carbon-characterization techniques and applications in the wastewater treatment, *InTech*.

Al-Qodah, Z. and Shawabkah, R. (2009). Production and characterization of granular activated carbon from activated sludge. *Brazilian Journal of Chemical Engineering*, 26(1)

Al-Swaidan, M.H. and Ahmad, A. (2011). Synthesis and characterization of activated carbon from saudi arabian dates tree's fronds wastes. *3rd International Conference on Chemical, Biological and Environmental Engineering*, Singapore.

Alzaydien, S.A. and Waleed, M. (2009). Equilibrium, kinetic and thermodynamic studies on the adsorption of phenol onto activated phosphate rock. *International Journal of Physical Sciences*, 4(4), 172-181

Amin, N.K (2008). Removal of reactive dye from aqueous solutions by adsorption onto activated carbons prepared from sugarcane bagasse pith. *Desalination*, 223, 152–161

Amini, M., Younesi, H. and Bahramifar, N. (2009). Statistical modeling and optimization of the cadmium biosorption process in an aqueous solution using Aspergillus Niger. *Colloids and Surfaces A: Physicochem. Eng. Aspects*, 337, 67–73

Amuda, O.S, Alade, A.O, Afolabi, A.O. and Adelewo, F.E (2012). Adsorption of acenaphthene unto activated carbon produced from agricultural wastes. *Journal of Environmental Science and Technology*, 5(4), 192-209

Ang, T.N., Ngoh, G.C. and May Chua, A.S. (2013). Comparative study of various pretreatment reagents on rice husk and structural changes assessment of the optimized pretreated rice husk. *Bioresource Technology*, 135, 116–119

Anupam, K., Duttab, S., Bhattacharjee, C. and Datta, S. (2011). Adsorptive removal of chromium (VI) from aqueous solution over powdered activated carbon: Optimization through response surface methodology. *Chemical Engineering Journal*, 173, 135– 143

APHA, (1998). *Standard Methods for the Examination of Water and Wastewater, 20th Edition, Washingon DC*. Available from http://www.apha.org/

Arulkumar, M., Sathishkumar, P. and Palvannan, T. (2011). Optimization of Orange G dye adsorption by activated carbon of Thespesia populnea pods using response surface methodology. *Journal of Hazardous Materials*, 186, 827–834

Awala, H.A. and El-Jamal, M.M. (2011). Equilibrium and kinetics study of adsorption of some dyes onto feldspar. *Journal of the University of Chemical Technology and Metallurgy,* 46, 1, 45-52

Aworn, A., Thiravetyan, P. and Nakbanpote, W. (2008). Preparation and characteristics of agricultural waste activated carbon by physical activation having micro- and mesopores. *J. Anal. Appl. Pyrolysis*, 82, 279−285

Baccar, R., Blánquez, P., Bouzid, J., Feki, M. Attiya, H. and Sarrà, M. (2013). Modeling of adsorption isotherms and kinetics of a tannery dye onto an activated carbon prepared from an agricultural by-product. *Fuel Processing Technology*, 106, 408–415

Bada, S.O. (2007). *Adsorption of Phenols onto Fly Ash*. M. Eng Thesis, University of the Witwatersrand, South Africa.

Bagheri, N. and Abedi, J. (2009). Preparation of high surface area activated carbon from corn by chemical activation using potassium hydroxide. *Chemical Engineering Research and Design*, 87, 1059−1064

Bansal, M., Garg, U., Singh, D. and Garg, V.K. (2009). Removal of Cr (VI) from aqueous solutions using pre-consumer processing agricultural waste: A case study of rice husk. *Journal of Hazardous Materials*, 162, 312–320

Baseri, R.J., Palanisamy, P.N. and Sivakumar, P. (2012). Preparation and Characterization of Activated Carbon from *Thevetia Peruviana* for the Removal of Dyes from Textile Wastewater, *Advances in Applied Science Research*, 3(1), 377-383

Basonde, R.R (2002). *Treatment of Organic and Inorganic Pollutants in Municipal Wastewater by Agricultural By-Product Based Granular Activated Carbons*. M. Tech Thesis, Louisiana State University, Louisiana, USA.

Basta, A.H., Fierro, V., El-Saied, H. and Celzard, A. (2009). 2-Steps KOH activation of rice straw: An efficient method for preparing high-performance activated carbons. *Bioresource Technology*, 100, 3941–3947

Basu, J.K., Monal, D. and Pinaki, G. (2012). Statistical optimization for the prediction of ibuprofen adsorption capacity by using microwave assisted activated carbon. *Archives of Applied Science Research*, 4(2), 1053-1060

Beker, U., Ganbold, B., Dertli, H. and Gulbayir, D.D. (2010). Adsorption of phenol by activated carbon: Influence of activation methods and solution pH. *Energy Conversion and Management*, 51, 235–240

Belgin, K., Fatma, T., Hakan, D. and İlknur D. (2008). Liquid phase adsorption of phenol by activated carbon derived from hazelnut bagasse. *International Journal of Environmental Application & Science*, 3(5), 373-380

Benyahia, F., Abdulkarim, M., Embaby, A. and Rao, M. (2004). Refinery Wastewater Treatment: A true Technological Challenge. *The Seventh Annual U.A.E. University Research Conference*, United Arab Emirate.

Bhantagar, A and Minocha, A.K. (2006). Conventional and non conventional adsorbents for removal of pollutants from water. *Indian Journal of Chemical Technology*, 13, 203-217

Bhatnagar, A., Hogland, W., Marques, M. and Sillanpa, M. (2013). An overview of the modification methods of activated carbon for its water treatment applications. *Chemical Engineering Journal*, 219, 499–511

Blanco-Martínez, D.A., Giraldo, L. and Moreno-Piraján, J.C. (2009). Effect of the pH in the adsorption and in the immersion enthalpy of monohydroxylated phenols from aqueous solutions on activated carbons. *Journal of Hazardous Materials*, 169, 291–296

Boumaza, S., Kaouah, F., Berrama, T., Trari, M. and Bendjama, Z. (2012). Optimization of preparation conditions for activated carbon from waste materials of agricultural origin for the removal of basic red 46. *Chemometrics and Intelligent Laboratory Systems*, 118, 311–316

Busca, G., Berardinelli, S., Resini, C. and Arrighi, L. (2008). Technologies for the removal of phenol from fluid streams: A short review of recent developments. *Journal of Hazardous Materials*, 160, 265–288

Butland, D.T. (2008). *Adsorption Removal of Tertiary Butyl Alcohol from Wastewater by Zeolite*. Master's Thesis, Worcester Polytechnic Institute, Worcester, USA.

Cadoni, P. and Angelucci, F. (2013). *Analysis of Incentives and Disincentives for Rice in Nigeria*. Retrieved February 27, 2014 from http://www.fao.org/fileadmin/templates/mafap/documents/technical_notes/NIGERIA/NIGERIA_Technical_Note_RICE_EN_Jul2013.pdf

Calero, M., Ronda, A., Martın-Lara, M.A., Perez, A. and Blazquez, G. (2013). Chemical activation of olive tree pruning to remove lead (II) in batch system: Factorial design for process optimization. *Biomass and Bioenergy*, 58, 322-332

Ceyhan, A. A., Sahin, O., Saka, C. and Yalcın, A. (2013). A novel thermal process for activated carbon production from thevetch biomass with air at low temperature by two-stage procedure. *Journal of Analytical and Applied Pyrolysis*, 104, 170–175

Chakraborty, S., Chowdhury, S. and Saha, P.D. (2011). Adsorption of Crystal Violet from aqueous solution onto NaOH-modified rice husk. *Carbohydrate Polymers*, 86, 1533– 1541

Chand, R., Watari, T., Inoue, K., Kawakita, H., Luitel, H.N., Parajuli, D., Torikai, T. and Yada, M. (2009). Selective adsorption of precious metals from hydrochloric acid solutions using porous carbon prepared from barley straw and rice husk. *Minerals Engineering*, 22, 1277–1282

Chandra, T.C., Mirna, M.M., Sunarso, J., Sudaryanto, Y. and Ismadji, S. (2009). Activated carbon from durian shell: Preparation and characterization. *Journal of the Taiwan Institute of Chemical Engineers*, 40, 457−462

Charles, O.I. and Odoemelam, I.S.A. (2010). Studies on adsorbent dosage, particle sizes and pH constraints on biosorption of Pb (II) and Cd (II) ions from aqueous solution using modified and unmodified Crasstrotrea Gasar (Bivalve) Biomass. *International Archives of Applied Science and Technology*, 1(1), 62-68

Chaudhary, N. and Balomajumder, C. (2013). Optimization study of adsorption parameters for removal of phenol on aluminum impregnated fly ash using response surface methodology. *Journal of the Taiwan Institute of Chemical Engineers*, http://dx.doi.org/10.1016/ j.jtice.2013.08.016

Chen, N., Zhang, Z., Feng, C., Li, M., Suiguira, N. and Chen, R. (2011a). Investigation on the batch and fixe-bed column performance of floride adsorption by kanuma mud. *Desalination*, 268, 76-82

Chen, Y., Zhai, S-R., Liu, N., Song, Y., An, Q-D. and Song, X-W. (2013). Dye removal of activated carbons prepared from NaOH-pretreated rice husks by low-temperature solution-processed carbonization and H_3PO_4 activation. *Bioresource Technology*, 144, 401–409

Chen, Y., Zhu,Y., Wang, Z., Li, Y., Wang, L., Ding, L.,….. and Guo, Y. (2011b). Application studies of activated carbon derived from rice husks produced by chemical-thermal process: A review. *Advances in Colloid and Interface Science*, 163, 39–52

Chowdhury, S., Mishra, R., Saha, P. and Kushwaha, P. (2011). Adsorption thermodynamics, kinetics and isosteric heat of adsorption of malachite green onto chemically modified rice husk. *Desalination*, 265, 159–168

Chowdhury, Z.Z., Zain, S.M., Rashid, A.K., Rafique, R.F. and Khalid, K. (2013). Breakthrough curve analysis for column dynamics sorption of Mn (II) ions from wastewater by using *Mangostana garcinia* peel-based granular-activated carbon. *Journal of Chemistry*, Volume 2013, Article ID 959761

Cronje, K.J., Chetty, K., Carsky, M., Sahu, J.N. and Meikap, B.C. (2011). Optimization of chromium(VI) sorption potential using developed activated carbon from sugarcane bagasse with chemical activation by zinc chloride. *Desalination*, 275, 276–284

Cuhadaroglu, D. and Uygun, O. A. (2008). Production and Characterization of Activated Carbon from a Bituminous Coal by Chemical Activation. *African Journal of Biotechnology*, 7(20), 3703-3710.

Dada, A.O., Olalekan, A.P., Olatunya, A.M. and Dada, O. (2012). Langmuir, Freundlich, Temkin and Dubinin-Radushkevich isotherms studies of equilibrium sorption of Zn (II) unto phosphoric acid modified rice husk**.** *IOSR Journal of Applied Chemistry*, 3(1), 38-45

Daffalla, S.B., Hilmi, M. and Maizatul S.S. (2012). Effect of organic and inorganic acid pretreatment on structural properties of rice husk and adsorption mechanism of phenol. *International Journal of Chemical and Environmental Engineering*, 3(3), 192-200

Daffalla, S.B., Hilmi, M. and Maizatul S.S. (n.d). *Batch Studies of Adsorption of Phenol from Aqueous Solutions Using Rice Husk Ash*. Retrieved February 9, 2013 from http://eprints.utp.edu.my/8817/1/1569558107-new.pdf

Daffalla, S.B., Mukhtar, H. and Shaharun, M.S. (2010). Characterization of adsorbent developed from rice husk: effect of surface functional group on phenol adsorption. *Journal of Applied Sciences*, 10(12), 1060-1067

Das, L., Praveen, K., Jason, A.O. and John, J.C. (2012). Adsorption of *p*-cresol on granular activated carbon. *CIGR Journal*, 14(4), 37-49

Demiral, H. and Gunduzoglu, G. (2010). Removal of nitrate from aqueous solutions by activated carbon prepared from sugar beet bagasse. *Bioresource Technology*, 101, 1675–1680

Demirbas, A. (2008). Heavy metal adsorption onto agro-based waste materials: A review. *Journal of Hazardous Materials*, 157, 220–229

Demirbas, A. (2009). Agricultural based activated carbons for the removal of dyes from aqueous solutions: A review. *Journal of Hazardous Materials*, 167, 1–9

Demirbas, E., Dizge, N., Sulak, M.T. and Kobya, M. (2009). Adsorption kinetics and equilibrium of copper from aqueous solutions using hazelnut shell activated carbon. *Chemical Engineering Journal*, 148, 480–487

Demirbas, E., Mehmet, K., Elif, S. and Tuncay O. (2004). Adsorption kinetics for the removal of chromium (VI) from aqueous solutions on the activated carbons prepared from agricultural wastes. *Water SA*, 30(4), 533-540

Deng, H., Li, G., Yang, H., Tang, J. and Jiangyun, T. (2010). Preparation of activated carbons from cotton stalk by microwave assisted KOH and K_2CO_3 activation. *Chemical Engineering Journal*, 163, 373–381

Dharmendirakumar, M., Vijayakumar, G. and Tamilarasan, R. (2012). Adsorption, kinetic, equilibrium and thermodynamic studies on the removal of basic dye Rhodamine-B from aqueous solution by the use of natural adsorbent perlite. *Journal of Mater. Environ. Science*, 3(1), 157-170

Dim, P.E and Okafor, J.O. (2012). Development and characterization of adsorbent from coconut shells for purification of dye wastewater. *Journal of Science, Technology, Mathematics and Education*, 8(3), 68-80

Djebbar, M., Djafri1, F., Bouchekara, M. and Djafri, A. (2012). Adsorption of phenol on natural clay. *African Journal of Pure and Applied Chemistry*, 6(2), 15-25

Dolas, H., Sahin, O., Saka, C. and Demir, H. (2011). A new method on producing high surface area activated carbon: The effect of salt on the surface area and the pore

size distribution of activated carbon prepared from pistachio shell. *Chemical Engineering Journal*, 166, 191–197

Dwivedi, C.P., Sahu, J.N., Mohanty, C.R., Mohana, B.R. and Meikap, B.C. (2008). Column performance of granular activated carbon packed bed for Pb (II) removal. *Journal of Hazardous Materials*, 156, 596–603

El-Naas, M.H., Al-Zuhair, S. and Alhaija, M.A. (2010). Removal of phenol from petroleum refinery wastewater through adsorption on date-pit activated carbon. *Chemical Engineering Journal*, 162, 997–1005

El-Shafey, E.I. (2007). Sorption of Cd (II) and Se (IV) from aqueous solution using modified rice. *Journal of hazardous materials*, doi:10.1016/j.jhazmat.2007.01.051

El-Shafey, E.I. (2010). Removal of Zn (II) and Hg (II) from aqueous solution on a carbonaceous sorbent chemically prepared from rice husk. *Journal of Hazardous Materials*, 175, 319–327

Farajzadeh, M.A. and Mohammad, R.F. (2005). Study of phenolic compounds removal from aqueous solution by polymeric sorbent. *Journal of the Chinese Chemical Society*, 52, 295-301

Fathy, N.A., Sayed-Ahmed, S.A. and Abo-El-Enin, R.M. (2012). Effect of activation temperature on textural and adsorptive properties for activated carbon derived from local reed biomass: Removal of p-Nitrophenol. *Environmental Research, Engineering and Management*, 1(59), 10-22

Fierro, V., Torne´-Fernandez, V., Montane, D. and Celzard, A. (2008). Adsorption of phenol onto activated carbons having different textural and surface properties. *Microporous and Mesoporous Materials*, 111, 276–284

Foo, K.Y. and Hameed, B.H. (2009). Utilization of rice husk ash as novel adsorbent: A judicious recycling of the colloidal agricultural waste. *Advances in Colloid and Interface Science*, 152, 39–47

Foo, K.Y. and Hameed, B.H. (2012). Preparation, characterization and evaluation of adsorptive properties of orange peel based activated carbon via microwave induced K_2CO_3 activation. *Bioresource Technology*, 104, 679–686

Galletti, C., Russo, N. and Fino, D. (2012). Zn (II) Removal from Wastewater Using Rice Husk as Adsorbent. *3rd International Conference on Industral and Harzadous Waste Management.*

Garg, U., Kaur, M.P., Jawa, G.K., Sud, D. and Garg, V.K. (2008). Removal of cadmium (II) from aqueous solutions by adsorption on agricultural waste biomass. *Journal of Hazardous Materials*, 154, 1149–1157

Gayatri, S.L. and Ahmaruzzaman, M.D. (2010). Adsorptive Technique for the Removal of Phenolic Compounds from Wastewater using Low-cost Adsorbent. *Asian University Journal of Science and Technology*, 5(2), 156-166

Ghaedi, M., Ghazanfarkhani, M.D., Khodadoust, S., Sohrabi, N. and Oftade, M. (2013). Acceleration of methylene blue adsorption onto activated carbon prepared from dross licorice by ultrasonic: Equilibrium, kinetic and thermodynamic studies. *Journal of Industrial and Engineering Chemistry*, http://dx.doi.org/10.1016/j.jiec.2013.10.039

Girgis, B.S., Smith, E., Louis, M.M. and El-Hendawy, A.A. (2009). Pilot production of activated carbon from cotton stalks using H_3PO_4. *J. Anal. Appl. Pyrolysis*, 86, 180-184

Girish, C.R. and Ramachandra, M.V. (2012). Adsorption of phenol from wastewater using locally available adsorbents. *Journal of Environmental Research and Development*, 6(3a), 763-772

Girods, P., Dufour, A., Fierro, V., Rogaume, Y., Rogaume, C., Zoulalian, A. and Celzard, A. (2009). Activated carbons prepared from wood particleboard wastes: Characterization and phenol adsorption capacities. *Journal of Hazardous Materials*, 166, 491–501

Godliving, Y.S.M. (2009). Recent advances in pretreatment of lignocellulosic wastes and production of value added products. *African Journal of Biotechnology*, 8(8), 1398-1415

Gottipati, R. (2012). *Preparation and Characterization of Microporous Activated Carbon from Biomass and its Application in the Removal of Chromium (VI) from Aqueous Phase*. PhD Thesis, National Institute of Technology, Rourkela, Odisha, India.

Gottipati, R. and Mishra, S. (2012). Application of response surface methodology for optimization of Cr (III) and Cr (VI) adsorption on commercial activated carbons. *Research Journal of Chemical Sciences*, 2(2), 40-48

Gratuito, M.K.B., Panyathanmaporn, T., Chumnanklang, R.-A., Sirinuntawittaya, N. and Dutta, A. (2008). Production of activated carbon from coconut shell: Optimization using response surface methodology. *Bioresource Technology*, 99, 4887–4895

Gueu, S., Yao, B., Adouby, K. and Ado, G. (2007). Kinetics and thermodynamics study of lead adsorption on to activated carbons from coconut and seed hull of the palm tree. *Int. J. Environ. Sci. Tech*., 4 (1), 11-17

Gulipalli, Ch., Prasad, B. and Wasewa, L. K. (2011). Batch study, equilibirum and kinetics of adsorption of selenium using rice husk ash (RHA). *Journal of Engineering Science and Technology*, 6(5), 586 – 605

Gundogdu, A., Duran, C., Senturk, H.B., Soylak, M., Imamoglu, M. and Onal, Y. (2013). Physicochemical characteristics of a novel activated carbon producedfrom tea industry waste. *Journal of Analytical and Applied Pyrolysis*, 104, 249–259

Hameed, B.H. and Foo, K.Y. (2010). Insights into the modeling of adsorption isotherm systems. *Chemical Engineering Journal*, 156, 2–10

Hameed, B.H. and Rahman, A.A. (2008). Removal of phenol from aqueous solutions by adsorption onto activated carbon prepared from biomass material. *Journal of Hazardous Materials*, 160, 576–581

Hameed, B.H., Mahmoud, D.K. and Ahmad, A.L. (2008). Equilibrium modeling and kinetic studies on the adsorption of basic dye by a low-cost adsorbent: Coconut (*Cocos nucifera*) bunch waste. *Journal of Hazardous Materials*, 158, 65–72

Han, C., Pu, H., Li, H., Deng, L., Huang, S., He, S. and Luo, Y. (2013). The optimization of As (V) removal over mesoporous alumina by using response surface methodology and adsorption mechanism. *Journal of Hazardous Materials*, 254, 301– 309

Han, R., Ding, D., Xu, Y., Zou, W., Wang, W., Li, Y. and Zou, L. (2008). Use of rice husk for the adsorption of congo red from aqueous solution in column mode. *Bioresources Technology*, 99, 2938-2946

Han, R., Wang, Y., Yu, W., Zou, W., Shi, J. and Liu, H. (2006). Biosorption of methylene blue from aqueous solution by rice husk in a fixed-bed column. *Journal of Hazardous Materials*, doi:10.1016/j.jhazmat.2006.07.031

Hapazari, I., Ntuli, V. and Parawira, W. (2011). Evaluation of single-step steam pyrolysis-activated carbons from Lesotho agro-forestry residues. *Tanzanian Journal of Science*, 37, 120-128

Hassani, A., Alidokht, L., Khataee, A.R. and Karaca, S. (2013). Optimization of comparative removal of two structurally different basic dyes using coal as a low-

cost and available adsorbent. *Journal of the Taiwan Institute of Chemical Engineers*, http://dx.doi.org/10.1016/ j.jtice.2013.10.014

Hema, H. and Arivoli, S. (2007). Comparative study on the adsorption kinetics and thermodynamics of dyes onto acid activated low cost carbon. *International Journal of Physical Sciences*, 2(1), 10-17

Herawan, S.G., Hadi, M.S., Ayob, Md.R. and Putra, A. (2013). Characterization of activated carbons from oil-palm shell by CO_2 activation with no holding carbonization temperature. *The Scientific World Journal*, Volume 2013, Article ID 624865

Hesas, R.H., Arami-Niya, A., Wan-Daud, W-M. A. and Sahu, J.N. (2013). Preparation of granular activated carbon from oil palm shell by microwave-induced chemical activation: Optimization using surface response methodology. *Chemical Engineering Research and Design*, 91, 2447–2456

Ho, S.Y. and McKay, G. (2004). Sorption of copper (II) from aqueous solution by peat. *Water, Air and Soil Pollution*, 158, 77-97

Ho, Y. (2004). Citation review of Lagergren kinetic rate equation on adsorption reactions. *Scientometrics*, 59(1), 171-177

Ho, Y., Mohammad, I.E. and Gihan, F.M. (2010). On the use of linearized pseudo-second-order kinetic equations for modeling adsorption systems. *Desalination*, 257, 93–101

Homagai, P.L., Ghimire, K.N. and Inoue, K. (2010). Adsorption behavior of heavy metals onto chemically modified sugarcane bagasse. *Bioresource Technology*, 101, 2067–2069

Hu, S., Xiang, J., Sun, L., Xu, M., Qiu, J. and Fu, P. (2008). Characterization of char from rapid pyrolysis of rice husk. *Fuel Processing Technology*, 89, 1096–1105

Ibrahim, F.B., Otun, J.A., Adie, D.B. and Jagaba, N.Z. (2011). Removal of some selected heavy metals from tannery wastewater using powdered limestone. *Nigerian Journal of Engineering*, 18(1), 89-95

Ibrahem, A.S., Sadon, F.N. and Kamariah, N.I. (2012). An overview of rice husk applications and modification techniques in wastewater treatment. *Journal of Purity, Utility Reaction and Environment*, 1(6), 338-364

Igboro, (2011). *Production of Biogas and Compost from Cow Dung in Zaria, Nigeria*. PhD Dissertation, Ahmadu Bello University, Zaria, Nigeria.

Imamoglu, M. and Tekir, O. (2008). Removal of copper (II) and lead (II) ions from aqueous solutions by adsorption on activated carbon from a new precursor hazelnut husks. *Desalination*, 228, 108–113

Inagaki, M. (2009). Pores in carbon materials-importance of their control. *New Carbon Materials*, 24(3), 193–232

Ioannidou, O. and Zabaniotou, A. (2007). Agricultural Residues as Precursors for Activated Carbon Production-A Review. *Renewable and Sustainable Energy Reviews*, 11, 1966-2005

Islam, M.S., Rouf, M.A., Fujimoto, S. and Minowa, T. (2012). Preparation and characterization of activated carbon from bio-diesel by-products (*Jatropha Seedcake*) by Steam Activation. *Bangladesh Journal of Scientific and Industrial Research*, 47(3), 257-264.

Ismail, A., Adie, D.B., Oke, I.A., Otun, J.A., Olarinoye, N.A., Lukman, S. and Okuofu, C.A. (2009). Adsorption kinetics of cadmium ions onto powdered corn cobs. *The Canadian Journal of Chemical Engineering*, 87, 896–909

Ji, F., Li, C., Xu, J. and Liu, P. (2013). Dynamic adsorption of Cu (II) from aqueous solution by zeolite/cellulose acetate blend fiber in fixed-bed. *Colloids and Surfaces A: Physicochem. Eng. Aspects*, 434, 88– 94

Jibril, B., Houache, O., Al-Maamari, R. and Al-Rashidi, B. (2008). Effects of H_3PO_4 and KOH in carbonization of lignocellulosic material. *J. Anal. Appl. Pyrolysis*, 83, 151−156

Jiménez, V., Díaz, J.A., Sánchez, P., Valverde, J.S. and Romero, A. (2009). Influence of the activation conditions on the porosity development of herringbone carbon nanofibers. *Chemical Engineering Journal*, 155, 931–940

Juárez-Galán, J.M., Silvestre-Albero, A., Silvestre-Albero, J. and Rodríguez-Reinoso, F. (2009). Synthesis of activated carbon with highly developed ‘‘mesoporosity”. *Microporous and Mesoporous Materials*, 117, 519–521

Kadhim, F. and Al-Seroury, F.A. (2012). Characterization the removal of phenol from aqueous solution in fluidized bed column by rice husk adsorbent. *Research Journal of Recent Sciences*, 1, 145-151

Kalalagh, S., Babazadeh, H., Nazemi, A.H. and Manshouri, M. (2011). Isotherm and kinetics studies on adsorption of Pb, Zn and Cu by Kaolite. *Capsian Journal of Environmental Science*, 9(2), 243-255

Kalavathy, H., Karthik, B. and Miranda, L.M. (2010). Removal and recovery of Ni and Zn from aqueous solution using activated carbon from Hevea brasiliensis: Batch and column studies. *Colloids and Surfaces B: Biointerfaces*, 78, 291–302

Kalavathy, M.H., Regupathi, I., Pillai, M.G. and Miranda, L.M. (2009). Modelling, analysis and optimization of adsorption parameters for H_3PO_4 activated rubber wood sawdust using response surface methodology (RSM). *Colloids and Surfaces B: Biointerfaces*, 70, 35–45

Kalderis, D., Bethanis, S., Paraskeva, P. and Diamadopoulos, E. (2008a). Production of activated carbon from bagasse and rice husk by a single-stage chemical activation method at low retention times. *Bioresource Technology*, 99, 6809–6816

Kalderis, D., Koutoulakis, D., Paraskeva, P., Diamadopoulos, E., Otal, E., Valle, J.O. and Fernandez-Pereira, C. (2008b). Adsorption of polluting substances on activated carbons prepared from rice husk and sugarcane bagasse. *Chemical Engineering Journal*, 144, 42–50

Kamble, S.P., Mangrulkar, P.A., Bansiwal, A.K. and Rayalu, S.S. (2008). Adsorption of phenol and *o*-chlorophenol on surface altered fly ash based molecular sieves. *Chemical Engineering Journal*, 138, 73–83

Kaouah, F., Boumaza, S., Berrama, T., Trari, M. and Bendjama, Z. (2013). Preparation and characterization of activated carbon from wild olive cores (oleaster) by H_3PO_4 for the removal of Basic Red 46. *Journal of Cleaner Production*, 54, 296-306

Karaca, S., Gurses, A., Acıkyıldız, M. and Ejder, M. (2008). Adsorption of cationic dye from aqueous solutions by activated carbon. *Microporous and Mesoporous Materials*, 115, 376–382

Karagoz, S., Tay, T., Ucar, S. and Erdem, M. (2008). Activated carbons from waste biomass by sulfuric acid activation and their use on methylene blue adsorption. *Bioresource Technology*, 99, 6214–6222

Karunarathne, H.D.S.S. and Amarasinghe, B.M.W.P.K. (2013). Fixed bed adsorption column studies for the removal of aqueous phenol from activated carbon prepared from sugarcane bagasse. *Energy Procedia*, 34, 83 – 90

Kennedy, L.J., Vijaya, J.J., Kayalvizhi, K. and Sekaran, G. (2007). Adsorption of phenol from aqueous solutions using mesoporous carbon prepared by two-stage process. *Chemical Engineering Journal*, 132, 279–287

Kermani, M., Bina, B., Khazaei, Z. and Pourmoghaddas, H. (2006). Removal of phenol from aquous solution by rice husk ash and activated carbon. *Pakistan Journal of Biologocal Sciences*, 9(10), 1905-1910

Khdeem, H.I. (2013). Adsorption isotherm of dyes from aqueous solutions on spent tea leaves, *International Journal of Advanced Scientific and Technical Research,* 3(1), 178-185

Khalir, W.K.A.W.M., Hanafiah, M.A.K.M., So'ad, S.Z.M., Ngah, W.S.W. and Majid, Z.A.A. (2012). Batch, column and thermodynamics of Pb (II) adsorption on xanthated rubber leaf powder. *Journal of Applied Sciences*, 12(11), 1142-1147

Khare, P. (2011). *Treatment of Phenolic Water Using Adsorption*. M.Tech Thesis, National Institute of Technology, Rourkela, India.

Khataee, A.R. (2009). Application of central composite design for the optimization of photodestruction of a textile dye using UV/S2O82-process. *Pol. J. Chem. Tech*., 11, 38-45.

Khataee, A.R. (2010). Optimization of UV-promoted peroxydisulphate oxidation of C.I. Acid Blue 25 using response surface methodology. *Environ. Technol*., 31, 73–86.

Khodadoust, S., Ghaedi, M., Sahraei, R. and Daneshfar, A. (2013). Application of experimental design for removal of sunset yellow by copper sulfide nanoparticles loaded on activated carbon. *Journal of Industrial and Engineering Chemistry,* http://dx.doi.org/10.1016/j.jiec.2013.10.053

Krishnan, A.K., Sreejalekshmi, K.G. and Baiju, R.S. (2011). Nickel (II) adsorption onto biomass based activated carbon obtained from sugarcane bagasse pith. *Bioresource Technology*, 102, 10239–10247

Krishnan, K.A. and Anirudhan, T.S. (2003). Removal of Cd (II) from aqueous solution by steam activated sulphurised carbon prepared from sugar cane baggase pith: Kinetics and equilibrium studies. *Water SA*, 29(2), 147-156

Krishnani, K.K., Meng, X., Christodoulatos, C. and Boddu, V.M. (2008). Biosorption mechanism of nine different heavy metals onto biomatrix from rice husk. *Journal of Hazardous Materials*, 153, 1222–1234

Kudaybergenov, K.K., Ongarbayev, E.K. and Mansurov, Z.A. (2012). Thermally treated rice husks for petroleum adsorption. *International Journal of Biology and Chemistry*, 1, 3-12

Kumagai, S., Shimizu, Y., Toida, Y. and Enda, Y. (2009). Removal of dibenzothiophenes in kerosene by adsorption on rice husk activated carbon. *Fuel*, 88, 1975–1982

Kumar, P.S. and Kirthika, K. (2009). Equilibrium and kinetic study of adsorption of nickel from aqueous solution onto bael tree leaf powder. *Journal of Engineering Science and Technology*, 4(4), 351-363

Kumar, U. and Bandyopadhyay, M. (2005). Fixed bed column study for Cd (II) removal from wastewater using treated rice husk. *Journal of Hazardous Materials*, doi:10.1016/j.jhazmat.2005.08.038

Kundu, S. and Gupta, A.K. (2005). Analysis and modeling of fixed bed column operations on As (V) removal by adsorption onto iron oxide-coated cement (IOCC). *Journal of Colloid and Interface Science*, 290, 52-57

Kwaghger, A. and Ibrahim, J.S. (2013). Optimization of conditions for the preparation of activated carbon from mango nuts using HCl. *American Journal of Engineering Research*, 2(7), 74-85

Kwak, J.S. (2005). Application of Taguchi and response surface methodologies for geometric error in surface grinding process. *Int. J. Mach. Tool. Manu*, 45, 327–334.

Lakshmi, U.R., Srivastava, V.C., Mall, I.D. and Lataye, D.H. (2009). Rice husk ash as an effective adsorbent: Evaluation of adsorptive characteristics for Indigo Carmine dye. *Journal of Environmental Management*, 90, 710-720

Lataye, D.H., Mishra, I.M. and Mall, I.D. (2008). Pyridine sorption from aqueous solution by rice husk ash (RHA) and granular activated carbon (GAC): Parametric, kinetic, equilibrium and thermodynamic aspects. *Journal of Hazardous Materials*, 154, 858–870

Lataye, D.H., Mishra, I.M. and Mall, I.D. (2009). Adsorption of picoline onto rice husk ash and granular activated carbon from aqueous solution: Equilibrium and thermodynamic study. *Chemical Engineering Journal*, 147, 139–149

Lazo-Cannata, J.C., Nieto-Márquez, A., Jacoby, A., Paredes-Doig, A.L., Romero, A., Sun-Kou, M.R. and Valverde, J.L. (2011). Adsorption of phenol and nitrophenols by carbon nanospheres: Effect of pH and ionic strength. *Separation and Purification Technology*, 80, 217–224

Li, B. (2012). Charaterization of pore structure and surface chemistry of activated carbons-a review, fourier transform-materials analysis, *InTech*

Li, K., Zheng, Z. and Li, Y. (2010). Characterization and lead adsorption properties of activated carbons prepared from cotton stalk by one-step H_3PO_4 activation. *Journal of Hazardous Materials*, 181, 440–447

Li, Y., Ding, X., Guo, Y., Rong, C., Wang, L., Qu, Y….. and Wang, Z. (2011a). A new method of comprehensive utilization of rice husk. *Journal of Hazardous Materials*, 186, 2151–2156

Li, Y., Ding, X., Guo, Y., Wang, L., Rong, C., Qu, Y….. and Wang, Z. (2011b). A simple and highly effective process for the preparation of activated carbons with high surface area. *Materials Chemistry and Physics*, 127, 495–500

Li, Y., Du, Q., Liu, T., Peng, X., Wang, J., Sun J.… and Xia, L. (2013). Comparative study of methylene blue dye adsorption onto activated carbon, graphene oxide, and carbon nanotubes. *Chemical Engineering Research and Design*, 91, 361-368

Lim, J.S., Manan, Z.A., Wan Alwi, S.R. and Hashim, H. (2012). A review on utilization of biomass from rice industry as a source of renewable energy. *Renewable and Sustainable Energy Reviews*, 16, 3084-3094

Lima, L.S., Araujo, M.D.M., Quináia, S.P., Migliorine, D.W. and Garcia, J.R. (2011). Adsorption modeling of Cr, Cd and Cu on activated carbon of different origins by using fractional factorial design. *Chemical Engineering Journal*, 166, 881–889

Lin, L., Zhai, R-S., Xiao, Z-Y., Song, Y., An, Q-D. and Song, X-W. (2013). Dye adsorption of mesoporous activated carbons produced from NaOH-pretreated rice husks. *Bioresource Technology*, 136, 437–443

Lin, S. and Juang, R. (2009). Adsorption of phenol and its derivatives from water using synthetic resins and low-cost natural adsorbents: A review. *Journal of Environmental Management*, 90, 1336–1349

Liou, T. (2010). Development of mesoporous structure and high adsorption capacity of biomass-based activated carbon by phosphoric acid and zinc chloride activation. *Chemical Engineering Journal*, 158, 129–142

Liou, T-H. and Wu, S-J. (2009). Characteristics of microporous/mesoporous carbons prepared from rice husk under base- and acid-treated conditions. *Journal of Hazardous Materials*, 171, 693–703

Liu, Q-S., Zheng, T., Wang, P., Jiang, J-P. and Li, N. (2010). Adsorption isotherm, kinetic and mechanism studies of some substituted phenols on activated carbon fibers. *Chemical Engineering Journal*, 157, 348–356

Liu, W-J., Zeng, F-X., Jiang, H. and Zhang, X-S. (2011). Preparation of high adsorption capacity bio-chars from waste biomass. *Bioresource Technology*, 102, 8247–8252

Liu, Z. and Zhang, F. (2011). Removal of copper (II) and phenol from aqueous solution using porous carbons derived from hydrothermal chars. *Desalination*, 267, 101–106

Lo, S-F., Wang, S-Y., Tsai, M-J. and Lin, L-D. (2012). Adsorption capacity and removal efficiency of heavy metal ions by Moso and Ma bamboo activated carbons. *Chemical Engineering Research and Design*, 90, 1397-1406

Lori, J.A., Lawal, A.O., and Ekanem, E.J. (2008). Active carbons from chemically mediated pyrolysis of agricultural wastes: Application in simultaneous removal of binary mixture of benzene and toluene from water. *International Journal of Environ. Res.,* 2(4), 411-418

Luo, X., Deng, Z., Lin, X. and Zhang, C. (2011). Fixed-bed column study for Cu^{2+} removal from solution using expanding rice husk. *Journal of Hazardous Materials*, 187, 182–189

Mahmoud, D.K., Mohamad, A.M.S. and Azlina, W.A. (2012). Langmuir model application on solid-liquid adsorption using agricultural wastes: Environmental application review. *Journal of Purity, Utility Reaction and Environment*, 1(4), 200-229

Mahvi, A.H., Maleki, A. and Eslami, A. (2004). Potential of rice husk and rice husk ash for phenol removal in aqueous systems. *American Journal of Applied Sciences*, 1(4), 321-326.

Malik, R., Ramtake, D.S. and Wate, S.R. (2006). Physico-chemical and surface characterization of adsorbent prepared from ground nut shell by $ZnCl_2$ activation and its ability to adsorb colour. *Indian Journal of Chemical Technology*, 13, 319-328

Mallikarjun, S.D. and Mise, S.R. (2012). A study of phosphate adsorption characteristics on different soils. *IOSR Journal of Engineering*, 2(7), 13-23.

Manase, A. (2012). Optimization of tea waste activated carbon preparation parameters for removal of cibacron yellow dye from textile wastewaters. *International Journal of Advanced Engineering Research and Studies*, I(IV), 50-56

Masoud, M.S., El-Saraf, W.M., Abdel-Halim, A.M., Ali, A.E., Mohamed, E.A. and Hasan, H.M.I. (2012). Rice husk and activated carbon for waste water treatment of El-Mex Bay, Alexandria Coast, Egypt. *Arabian Journal of Chemistry*, http://dx.doi.org/10.1016/j.arabjc.2012.04.028

Maximova, A. and Koumanova, B. (2008). Equilibrium and kinetics study of adsorption of basic dyes onto perfil from aqueous solutions. *Journal of the University of Chemical Technology and Metallurgy*, 43(1), 101-108

Mina, G., Rafsanjani, H.H. and Goharrizi, A.S. (2011). Optimization and modeling of hexavalent chromium removal from aqueous solution via adsorption on multiwalled carbon nanotubes. *Research Journal of Applied Sciences, Engineering and Technology*, 3(9), 880-886

Mohamed, A.R., Mohammadib, M. and Darzi, G.N. (2010). Preparation of carbon molecular sieve from lignocellulosic biomass: A review. *Renewable and Sustainable Energy Reviews*, 14, 1591-1599

Mohammad, Y.S, Shaibu-Imodagbe, E.M. and Okuofu, C.A. (2012). Pyrolysis for solid waste management and biofuel production. *Journal of Occupational Safety and Environmental Health*, 1(1), 52-55

Mohammad-Khan, A. and Ansari, R. (2009). Activated Charcoal: Preparation, characterization and Applications: A review article. *International Journal of Chemical Tech. Research*, 1(4), 859-864

Mohan, D., Singh, K.P. and Singh, V.K. (2008). Wastewater treatment using low cost activated carbons derived from agricultural byproducts-A case study. *Journal of Hazardous Materials*, 152, 1045–1053

Mohd-Din, A.T., Hameed, B.H and Ahmad, A.L. (2009). Batch adsorption of phenol onto physiochemical-activated coconut shell. *Journal of Hazardous Materials*, 161, 1522-1529

Moreno-Virgen, M., Rigoberto, T., Mendoza-Castillo, I.D. and Bonilla-Petriciolet, A. (2012). Applications of activated carbons obtained from lignocellulosic materials for the wastewater treatment, lignocellulosic precursors used in the synthesis of activated carbon -characterization techniques and applications in the wastewater treatment, *InTech*

Moussavi, G., Alahabadi, A., Yaghmaeian, K. and Eskandari, M. (2013). Preparation, characterization and adsorption potential of the NH_4Cl-induced activated carbon for the removal of amoxicillin antibiotic from water. *Chemical Engineering Journal*, 217, 119–128

Moyo, M., Eusebia, M., Fidelis, C. and Benias, C.N. (2012). Removal of phenol from aqueous solution by adsorption on yeast. *IJRRS*, 11(3), 486-494

Mukosha, L., Onyango, M.S., Ochieng, A. and Kasaini, H. (2013). Development of better quality low-cost activated carbon from South African pine tree (*Pinus patula*) sawdust: characterization and comparative phenol adsorption. *World Academy of Science, Engineering and Technology*, Vol. 79

Nabais, J.M.N., Gomes, J.A., Suhas, Carrott, P.J.M., Laginhas, C. and Roman, S. (2009). Phenol removal onto novel activated carbons made from lignocellulosic precursors: Influence of surface properties. *Journal of Hazardous Materials*, 167, 904–910

Nabais, J.V., Carrott, P., Carrott, R., Luz, V. and Ortiz, A.L. (2008). Influence of preparation conditions in the textural and chemical properties of activated carbons from a novel biomass precursor: The coffee endocarp. *Bioresource Technology*, 99, 7224–7231

Nadavala, S.K., Swayampakula, K., Boddu, V.M. and Abburi, K. (2009). Biosorption of phenol and *o*-chlorophenol from aqueous solutions on to chitosan–calcium alginate blended beads. *Journal of Hazardous Materials*, 162, 482–489

Nadeem, M., Mahmoud, A., Shahid, S.A., Shah, S.S., Khalid, M.A. and McKay, G. (2006). Sorption of Lead from Aqueous Solution by Chemically Modified Adsorbents. *Journal of Hazardous Materials,* doi:10.1016/jhazmat.2006.05.098

Nahil, M.A. and Williams, P.T. (2012). Pore characteristics of activated carbons from the phosphoric acid chemical activation of cotton stalks. *Biomass and Bioenergy*, 37, 142-149

Naiya, T.K., Bhattacharya, A.K., Mandal, S. and Das, S.K. (2009). The sorption of lead (II) ions on rice husk ash. *Journal of Hazardous Materials*, 163, 1254–1264

Nasehir-Khan, E.M Y., Faizal, L.M., Ismail, A., Olugbenga, S.B. and Mohd, A.A. (2010a). Effect of preparation conditions of activated carbon prepared from rice husk by CO_2 activation for removal of Cu (II) from aqueous solution. *International Journal of Engineering & Technology*, 10(6), 47-51

Nasehir-Khan, E.M.Y., Faizal, L.M., Ismail, A., Olugbenga, S.B. and Mohd, A.A. (2010b). Process optimization for Zn (II) removal by activated carbon prepared from rice husk using chemical activation. *International Journal of Basic & Applied Sciences*, 10(6), 132-136

Nasehir-Khan, E.M Y., Faizal, L.M., Ismail, A., Olugbenga, S.B. and Mohd, A.A. (2011). Fixed-bed column study for Cu (II) removal from aqueous solutions using rice husk based activated carbon. *International Journal of Engineering & Technology*, 11(1), 248-253

Ngah, W.S.W and Hanafiah, M.A.K.M. (2008). Removal of heavy metal ions from wastewater by chemically modified plant wastes as adsorbents. *Bioresource Technology*, 99, 3935–3948

Nhapi, I., Banadda, N., Murenzi, R., Sekomo, C.B. and Wali, U.G. (2011). Removal of heavy metals from industrial waste water using rice husks. *The Open Environmental Engineering Journal*, 4, 170-180

Njoku, V.O. and Hameed, B.H. (2011). Preparation and characterization of activated carbon from corncob by chemical activation with H_3PO_4 for 2,4-dichlorophenoxyacetic acid adsorption. *Chemical Engineering Journal*, 173, 391–399

Noreen, S., Bhatti, H.N., Nausheen, S., Sadaf, S. and Ashfaq, M. (2013). Batch and fixed bed adsorption study for the removal of DrimarineBlack CL-B dye from aqueous solution using a lignocellulosic waste: A cost affective adsorbent. *Industrial Crops and Products*, 50, 568– 579

Nwabunne, J.T. and Igbokwe, P.K. (2012). Adsorption performance of packed bed column for the removal of lead (II) using oil palm fibre. *International Journal of Applied Science and Technology*, 2(5), 106-115

Obeng, D.P., Morrell, S. and Napier-Munn, T.J. (2005). Application of central composite rotatable design to modeling the effect of some operating variables on the performance of the three-product cyclone. *Int. Journal of Miner. Process*., 76, 181–192.

Ocholi, O.J. (2012). *Adsorption of Simulated and Real Effluents onto Activated Carbon Surfaces*. PhD Thesis, Ahmadu Bello University, Zaria, Nigeria

Omar, H.A. (2012). Adsorptive removal of phenol from aqueous solution using natural and immobilized chitin by dithiazone. *New York Science Journal*, 5(8), 47-55

Osakwe, E.C. (2011). *Study of Heavy Metals Removal from Synthetic Wastewater Using Borassus Aethlopum and Cocos Nucifera*. M.Sc Thesis, Ahmadu Bello University, Zaria, Nigeria

Oscar, H-R. and Stuart, M.H. (2008). Novel and modified materials for wastewater treatment applications. *Journal of Materials Chemistry*, 18, 2751–2761

Otokunefor, T.V. and Obiukwu, C. (2005). Impact of refinery effluent on the physicochemical properties of a water body in the Niger Delta. *Applied Ecology and Environmental Research,* 3(1), 61-72

Ozdemir, M., Bolgaz, T., Saka, C. and Sahin, O. (2011). Preparation and characterization of activated carbon from cotton stalks in a two-stage process. *Journal of Analytical and Applied Pyrolysis*, 92, 171–175

Ozturk, N. and Kavak, D. (2005). Adsorption of boron from aqueous solutions using fly ash: Batch and column studies. *Journal of Hazardous Materials*, (B127) 81–88

Pan, B., Qui, H., Lv, L., Zhang, Q., Zhang, W. and Zhang, Q. (2009). Critical review in adsorption kinetic models. *Journal of Zhejiang University Science,* 10(5), 716-724

Patel, P.M. (2005). *Supercritical Fluid Extraction of Rice Bran with Adsorption on Rice Hull Ash*. PhD Dissertation, Louisiana State University, Louisiana, USA.

Patnukao, P. and Pavasant, P. (2008). Activated carbon from *Eucalyptus camaldulenis Dehn* bark using phosphoric acid activation. *Bioresource Technology*, 99, 8540-8543

Potgieter, J.H., Bada, S.O. and Potgieter-Vermaak, S.S. (2009). Adsorptive removal of various phenols from water by South African fly ash. *Water SA*, 35(1), 89-96

Purnomo, C.W., Salim, C. and Hinode, H. (2011). Preparation and characterization of activated carbon from bagasse fly ash. *Journal of Analytical and Applied Pyrolysis*, 91, 257–262

Qadeer, R. and Akhtar, S. (2005). Kinetics Study of Lead ion Adsorption on Active Carbon. *Turk Journal of Chemistry,* 29, 95- 99.

Rangabhashiyam, S., Anu, N. and Selvaraju, N. (2013). Sequestration of dye from textile industry wastewater using agricultural waste products as adsorbents, *Journal of Environmental Chemical Engineering*, 1, 629-641

Reddy, K.S.K., Al Shoaibi, A. and Srinivasakannan, C. (2012). A comparison of microstructure and adsorption characteristics of activated carbons by CO2 and H_3PO_4 activation from date palm pits. *New Carbon Materials,* 27(5), 344–351

Rivera-Utrilla, J., Sanchez-Polo, M., Gomez-Serrano, V., Alvarez, P. M., Alvim-Ferraz, M.C.M. and Dias, J.M. (2011). Activated carbon modifications to enhance its water treatment applications: An overview. *Journal of Hazardous Materials,* 187, 1–23

Roosta, M., Ghaedi, M., Shokri, N., Daneshfar, A., Sahraei, R. and Asghari, A. (2014). Optimization of the combined ultrasonic assisted/adsorption method for the removal of malachite green by gold nanoparticles loaded on activated carbon: Experimental design. *Spectrochimica Acta Part A: Molecular and Biomolecular Spectroscopy*, 118, 55–65

Rosas, J. M., Bedia, J., Rodríguez-Mirasol, J. and Cordero, T. (2009). HEMP-derived activated carbon fibers by chemical activation with phosphoric acid. *Fuel,* 88, 19–26

Rosas, J. M., Bedia, J., Rodríguez-Mirasol, J. and Cordero, T. (2010). On the preparation and characterization of chars and activated carbons from orange skin. *Fuel Processing Technology,* 91, 1345–1354

Roy, P., Mondal, N.K. and Das, K. (2013). Modeling of the adsorptive removal of arsenic: A statistical approach. *Journal of Environmental Chemical Engineering*, http://dx.doi.org/10.1016/j.jece.2013.10.014

Rusly, S.M. and Shaliza, I. (2010). Adsorption of textile reactive dye by palm shell activated carbon: Response surface methodology. *World Academy of Science, Engineering and Technology*, 43, 892-895

Saad, S.A., Isa, K.M.D. and Bahari, R. (2010). Chemically modified sugarcane bagasse as a potentially low-cost biosorbent for dye removal. *Desalination*, 264, 123–128

Saadat, S. and Karimi, J.A. (2011). Optimization of Pb (II) adsorption onto modified walnut shells using factorial design and simplex methodologies. *Chemical Engineering Journal*, 173, 743– 749

Sadaf, S. and Bhatti, H.N. (2013). Batch and fixed bed column studies for the removal of Indosol Yellow BG dye by peanut husk. *Journal of the Taiwan Institute of Chemical Engineers,* http://dx.doi.org/10.1016/j.jtice.2013.05.004

Sadon, F.N., Ahmmed, S.I. and Kamariah, N.I. (2012). An overview of rice husk applications and modification techniques in wastewater treatment. *Journal of Purity, Utility Reaction and Environment*, 1(6), 338-364

Saetea, P. and Tippayawong, N. (2013). Characterization of adsorbent from hydrothermally carbonized and steam activated sewage sludge. *Proceedings of the World Congress on Engineering*, London, U.K

Sahin, O. and Saka, C. (2013). Preparation and characterization of activated carbon from acorn shell by physical activation with H_2O–CO_2 in two-step pretreatment. *Bioresource Technology*, 136, 163–168

Sahu, J.N., Acharya, J. and Meikap, B.C. (2010). Optimization of production conditions for activated carbons from Tamarind wood by zinc chloride using response surface methodology. *Bioresource Technology*, 101, 1974–1982

Sahu, J.N., Acharya, J. and Meikapa, B.C. (2009a). Response surface modeling and optimization of chromium (VI) removal from aqueous solution using Tamarind wood activated carbon in batch process. *Journal of Hazardous Materials*, 172, 818–825

Sahu, J.N., Agarwal, S., Meikap, B.C. and Biswas, M.N. (2009b). Performance of a modified multi-stage bubble column reactor for lead (II) and biological oxygen demand removal from wastewater using activated rice husk. *Journal of Hazardous Materials*, 161, 317–324

Saka, C. (2012). BET, TG–DTG, FT-IR, SEM, iodine number analysis and preparation of activated carbon from acorn shell by chemical activation with $ZnCl_2$. *Journal of Analytical and Applied Pyrolysis*, 95, 21–24

Santhi, T., Manonmani, S. and Smitha, T. (2010). Kinetics and isotherm studies on cationic dyes adsorption onto Annona *Squmosa* seed activated carbon. *International Journal of Engineering Science and Technology*, 2(3), 287-295

Schroder, E., Klaus, T., Benjamin, O. and Sabrina, H. (2011). Activated carbon from waste biomass, progress in biomass and bioenergy production, *InTech*

Shen, W., Zhijie, L. and Yihong, L. (2008). Surface chemical functional groups modification of porous carbon. *Recent Patents on Chemical Engineering*, 1, 27-40

Shi, Q., Zhang, J., Zhang, C., Li, C., Zhang, B., Hu, W….. and Zhao, R. (2010). Preparation of activated carbon from cattail and its application for dyes removal. *Journal of Environmental Sciences*, 22(1), 91-97

Shih, M. (2012). Kinetics of the batch adsorption of methylene blue from aqueous solutions onto rice husk: effect of acid-modified process and dye concentration. *Desalination and Water Treatment*, 37(1), 200-214

Shri, M.W.B. and Vijayababu, P.V. (2013). Some studies on removal of phenol from waste water using low cost adsorbent. *International Journal of Scientific & Engineering Research*, 4(8), 1790-1798

Sincero, A.P. and Sincero, G.A. (2006). *Environmrntal Engineering: A Design Approach*. Prince-Hall of India, New Delhi**.**

Singh, K.P., Malik, A., Sinha, S. and Ojha, P. (2008). Liquid-phase adsorption of phenols using activated carbons derived from agricultural waste material. *Journal of Hazardous Materials*, 150, 626–641

Singh, K.P., Singh, A.K., Gupta, S. and Sinha, S. (2010). Experimental design and response surface modeling for optimization of Rhodamine B removal from water by magnetic nanocomposite. *Chemical Engineering Journal*, 165, 151–160

Singh, K.P., Singh, A.K., Gupta, S. and Sinha, S. (2011a). Optimization of Cr (VI) reduction by zero-valent bimetallic nanoparticles using the response surface modeling approach. *Desalination*, 270, 275–284

Singh, K.P., Singh, A.K., Gupta, S. and Sinha, S. (2011b). Optimizing adsorption of crystal violet dye from water by magnetic nanocomposite using response surface modeling approach. *Journal of Hazardous Materials*, 186, 1462–1473

Sivarajasekar, N. and Baskar, R. (2013). Adsorption of Basic Red 9 on activated waste Gossypium hirsutum seeds: Process modeling, analysis and optimization using statistical design. *Journal of Industrial and Engineering Chemistry*, http://dx.doi.org/10.1016/j.jiec.2013.10.058

Sivasubramanian, S. Rengasamy, M. and Brinda L.A. (2012). Potential of phenol removal by low-cost adsorbent in a batch reactor. *International Journal on Applied Bioengineering*, 6(1), 39-43

Somasundaram, S., Sekar, K., Gupta, V. K. and Ganesan, S. (2013). Synthesis and characterization of mesoporous activated carbon from rice husk for adsorption of glycine from alcohol-aqueous mixture. *Journal of Molecular Liquids*, 177, 416–425

Song, J., Zou, W., Bian, Y., Su, F. and Han, R. (2011). Adsorption characteristics of methylene blue by peanut husk in batch and column modes. *Desalination*, 265, 119–125

Song, X., Zhang, Y., Yan, C., Jiang, W. and Chang, C. (2013). The Langmuir monolayer adsorption model of organic matter into effective pores in activated carbon. *Journal of Colloid and Interface Science*, 389, 213-219

Soto, M.L., Moure, A., Dominguez, H. and Parajo, J.C. (2011). Recovery, concentration and purification of phenolic compounds by adsorption: A review. *Journal of Food Engineering*, 105, 1–27

Srihari, V. and Das, A. (2008). Comparative studies on adsorptive removal of phenol by three agro-based carbons: Equilibrium and isotherm studies. *Ecotoxicology and Environmental Safety*, 71, 274–283

Srinivasakannan, C. (2003). High surface area activated carbon from waste biomass. *Proceedings of the 2nd Regional Conference on Energy Technology towards a Clean Environment*, Phuket, Thailand

Srivastava, V.C., Mall, I.D. and Mishra, I.M. (2008). Removal of cadmium (II) and zinc (II) metal ions from binary aqueous solution by rice husk ash. *Colloids and Surfaces A: Physicochem. Eng. Aspects*, 312, 172–184

Stavropoulos, G.G., Samaras, P. and Sakellaropoulos, G.P. (2008). Effect of activated carbons modification on porosity, surface structure and phenol adsorption. *Journal of Hazardous Materials*. 151, 414–421

Sud, D., Mahajan, G. and Kaur, M.P. (2008). Agricultural waste material as potential adsorbent for sequestering heavy metal ions from aqueous solutions: A review. *Bioresource Technology*, 99, 6017–6027

Sugashini, S. and Meera, S.B.K.M. (2013). Column adsorption studies for the removal of Cr (VI) ions by ethylamine modified chitosan carbonized rice husk composite beads with modeling and optimization. *Journal of Chemistry*, Volume 2013, Article ID 460971

Sugumaran, P., Priya Susan, V., Ravichandran, P. and Seshadri, S. (2012). Production and characterization of activated carbon from banana empty fruit bunch and *Delonix regia* fruit pod. *Journal of Sustainable Energy & Environment*, 3, 125-132

Suresh, S., Srivastava, V.C. and Mishra, I.M. (2011). Adsorptive removal of phenol from binary aqueous solution with aniline and 4-nitrophenol by granular activated carbon. *Chemical Engineering Journal*, 171, 997– 1003

Suteu, D. and Malutan, T. (2013). Adsorption of cationic dye on cellolignin. *BioResource*, 8(1), 427-446

Tan, I.A.W., Ahmad, A.L. and Hameed, B.H. (2008a). Adsorption of basic dye on high-surface-area activated carbon prepared from coconut husk: Equilibrium, kinetic and thermodynamic studies. *Journal of Hazardous Materials*, 154, 337–346

Tan, I.A.W., Ahmad, A.L. and Hameed, B.H. (2008b). Preparation of activated carbon from coconut husk: Optimization study on removal of 2,4,6-trichlorophenol using response surface methodology. *Journal of Hazardous Materials*, 153, 709-717

Tan, I.A.W., Ahmad, A.L. and Hameed, B.H. (2009). Fixed-bed adsorption performance of oil palm shell-based activated carbon for removal of 2,4,6-trichlorophenol. *Bioresource Technology*, 100, 1494–1496

Tay, T., Ucar, S. and Karagöz, S. (2009). Preparation and characterization of activated carbon from waste biomass. *Journal of Hazardous Materials*, 165, 481–485

Thamilarasu, P., Sharmila, R. and Karunakaran, K. (2012). Kinetic, equilibrium and thermodynamic studies on removal of Cr (VI) by modified activated carbon prepared from Ricinus Communis seed shell. *Coromandal Journal of Science*, 1(1), 30-39

Theydan, S.K. and Ahmed, M.J. (2012). Adsorption of methylene blue onto biomass-based activated carbon by $FeCl_3$ activation: Equilibrium, kinetics, and thermodynamic studies. *Journal of Analytical and Applied Pyrolysis*, 97, 116–122

Ucar, S., Erdem, M., Tay, T. and Karagoz, S. (2009). Preparation and characterization of activated carbon produced from pomegranate seeds by $ZnCl_2$ activation. *Applied Surface Science*, 255, 8890-8896

Valix, M., Cheung, W.H. and Zhang, K. (2008). Role of chemical pre-treatment in the development of super-high surface areas and heteroatom fixation in activated carbons prepared from bagasse. *Microporous and Mesoporous Materials*, 116, 513–523

Verla, A.W, Horsfall, M., Verla, E.N., Spiff, A.I. and Ekpete, O.A. (2012). Preparation and characterization of activated carbon from fluted pumpkin (*Telfairia Occidentalis* Hook.F) seed shell. *Asian Journal of Natural & Applied Sciences*, 1(3), 39-50

Vijayakumar, G., Tamilarasan, R. and Dharmendirakumar, M. (2012). Adsorption kinetics, equililibrium and thermodynamics studies on the removal of basic dye Rhodamine-B from aqueous solution by natural adsorbent perlite. *Journal of Material Environmental Science*, 3(1), 157-170

Wang, L. (2012). Application of activated carbon derived from 'waste' bamboo culms for the adsorption of azo disperse dye: Kinetic, equilibrium and thermodynamic studies. *Journal of Environmental Management*, 102, 79-87

Wang, L., Guo, Y., Zou, B., Rong, C., Ma, X., Qu, Y….. and Wang, Z. (2011a). High surface area porous carbons prepared from hydrochars by phosphoric acid activation. *Bioresource Technology*, 102, 1947–1950

Wang, L., Wang, X., Zou, B., Rong, C., Ma, X., Qu, Y….. and Wang, Z. (2011b). Preparation of carbon black from rice husk by hydrolysis, carbonization and pyrolysis. *Bioresource Technology*, 102, 8220-8224

Wang, L., Zhang, J., Zhao, R., Li, C., Li, Y. and Zhang, C. (2010). Adsorption of basic dyes on activated carbon prepared from Polygonum Orientale Linn: Equilibrium, kinetic and thermodynamic studies. *Desalination*, 254, 68–74

Wong, K.K., Lee, C.K., Low, K.S. and Haron, M.J. (2003). Removal of Cu and Pb by tartaric acid modified rice husk from aqueous solutions. *Chemosphere*, 50, 23–28

Xin-hui, D., Srinivasakannan, C., Qu, W-W., Xin, W., Jin-hui, P. and Li-bo, Z. (2012). Regeneration of microwave assisted spent activated carbon: Process optimization, adsorption isotherms and kinetics. *Chemical Engineering and Processing*, 53, 53–62

Yadanaparthi, S.K.R., Graybill, D. and Wandruszka, R. (2009). Adsorbents for the removal of arsenic, cadmium, and lead from contaminated waters. *Journal of Hazardous Materials*, 171, 1–15

Yakout, S.M. and Sharaf-El-Deen, G. (2011). Characterization of activated carbon prepared by phosphoric acid activation of olive stones. *Arabian Journal of Chemistry*, dx.doi.org/10.1016/j.arabjc.2011.12.002

Yang, J. and Qiu, K. (2011). Development of high surface area mesoporous activated carbons from herb residues. *Chemical Engineering Journal*, 167, 148–154

Ye, H., Zhu, Q. and Du, D. (2010). Adsorptive removal of Cd (II) from aqueous solution using natural and modified rice husk. *Bioresource Technology*, 101, 5175–5179

Zahangir-Alam, M., Muyibi, S.A., Mansor, M.F. and Wahid, R. (2007). Activated carbons derived from oil palm empty-fruit bunches: Application to environmental problems. *Journal of Environmental Sciences*, 19, 103–108

Zanzi, R., Bai, X., Capdevila, P. and Bjornbom, E. (2001). Pyrolysis of biomass in presence of steam for preparation of activated carbon, liquid and gaseous products. *6th World Congress of Chemical Engineering*, Melbourne, Australia

Zawani, Z., Luqman, C.A. and Thomas, S.Y.C. (2009). Equilibrium, kinetics and thermodynamic studies: adsorption of Remazol Black 5 on the palm kernel shell activated carbon (PKS-AC). *European Journal of Scientific Research*, 37(1), 63-71

Zhang, J., Fu, H., Lv, X., Tang, J. and Xu, X. (2011a). Removal of Cu (II) from aqueous solution using the rice husk carbons prepared by the physical activation process. *Biomass and Bioenergy*, 35, 464-472

Zhang, W., Dong, L., Yan, H., Li, H., Jiang, Z., Kan, X….. and Cheng, R. (2011b). Removal of methylene blue from aqueous solutions by straw based adsorbent in a fixed-bed column. *Chemical Engineering Journal*, 173, 429– 436

Zhang, Y., Cui, H., Ozao, R., Cao, Y., Bobby, I.T.C., Wang, C. and Pan, W. (2007). Characterization of activated carbon prepared from chicken waste and coal. *Energy & Fuels*, 21, 3735–3739

Zhu, K., Fu, H., Zhang, J., Lv, X., Tang, J. and Xu, X. (2012). Studies on removal of NH_4^+-N from aqueous solution by using the activated carbons derived from rice husk. *Biomass and Bioenergy*, 43, 18-25

Zuo, S., Yang, J., Liu, J. and Cai, X. (2009). Significance of the carbonization of volatile pyrolytic products on the properties of activated carbons from phosphoric acid activation of lignocellulosic material. *Fuel Processing Technology*, 90, 994–1001

APPENDIX A

Appendix A1: Results on Effect of Solution pH

pH	C_e (mg/l)	q_e (mg/g)	RE (%)
2	2.193	0.960	94.600
4	2.018	0.965	95.032
6	2.105	0.963	94.816
8	2.368	0.956	94.168
10	2.544	0.952	93.736

Appendix A2: Results on Effect of Process Temperature

T (^oC)	C_e (mg/l)	q_e (mg/g)	k (g/l)	RE (%)
30	2.281	0.958	0.420	94.384
40	2.544	0.952	0.374	93.736
50	2.632	0.949	0.361	93.520

Appendix A3: Breakthrough Curve, Yoon Nelson and Thomas model plot data for *z=4.5cm, f=3ml/min, C_o=51.32mg/l*

t (min)	C_t (mg/l)	q_B (mg/g)	RE (%)	C_t/C_o	$\ln(C_t/C_o-C_t)$	$\ln(C_o/C_t -1)$
10	2.807	0.513	94.530	0.055	-2.850	2.850
20	3.421	1.026	93.334	0.067	-2.639	2.639
30	5.439	1.540	89.403	0.106	-2.133	2.133
40	6.228	2.053	87.864	0.121	-1.980	1.980
50	9.123	2.566	82.224	0.178	-1.532	1.532
60	12.632	3.079	75.387	0.246	-1.119	1.119
70	15.877	3.592	69.062	0.309	-0.803	0.803
80	16.667	4.106	67.524	0.325	-0.732	0.732
90	16.667	4.619	67.524	0.325	-0.732	0.732
100	21.930	5.132	57.268	0.427	-0.293	0.293
110	21.930	5.645	57.268	0.427	-0.293	0.293
120	21.404	6.158	58.294	0.417	-0.335	0.335

Appendix A4: Breakthrough Curve, Yoon Nelson and Thomas model plot data for *z=6cm, f=3ml/min, C_o=51.32mg/l*

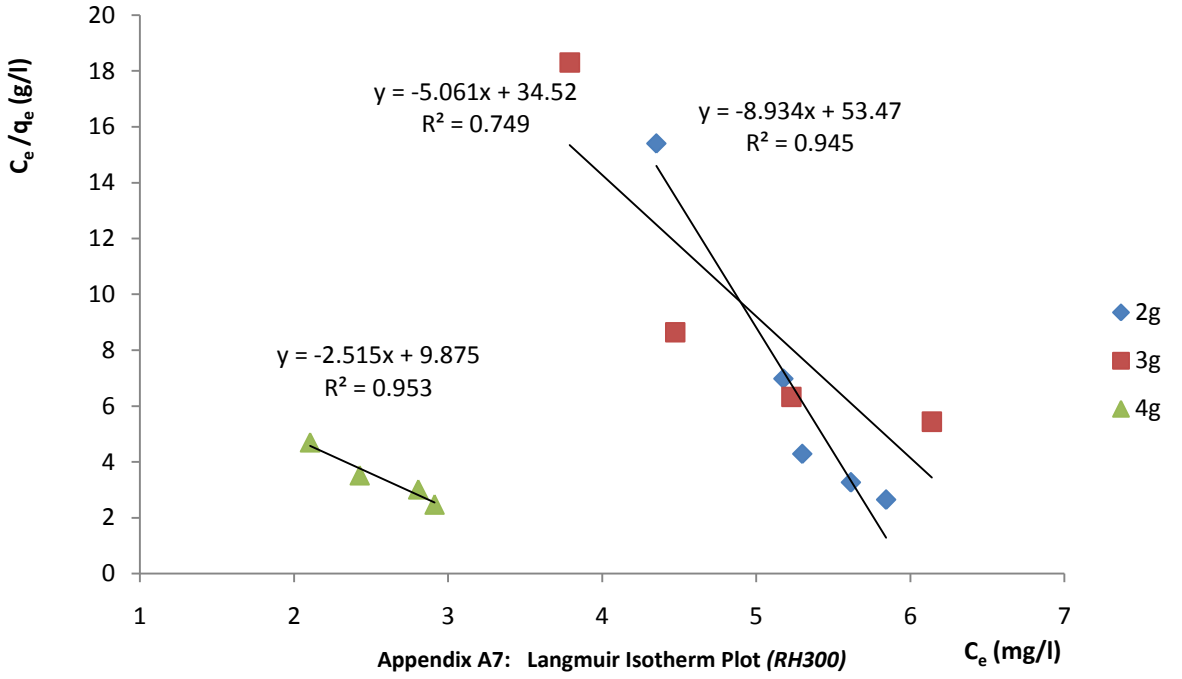
t (min)	C_t (mg/l)	q_B (mg/g)	RE (%)	C_t/C_o	$\ln(C_t/C_o-C_t)$	$\ln(C_o/C_t -1)$
10	2.456	0.385	95.214	0.048	-2.990	2.990
20	3.246	0.770	93.676	0.063	-2.695	2.695
30	3.509	1.155	93.163	0.068	-2.612	2.612
40	4.912	1.540	90.428	0.096	-2.246	2.246
50	5.439	1.925	89.403	0.106	-2.133	2.133
60	6.140	2.309	88.035	0.120	-1.996	1.996
70	6.579	2.694	87.181	0.128	-1.917	1.917
80	11.404	3.079	77.780	0.222	-1.253	1.253
90	13.158	3.464	74.361	0.256	-1.065	1.065
100	16.667	3.849	67.524	0.325	-0.732	0.732
110	18.596	4.234	63.764	0.362	-0.565	0.565
120	18.246	4.619	64.447	0.356	-0.595	0.595
130	18.509	5.004	63.935	0.361	-0.573	0.573
140	19.298	5.389	62.396	0.376	-0.506	0.506
150	19.298	5.774	62.396	0.376	-0.506	0.506
160	19.298	6.158	62.396	0.376	-0.506	0.506
170	21.930	6.543	57.268	0.427	-0.293	0.293

Appendix A5: Breakthrough Curve, Yoon Nelson and Thomas model plot data for *z=7.5cm, f=3ml/min, C_o=51.32mg/l*

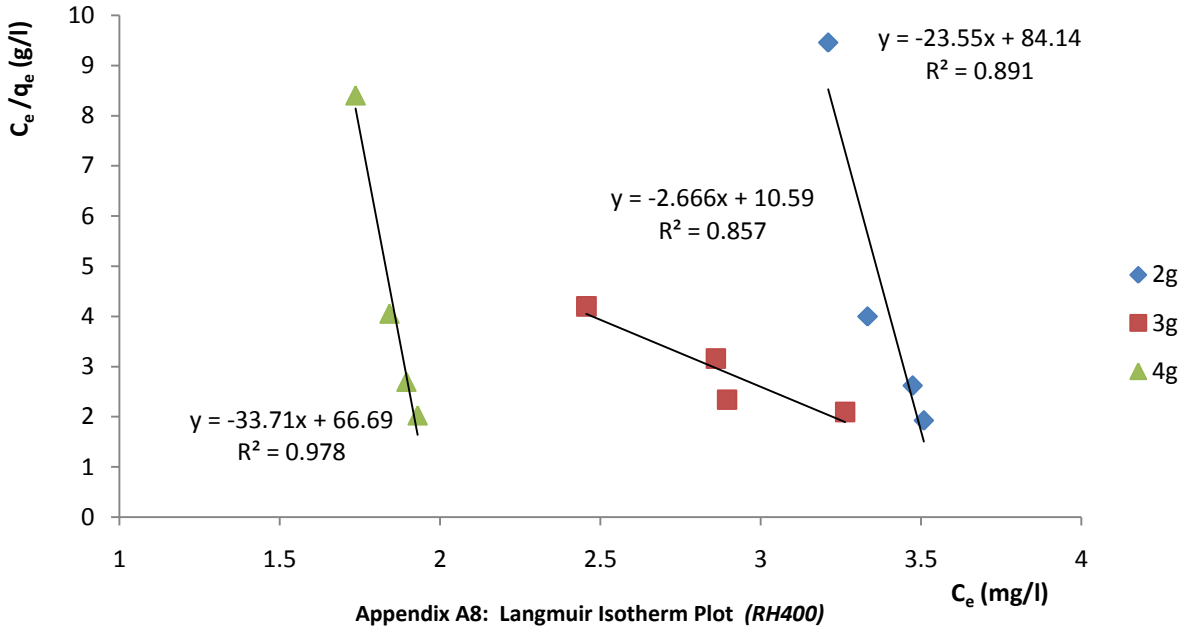
t (min)	C_t (mg/l)	q_B (mg/g)	RE (%)	C_t/C_o	$\ln(C_t/C_o-C_t)$	$\ln(C_o/C_t-1)$
10	1.754	0.308	96.581	0.034	-3.341	3.341
20	2.193	0.616	95.727	0.043	-3.109	3.109
30	2.456	0.924	95.214	0.048	-2.990	2.990
40	2.719	1.232	94.701	0.053	-2.883	2.883
50	3.860	1.540	92.479	0.075	-2.509	2.509
60	4.474	1.848	91.283	0.087	-2.349	2.349
70	5.351	2.155	89.574	0.104	-2.151	2.151
80	6.754	2.463	86.839	0.132	-1.887	1.887
90	7.807	2.771	84.788	0.152	-1.718	1.718
100	9.035	3.079	82.395	0.176	-1.543	1.543
110	9.386	3.387	81.711	0.183	-1.497	1.497
120	12.105	3.695	76.412	0.236	-1.175	1.175
130	12.544	4.003	75.558	0.244	-1.129	1.129
140	13.070	4.311	74.532	0.255	-1.074	1.074
150	12.544	4.619	75.558	0.244	-1.129	1.129
160	13.509	4.927	73.677	0.263	-1.029	1.029
170	13.246	5.235	74.190	0.258	-1.056	1.056
180	13.684	5.543	73.336	0.267	-1.012	1.012
190	13.860	5.850	72.994	0.270	-0.994	0.994
200	14.561	6.158	71.626	0.284	-0.926	0.926
210	12.632	6.466	75.387	0.246	-1.119	1.119
220	14.737	6.774	71.284	0.287	-0.909	0.909
230	14.912	7.082	70.943	0.291	-0.893	0.893
240	15.263	7.390	70.259	0.297	-0.860	0.860
250	15.351	7.698	70.088	0.299	-0.851	0.851
260	15.702	8.006	69.404	0.306	-0.819	0.819
270	19.123	8.314	62.738	0.373	-0.521	0.521
280	20.351	8.622	60.345	0.397	-0.420	0.420
290	20.614	8.930	59.832	0.402	-0.398	0.398

Appendix A6: Breakthrough Curve, Yoon Nelson and Thomas model plot data for *z=6cm, f=4.5ml/min, C_o=51.32mg/l*

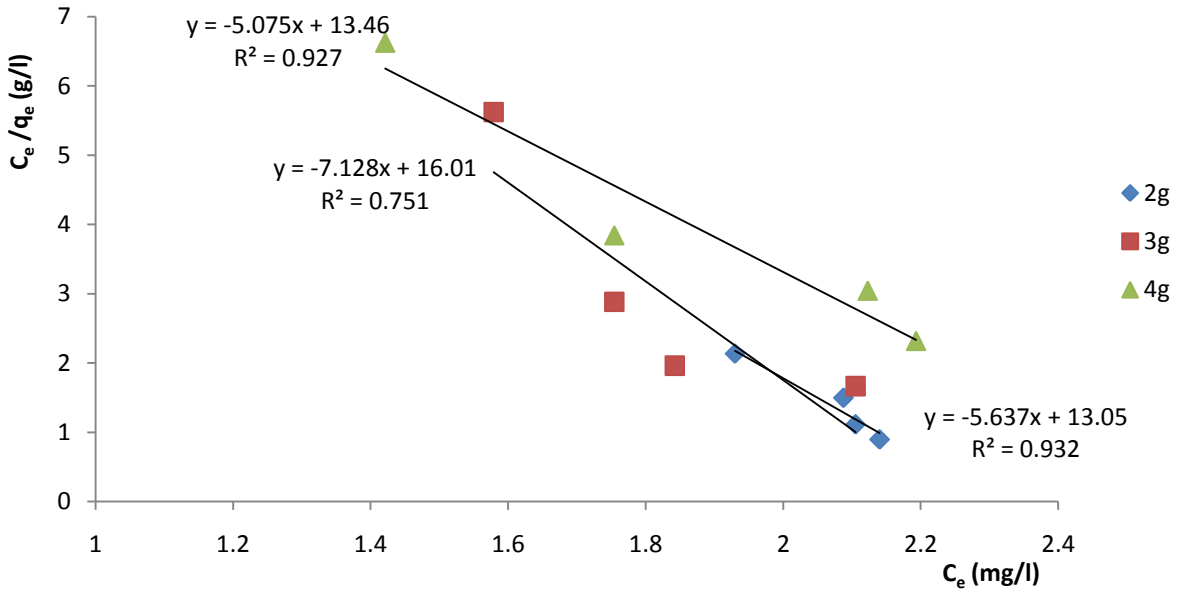
t (min)	C_t (mg/l)	q_B (mg/g)	RE (%)	C_t/C_o	$\ln(C_t/C_o-C_t)$	$\ln(C_o/C_t-1)$
10	3.684	0.385	92.821	0.072	-2.560	2.560
20	5.175	0.770	89.915	0.101	-2.188	2.188
30	6.404	1.155	87.522	0.125	-1.948	1.948
40	10.000	1.540	80.514	0.195	-1.419	1.419
50	14.035	1.925	72.652	0.273	-0.977	0.977
60	16.754	2.309	67.353	0.326	-0.724	0.724
70	17.632	2.694	65.644	0.344	-0.647	0.647
80	17.895	3.079	65.131	0.349	-0.625	0.625
90	17.544	3.464	65.815	0.342	-0.655	0.655
100	18.158	3.849	64.618	0.354	-0.602	0.602
110	20.702	4.234	59.661	0.403	-0.391	0.391
120	21.053	4.619	58.978	0.410	-0.363	0.363



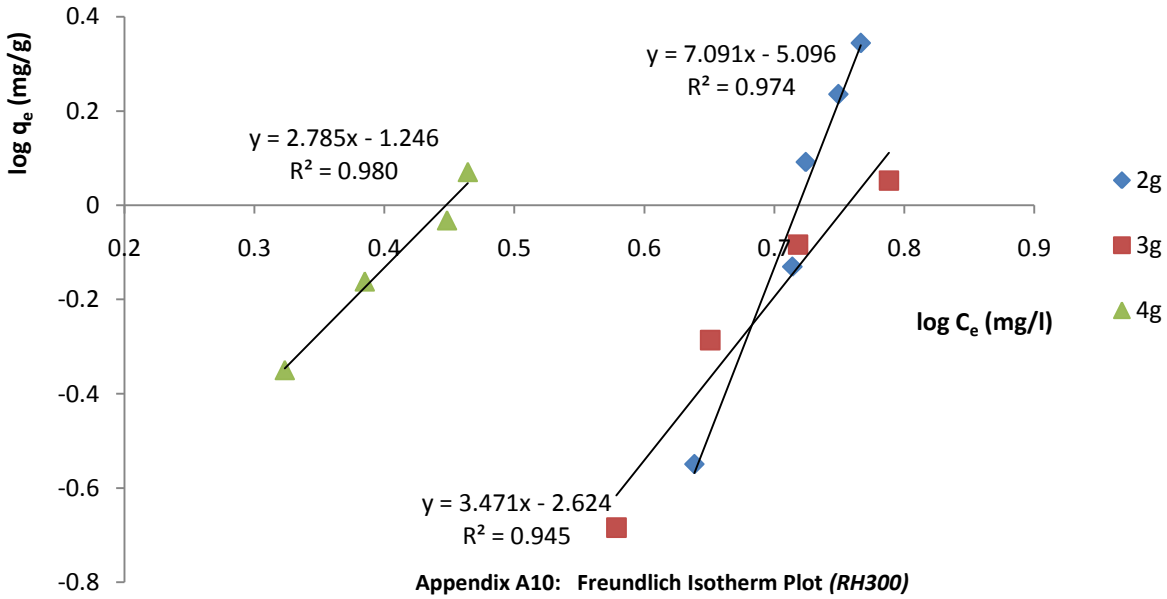
Appendix A7: Langmuir Isotherm Plot *(RH300)*



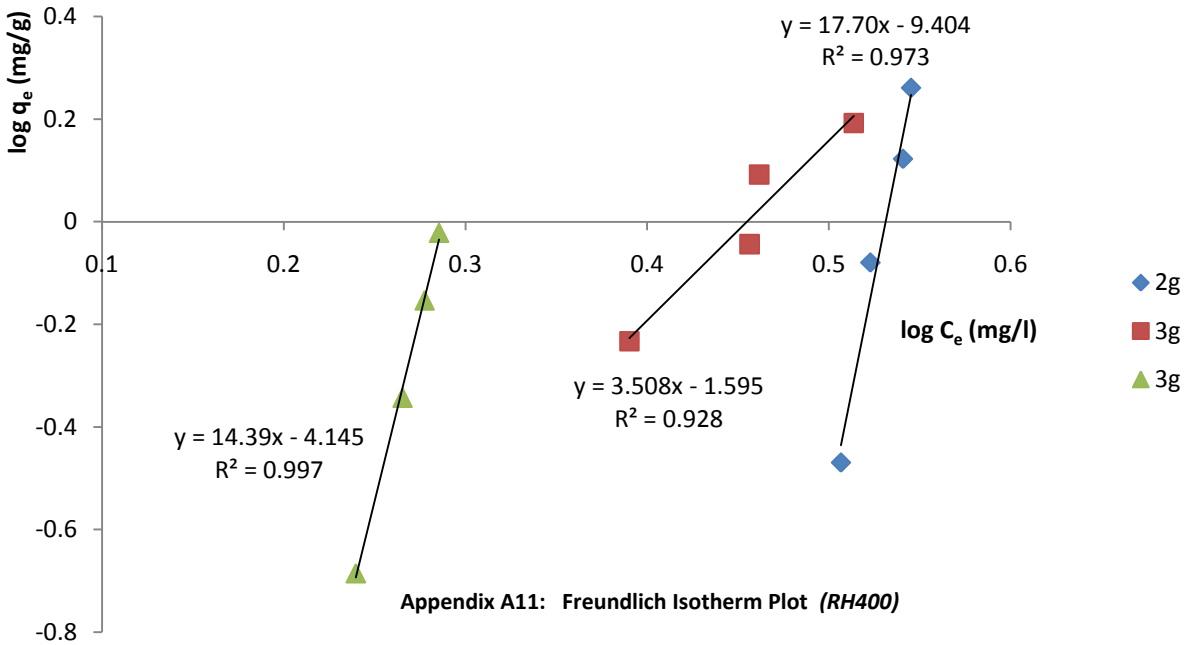
Appendix A8: Langmuir Isotherm Plot *(RH400)*



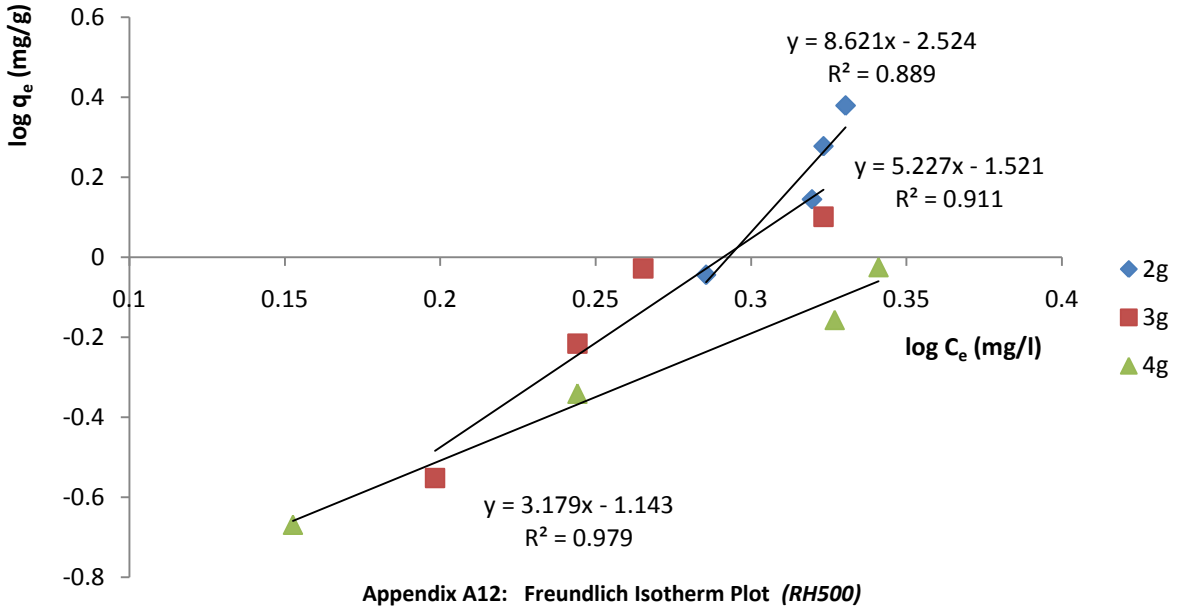
Appendix A9: Langmuir Isotherm Plot *(RH500)*



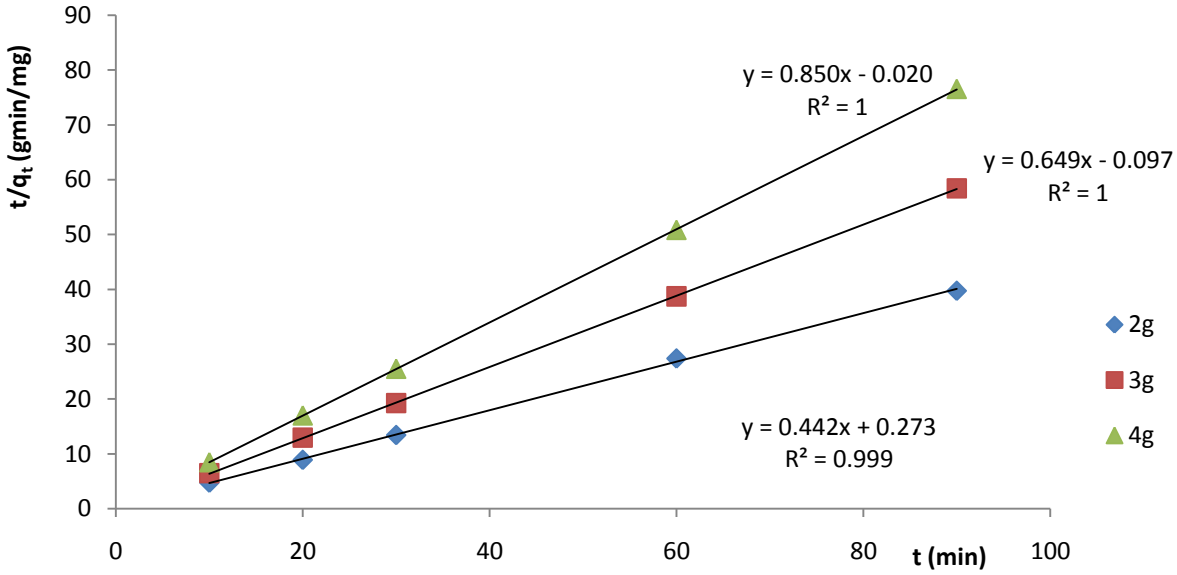
Appendix A10: Freundlich Isotherm Plot *(RH300)*



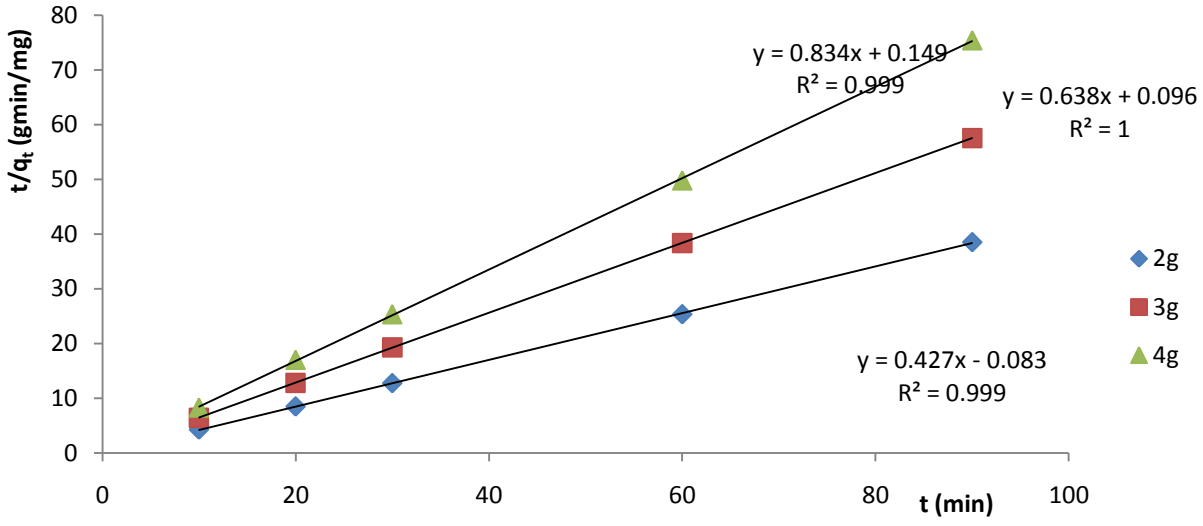
Appendix A11: Freundlich Isotherm Plot *(RH400)*



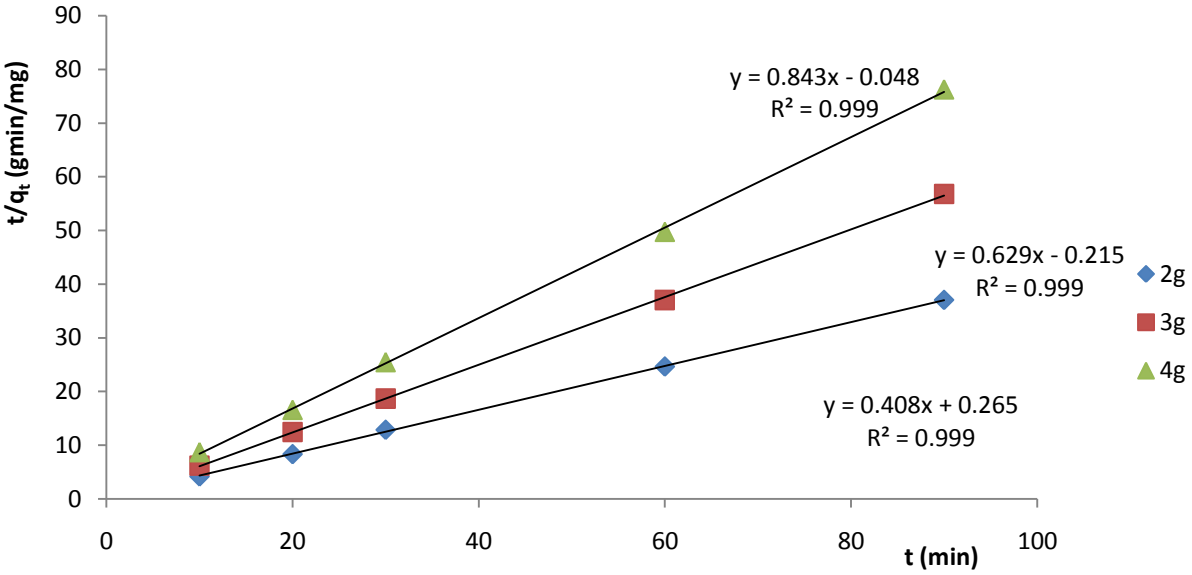
Appendix A12: Freundlich Isotherm Plot *(RH500)*



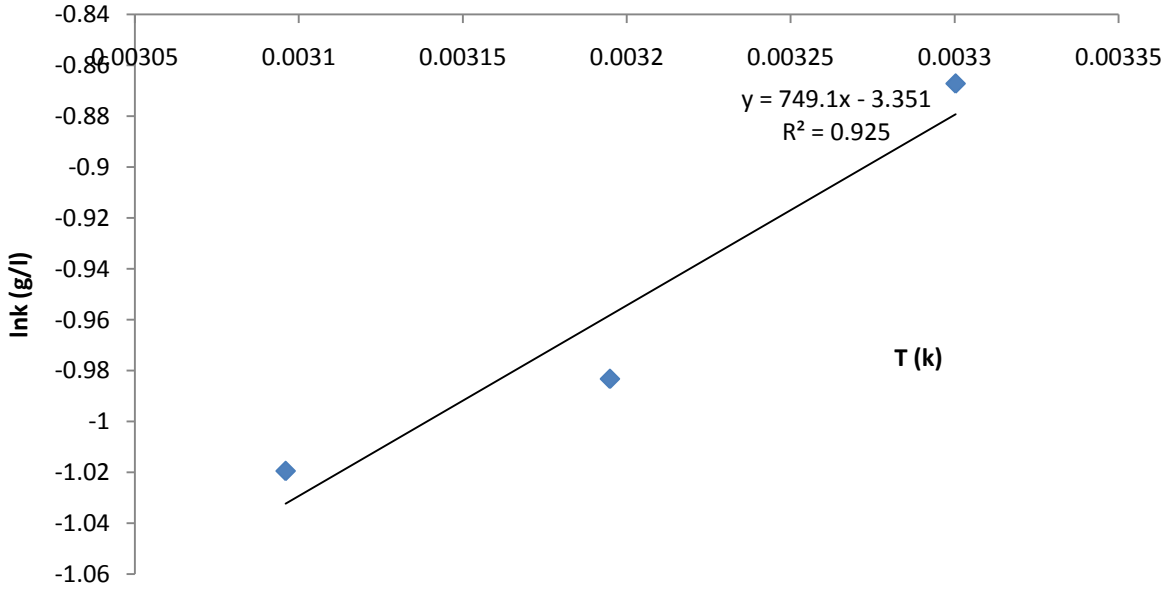
Appendix A13: Pseudo-Second Order Kinetics Plot *(RH300)*



Appendix A14: Pseudo-Second Order Kinetics Plot *(RH400)*



Appendix A15: Pseudo-Second Order Kinetics Plot *(RH500)*



Appendix A16: Thermodynamic model plot

APPENDIX B

The manuscripts published or accepted for publication from this study are:

(i) **Mohammad, Y.S.**, Shaibu-Imodagbe, E.M., Igboro, S.B., Giwa, A. and Okuofu, C.A. (2014). Adsorption of phenol from refinery wastewater using rice husk activated carbon, *Iranica Journal of Energy and Environment*, 5(4), 393-399

(ii) **Mohammad, Y.S.**, Shaibu-Imodagbe, E.M., Igboro, S.B., Giwa, A. and Okuofu, C.A. (2014). Modeling and optimization for production of rice husk activated carbon and adsorption of phenol, *Journal of Engineering*, Volume 2014, http://dx.doi.org/10.1155/2014/278075

(iii) **Mohammad, Y.S.**, Shaibu-Imodagbe, E.M., Igboro, S.B., Giwa, A. and Okuofu, C.A. (2014). Application of low-cost adsorbent in the treatment of Samaru stream water, *Journal of Engineering Studies and Research*, 20(4), 61-65

(iv) **Mohammad, Y.S.**, Shaibu-Imodagbe, E.M., Igboro, S.B., Giwa, A. and Okuofu, C.A. (2015). Effect of phosphoric acid modification on characteristics of rice husk activated carbon, *Iranica Journal of Energy and Environment*, 6(1), 20-25

(v) **Mohammad, Y.S.**, Shaibu-Imodagbe, E.M., Igboro, S.B., Giwa, A. and Okuofu, C.A. (2015). Isotherms, kinetics and thermodynamics of phenol adsorption onto rice husk activated carbon. *Leonardo Electronic Journal of Practices and Technologies*, Accepted.

(vi) **Mohammad, Y.S.,** Shaibu-Imodagbe, E.M., Igboro, S.B., Giwa, A. and Okuofu, C.A. (2013). Activated Carbons from Biomass: Development, Characterization and Application, *Conference Proceedings of the 12th Annual Nigerian Materials Congress*, Held at African University of Science and Technology, Abuja